FRIENDS OF THE PLEISTOCENE, ROCKY MOUNTAIN-CELL, 45TH FIELD CONFERENCE

PLIO-PLEISTOCENE STRATIGRAPHY AND GEOMORPHOLOGY OF THE CENTRAL PART OF THE ALBUQUERQUE BASIN

OCTOBER 12-14, 2001

SEAN D. CONNELL
New Mexico Bureau of Geology and Mineral Resources-Albuquerque Office, New Mexico Institute of Mining and Technology, 2808 Central Ave. SE, Albuquerque, New Mexico 87106

DAVID W. LOVE
New Mexico Bureau of Geology and Mineral Resources, New Mexico Institute of Mining and Technology, 801 Leroy Place, Socorro, NM 87801

JOHN D. SORRELL
Tribal Hydrologist, Pueblo of Isleta, P.O. Box 1270, Isleta, NM 87022

J. BRUCE J. HARRISON
Dept. of Earth and Environmental Sciences, New Mexico Institute of Mining and Technology
801 Leroy Place, Socorro, NM 87801

Open-File Report 454C and D
Initial Release: October 11, 2001

New Mexico Bureau of Geology and Mineral Resources
New Mexico Institute of Mining and Technology
801 Leroy Place, Socorro, NM 87801

INTRODUCTION

This field-guide accompanies the 45th annual Rocky Mountain Cell of the Friends of the Pleistocene (FOP), held at Isleta Lakes, New Mexico. The Friends of the Pleistocene is an informal gathering of Quaternary geologists, geomorphologists, and pedologists who meet annually in the field.

The field guide has been separated into two parts. Part C (open-file report 454C) contains the three-days of road logs and stop descriptions. Part D (open-file report 454D) contains a collection of mini-papers relevant to field-trip stops. This field guide is a companion to open-file report 454A and 454B, which accompanied a field trip for the annual meeting of the Rocky Mountain/South Central Section of the Geological Society of America, held in Albuquerque in late April. Errors in compiling this field-excursion are undoubtable. Please kindly inform the authors of any errors or omissions. We appologize for any unintended omissions or citations.

In keeping with the informal character of Rocky Mountain Cell FOP field excursions, this guidebook contains preliminary findings of a number of concurrent projects being worked on by the trip leaders. Thus, this guidebook should be considered as a type of progress report on geologic mapping, stratigraphic work, and radioisotopic dating.

The contents of the road logs and mini-papers have been placed on open file in order to make them available to the public as soon as possible. Revision of these papers is likely because of the on-going nature of work in the region. The papers have not been edited or reviewed according to New Mexico Bureau of Geology and Mineral Resources standards. The contents of this report should not be considered final and complete until published by the New Mexico Bureau of Geology and Mineral Resources. Comments on papers in this open-file report are welcome and should be made to authors. The views and preliminary conclusions contained in this report are those of the authors and should not be interpreted as necessarily representing the official policies, either expressed or implied, of the State of New Mexico, Pueblo of Isleta, or the U.S. Government.

ACKNOWLEDGEMENTS

The New Mexico Bureau of Geology and Mineral Resources (P.A. Scholle, Director) supported this field trip. Much of the data presented during this field trip are from numerous open-file reports released by the New Mexico Bureau of Geology and Mineral Resources during the course of cooperative geologic mapping with the U.S. Geological Survey (New Mexico Statemap Project, P.W. Bauer, Program Manager). We are particularly grateful to the people of the Pueblo of Isleta for granting access during many of the stratigraphic and mapping studies discussed during the field trip. In particular, we thank the Honorable Alvino Lucero, Governor of Isleta, for granting access to study stratigraphically significant sites on the reservation.

We are indebted to Florian Maldonado for his help and important work on the western part of the Isleta Reservation. Bill McIntosh and Nelia Dunbar provided the many important dates and tephrochronologic correlations in the Albuquerque Basin. We are grateful to John Hawley, Steven Cather, Dan Koning, and Richard Chamberlin for their assistance and advice. We thank Tien Grauch, Dirk Van Hart, and Keith Kelson for freely sharing their ideas on the geology and structure of the Isleta Reservation and Sandia National Laboratories area. In particular, the site-wide hydrologic project at Sandia National Laboratories conducted by GRAM Inc. and William Lettis and Associates (Thomas et al., 1995) was especially helpful in documenting the geology of Kirtland Air Force Base and the Sandia Labs. We also thank Jim Cole and Byron Stone for sharing some of their ideas on the late-stage development of the basin. David McCraw and Patricia Jackson-Paul assisted in the field and in the preparation of some of the map and poster figures. Leo Gabaldon assisted with drafting of the simplified geologic map of the Isleta Reservation. Glen Jones and Mark Mansell produced the shaded-relief images from 10-m DEM data released by the U.S. Geological Survey.

GUIDEBOOK TABLE OF CONTENTS
OPEN-FILE REPORT 454C

First Day Road Log: Geology of the Isleta Reservation
S.D. Connell, D. W. Love, and J.D. Sorrell *1-1*

Second Day Road Log: Geology of southern Albuquerque and Tijeras Arroyo
S.D. Connell, D.W. Love, J.B.J. Harrison *2-1*

Third Day Road Log: Geology of Los Lunas volcano
D.W. Love, W.C. McIntosh, N. Dunbar, and S.D. Connell *3-1*

MINI-PAPER TABLE OF CONTENTS
OPEN-FILE REPORT 454D

Terraces of Hell Canyon and its tributaries, Memorial Draw and Ojo de la Cabra
D. W. Love *A-1*

Surface geology and liquefaction susceptibility in the inner valley of the Rio Grande near Albuquerque, New Mexico
K.I. Kelson, C.S. Hitchcock, and C.E. Randolph *B-1*

Stratigraphy of middle and upper Pleistocene fluvial deposits of the Rio Grande Valley (Post-Santa Fe Group) and the geomorphic development of the Rio Grande Valley, northern Albuquerque Basin, central New Mexico
S.D. Connell and D. W. Love *C-1*

Summary of Blancan and Irvingtonian (Pliocene and early Pleistocene) mammalian biochronology of New Mexico (*reprinted from NMBMMR Open-file report 454B*)
G.S. Morgan, and S.G. Lucas *D-1*

Plio-Pleistocene mammalian biostratigraphy and biochronology at Tijeras Arroyo, Bernalillo County, New Mexico (*reprinted from NMBMMR Open-file report 454B*)
G.S. Morgan and S.G. Lucas *E-1*

Cuspate-lobate folds along a sedimentary contact, Los Lunas volcano, New Mexico
(*reprinted from NMBMMR Bulletin 137*)
W.C. Haneberg........ *F-1*

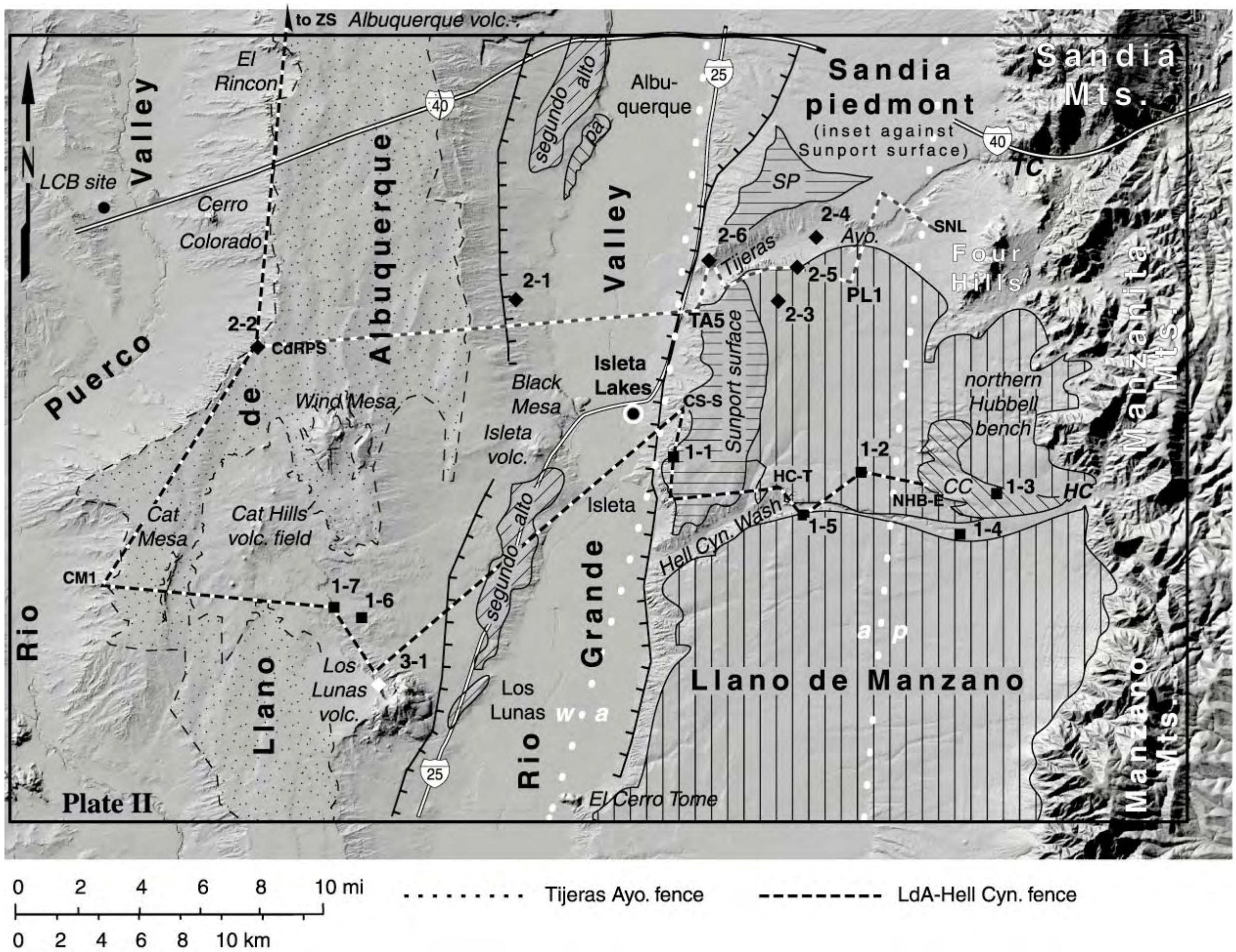

Plate I. Shaded-relief map of the Isleta Reservation and southern Albuquerque field-trip area illustrating the locations of day 1 (black square), day 2 (black diamond), and day 3 (white diamond) stops. All trips start from the Isleta Lakes Campground (black circle) in the inner valley of the Rio Grande. The Llano de Albuquerque is a broad, south-sloping interfluve between the Rio Puerco and Rio Grande Valleys, which was formed during late Pliocene time. The hachured lines indicate the approximate boundary of inset fluvial terrace deposits of the Rio Grande Valley. The broad low-relief surfaces east of the Rio Grande Valley contain the Pleistocene Sunport (SP) and Llano de Manzano surfaces, and the Pliocene Cañada Colorada surface (CC). The approximate eastern and western limits of the axial-fluvial Rio Grande (a) is denoted depicted by white dotted lines. TC and HC indicate the mouths of Tijeras, and Hell Canyons, respectively. Nearly all of the north- and northwest-trending scarps are faults that cut these geomorphic surfaces. Base from shaded-relief image in Maldonado et al. (1999) and was prepared from 10-m DEM data from the National Elevation Database of the U.S. Geological Survey.

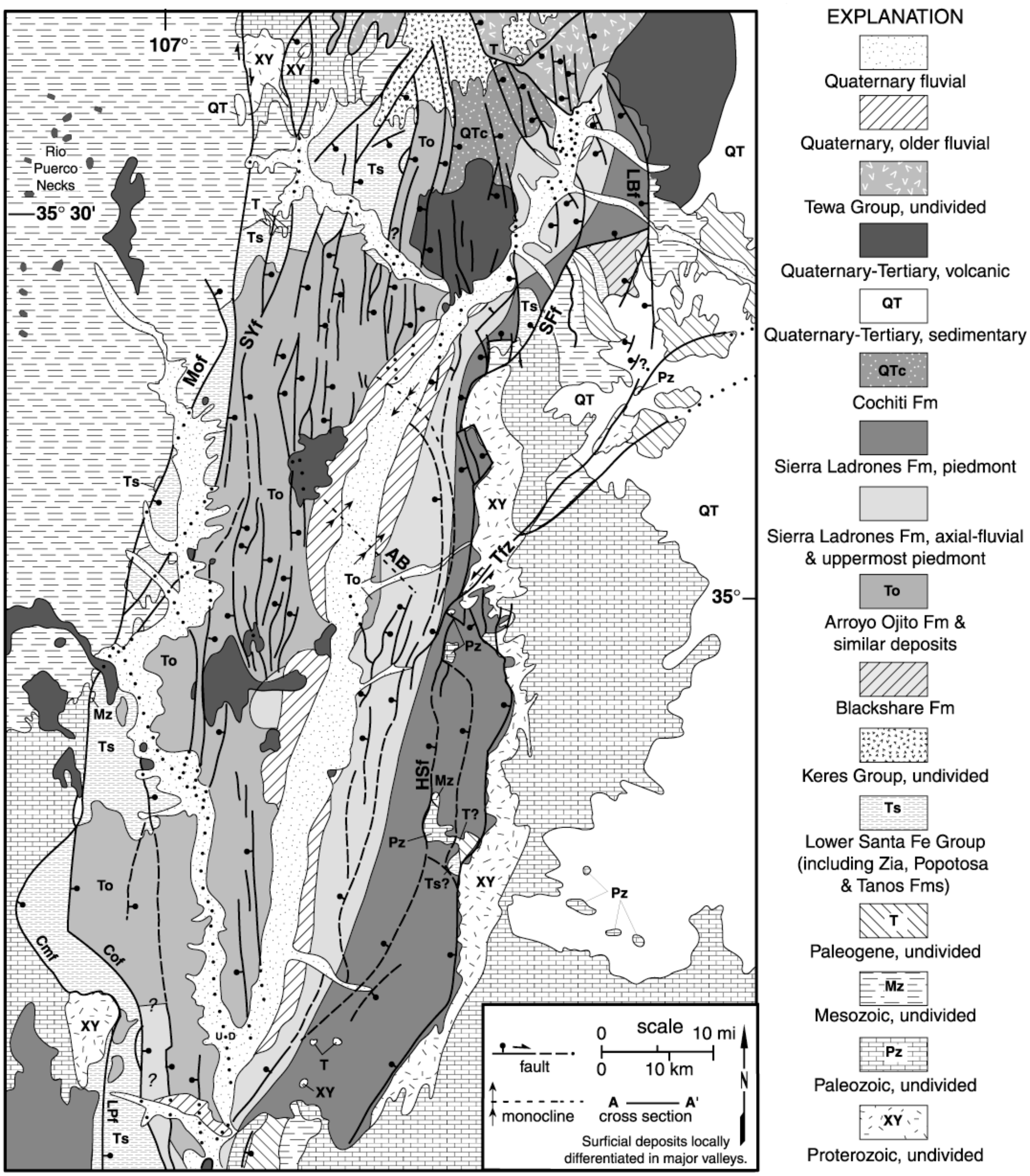

Plate II. Simplified geologic map of the Albuquerque Basin (Connell, in preparation).

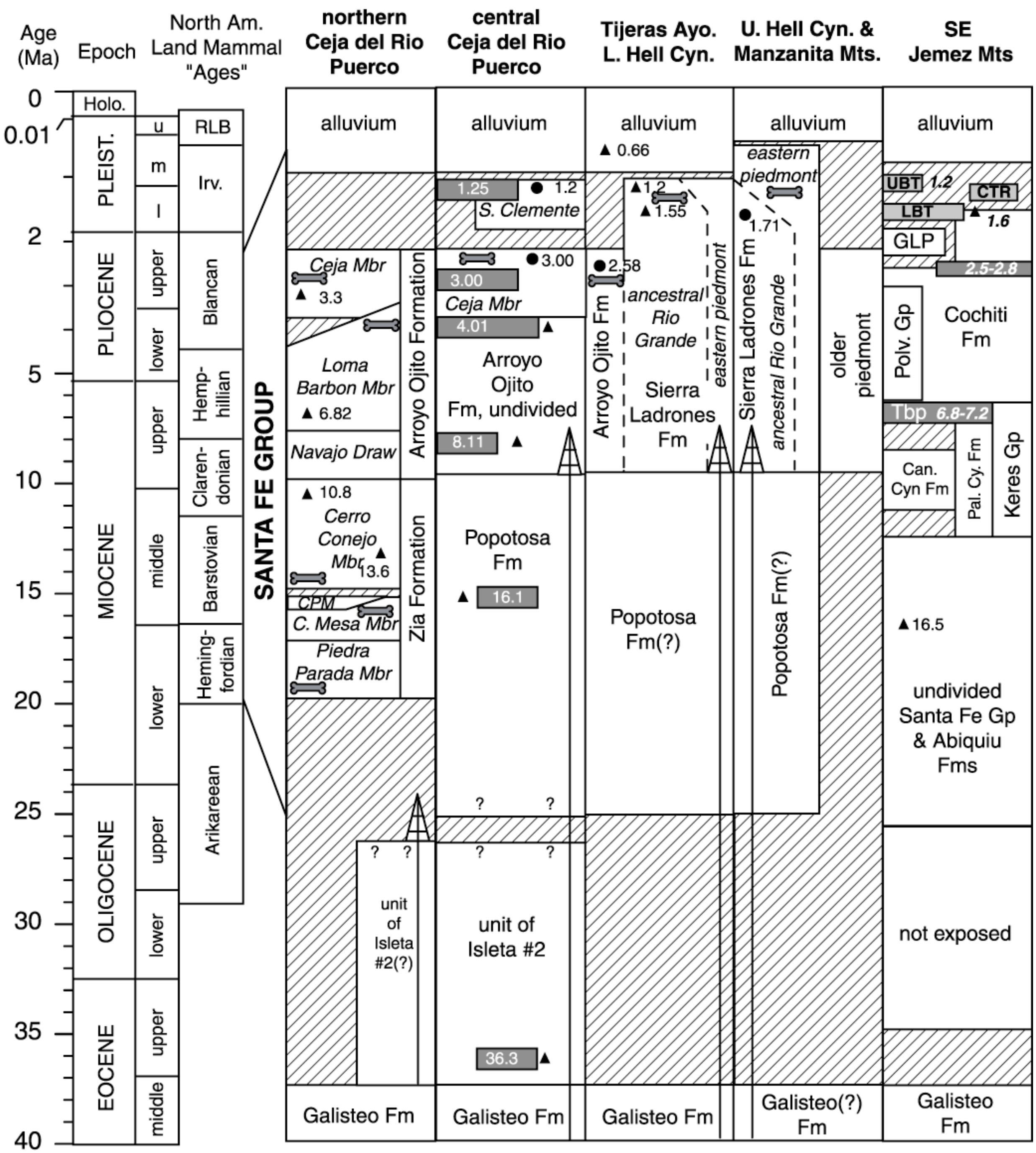

Plate III. Stratigraphic correlation diagrams of deposits in the central Albuquerque Basin and southern Jemez Mountains. Black triangles and circles denote radioisotopically dated primary, and fluvially recycled volcanic products, respectively. Bones denote biostratigraphically significant fossil mammal sites. Volcanic units are shaded. Dates are from various sources and noted in Ma. Deposits of Zia Fm include the Chamisa Mesa (C. Mesa) and Cañada Pilares (CPM) mbrs. Rancholabrean (RLB) and Irvingtonian (Irv) are Pleistocene divisions of the North American Land Mammal "ages."

FRIENDS OF THE PLEISTOCENE, ROCKY MOUNTAIN CELL, 45TH FIELD CONFERENCE

PLIO-PLEISTOCENE STRATIGRAPHY AND GEOMORPHOLOGY OF THE CENTRAL PART OF THE ALBUQUERQUE BASIN

FIRST-DAY ROAD LOG, OCTOBER 12, 2001

Geology of the Isleta Reservation

SEAN D. CONNELL
New Mexico Bureau of Geology and Mineral Resources-Albuquerque Office, New Mexico Institute of Mining and Technology, 2808 Central Ave. SE, Albuquerque, New Mexico 87106

DAVID W. LOVE
New Mexico Bureau of Geology and Mineral Resources, New Mexico Institute of Mining and Technology, 801 Leroy Place, Socorro, NM 87801

JOHN D. SORRELL
Tribal Hydrologist, Pueblo of Isleta, P.O. Box 1270, Isleta, NM 87022

The following road log examines some of the many outstanding geologic and geomorphic features on the Isleta Reservation. The first day of this field excursion examines lower Pleistocene deposits of the ancestral Rio Grande, the axial-river of the Albuquerque Basin and the namesake of the Rio Grande rift, and interfingering deposits of the eastern-margin piedmont. We also examine the role of faulting on the preservation of early Pleistocene and Pliocene geomorphic surfaces along the eastern margin of the basin. The day-one trip will conclude with a traverse to the eastern slopes of the late Pleistocene Cat Hills volcanic field to a visit to a graben on the San Clemente land grant. This graben preserves a sequence of sand and mud that overlies a buried soil developed on upper Pliocene fluvial deposits associated with rivers that drained the western margin of the basin. Many of the dates cited here are from Maldonado et al. (1999) and from unpublished data of Bill McIntosh and Nelia Dunbar (NM Bureau of Geology and Mineral Resources).

Nearly the entire following road log is on tribal lands administered by the Pueblo of Isleta, which are restricted to the public. Access to Pueblo lands must be made through the tribal administrator or governors office (Pueblo of Isleta, P.O. Box 1270, Isleta, New Mexico) prior to travelling on Pueblo lands. In respect for the privacy of the tribal community, we ask that you discuss access for geologic study or to access Pueblo lands to examine the exposures discussed herein with John Sorrell, Dave Love, or Sean Connell, prior to contacting the Governor's Office for permission. Road-log mileage has not been checked for accuracy. Field-trip stops illustrated on Plate I.

Mi. **Description**

0.0 Begin trip at south side of store at the Isleta Lakes Campground, *Isleta 7.5' quadrangle (1991), GPS: NAD 83, UTM Zone 013 S, N: 3,867,855 m; E: 346,955 m. (Note that the UTM ticks on this quad are incorrect)*. Drive east and leave Isleta Lakes Campground. **0.3**

0.3 Railroad Crossing. **0.1**

0.4 Isleta Eagle Golf Course to south, a 27-hole course operated by the tribe and is part of their growing resort complex. **0.1**

0.5 Exposures of Arroyo Ojito Fm in bluffs to south. Basin-fill deposits are assigned to the upper Oligocene to lower Pleistocene Santa Fe Group, which comprises the synrift volcanic and sedimentary rocks of the Rio Grande rift. The Santa Fe Group is commonly subdivided into a lower subgroup representing deposition within internally drained (hydrologically closed) basins containing playa-lake, eolian, and piedmont deposits. Fluvial deposits from the proto-Rio Grande and Rio Puerco systems probably emptied into the northern and northwestern parts of the basin before these river systems integrated south into southern New Mexico during latest Miocene (?) or early Pliocene time. The upper sub-group represents deposition within externally drained (hydrologically open) basins where the Rio Grande represents the through-going axial river and contains a generally consistent pattern of lithofacies assemblages. Within externally drained half-graben basins, axial-fluvial deposits are bounded on either side by deposits derived from the footwall and hanging walls of the basin (Fig. 1-1). Hanging-wall deposits typically comprise the bulk of deposition, both spatially and areally. Axial-river deposits interfinger with piedmont deposits derived from rift-flank uplifts, such as the prominent chain of mountains of the Sandia-Manzanita-Manzano-Los Pinos uplifts along the eastern rift border, and the Ladron Mountains to the southwest. In the Albuquerque area, upper Santa Fe Group deposits are three major lithofacies assemblages that represent distinctive depositional systems. The most abundant (both spatially and volumetrically) are deposits of the Arroyo Ojito Fm, which is a middle Miocene to Pliocene (and possibly earliest Pleistocene) fluvial succession associated with major western tributaries to the axial Rio Grande, such as the Rio Puerco, Rio Jemez/Guadalupe, and Rio San Jose systems (Fig. 1-2). These western rivers joined deposits of the ancestral Rio Grande just east of the present Rio Grande Valley during late Pliocene time. The present-day confluence of the Rio Puerco and Rio Grande is just south of Bernardo, New Mexico, about 55 km south of Isleta, New Mexico

Deposits of the axial-fluvial ancestral Rio Grande are provisionally assigned to the Sierra Ladrones Fm of Machette (1978) as are also locally derived deposits of the eastern margin that interfinger with these extrabasinal fluvial sediments. The Sierra Ladrones Fm has been extended from its type area at the southern edge of the basin, about 65 km to the south, by a number of workers (Hawley, 1978; Lucas et al., 1993; Smith et al., 2001), however, the stratigraphic and lithologic relationship between these deposits and those of the type area is ambiguous. The Sierra Ladrones Fm was defined without a type section and age control is generally poor in the type area. Studies of the type area of the Sierra Ladrones Fm (Connell et al., 2001a) are underway and results of this study should aid in its correlation throughout the basin. **0.1**

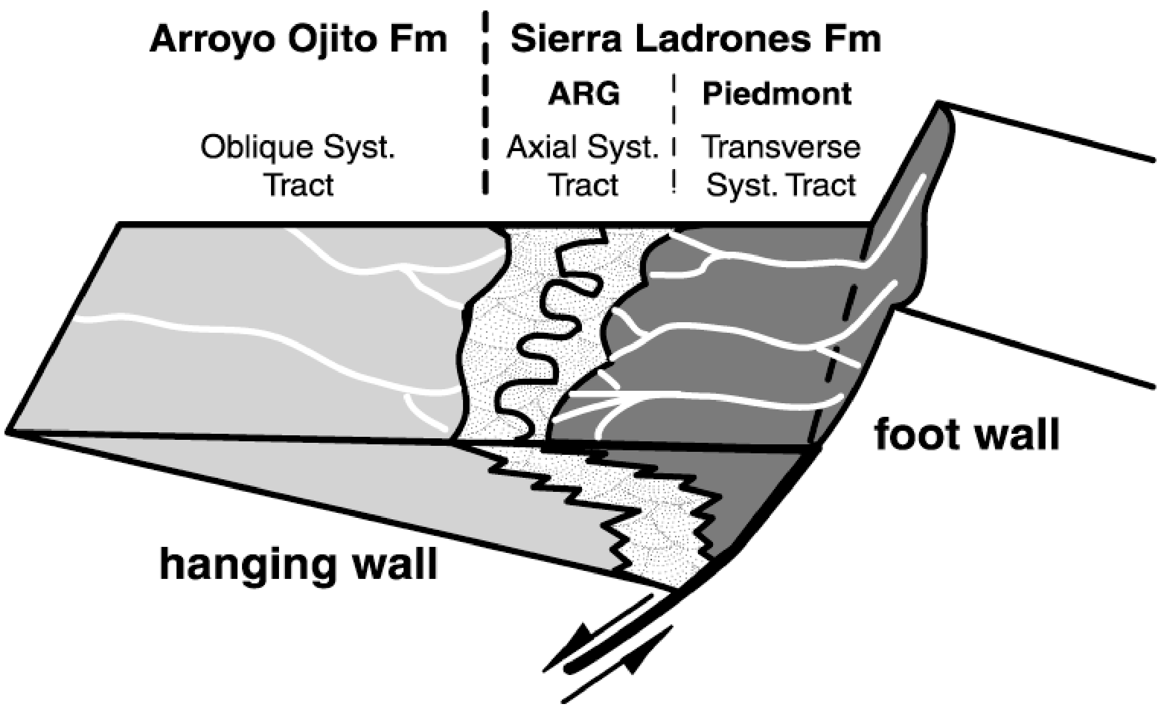

Figure 1-1. Diagram illustrating the distribution of sediments in a half-graben during deposition of the upper Santa Fe sub-Group (modified from Mack and Seager, 1990). This figure depicts the spatial distribution of major fluvial components. The axial-river is bounded on either side by deposits derived from the footwall and hanging wall of the half graben. This diagram represents a “post orogenic” stage of basin development where footwall-derived deposits prograde basinward during times of relative tectonic quiescence (see Blair and Bilodeau, 1988).

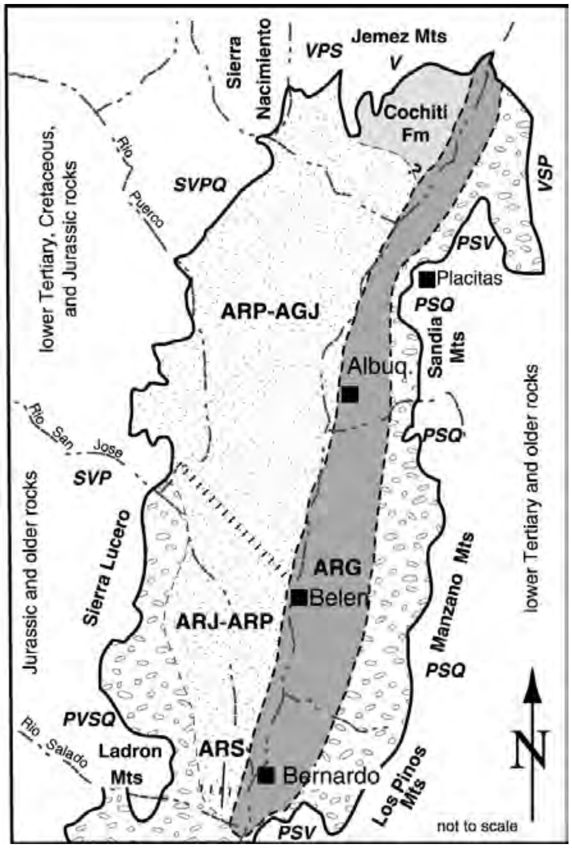

Figure 1-2. Schematic map showing the approximate areal distribution of major lithofacies in Pliocene sediments of the upper Santa Fe Group (modified from Connell et al., 1999; Love et al., 2001). The south-flowing ancestral Rio Grande (ARG) is the axial-fluvial facies (gray shading). The Arroyo Ojito Fm (stippled pattern) represents deposition by a series of large S-SE-flowing tributary drainages originating on the Colorado Plateau, San Juan Basin, Sierra Nacimiento, and western Jemez Mts. These deposits are associated with the ancestral Rio Puerco (ARP), Rio Guadalupe/Jemez (AGJ), ancestral Rio San Jose (ARJ), and ancestral Rio Salado (ARS). These fluvial deposits merge into a single axial-fluvial system at the southern margin of the basin. The conglomerate pattern delineates locally derived deposits from rift-margin uplifts. The Cochiti Fm (light-gray shading) consists of volcanic-bearing sediments shed off the southeast flank of the Jemez Mts. The boundaries among sub-drainages of the Arroyo Ojito Fm are approximate and diagrammatic. Sediment sources to deposits of the Albuquerque Basin include sedimentary and chert (S), volcanic (V), plutonic/metamorphic (P), and metaquartzite (Q).

0.7 Two normal faults with down-to-the-east displacement are exposed in Arroyo Ojito Fm to north on eastern edge of borrow pit. These faults are part of a wider zone included within the down-to-the-west Palace-Pipeline fault zone. This zone may be responsible for the presence of H_2S in groundwater in this area. **0.2**

0.9 Turn right (south) onto highway NM-47 at the Conoco Gas Station and Convenience Store. **0.1**

1.0 The upper Pliocene basaltic centers west of the Rio Grande Valley, include the 2.72-2.79 Ma Isleta volcano at 2:00, and the 4.01 Ma Wind Mesa volcano at 2:00-3:00 ($^{40}Ar/^{39}Ar$ dates summarized in Maldonado et al., 1999). Bluffs to the east are of the Arroyo Ojito Fm, overlain by a thin cap of ancestral Rio Grande deposits of the Sierra Ladrones Fm. The Arroyo Ojito Fm here contains base surge from Isleta volcano and fluvially recycled 2.75 Ma pumice. **0.2**

1.2 Cross arroyo. Fault exposed to your right cuts the Arroyo Ojito Fm and younger alluvium, locally. **0.2**

1.4 Milepost 40 and stop light. Isleta Casino and Resort to your left. **1.0**

2.4 Milepost 39. Arroyo Ojito Fm in road cuts ahead. **0.5**

2.9 Just west of the highway and near the level of the floodplain are exposures of the Arroyo Ojito Fm that contain fluvially recycled pumice dated at 2.68 Ma ($^{40}Ar/^{39}Ar$ date, W.C. McIntosh, unpubl.) and basaltic tephra (cinders) that were probably derived from 2.72-2.79 Ma Isleta volcano (Fig. 1-3). The contact between ancestral Rio Grande and western-fluvial deposits of the Arroyo Ojito Fm is unconformable here. At least 25-68 m of the underlying Arroyo Ojito Fm is missing here. **0.6**

3.5 Merge into left lane. **0.4**

3.9 Turn left (east) at stop light at intersection with NM-47 and SP-60/NM-147. Travel on Pueblo lands is restricted and permission must be obtained prior to entry. All tribal laws and customs must be obeyed on Pueblo lands. Permission to take photographs and samples must be obtained from tribal officials. Please drive slow (<10 MPH) through housing area. **0.4**

4.3 Cross cattle guard and ascend valley border. **0.5**

4.8 Exposures to south (right) are of the Isleta South Powerline stratigraphic section (Fig. 1-4). The uppermost gray beds are pumice-bearing deposits of the ancestral Rio Grande. Pumice pebbles and cobbles are fluvially recycled gravel of the Cerro Toledo Rhyolite (1.6-1.2 Ma) and Bandelier Tuff (1.2 and 1.6 Ma; Izett and Obradovich, 1994), which are early Pleistocene ignimbrite sheets that were emplaced during the development of the Jemez Mountains, about 80 km to the north. These deposits also contain pebbles to small cobbles of black obsidian, which has been geochemically correlated to the 1.43-1.52 Ma Rabbit Mountain obsidian of the Cerro Toledo Rhyolite (Stix et al., 1988). These deposits are part of the axial-fluvial facies of the Sierra Ladrones Fm, which forms a 10-12-km wide axial ribbon that is typically exposed east of the present Rio Grande Valley. Deposits of the ancestral Rio Grande are recognized in drillholes within 2 km west of the front of the Sandia Mountains in the Northeast Heights section of Albuquerque and within 6 km of the Manzanita Mts. **0.3**

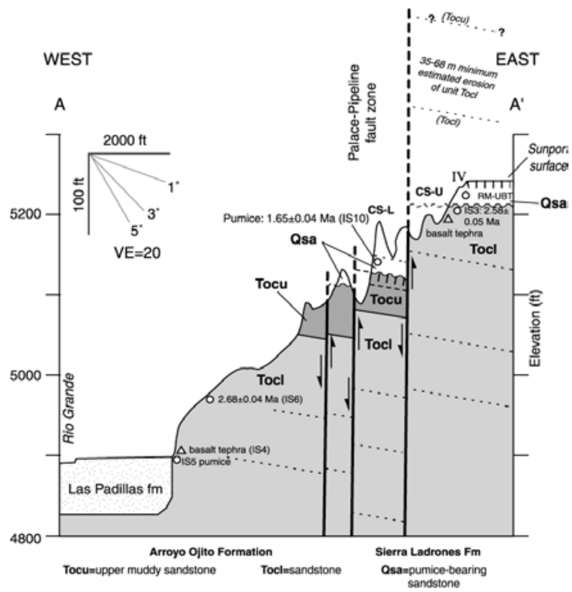

Figure 1-3. Cross Section of eastern bluff of Rio Grande Valley, illustrating age and stratigraphic relationships between the upper Arroyo Ojito Fm (Tocl, Tocu) and Sierra Ladrones Fm (Qsa). Unit Tocu contains abundant mudstone and overlies the sandstone dominated Tocl, which is similar to the Ceja Member of the Arroyo Ojito Fm. The amount of eroded and faulted section on the east (right) side of this cross section are based on estimates of the thickness of the sediment between the 2.68 Ma tephra and the highest preserved part of unit Tocu. Primary tephra indicated by open triangles, recycled pumice denoted by open circles. Hachures denote soils. Roman numerals indicate pedogenic carbonate morphologic stage. Dotted lines denote apparent dip of beds.

5.1 Turn right onto two-track dirt road. **0.2**

5.3 Intersection with two-track road. Continue straight. **0.1**

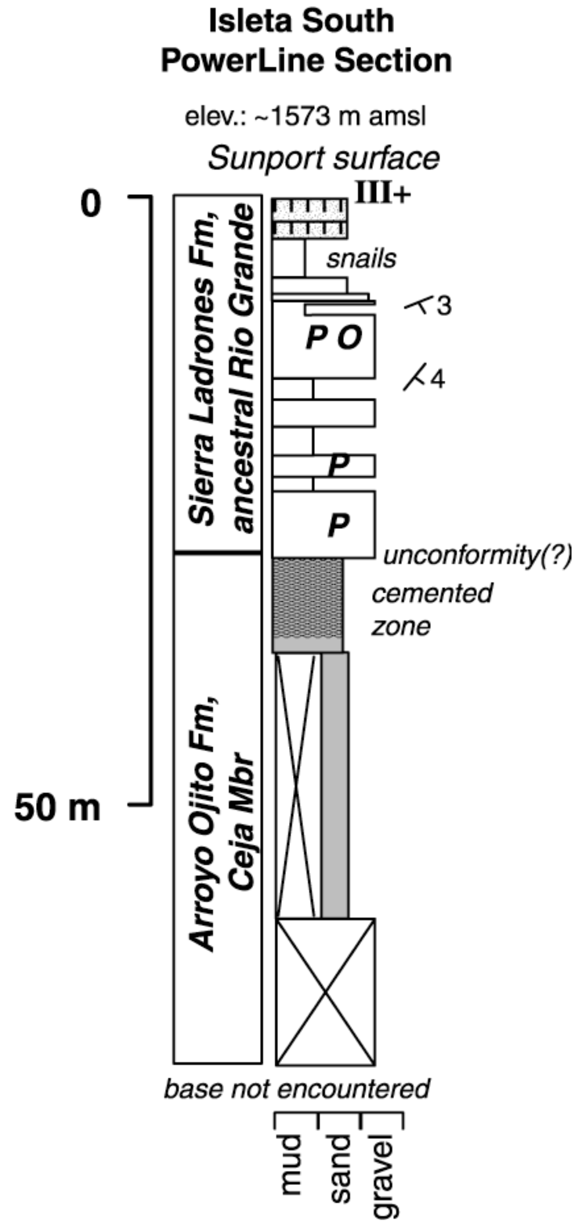

Figure 1-4. Stratigraphic column of the Isleta South Powerline composite section. Deposits of the ancestral Rio Grande contain fluvially recycled pumice (P) from the upper and lower Bandelier Tuff (BT) and Rabbit Mountain obsidian (O) of the Cerro Toledo Rhyolite. Fallout ashes and fluvially recycled pumice of the Cerro Toledo Rhyolite (1.55 Ma) and upper Bandelier Tuff (1.26 Ma, not shown here) are also found near the top of this section. These deposits overlie a moderately cemented and rhizoconcretionary-bearing interval in the Arroyo Ojito Formation, however, no distinctive unconformity is recognized here. Elsewhere, most notably near faults, this contact is unconformable. Bedding dips slightly to the southeast. Hachures denote soils. Roman numerals indicate pedogenic carbonate morphologic stage.

5.4 Ascend onto the Sunport surface, which is faulted by a number of down-to-the-west faults. The Sunport surface is a constructional surface named by Lambert (1968) for the Albuquerque International Airport (a.k.a. Sunport) on the north side of Tijeras Arroyo. This surface is part of the Llano de Manzano of Machette (1985). The Llano de Manzano was considered by Machette (1985) to represent a surface that graded to an alluvial terrace about 92-113 m above the modern Rio Grande. The Llano de Manzano is considerably lower than the Llano de Albuquerque surface to the west, which is about 110-215 m above the modern Rio Grande (Machette, 1985) and represents the upper constructional surface of the Arroyo Ojito Fm. Recent studies (Connell et al., 2000; Maldonado et al., 1999) indicate that the Llano de Manzano is composed of a number of different geomorphic surfaces, rather than a single surface. We use Lambert's (1968) Sunport surface to distinguish it from the slightly younger Llano de Manzano surface complex to the south and east, which contains piedmont deposits that prograde across much of this abandoned fluvial surface. We concur with Machette (1985) on the differences in age and geomorphic position between the Sunport/Llano de Manzano surfaces and the Llano de Albuquerque. Stratigraphic and geomorphic data suggest that the Sunport and Llano de Albuquerque surfaces are about two to five times older than estimated by Machette (1985). During Day 1 and 2 stops, we present evidence that the Sunport and Llano de Manzano surfaces should be considered part of the basin-fill succession, rather than as inset deposits that are stratigraphically disconnected from early depositional events.

The Sunport surface contains a petrocalcic soil that exhibits Stage III+ pedogenic carbonate morphology. Platy structure is locally recognized in natural exposures, but a laminar carbonate horizon is only weakly developed in places. On the basis of pedogenic carbonate development, Machette (1985) originally estimated the age of the Llano de Manzano surface to be about 300 ka. $^{40}Ar/^{39}Ar$ dates and geochemical correlations on tephra inset against and beneath the Sunport surface constrain the development of this constructional fluvial surface to between 1.2-0.7 Ma. **0.1**

5.5 **STOP 1-1.** East edge of Rio Grande Valley and ancestral Rio Grande deposits. Stop near trace of northeast-trending fault with down-to-the-west normal movement. *Isleta 7.5' quadrangle, GPS: NAD 83, UTM Zone 013 S, N: 3,864,180 m; E: 348,495 m.*

Light-gray, loose, sand and pebbly sand exposed just beneath the broad mesa of the Sunport surface are correlated to axial-river deposits of the ancestral Rio Grande, which is provisionally assigned to the Sierra Ladrones Fm. Gravelly intervals contain abundant rounded volcanic and metaquartzite cobbles and pebbles with minor granite. Chert is very sparse. Deposits of the ancestral Rio Grande unconformably overlie deposits of the Arroyo Ojito Fm along the eastern margin of the valley in the field-trip area (Fig. 1-4). Just north of this stop, this contact is slightly angular near a series of north-trending normal faults of the Palace-Pipeline fault zone exposed along the eastern margin of the Rio Grande Valley. Gravel contains scattered, fluvially recycled cobbles and rare boulders of the 1.22 Ma upper Bandelier Tuff. Fallout and fluvially reworked ashes are locally recognized in these deposits and have been dated and geochemically correlated to the 1.2 Ma Bandelier Tuff and the 1.55 Ma Cerro Toledo Rhyolite. Scattered rounded obsidian pebbles are also in this deposit. Some of these have been geochemically correlated to the 1.43-1.52 Ma Rabbit Mountain obsidian (Stix et al., 1988) of the Cerro Toledo Rhyolite. A mudstone containing aquatic and terrestrial gastropods is locally preserved between the loose sand and gravel and overlying fine-to medium-grained eolian sand and petrocalcic soil of the Sunport surface, which exhibits Stage III+ to locally weak Stage IV pedogenic carbonate morphology (Fig. 1-5). Cessation of deposition of the ancestral Rio Grande and development of the Sunport surface is constrained by deposits of the Lomatas Negras fm, which contains a fallout ash of the ~0.66 Ma Lava Creek B (Yellowstone National Park area, Wyoming and Montana). This terrace deposit is topographically lower than the Sunport surface, which contains a 1.26 Ma ash in Tijeras Arroyo. These stratigraphic and geomorphic relationships demonstrate that the Sunport surface developed between 0.7-1.2 Ma. This age is similar to ages of major erosional events reported for the abandonment of the lower La Mesa geomorphic surface and subsequent entrenchment of the Rio Grande in southern New Mexico (Mack et al., 1993, 1996), and for an unconformity between the St. David Fm and overlying alluvium in a tectonically quiescent basin in southeastern Arizona (Smith, 1994). The mudstone at the top of this section has been sampled for paleomagnetic studies by John Geissman (University of New Mexico) to better constrain the timing of development of the Sunport surface.

Figure 1-5. View looking north of Isleta South Powerline Section (Fig. 1-5) from footwall of northeast-trending normal fault. The white band at along the edge of exposures is the Sunport surface, which exhibits Stage III+ to locally weak Stage IV pedogenic carbonate morphology. Dave Love and 1.5-m scale on a snail-bearing mudstone bed preserved on hanging wall of unnamed northeast-trending fault. This mudstone pinches out at the left side of the photograph, near the lone juniper bush.

A major focus of this field trip is to document the timing late-stage filling of the Albuquerque Basin and subsequent entrenchment and development of smaller aggradational events associated with a long-term net decrease in local base level during Quaternary time. During aggradation of the Santa Fe Group, regional base level, as controlled by the Rio Grande, would have been increasing with a concomitant rise in groundwater levels (Fig. 1-6) and local development of phreatic cements. Using conceptual models of sedimentation in extensional basins (see summaries in Leeder and Jackson, 1993; Gawthorpe and Leeder, 2000), axial-fluvial sedimentation would be focussed along active eastern basin margin faults and rift-margin piedmont deposits would be limited to a rather narrow band near the eastern structural margin of the basin. The axial-fluvial system flowed longitudinally, whereas, hanging-wall deposits typically drained obliquely to the axial river. Deposits derived from the footwall flowed in a transverse orientation relative to the axial river. Concomitant deposition and tectonic subsidence along the basin-bounding fault would result in the development of interfingering and wedge-shaped stratal packages.

During entrenchment, the Rio Grande Valley formed in a series of episodic entrenchment and partial aggradation events. This net decline in base level would result in the removal of water in the aquifer. Deposits associated with the development of incised valleys contain somewhat tabular fluvial successions of extrabasinal detritus. The margins of these deposits are bounded by locally derived alluvium from bluffs. These deposits have bounding disconformities along the base and margins. In particular, the margins of such deposits are distinctive in their development of buttress unconformities, which include buried paleobluffs.

A recent model of late-stage basin sedimentation and entrenchment, based upon the work of Machette (1985) and Reneau and Dethier (1996), was proposed by Cole (2001a, b) and Stone (2001a, b). This, termed herein as the Cole-Stone (CS) model for convenience, proposes that widespread aggradation of synrift basin filling ceased during late Pliocene time, by about 2.5 Ma, when the ancestral Rio Grande entrenched into older deposits of the upper Santa Fe Group. They proposed that this late Pliocene entrenchment created the constructional surface of the Llano de Albuquerque, the interfluve between the valleys of the Rio Puerco and Rio Grande.

The CS model agrees with Machette's (1985) interpretation of the early Pleistocene deposits of the Sunport surface representing the oldest inset fluvial terrace deposit in the basin (Stone et al., 2001a,b). This inset relationship is based on inferences regarding the location of the paleo-groundwater table using the spatial and temporal distributions of phreatomagmatic and non-phreatomagmatic eruptions in the region (Cole et al., 2001a), and in a record of repeated entrenchment and aggradation events dating back to early Pliocene time in White Rock Canyon (Reneau and Dethier, 1996) at the margin of the Española and Albuquerque basins, about 80 km to the north (Fig. 1-7).

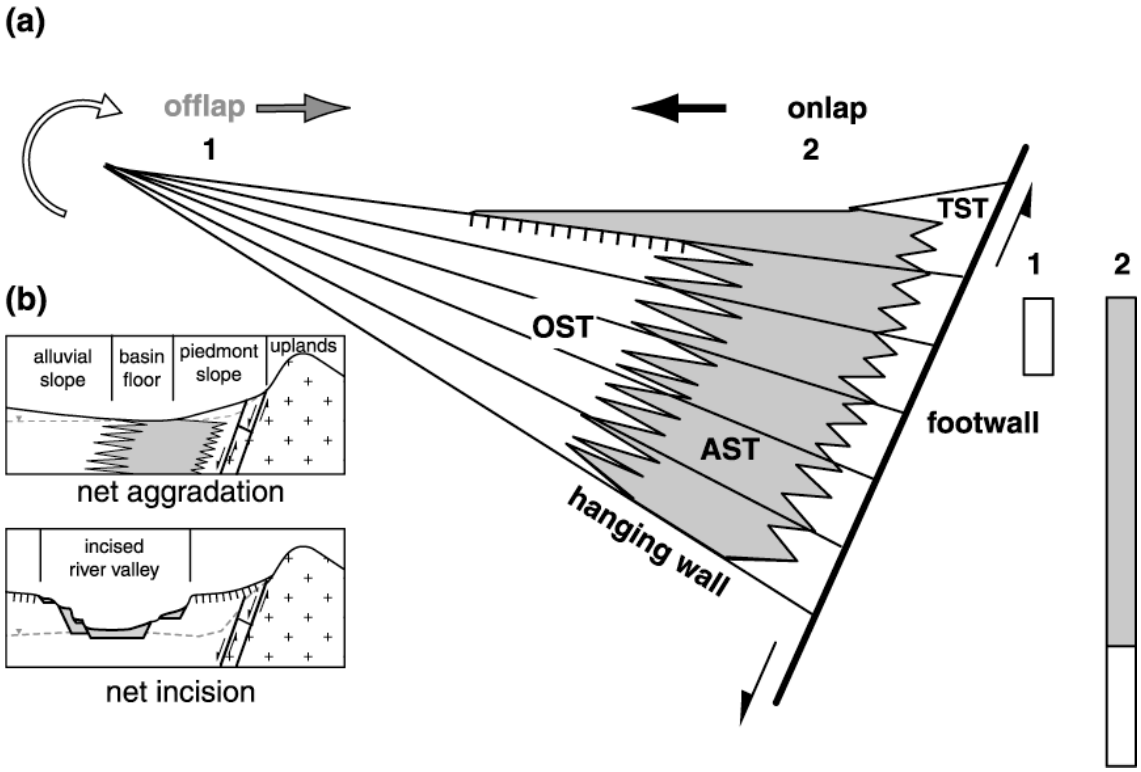

Figure 1-6. Hypothetical stratigraphic relationships of sedimentation in an actively subsiding half-graben basin; intrabasinal faulting is not accounted for in this conceptual model. Intrabasinal faults can create local fault-wedge stratigraphic successions that would have similar stratal geometries to this model; however, deposition would be dominated by eolian and colluvial processes, rather than fluvial. Deposits from the hanging wall (Oblique systems tract; Arroyo Ojito Fm) are volumetrically the largest component of the basin fill. The axial-fluvial system (AST) occupies the central part of the basin and interfingers with OST and locally derived transverse deposits (TST) from the footwall uplift. During times of significant footwall upflift (or basin subsidence), AST and TST will be close to the uplifting footwall block (*cf*. Blair and Bilodeau, 1988). During times of relative tectonic quiescence or slower subsidence rates, TST will onlap onto AST and AST will onlap onto OST (*cf*. Blair and Bilodeau, 1988; Mack and Seager, 1990). Offlap and the development of sediment bypass surfaces on the OST could occur along the hanging-wall border because of the relative lack of space developed in this simple block rotational model. If the OST has been abandoned, then an unconformity between AST and OST will develop during westward onlap of AST onto older OST deposits as AST and TST progrades basinward. This interaction between deposition and subsidence in this simplified fault block results in the development of wedge-shaped stratal units and eastward thickening from the up-dip portion of the hanging wall (1) and the continually subsiding footwall (2). Offlap of the western-fluvial facies could occur as progressive rotation of the hanging wall creates subsidence along the footwall. This would likely result in the development of unconformities along the up-dip portions of the hanging wall. Progradation of axial-river and piedmont deposits could occur during onlap of these deposits onto the hanging wall surface of western-fluvial deposits, resulting in the development of a wedge of axial-river and piedmont deposits near the footwall. The hachured area denotes the development of an unconformity along the boundary between western fluvial deposits (oblique depositional systems tract, OST), and the axial-fluvial systems tract (AST) of the ancestral Rio Grande. Westward onlap of the AST would result in the preservation of an unconformity that would increase in magnitude towards the up-dip portion of the hanging wall. Continued deposition between the AST and the eastern piedmont (transverse systems tract, TST) would occur towards the footwall. B) Hypothetical diagram contrasting deposition in an aggrading basin (i.e., Santa Fe Group time) and episodic deposition during periods of long-term net entrenchment. During net aggradation, base level rises and facies interfinger with one another and deposits tend to have a wedge-shaped geometry and thicken towards the basin-bounding fault. During net entrenchment, base level fall and the upper parts of the basin fill system are drained of water. Episodic aggradational events are recorded as unconformity bounded tabular sedimentary units. Progressive net decline in base level and groundwater levels, which drained out of the upper part of the basin-fill aquifer. Dashed lines represent paleo-base level positions of the axial river.

Basic elements, either explicitly required, or reasonably inferred by the CS model include:

- Development of phreatomagmatic volcanism during aggradational phase of basin because of near surface groundwater.
- Lack of thick or extensive fluvial deposits during a nearly 2 m.y. interval, between about 2.8-0.8 Ma. An exception is along the La Bajada fault zone, which defines the Albuquerque- Española basin boundary.
- Widespread hiatus in deposition indicates that the drainage system had begun to erode into upper Santa Fe Group strata by 2.5 Ma.
- Oldest significant post-phreatomagmatic-basalt fluvial deposits are preserved as a terrace east of the Rio Grande Valley.

The model proposed by Connell et al. (2000; 2001c) and Love et al. (2001) and modified herein, suggests that:

- Basin-fill aggradation occurred during Pliocene and Pleistocene changes in climate. Stratigraphic and subsurface studies (Connell et al., 1998a, 1999; Hawley et al., 1995) note that deposits become markedly coarser near the top of the Santa Fe Group. Incision of the Santa Fe Group occurred between 0.7-1.2 Ma here. This bracketed age is similar to well documented entrenchment events in the Camp Rice Fm (southern New Mexico correlative of the Sierra Ladrones Fm), suggesting that entrenchment was of a regional nature.
- Late-stage deposition of the Santa Fe Group was strongly controlled by the activity and location of intrabasinal faults. This tectonic influence on sedimentation would be increased if sedimentation rates were slow, too.
- Determination "normal" aggradational stratigraphic successions vs. incised fluvial-terrace suites can be difficult, especially in the Albuquerque Basin, where most of the basin-fill and post-basin-fill deposits are lithologically similar. However, stratal geometries and unconformity development can be useful tools in discriminating between these two different depositional processes.

Landscape evolution can be inferred by reconstructing pre-faulting positions, ages, and stratigraphic-geomorphic setting of volcanic deposits, which are useful because they are resistant to erosion and have reasonably predictable surface forms. In particular, topographic inversion of basaltic flows are useful in determining the rate and magnitude of valley entrenchment. However, care must be used when inferring paleo-groundwater conditions because phreatomagmatic eruptions could occur where perched groundwater is present. Volcanic features bury and preserve paleo-topography, however, the relative stability a particular paleo-topographic surface (i.e., stable geomorphic surface, or just a preserved bed in an otherwise conformable stratigraphic sequence) can only be deduced with confidence where indicators of surface stability, such as soils, are present.

Rates of Plio-Pleistocene fluvial deposition are poorly constrained by are on the order of about 100 m/m.y. or less near San Felipe Pueblo (Derrick and Connell, unpubl. data). This rate is significantly slower than rates of deposition of the Popotosa Fm (lower Santa Fe sub-Group), which were near 400 m/m.y. during late Miocene time (Lozinsky, 1994). Thus, rates of deposition slowed by Pliocene time, but deposition was occurring in the basin (see Smith et al., 2001).

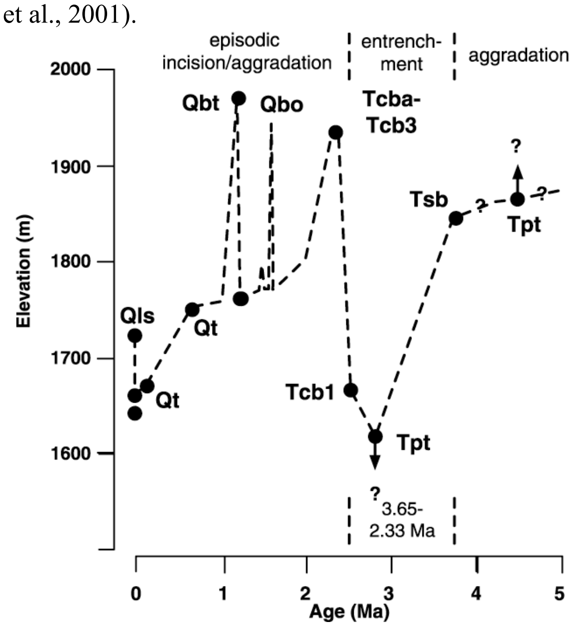

Figure 1-7. Graph depicting timing of major entrenchment and aggradation events in the southern Española Basin at White Rock Canyon (Reneau and Dethier, 1996), about 85 km north of Stop 1-1. The black circles represent dated deposits and the projected position of the ancestral Rio Grande. The dashed line represents projected levels of the ancestral Rio Grande through time in White Rock Canyon, which is on the footwall of the La Bajada fault and has been strongly affected by repeated Plio-Pleistocene volcanic events. Refer to Reneau and Dethier (1996) for discussion of methods and dates. Deep incision occurred between about 3.65-2.33 Ma in White Rock Canyon. This was followed by repeated aggradation and deep incision events throughout late Pliocene and Pleistocene time. Note that the Rio Grande was aggraded to 1970 m)and above its former position prior to ~3 Ma) after 1.2 Ma and before White Rock Canyon was entrenched.

In the Española Basin, Reneau and Dethier (1996) provide excellent evidence for repeated Pliocene and Pleistocene entrenchment events that may be related to climatically and geomorphically (e.g., volcanically and tectonically) driven incision. Their study area is near the structural margin of the Española and Albuquerque basins and lies within a geomorphically, volcanically, and tectonically active area, where deposition and incision were strongly influenced by faulting and episodic damming of the river valley. Here at Isleta, local unconformities are interpreted as the result of concurrent deposition and tilting (Connell et al., 2001b) and local uplift of an intrabasinal horst (Love et al., 2001). We suggest that these apparently disparate controls on sedimentation influence the depositional system in different, but not mutually exclusive, manners. For instance, deposits of the upper Santa Fe Group generally coarsen upwards (see Connell et al., 1998b). The development of these coarsening upwards sequences in the uppermost Santa Fe Group demonstrate increased competence of Plio-Pleistocene rivers and could be associated with an increase in effective moisture during Plio-Pleistocene times; however, coarsening of piedmont deposits could also be attributed to basinward progradation during times of tectonic quiescence (Leeder and Gawthorpe, 1987; Blair and Bilodeau, 1988).

The CS model differs from part of the model of Connell et al. (2000, 2001c), which suggests that spatially time-transgressive sedimentation and development of local stratigraphic tops in the Santa Fe Group occurred into Pleistocene time. This diachroneity of sedimentation is strongly influenced by continued faulting and tilting in the basin during late Pliocene and Pleistocene time, which resulted in the development of unconformities on the up-dip portions of hanging wall blocks and concomitant aggradation near basin depocenters (Connell et al., 2001c). The presence of numerous scarps cutting Pleistocene deposits attests to continued deformation within the basin. This is supported by paleoseismic studies of the basin that indicate Quaternary movement of intrabasinal faults between 2-20 m/m.y. (Machette et al., 1998; Personius et al., 1999; Personius, 1999; Wong et al., *in prep*).

The CS model proposes that the Sunport surface represents the highest inset fluvial terrace deposit in the Albuquerque Basin (Stone et al., 2001a,b). If this interpretation is true, then this rather broad (5-10 km wide) terrace deposit should be inset against older basin fill deposits along the eastern margin. Geologic mapping of the Isleta Reservation to the northeastern edge of the basin (Cather and Connell, 1998; Cather et al., 2001; Connell and Wells, 1999; Maldonado et al., 1999; Smith et al., 2001) does not recognize such a buttress unconformity. Instead deposits of the ancestral Rio Grande system interfinger with deposits shed off of eastern margin uplifts and are buried by progradation of eastern-margin piedmont detritus.

Stratigraphic evidence along strands of the Hubbell Spring fault zone shows early Pleistocene deposits of the ancestral Rio Grande are an integral part of the basin-fill depositional system in an asymmetric or complexly faulted half-graben basin. We argue that deposition of the Santa Fe Group generally ceased when the Rio Grande unequivocally entrenched into older fluvial deposits during early Pleistocene time, forming discontinuous flights of unpaired terrace deposits that border the Rio Grande Valley. Deposition of the Santa Fe group continued locally into the Pleistocene, where smaller non-integrated drainages deposited sediment onto broad abandoned plains and piedmont-slopes of the Llano de Manzano. Intrabasinal faulting and coeval sedimentation resulted in the formation of a number of distinct geomorphic surfaces on local uplifted fault blocks, resulting in the development of a number of local tops of the basin fill. South of the Española Basin, many workers generally consider the Santa Fe Group basin-fill system to have aggraded until early Pleistocene time, when the Rio Grande Valley formed (Smith et al., 2001; Connell and Wells, 1999; Connell et al., 1998; Maldonado et al., 1999; Hawley et al., 1995).

Our interpretation of the stratigraphy has the distinct advantage of distinguishing basin-fill from younger entrenched deposits with less ambiguity that the C-S model. The determination of hiatal surfaces along the eastern margin of the basin would be difficult, mainly because of the influence of faulting on sedimentation and because age control is generally lacking for much of the sedimentary succession. Along the eastern margin of the Albuquerque Basin, between Cochiti Pueblo and Hell Canyon Wash, exposures and drillhole data indicate the presence of conformable stratigraphic successions of Plio-Pleistocene age. The presence of soils locally marks unconformities or hiatuses in the section. However, these would be rather difficult to extend across a tectonically active basin. By picking a broader set of criteria for basin-fill aggradation, these ambiguities are diminished, especially in areas with little subsurface control or exposure.

Problems with reconciling these two models is important because the CS model requires the presence of a rather profound unconformity beneath the eastern side of the basin to accommodate their Sunport terrace. The removal of over 70 m of Pliocene sediment would create a previously unrecognized major hydrogeologic discontinuity in Albuquerque's aquifer. The presence of such a discontinuity would also significantly revise estimates of the amount of drawdown required for irreversible subsidence, as was recently estimated by Haneberg (1999).

Stratigraphic evidence amassed by Sean Connell and Dave Love since 1997, indicates the presence of an intraformational unconformity between early Pleistocene deposits of the ancestral Rio Grande and the Arroyo Ojito Formation on Isleta Pueblo and Tijeras Arroyo. To the south, the unconformity between the Sierra Ladrones and Arroyo Ojito formations diminishes. A major unconformity within the ancestral Rio Grande is recognized locally between deposits containing the Cerro Toledo ash and overlying coarse gravels of the Rio Grande north of the mouth of Hell Canyon Wash (see Day 2). This unconformity is related to local faulting and migration of the ancestral Rio Grande. This unconformity may die out to the east. Such unconformable relationships are recognized in a few areas, and thus may not be applicable in a regionally consistent manner without precise age constraints.

Turn vehicles around and drive towards SP-60. **0.3**

5.8 Hard right onto east-trending two-track road, which rejoins SP-60 heading east. **0.2**

6.0 Turn east onto SP-60. **0.4**

6.4 Ascend scarp of Palace-Pipeline fault, which cuts deposits of the ancestral Rio Grande. The trace of the Palace-Pipeline fault, which is about 19-m high here, is named for its proximity to the old Isleta Gaming Palace and a gas pipeline. This fault roughly corresponds with the location of the Rio Grande fault of Russell and Snelson (1994) south of Albuquerque. Russell and Snelson (1994) proposed the Rio Grande fault as a prominent intrabasinal normal fault that cut off the range-bounding normal faults of the Manzanita and Sandia Mountains after late Miocene or Pliocene time (Russell and Snelson, 1994). Russell and Snelson (1994) projected their Rio Grande fault northward and beneath the inner valley. Their Rio Grande fault was projected beneath downtown Albuquerque, New Mexico, and extended north to Bernalillo, New Mexico. Russell and Snelson (1994) proposed this projection on the basis of drillhole data on the Isleta Reservation and on two partial lines of seismic reflection data and drillhole data that demonstrate the presence of a major intrabasinal graben beneath the present Rio Grande Valley (Fig. 1-8). Gravity data (Grauch et al., 1999) and geologic studies of the basin (Maldonado et al., 1999; Connell and Wells, 1999; Connell et al., 1998) suggest that this intrabasinal structure is likely an older feature that probably trended to the northwest rather than to the north (Maldonado et al., 1999). The presence of thick early Pleistocene deposits on the footwall of the Rio Grande fault does not support the presence of significant Pleistocene activity along this fault. However, the presence of an unconformity and intrabasinal faults exposed along the eastern margin of the Rio Grande Valley at Stop 1 does support significant late(?) Pliocene tectonism near the present day valley. **0.2**

6.6 Cross cattle guard and descend broad east-tilted footwall block of Palace-Pipeline fault. This block generally slopes towards west-facing scarps of splays between the Palace-Pipeline fault and the McCormick Ranch fault zone. The TransOcean Isleta #1 well, about 1.8 km to the north, was drilled to 3163 m below land surface (bls) and encountered 1563 m of Santa Fe Group basin fill (Fig. 1-8; Lozinsky, 1994). The Shell Isleta #2 well, drilled just west of Isleta volcano, was drilled to 6482 m bls and encountered 4407 m of Santa Fe Group strata (Lozinsky, 1994). **0.6**

7.2 Borrow pit on north side of road exposed strongly developed petrocalcic soil of the Sunport surface, which exhibits Stage III+ carbonate morphology. This soil is overlain by eolian sand that contains weakly developed buried soils (Fig. 1-9). **0.3**

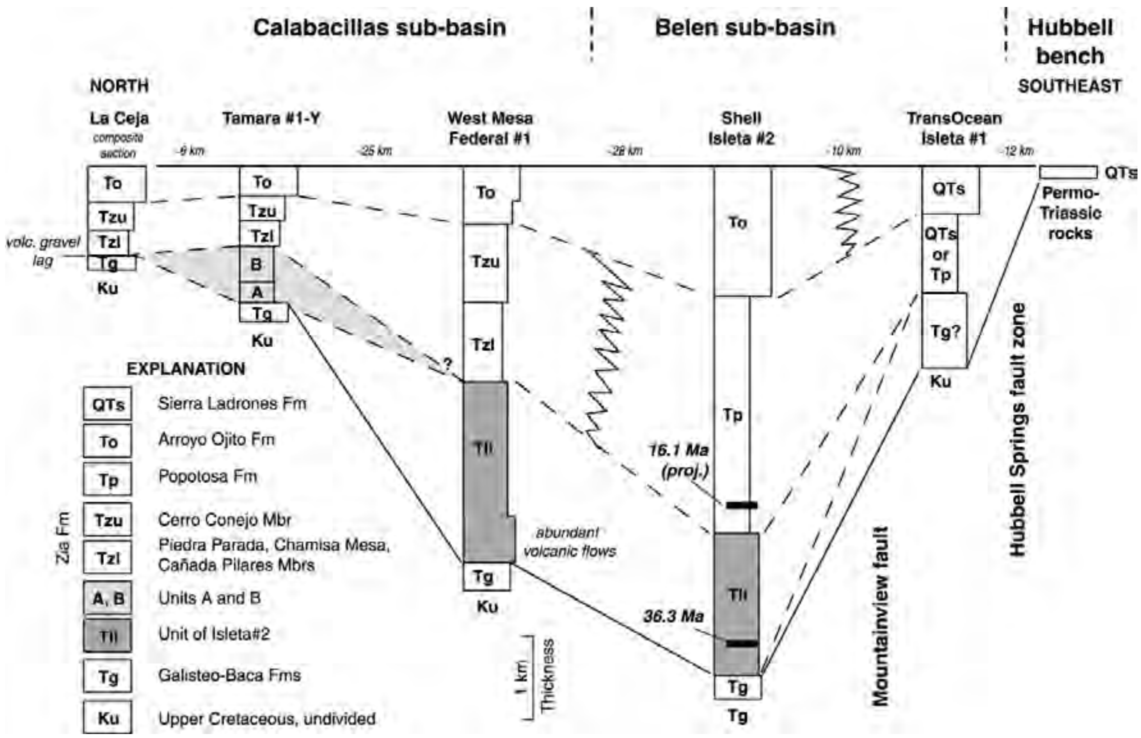

Figure 1-8. Stratigraphic fence of Cenozoic deposits in the Calabacillas and northern Belen sub-basins. Data from oil test wells (Lozinsky, 1988, 1994; Connell et al., 1999; Tedford and Barghoorn, 1999; Maldonado et al., 1999; Black and Hiss, 1974). From Connell, Koning, and Derrick (2001).

Figure 1-9. Photograph of petrocalcic soil of the Sunport surface, exhibiting Stage III+ pedogenic carbonate morphology overlain by fine- to medium-grained sand of eolian origin. The overlying eolian sand commonly forms an extensive cover over the carbonate of the Sunport surface. Scale is 1.5 m.

7.5 Cross west-facing scarp of fault cutting ancestral Rio Grande deposits that are overlain by a thin veneer of eolian sand. **0.4**

7.9 Cross west-facing scarp of fault cutting ancestral Rio Grande deposits. Descend east-sloping footwall dip slope. **0.5**

8.4 Cross west-facing scarp of fault cutting ancestral Rio Grande deposits. **0.1**

8.5 Descend into unnamed northern tributary valley to Hell Canyon Wash. Prominent bench ahead just west of the front of the Manzanita Mountains is the northern Hubbell bench, which exposes Permo-Triassic rocks and thin well cemented conglomerate and sandstone of older Santa Fe Group deposits. **0.4**

8.9 Tributary valley of Hell Canyon Wash. **0.3**

9.2 On east-facing scarp of down-to-the-east McCormick Ranch fault. **0.3**

9.5 Near western pinchout of piedmont deposits, which overlie ancestral Rio Grande deposits here. Note that gravel is typically subrounded to angular and composed of limestone, quartzite, schist, and granite. **0.2**

9.7 Road is on terrace of Memorial Draw, a tributary to Hell Canyon Wash. It is named for a small memorial erected by the parents of one of several Navy fliers killed in a crash here in 1946. This terrace is buried by Holocene alluvium upstream and was removed by erosion downstream. Higher terraces are cut by strands of the Hubbell Spring fault zone. **0.6**

10.3 Cross gas pipeline. **0.7**

11.0 Cross cattle guard. Large cottonwood at 11:00 is Hubbell Spring, on the eastern strand of the Hubbell Spring fault zone. The

Hubbell Spring fault zone is subdivided into three major strands (Maldonado et al., 1999; Personius et al., 1999). The eastern strand forms the embayed escarpment of the Hubbell bench and juxtaposes reddish-brown Permo-Triassic sandstone and mudstone against deposits of the Santa Fe Group. The central and western strands of the Hubbell Spring fault zone commonly have prominent scarps and are geomorphically young and have rather distinct linear traces. Note the large Cottonwood at 1:00, which is on the central strand of Hubbell Spring fault zone and is the location of Stop 2-2. **0.4**

11.4 Pass intersection with road to Hubbell Spring to left. **0.6**

12.0 Pull off road. **STOP 1-2. Hubbell Spring fault zone.** *Hubbell Spring 7.5' quadrangle, GPS: NAD 83, UTM Zone 013 S, N: 3,865,030 m; E: 358,090 m.*

At this stop we examine some spring deposits on the footwall of the central strand of Hubbell Spring fault zone, tectonic controls on groundwater and sedimentation, and paleoseismicity of the Hubbell Spring fault zone. Wells on south side of road encounter water at about 6 m below land surface. A deeper groundwater monitoring well (28D), drilled about 25 m north of the road, exhibits decreasing water levels with depth, indicating that this is a groundwater recharge area associated with this fault (Fig. 1-10). The high level of groundwater is also indicated by the presence of the large Cottonwood on the hanging wall of this fault strand. There are two prominent springs associated with this strand of the Hubbell Spring fault zone. Hubbell Spring and Ojo de la Cabra (Goat Spring) are about 2.5 km north and south of this stop. Deposits encountered in well 28D indicate that fluvial deposits of the ancestral Rio Grande interfinger with limestone-bearing piedmont deposits derived from the front of the Manzanita Mountains. The presence of fluvial deposits of the ancestral Rio Grande is supported by observations of similar strata exposed in a trench on the footwall of the central Hubbell Spring fault zone to the north (Personius et al., 2000). This well bottomed in limestone that we interpret to represent conglomerate from the piedmont member of the Sierra Ladrones Fm, rather than from the Madera Group, which would be much lower in the stratigraphic section, and below Paleogene-Triassic red beds, which were not encountered in cuttings sampled from this well. If this limestone interval is the Pennsylvanian Madera limestone, it then requires that about 580 m of Permo-Triassic rocks (estimated from eastern slope of Sandia Mountains; Ferguson, 1996) be missing from the drillhole section. This interpretation would suggest the presence of reverse faulting, probably of Laramide age; however, the presence of Permo-Triassic strata on the footwall of the eastern strand of the Hubbell Spring fault zone does not support this interpretation. Also, the presence of dark-gray Paleocene mudstone in wells on the Isleta-Sandia National Labs boundary (Thomas et al., 1995) indicate fine-grained, low energy deposition during early Cenozoic time. Another possible explanation is that the limestone was deposited by streams draining the western front of the Manzanita Mts. Pennsylvanian limestone is well exposed along the eastern basin margin and is also exposed on the footwall of the eastern Hubbell Spring fault on the lands of the Sandia National Laboratories and Kirtland Air Force Base, which abuts the northern boundary of the Isleta Reservation.

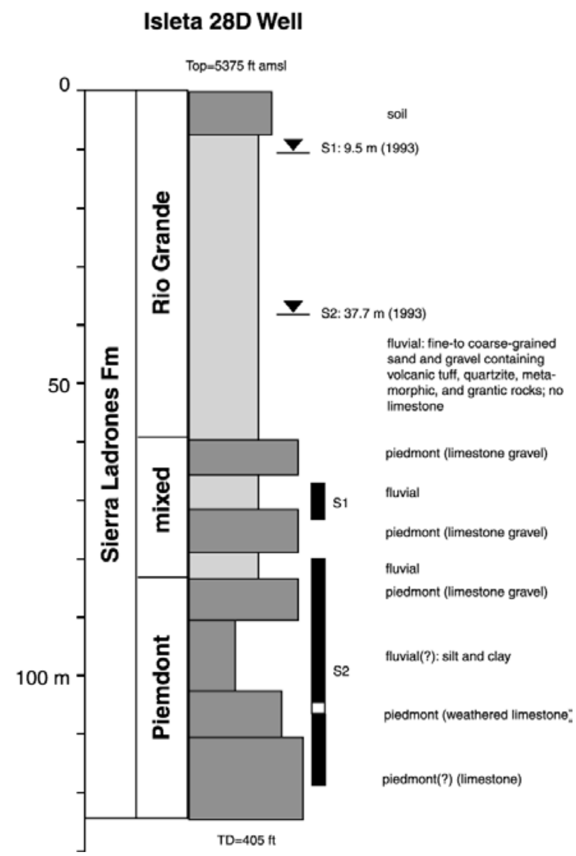

Figure 1-10. Stratigraphic column of monitoring well MW28D drillhole and stratigraphic interpretations. The black rectangles depict upper (S1) and lower (S2) screens, which have associated water levels of 9.5 m and 37.7 m bls, respectively.

The presence of ancestral Rio Grande deposits less than 2 km west of the Hubbell bench, which is underlain Permo-Triassic red beds indicates that the Rio Grande was at least 12 km east of its present course. Geologic mapping of the region and stratigraphic studies within the two largest tributary canyons to the Rio Grande, Hell Canyon Wash and Tijeras Arroyo, do not support the presence of a buttress unconformity or paleobluff line between early Pleistocene deposits of the ancestral Rio Grande and eastern-margin piedmont deposits. Instead the stratigraphic relationships in these arroyos suggests an interfingering relationship between the axial-fluvial and transverse piedmont system, as recognized in elsewhere in Plio-Pleistocene basin-fill systems, such as the Palomas Fm of southern New Mexico (Mack and Seager, 1990; Gile et al., 1981). In contrast, the CS model implies the presence of a major stratal discontinuity along the eastern basin margin that would juxtapose early Pleistocene deposits against older (Pliocene) strata. Intrabasinal normal faults could act as this unconformable boundary; however, the presence of ancestral Rio Grande deposits across traces of the central Hubbell Spring fault suggests that this fault strand does not exert enough control over the eastern limit of the axial-fluvial system during late Pliocene(?) time. The stratigraphic relationship in MW28D indicates structural control on the stratigraphic position of ancestral Rio Grande deposits, however, the relative lack of reworked extrabasinal detritus in the piedmont section suggests that faulting did not produce a significant escarpment during Plio-Pleistocene deposition.

One of the younger strands of the Hubbell Spring fault zone was studied by Steve Personius of the U.S. Geological Survey in the fall of 1997 (Personius et al., 2000). A trench was excavated on the steepest, most youthful looking fault scarp near the northern end of this fault zone, about 2 km to the north of this stop (Figs. 1-11 and 1-12). Seven stratigraphic units were described in the excavation. These deposits consist of a lower light-gray fluvial deposit (unit 1) that is overlain by locally derived alluvial deposits (unit 2). These are overlain by a series of eolian and alluvial deposits (3-8). The lowest deposit was recognized as fluvial and correlated with the early Pleistocene Santa Fe Group (Personius et al., 2000), however, provenance of this deposit was not indicated. These deposits contain rounded volcanic and metaquartzite pebbles having a strong affinity to ancestral Rio Grande deposits, which were also recognized on the footwall of this strand of the Hubbell Spring fault at monitoring well MW28D. Soils described on alluvium on the far-field part of the footwall block indicate the development of Stage IV pedogenic carbonate morphology (Personius et al., 2000). The younger eolian sediments of units 4, 5, and 7 are composed of eolian sand and were dated using thermoluminescence (TL) and infra-red stimulated luminescence (IRSL) methods at 52-60 ka, 27-34 ka, and 11-14 ka , respectively (Personius et al., 2000). Unit 5 is offset by the fault and unit 9 buries the fault. Stratigraphic relationships of units 6-8 relative to the fault are not apparent. The older alluvial deposits were dated using Uranium-series disequilibrium methods and yielded ages ranging from 70-244 ka, with the best date of 92±7 ka (Personius et al., 2000) for a trench containing the Stage IV carbonate soil on the footwall. Interpretation of the fault-rupture history for this strand of the Hubbell Spring fault indicate three episodes of movement during late Pleistocene time (Fig. 1-13). The latest event is estimated to have occurred during latest Pleistocene time.

Slip-rate estimates for basin-margin faults that cut across the seismogenic crust are on the order of 0.02-0.2 mm/yr (20-200 m/m.y.). Slip-rate estimates for intrabasinal faults in the Albuquerque area are on the order of 0.004-0.05 mm/yr (4-50 m/m.y.) (Personius, 1999). Estimated recurrence intervals for basin-margin and intrabasinal faults are 10-50 ka and 10-200 ka, respectively (Personius, 1999). Thus, faulting of the 0.7-1.2 Ma Sunport surface would result in between 3-60 m of movement across intrabasinal faults.

East and southeast of the water tank at Stop 1-2 are low hills interpreted to be former spring mounds. At the surface of these mounds and in interbedded alluvial and eolian deposits are layers of fragmented plates and nodules of micritic calcium-carbonate sandstone. One such spring mound is exposed along the footwall of the Hubbell Spring fault on the north side of the road (Fig. 1-14). This exposure has a sharp base with underlying uncemented sand. Other exposures of spring deposits have sharp bases and large masses of oxidized and hydrated iron and manganese stain deposits red, orange, yellow, and black. In reduced environments, reduced iron, and stains sediments green, gray, and black. These deposits commonly contain root molds or casts and represent precipitation in poorly drained sediment, such as those along springs. These features differ from more common pedogenic features that are typical of the well-drained semi-arid soils. Features common in well-drained, semi-arid soils include distinctive horizonization, and a gradual downward decrease in calcium-carbonate cement and soil structure. Exceptions to these morphologic differences can occur across major textural boundaries. Also, spring and pedogenic carbonates may be reworked or superimposed along fault zones or major escarpments, such as along the edges of the Cañada Colorada surface to the east. (Fig. 1-15).

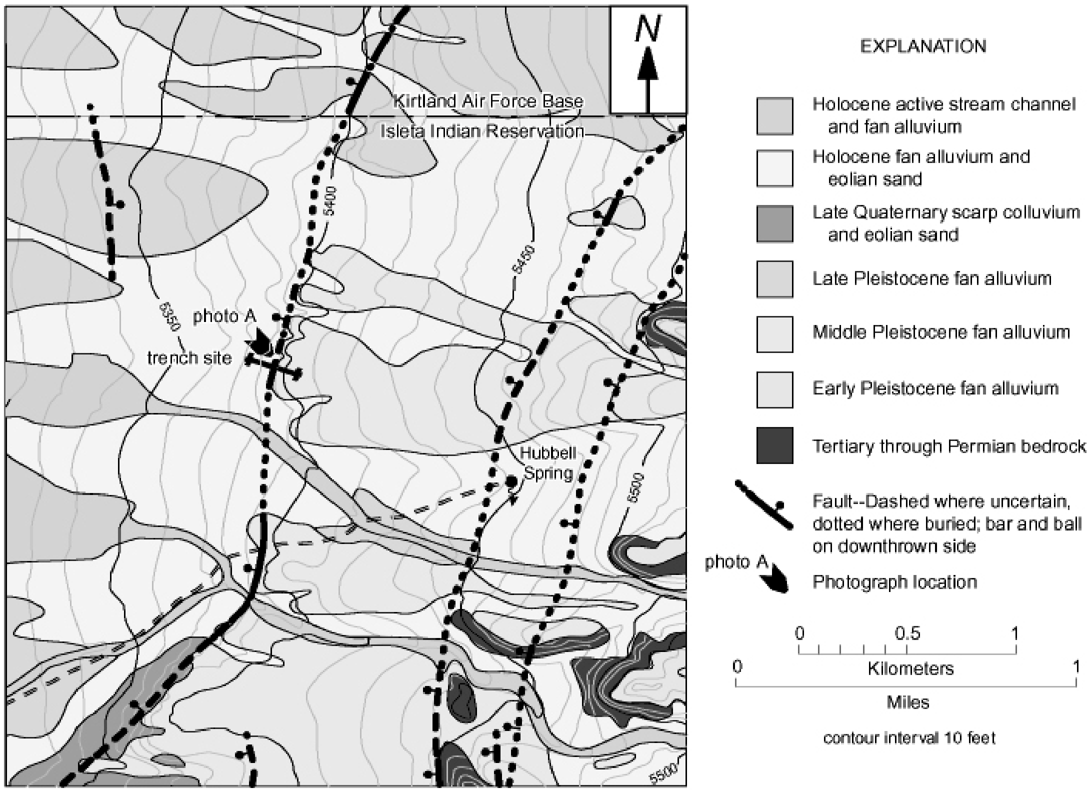

Surficial geologic map of Hubbell Spring trench site and vicinity; modified from Love and others (1996). See Quaternary fault map for location.

Figure 1-11. Geologic map of trench site area, northern Hubbell Spring fault zone (Personius et al., 2000). The trench site is about 2 km north of stop 1-2.

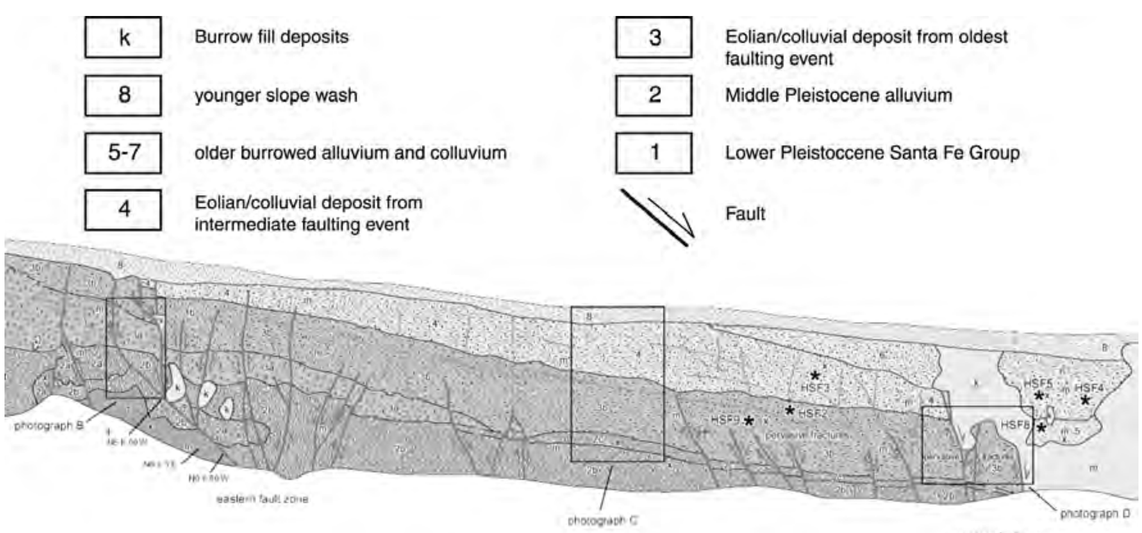

Figure 1-12. Part of paleoseismic trench across central strand of the Hubbell Spring fault zone (Personius et al., 2000), illustrating displacements of units 1-4.

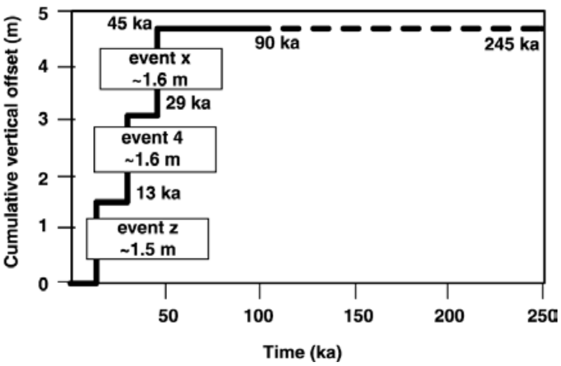

Figure 1-13. Time-displacement diagram for the Hubbell Spring fault zone (Personius, 1999). The two oldest dates are U-series ages on calcic soil rinds developed on alluvial gravels that predate the oldest event. The younger dates are based on thermoluminescence (TL) ages on sandy colluvial/eolian deposits that are interpreted to closely post-date surface-faulting events.

Figure 1-14. Photograph of spring deposits on footwall of central strand of the Hubbell Spring fault zone. Note sharp base and top of this <10-cm thick deposit of micritic calcium-carbonate cemented sandstone.

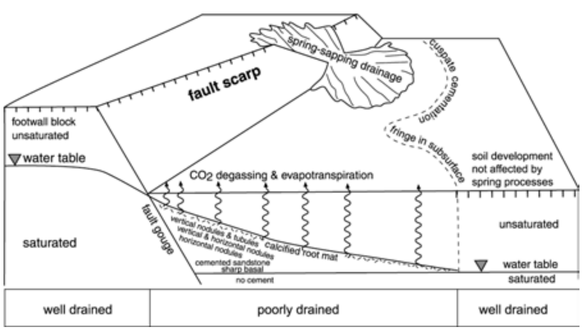

Figure 1-15. Conceptual diagram of spring-deposit formation and the spatial and hydrologic relationship to soil development in fault blocks with identical alluvium on both sides. As calcium-carbonate saturated water drains from the uplifted block to the downthrown block, calcium-carbonate is precipitated in a narrow wedge (Love and Whitworth, 2001). Hachures indicate soils.

Continue driving east on SP-60. **1.0**

13.0 Whaleback feature at 9:00 is deformed piedmont conglomerate and underlying Permian sandstone on footwall of eastern strand of the Hubbell Spring fault zone (Fig. 1-16). The northern Hubbell bench is deeply embayed by streams originating from the Manzanita Mountains. The escarpment formed by the central Hubbell Spring fault has been eroded to the east by as much as 640 m by Cañada Colorada, resulting in the development of a sinuosity value (Bull, 1984) of 3.7 (Karlstrom et al., 1997). **0.3**

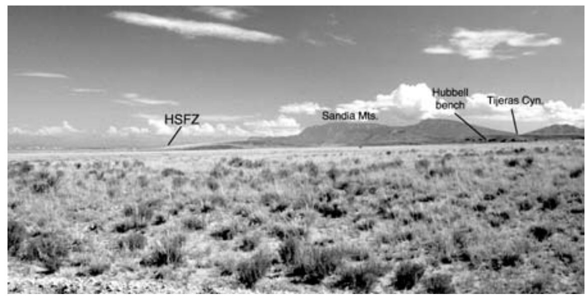

Figure 1-16. Photograph look north of trace of central strand of Hubbell Spring fault zone, marked by low hill in the middle ground. Sandia Mountains in distance.

13.3 Cross cattle guard. Road to southeast is SP-603. Continue straight and ascend deposits of colluvium, alluvium, and spring deposits along edge of northern Hubbell bench. **0.3**

13.6 Contact between east-tilted Yeso Fm (Permian) overlain by 15-20 m of well-cemented, clast- and matrix-supported, limestone-bearing conglomerate (Fig. 1-17). This conglomerate is well cemented by fine-grained sparry calcite. The gorge to the south is Hell Canyon Wash. Note older surfaces above piedmont-plain south of Hell Canyon. **0.3**

13.9 Limestone cobbles and boulders next to road are completely covered with thick calcium-carbonate. Ascend onto the Cañada Colorada surface, a gently west-sloping constructional surface of probable Pliocene age formed on a wedge of well-cemented conglomerate and sandstone derived from the front of the Manzanita Mountains. White pebble gravel on road to the east is composed mostly of hard petrocalcic peds of the Cañada Colorada soil. Mouth of Hell Canyon at 12:00. Mouth of Cañada Colorada at 10:00. Note that the banded rocks (limestone of the Pennsylvanian Madera Group), which form the topographic divide of the Manzanita Mountains, are dropped down-to-the-west by a series of faults at 10:00. Buildings to the north are research facilities of Sandia National Laboratories. The northern Manzanita Mountains are deeply embayed and have a range front sinuosity of about 6. The shiny metallic structures on the lone hill, just west of the mountain front, are the Starfire Optical Observatory, built as part of the Strategic Defense Initiative of the 1980s. This structure sits on an inselberg of Proterozoic schist on the footwall of the "range-bounding" Coyote fault. The range is deeply embayed and the Coyote fault only marks the range-front at the toes of major spur ridges. This degree of embayment suggests that the Manzanita Mountains are tectonically inactive. Scattered inliers of Pennsylvanian limestone are locally exposed on the piedmont-slope between the Coyote and Tijeras fault zones.

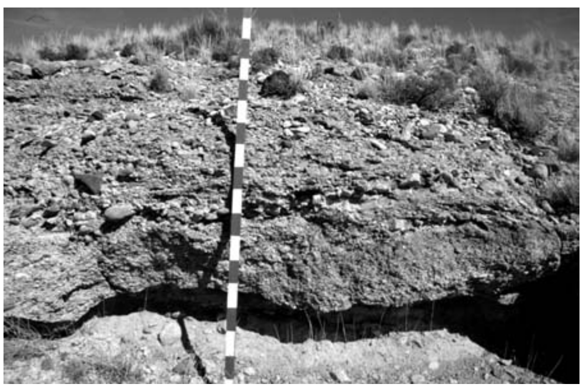

Figure 1-17. Photograph of well cemented, clast-supported, locally derived piedmont deposits exposed on the northern Hubbell bench. Gravel is mostly rounded limestone and reddish-brown sandstone with minor granitic and metamorphic clasts.

The Tijeras fault is a northeast-trending fault that has a long and complicated history of recurrent movement ranging from Quaternary to Proterozoic in age (Connolly et al., 1982; Kelson et al., 1999; Abbott et al., 1995). The southwest projection of this feature into the Albuquerque Basin nearly coincides with the zone of Plio-Pleistocene basalt fields on the Llano de Albuquerque and generally corresponds to a shift in regional patterns of stratal tilt. These features were used as evidence to suggest that the Tijeras fault zone continued across the Albuquerque Basin as an accommodation zone (Russell and Snelson, 1994). The Tijeras accommodation zone was considered to represent a zone of weakness that resulted in accommodating stratal tilts of the Calabacillas and Belen sub-basins (northern Albuquerque and Belen basins) in a scissors fault manner. Geologic mapping and aeromagnetic studies (Maldonado et al., 1999; Grauch, 2001) indicate that the Tijeras fault zone appears to merge into, and probably connects with or is cut by, faults of the Hubbell Spring fault zone, instead of continuing across the basin as a discrete, sub-basin bounding structure as suggested by Russell and Snelson (1994). The east-tilted dip-slope of the Sandia Mountains are clearly visible to the north. **0.5**

14.4 Note lower, inset surfaces associated with Cañada Colorada to the north. **0.6**

15.0 Gate to north pasture. Junipers are present at this elevation (~5680 ft). **0.6**

15.6 Turn right (south) onto two-track road towards windmill at 11:00. **0.4**

16.0 Bottom of Memorial Draw. **0.2**

16.2 **STOP 1-3. Northern Hubbell bench.** Park near windmill. *Mount Washington 7.5' quadrangle, GPS: NAD 83, UTM Zone 013 S, N: 3,862,250 m; E: 363,665 m.*

At this stop, we compare the deep dissection of the northern Hubbell bench and the broad, feature-poor landscape of the Llano de Manzano. Piedmont deposits of the eastern margin are locally derived and form typical proximal, medial, and distal facies. They commonly consist of subangular limestone, metamorphic, sandstone, and granitic pebbles and cobbles; boulders are common near the mountain front. Eolian sand sheets are common on medial and distal portions of the piedmont. The eastern margin of the basin can be divided into three geomorphic domains: 1) incised axial and tributary river valley; 2) weakly dissected piedmont; 3) deeply dissected piedmont (Fig. 1-18 and 1-19).

The front of the Manzanita Mts is deeply embayed and contains exposed or shallowly buried Pennsylvanian-Triassic rocks on the hanging wall of the range-bounding fault. Pleistocene-age fault scarps are recognized on the intrabasinal Hubbell Spring fault zone. In contrast, the front of the northern Manzano Mts is rather linear and contains Pleistocene fault scarps near the mountain front. South of the northern Hubbell bench, a well drilled about 3.7 km west of the mountain front on the Bosque Peak quadrangle (Bonita Land and Livestock well, Karlstrom et al., 1999) encountered deposits of the Santa Fe Group to at least 186 m bls. Cuttings from this well indicated conglomeratic deposits extend to about 64 m and overlie muddy sandstone to the bottom of the hole.

The broad west-sloping piedmont is the Cañada Colorada surface, which is preserved on the footwall of the eastern Hubbell Spring fault zone. This surface lies within the deeply dissected piedmont domain. I contrast the Llano de Manzano is only slightly dissected and rift-border drainages deposit sediment onto the abandoned piedmont slope and basin-plain of this geomorphic surface complex (Fig. 1-19). A Pliocene age for the Cañada Colorada surface is suggested by geomorphic criterion: it lies about 52 m above the plain of the Llano de Manzano, is deeply embayed, having a range-front sinuosity value of 3.7, and contains a 2 m thick petrocalcic soil that has affinities to Stage V carbonate morphologic development. Soils in a pit (MW10S) about 30 m north of the windmill are more than 2.2 m in thickness and contain Stage III+ to V(?) pedogenic carbonate morphology (Fig. 1-20). Another trench excavated about 2.7 km to the east (MW15) exhibits a similar soil that is over 2.1 m thick.

Driller's notes from the nearby windmill (RWP-27, range water project) indicate the presence of about 20 m of conglomerate over reddish-brown shale to 91 m below land surface. The upper 20 m is correlative to the older, well cemented piedmont conglomerate and sandstone of the Santa Fe Group that forms a thin cap on the northern Hubbell bench. These deposits are well cemented and are Pliocene, and perhaps Miocene in age. The age of this deposit is not well constrained but is older than the early Pleistocene deposits on the hanging walls of the central and eastern Hubbell Spring fault zone.

Longitudinal profiles of paleo-stream positions on the Cañada Colorada surface tend to diverge towards the basin. This basinward divergence results in the development of flights of inset deposits and suggests that streams are progressively entrenching into the northern Hubbell bench, presumably in response to base-level adjustments imposed by activity on the many downstream strands of the Hubbell Spring fault zone.

In contrast, the Llano de Manzano is a low-relief basin-floor and piedmont slope with little constructional topography, except locally along intrabasinal fault scarps. With the exception of Tijeras, Hell Canyon, and Abo Arroyos, the largest drainages of the eastern margin, all other drainages of the mountain front are not integrated with the Rio Grande, but instead have their base level set by the Llano de Manzano (Fig. 1-21). Thus, deposits of these smaller, non-integrated drainages are nearly indistinguishable from the underlying strata. The upper part of the basin-fill succession does contain soils that could be used to discriminate the boundary between basin-fill and younger deposition; however, exposures are not sufficient to do this on a regional basis. Also the selection of stratigraphically lower soils to define the end of Santa Fe Group deposition posses considerable problems in correlation across the basin. Much of the deposition on this broad basin-plain/piedmont-slope occurred after development of the Rio Grande Valley. Late Pleistocene and Holocene deposits can be differentiated on the Llano de Manzano by the relatively weak soil development and incision into older deposits that have more strongly developed soils.

Intrabasinal faulting also creates local conditions where suites of inset terrace deposits on the footwall become part of a soil-bounded aggradational succession on the hanging wall. From a practical standpoint, inclusion of deposits with the stratigraphically highest, moderately developed soils is easier to differentiate and is less ambiguous that interpreting lower, poorly dated, soil-bounded unconformities in the section.

Following a number of models of rift-sedimentation (see among others, Gawthorpe and Leeder, 2000; Mack and Seager, 1990; Leeder and Jackson, 1993; Leeder and Gawthorpe, 1987; Blair and Bilodeau, 1988; Dart et al., 1995), we propose that deposition along the eastern margin of the basin is strongly controlled by the activity of basin-margin and intrabasinal faults. The activity of these faults strongly influences the location of the axial-river (ancestral Rio Grande) and interfingering piedmont deposits derived from the Manzanita and Manzano Mts. During basinward migration of the rift-border structure, portions of the former piedmont-slope and basin-floor are uplifted. Younger deposits bypass this footwall block, which becomes a local stratigraphic top (Fig. 1-22). Smaller drainages that are not integrated with the axial-river tend to have their base level set by these abandoned surfaces. Intrabasinal faulting also tends to create local fault wedges. Many of these wedges can be observed near the constructional tops of the basin-fill succession; however, these wedges can also be recognized in the late Miocene (see map of Connell, 1998).

Retrace route back to SP-60. **0.6**

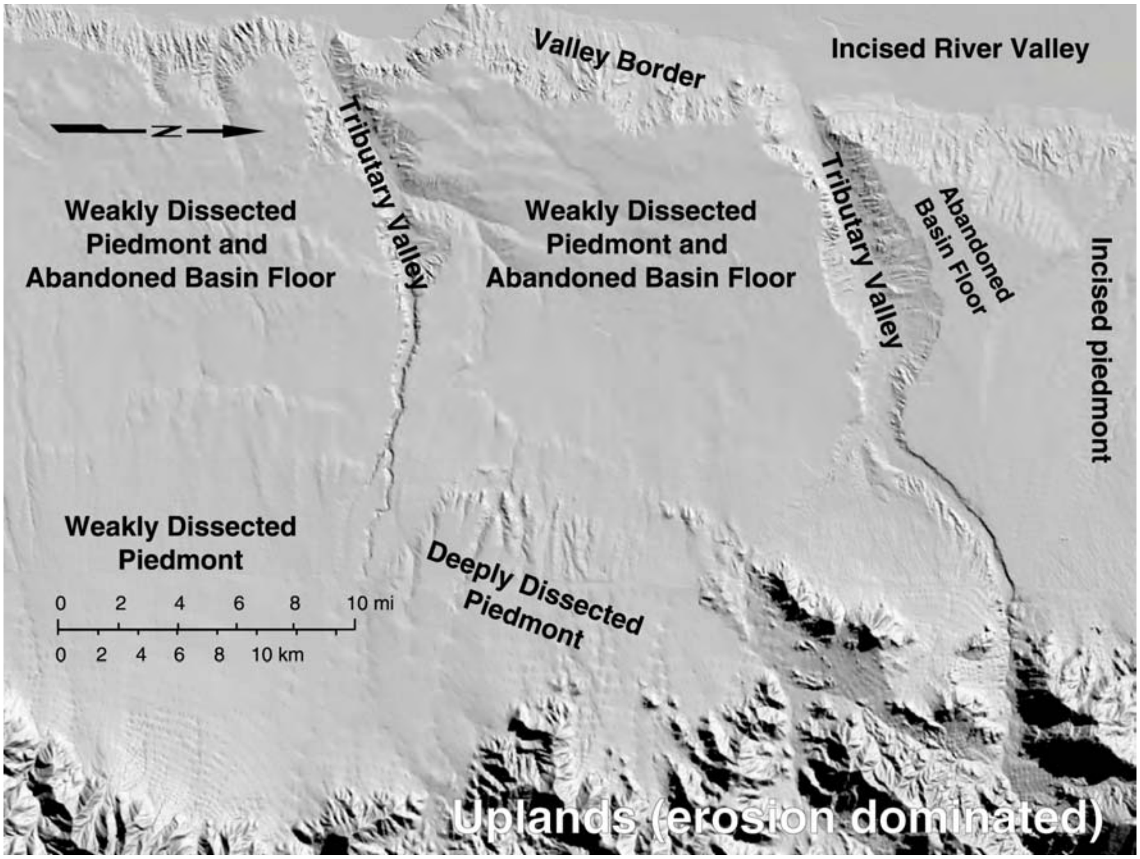

Figure 1-18. Shaded-relief map illustrating variations in mountain-front morphology and piedmont dissection where streams that are not integrated with the Rio Grande and its entrenched tributaries deposit sediment across the low-relief slope of the Llano de Manzano.

Figure 1-19. View of Llano de Manzano south of northern Hubbell bench, illustrating deposition of range-front alluvial fans that prograded over the low-relief, feature-challenged slope of the Llano de Manzano.

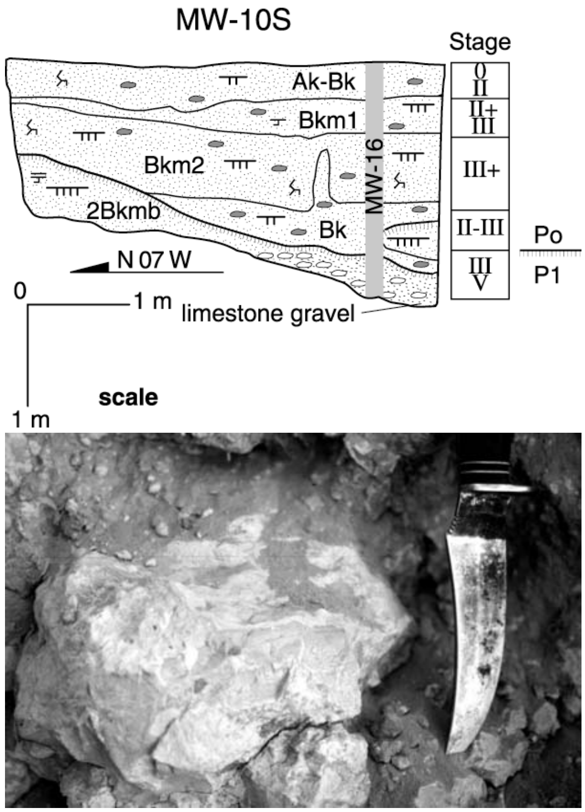

Figure 1-20. Top: Log of soil pit in Cañada Colorado surface. Ticks indicate pedogenic carbonate morphology of each horizon (e.g., single tick= Stage I, double tick=Stage II, triple tick=Stage III). Bottom: Photograph of extremely hard carbonate peds from MW-10S soil pit. Po and P1 denote older and younger soils, respectively.

16.8 Turn right onto SP-60. **1.6**

18.4 To your left is a clear view of down-to-the-west normal faulting within the Manzanita Mountains drops the banded limestone of the Madera Group towards the mountain front. **0.2**

18.6 Turn right (south) onto SP-604. **0.3**

18.9 Descend Cañada Colorada surface into Hell Canyon valley. Note buildings and abandoned mine workings to left on face of Manzanita Mountains. **0.1**

19.0 Descend riser onto middle Pleistocene terrace of Hell Canyon. **0.2**

19.2 The short red pipe about 20 m east of road is the upper East Side Monitoring Well. This well encountered about 21 m of limestone-bearing conglomerate that overlies over 75 m of red clay and sand with limestone layers near the bottom of the hole (at 88 m bls). Groundwater is at about 34 m bls. About 2.9 km to the northeast, just west of the mountain front, a driller's log of a windmill (RWP29) indicates about 21-32 m of gravel over probably Pennsylvanian or Permian rocks. Other monitoring wells drilled on the northern Hubbell bench indicate the presence of about 25-42 m of limestone-bearing gravel correlated to the piedmont deposits of the Santa Fe Group. These conglomerates overlie dark red shale and sandstone of the Permo-Triassic succession. Soil pit (MW8S) just south of road indicates that this deposit contains a soil with Stage III pedogenic carbonate morphology (Fig. 1-23). **0.1**

19.3 Descend riser to Holocene valley of Hells Canyon Wash. Guadalupe Peak at 12:00 with Pennsylvanian limestone nonconformably overlying Ojito granite (Karlstrom et al., 2000). **0.1**

19.4 Crossing modern channel of Hell Canyon Wash. A low (<2 m high) terrace contains charcoal that was dated at 1220±60 yr BP (Beta 106204; dendrochronologically calibrated to 675-975 yr AD, ±2σ). **0.1**

19.5 Note toes of mountain-front fans to your left. Canon de los Seis to southeast. Topography is slightly undulatory and buried soils are common. Exposures of gas line to south indicate an extensive, but locally discontinuous cover of grus-dominated sand with Stage I and II pedogenic carbonate development, overlying moderately developed calcic soil with Stage II to III carbonate morphology. **1.1**

20.6 Note large cobbles and boulders in deposits. **0.2**

20.8 Descend riser onto terrace of Canon de los Seis. **0.2**

21.0 Arroyo exposures of late Quaternary cut and fill terrace sequences. Windmill (RWP-10) to left. **0.1**

21.1 Bear right and head south along fence. **0.6**

21.7 Turn right onto SP-59. **0.2**

21.9 Cross gas pipeline. **0.2**

22.1 Descend low riser into younger grus-dominated alluvium of Cañon de los Seis. **1.8**

23.9 Limestone boulders along edge of Sanchez Canyon, a tributary to Hell Canyon. Suite of inset terrace deposits of Hell Canyon to north. **0.9**

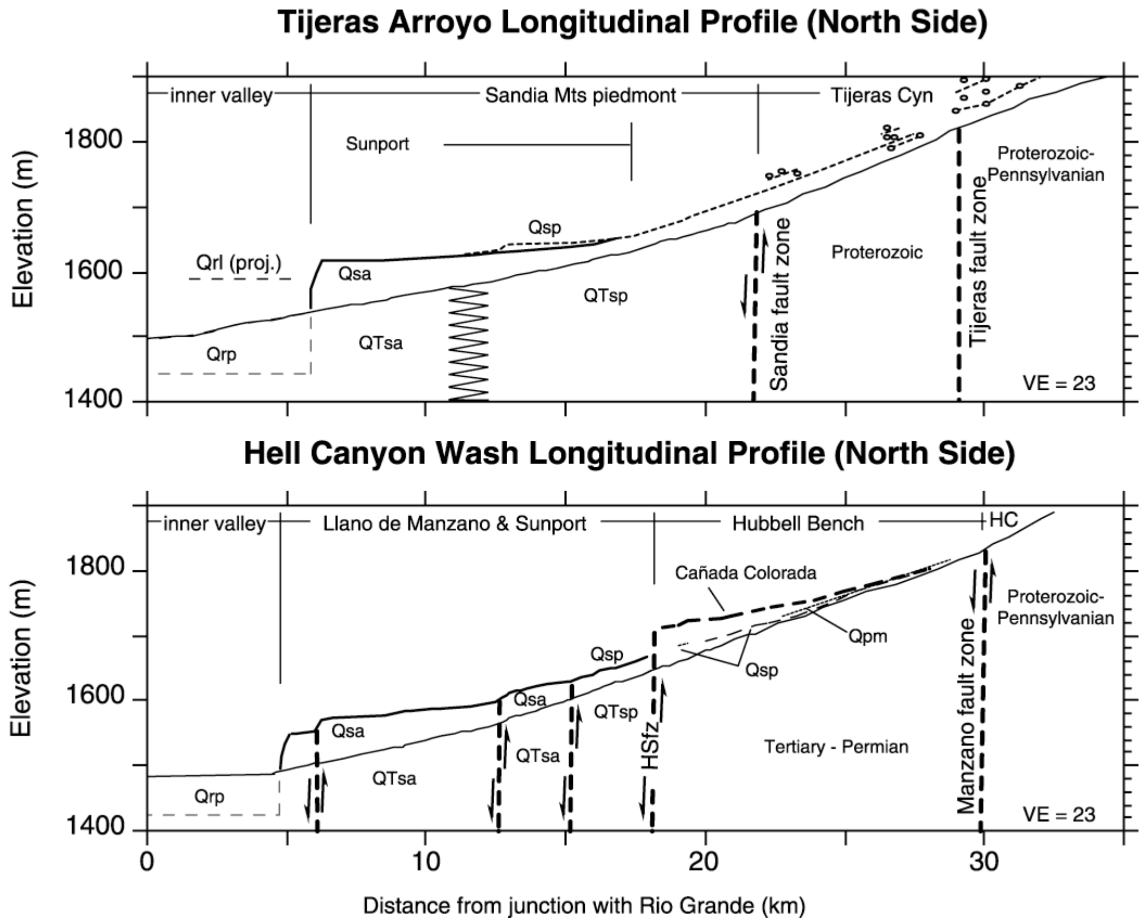

Figure 1-21. Longitudinal profiles of major tributary drainages to the Rio Grande. Top: Tijeras Arroyo, which enters the basin at the junction of the Manzanita and Sandia Mountains. Subsurface work (Hawley and Hasse, 1992; Hawley et al., 1995; Hawley, 1996; Connell et al., 1998) indicate the presence of a number of intrabasinal faults west of the range-bounding Sandia fault. These faults, however, do not significantly influence development of piedmont-slope surfaces. Bottom: Longitudinal profile of Hell Canyon Wash. Intrabasinal faulting by the Hubbell Spring fault zone significantly influences late-stage sedimentation of the Santa Fe Group and the development of piedmont surfaces. Uplift of footwall blocks resulted in the preservation of flights of piedmont and valley-fill units that become nearly indistinguishable from the aggradational succession on the hanging wall.

24.8 Cut in low, middle Pleistocene terrace across tributary to north contains a stack of calcic soils (MW1S), illustrating a succession of soils containing I+ (25 cm thick), and III+ (90-125 cm thick) pedogenic carbonate morphology. A gas line excavated across the piedmont exposed much of the piedmont-slope south of Hell Canyon Wash. This trench contained a strongly developed soil with Stage III carbonate morphology and clay-rich Bt horizons. Younger grus-dominated sands overlie this soil. **0.2**

25.0 Cross cattle guard. **0.2**

25.2 Cross over interfluve between Ojo de la Cabra and Hell Canyon drainages. **0.5**

25.7 Turn to right and stay on SP-59. Descend onto terrace tread. **0.5**

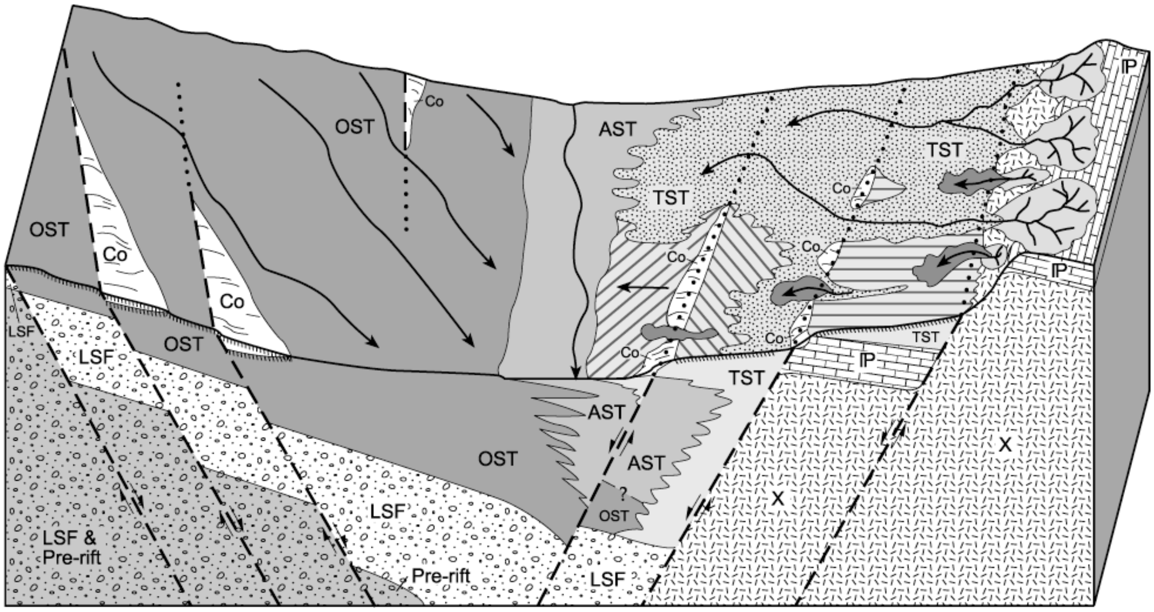

Figure 1-22. Conceptual block diagram, illustrating regional patterns of Santa Fe Group sedimentation (inspired after Gawthorpe and Leeder, 2000). Deposition along the footwall of the basin (transverse and axial systems tracts, TST and OST, respectively) are influenced by the location and activity of intrabasinal normal faults. In particular, basinward migration of the eastern rift-border structure results in the preservation of a number of geomorphic surfaces on the footwalls of intrabasinal faults. Depending on the size and lithology of the footwall drainages, piedmont deposition may be integrated with the axial river (AST) or will grade to local base levels along the eastern margin. Stratigraphic (or syntectonic) wedges are locally preserved along exposed fault scarps (co).

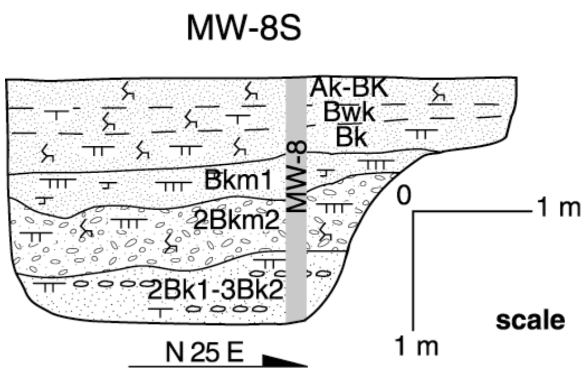

Figure 1-23. Log of soil pit on inset middle(?) Pleistocene terrace deposit of Hell Canyon Wash. Ticks indicate pedogenic carbonate morphology of each horizon (e.g., single tick= Stage I, double tick=Stage II, triple tick=Stage III).

26.2 Descend riser. Junipers on lower tread surfaces. **STOP 1-4**. **Inset terrace deposits of Hell Canyon Wash**. *Hubbell Spring 7.5' quadrangle, GPS: NAD 83, UTM Zone 013 S, N: 3,861,415 m; E: 362,310 m.*

This stop is an overview of the suite of inset terrace deposits associated with Hell Canyon Wash. Upstream and to the east, Hell Canyon Wash is a rather broad valley. West of here is the canyon of Hell Canyon Wash, which entrenched into the upper Santa Fe Group basin fill during early(?) or middle Pleistocene time. To the south, drainages developed on the footwall of the Manzano Mountains are not integrated with Hell Canyon Wash or the Rio Grande. These drainages terminate on abandoned, early Pleistocene basin-plain and piedmont-slope surfaces, which constitute base level control for such streams. At this stop four terrace levels are visible above the modern channel. The lowest terrace is 2.5-3 m above the modern channel and functioned as the floodplain/valley floor during the 20th Century and probably consists of Holocene fill. The second level is discontinuous and is ~6 m above the modern channel. This small local terrace deposit is cut into an adjacent 9-m high terrace level and could represent local (autocyclic?) variations in arroyo cutting and filling, rather than being related to tectonically or climatically driven changes in the landscape. However, other 6-m high terraces are present downstream. An extensive terrace is 9 m above the modern channel here. This terrace deposit is not preserved down stream. The next highest terrace is 10-11 m above the modern channel. This unit becomes a broad, extensive terrace deposit downstream and is preserved on both sides of Hell Canyon Wash. The highest terrace is 12-13 m above the modern channel and locally forms a broad rounded drainage-divide that SP-59 follows. To the west is an older surface that is 27 m above the modern channel. The problem with correlating terraces in this geomorphic setting is that they become discontinuous downstream and are buried by eolian and alluvial sediments upstream. Their age, climate and tectonic significance remain elusive.

Turn around and head back to MM 25.7. **0.2**

26.4 Turn right (west) onto Hell Canyon Road (SP-625), heading west on interfluve of Ojo de la Cabra (Goat Spring) drainage. **0.5**

26.9 Cross cattle guard. **0.6**

27.5 Descend into Ojo de la Cabra drainage. **0.1**

27.6 Road crosses terrace remnant, which merges into the valley floor upstream and is buried by piedmont alluvium farther east. **0.1**

27.7 Road parallels Holocene terrace to south that contains charcoal and snails. **0.2**

27.9 Notice the presence of phreatophytes (e.g., reeds and rushes) as you pass the spring of Ojo de la Cabra (Goat Spring). Note the abundance of Mesquite and Creosote down stream. We are near the northern limit of Creosote, which defines the northern limit of Chihuahuan Desert vegetation. **0.2**

28.1 Confluence between Ojo de la Cabra drainage with Hell Canyon Wash. Two discontinuous levels of terraces are present here. Piedmont deposits consist of sandstone with interbedded clast-supported conglomerate composed mostly of limestone with subordinate metamorphic and minor reddish-brown sandstone cobbles and boulders. **0.4**

28.5 Note terrace deposits midway up margins of Hell Canyon Wash. **0.5**

29.0 Buried paleocanyon on north side of drainage contains about 10-15 m of bouldery piedmont sediments. **0.2**

29.2 Arroyo terrace deposit to north is inset against upper Santa Fe Group. **0.1**

29.3 Hell Canyon Wash broadens, presumably because of the presence of weakly cemented fluvial deposits of the ancestral Rio Grande below just level of valley floor. Drainages developed in ancestral Rio Grande deposits commonly form broad tributary valleys, whereas, tributary drainages incised into the better cemented piedmont deposits commonly contain narrower and steeper-walled valleys. **0.4**

29.7 Paleo-canyon backfill (s) exposed on north rim of Hell Canyon Wash. Historic gravel bars on valley floor may have been deposited during flood in the 1920s(?). There are anecdotal accounts of a flood in Hell Canyon that reached the Rio Grande in the 1920s, however, the extent of this flood has not been independently verified. **0.6**

30.3 To your right at valley floor level are well cemented, gently east-tilted exposures of early Pleistocene pumice-bearing ancestral Rio Grande deposits. **0.1**

30.4 Cross cattle guard. **0.3**

30.7 **STOP 1-5. Hell Canyon Wash**. *Hubbell Spring 7.5' quadrangle, GPS: NAD 83, UTM Zone 013 S, N: 3,862,700 m; E: 355,420 m.*

A stratigraphic section measured along the southern margin of the arroyo is on the footwall of an intrabasinal fault. The lower part of this section contains deposits of the ancestral Rio Grande that contain locally abundant pumice pebbles. A pumice was dated using the $^{40}Ar/^{39}Ar$ method at 1.71 Ma. Geochemistry of this dated pebble indicates that it is chemically similar to the Bandelier Tuff (N. Dunbar, 2001, personal commun.). However, its age is slightly older than the lower Bandelier and may be related to the pre-caldera San Diego Canyon ignimbrite. About half-way up the slope is a cross-bedded pumice-bearing pebble conglomerate that is well cemented with sparry calcite and forms elongate concretions (Fig. 1-24). The orientations of such elongate concretions are bi-directional indicators of paleo-groundwater flow (Mozley and Davis, 1996). Assuming that paleo-groundwater flow directions roughly mimic the present southward course of the Rio Grande, the orientations of these elongate concretions are south-southeast. Paleocurrent orientations determined from cross bedding are south-southwest, but similar to the paleo-groundwater flow indicators. A succession of fine- to medium-grained sand with scattered concretionary sandstone and rhizoconcretionary intervals is typically present between the underlying fluvial and overlying piedmont deposits. Cementation of the underlying fluvial succession is also common near the boundary (laterally or vertically) with eastern-margin piedmont deposits. Fluvial and eolian-dominated deposits interfinger with, and are overlain by, locally derived piedmont deposits of the Manzano Mts.

The top of the section contains a strongly developed soil with Stage IV pedogenic carbonate morphology and a strongly developed stone pavement. This surface is a remnant of the footwall of a strand of the Hubbell Spring fault zone. Later piedmont deposits bypassed this remnant to the north and south of Hell Canyon. Deposits of these later piedmont systems are only slightly offset by this fault strand, but are displaced more by other strands to the west. The tops of limestone pebbles on this constructional surface are commonly flattened, probably by the dissolution of carbonate. The undersides of these clasts are quite deeply pitted and have a pendant morphology caused by the dissolution of calcite. Later re-precipitation of white micritic carbonate indicates deposition after an earlier stage of dissolution. These cements are quite different than the sparry, phreatic calcite exposed below in the fluvial deposits of the ancestral Rio Grande (Fig. 1-25 and 1-26).

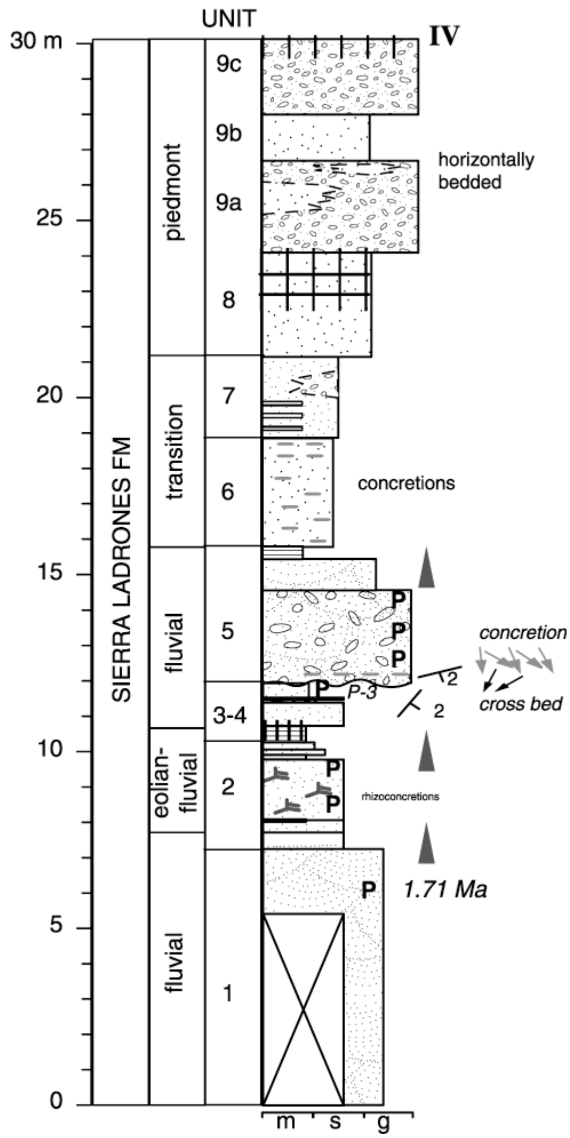

Figure 1-24. Stratigraphic section of Hell Canyon Central Section measured along southern margin of Hell Canyon. This marks the approximate eastern limit of exposure of pumice-bearing fluvial deposits of the ancestral Rio Grande, which become buried to the east. Hachures denote soils. Roman numerals indicate pedogenic carbonate morphologic stage.

Comparisons of surface and available subsurface stratigraphic data indicate the development of a westard-prograding wedge of ancestral Rio Grande and eastern-margin piedmont deposits (Fig. 1-27). This westward progradation of the ancestral Rio Grande would result in onlap onto deposits of the Arroyo Ojito Fm (the western oblique fluvial system). The top of the Arroyo Ojito Fm is defined by the Llano de Albuquerque surface, which is late Pliocene in age (see discussions in Day 2 road log).

Figure 1-25. Photograph looking to the east at well cemented extrabasinal, cross bedded sandstone and rounded conglomerate of the ancestral Rio Grande deposits of the Sierra Ladrones Fm. The banded appearance is the result of southerly oriented sandstone concretions indicating a southerly direction of paleo-groundwater flow. Scale is 1.5 m high.

Thus, this westward progradation of the Rio Grande would result in the development of an unconformity of increasing temporal magnitude to the west (see Fig. 1-6). The nature of this contact will be explored on Day 2. This westward progradation of the ancestral Rio Grande and piedmont deposits is recognized throughout much of the basin (see Connell et al., 1995; Cather et al., 2000; Smith et al., 2001 for examples) and may be responsible for the present position of the Rio Grande Valley, prior to 0.7-1.2 Ma entrenchment. This relationship may also explain why deposits of the ancestral Rio Grande in the Albuquerque area are rather sparse west of the Rio Grande Valley.

Geologic studies of the Isleta Reservation do not support the presence of an eastern buttress unconformity between early Pleistocene fluvial deposits of the ancestral Rio Grande and older basin fill. Figure 1-28 is a conceptual model showing interpreted differences in bounding unconformities and stratal geometries one might expect between aggrading basin fill and incised river valley deposition.

Continue driving west on SP-625. **0.5**

31.2 Ancestral Rio Grande deposits low in canyon walls, east of a strand of the Hubbell Spring fault zone. These deposits commonly form “flat irons” (Gerson, 1982) that are separated from the modern valley border slopes. These are probably the result of differential permeability and runoff contrasts between the more permeable ancestral Rio Grande deposits and the less permeable piedmont alluvium. North side of Hell Canyon Wash widens. Badlands contain interfingering distal piedmont and ancestral Rio Grande deposits. **0.1**

31.3 Pass connecting road to SP-624. Bear left. **0.2**

31.5 Road to right across dam leads to exposures of interfingering transition between piedmont and fluvial deposits. **0.2**

31.7 Valley broadens and interfingering piedmont deposits become thinner. **0.4**

32.1 High terrace deposits across valley to your right. Piedmont deposits above are generally less than 2 m thick and cap both edges of Hell Canyon Wash. **0.4**

32.5 Low terrace deposit from Memorial Draw, to north, which follows the McCormick Ranch fault. **0.5**

33.0 Cross road from northeast. Large boulders of upper Bandelier Tuff found to south (Fig 1-29). Note terrace, about 7 m above road, along south side of Hell Canyon Wash. **0.3**

33.3 Terrace deposit continues on south side of Hell Canyon but become more dissected to the west. **1.2**

34.5 Cross trace of Palace-Pipeline fault zone, which displaces the Llano de Manzano by about 18 m on south side of Hell Canyon Wash. Terrace to your left (south) terminates near trace of fault. This terrace is probably middle to late Pleistocene in age. It is not clear whether the fault displaces this terrace to the extent that it is buried below the valley to the west. Rather, this terrace is probably too thick to be offset that much. Capture of new tributaries west of the Palace-Pipeline fault and erosion of the valley margins may provide a better explanation for the lack of terraces to the west. **0.7**

35.2 Cross cattle guard. Exposures at 9:00 and 2:00 contain an ash preliminarily dated at 1.55 Ma and correlated to the Cerro Toledo Rhyolite. Earlier attempts to date this fine-grained ash yielded a range in ages from 1.05-1.6 Ma. **0.6**

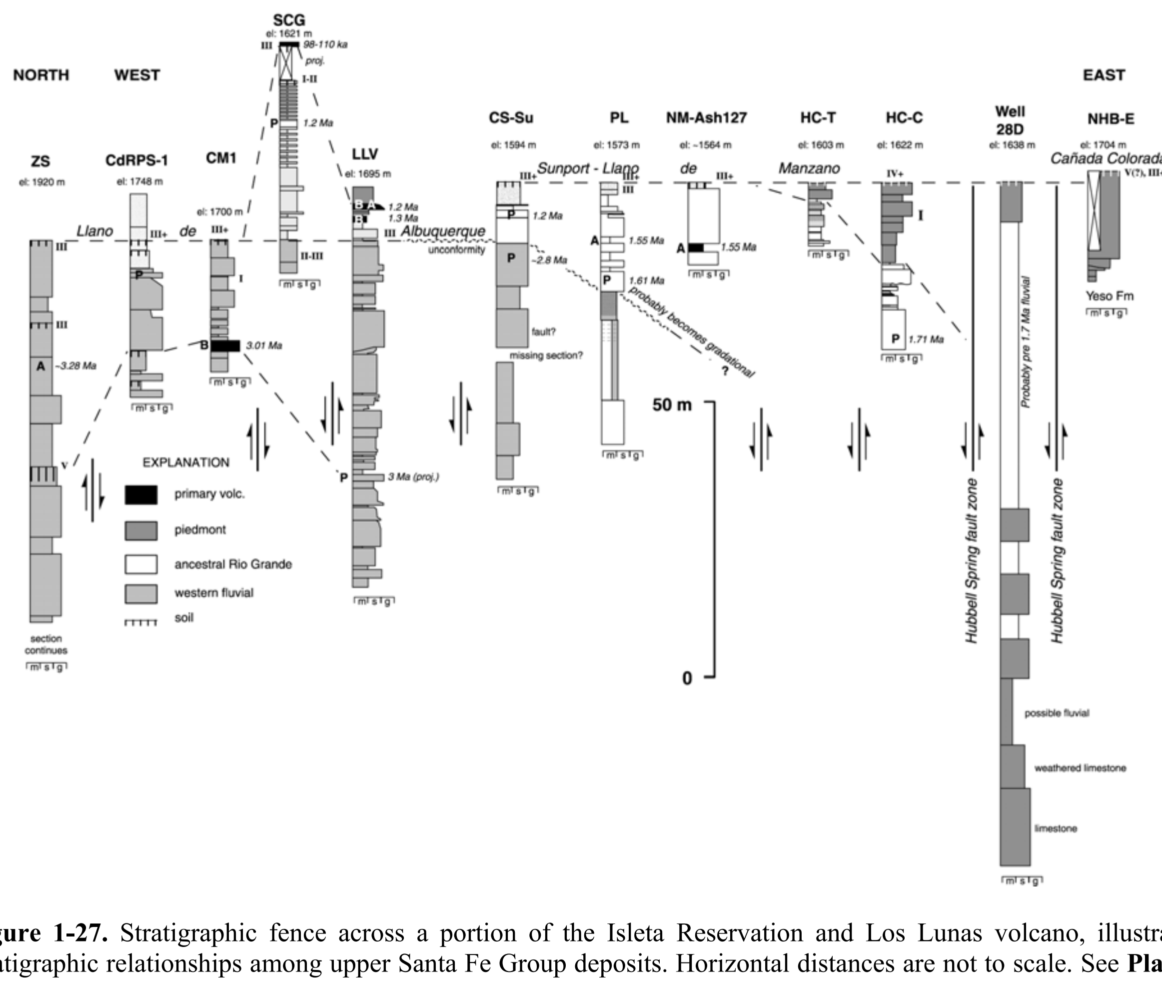

Figure 1-27. Stratigraphic fence across a portion of the Isleta Reservation and Los Lunas volcano, illustrating stratigraphic relationships among upper Santa Fe Group deposits. Horizontal distances are not to scale. See **Plate II** for approximate locations of stratigraphic sections. The Zia fault section (ZS) is about 45 km north of CdRPS-1 and contains the ~3.3 Ma Nomlaki Tuff (Connell et al., 1999). Hachures denote soils. Roman numerals indicate pedogenic carbonate morphologic stage.

Figure 1-26. Photograph of constructional surface at top of stratigraphic section, illustrating a deeply pitted limestone pebble covered with micritic carbonate. The interlocking flat pebbles form a moderately to well developed desert pavement. Limestone pebble tops are commonly flattened and subparallel to the ground surface.

35.8 Turn right (north) towards cattle guard at north end of Hell Canyon Wash. **0.2**

36.0 Cross cattle guard. **0.1**

36.1 Begin pavement, turn north and drive on floodplain of Rio Grande. Bluffs to east contain pumice-bearing ancestral Rio Grande deposits. **0.7**

36.8 White bed at 3:00 is ash dated at 1.55 Ma and correlated to Cerro Toledo Rhyolite. This ash is about 10 m below the Sunport surface. (Fig. 1-30). **0.8**

37.6 Bluffs to east expose fine-grained light-brown sand overlain by gray deposits of the ancestral Rio Grande. This contact descends to the south and is buried at the mouth of Hell Canyon Wash. **0.8**

38.4 Cross cattle guard and turn right onto state highway NM-47. Merge into left lane. **0.4**

38.8 Turn left onto state highway NM-147 towards Isleta Pueblo. Bluff to north is low terrace. **0.2**

39.0 Cross Rio Grande. The concrete structure that spans the river is the Isleta Diversion Dam of the Middle Rio Grande Conservancy District, which diverts water from the Rio Grande to a number of acequias (*ditches*) for irrigation agriculture between of Isleta and San Acacia, New Mexico. Much of this water is returned to the river via a series of drains. **0.3**

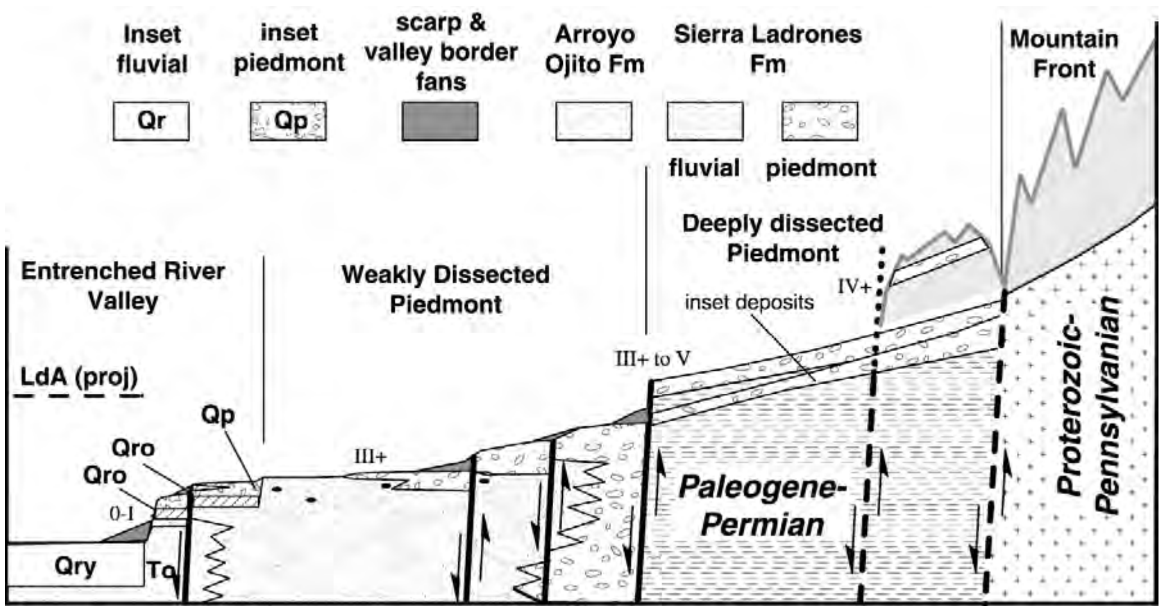

Figure 1-28. Schematic stratigraphic relationships comparing deposition on deeply dissected and weakly dissected piedmonts and the entrenched river valley. Units Qro and Qry denote younger and older inset fluvial deposits.

Figure 1-29. Photograph of boulder of upper Bandelier Tuff within early Pleistocene sand and gravel of the ancestral Rio Grande deposits of the Sierra Ladrones Fm. This boulder is exposed in a gully just south of Hell Canyon Wash.

Figure 1-30. Photograph of white fluvially reworked ash of Cerro Toledo Rhyolite exposed along eastern margin of Rio Grande Valley. This ash lies about 30 m above the local base of early Pleistocene sand and gravel of the ancestral Rio Grande deposits of the Sierra Ladrones Fm.

39.3 Turn left to Isleta Pueblo (pop: 4409). The Pueblo of Isleta (Spanish for *island*) was built on a slightly elevated fluvial-terrace deposit of the Rio Grande. A basalt flow crops out on the northern side of the "island of Isleta." The original pueblo was located on the site of the present pueblo when Coronado visited the area in 1540.The Spanish established the Mission of San Antonio de Isleta by 1613. Plains-Indian raids caused the Pueblo Indians living east of the Manzano Mountains to move to Isleta around 1675. The Isleta Pueblo did not actively participate in the Pueblo Revolt against the Spanish in 1680 and became a refuge for Spanish settlers. In spite of this Governor Otermin captured the pueblo in 1681 and took 400 to 500 prisoners with him to El Paso where they settled at Ysleta del Sur. The remaining population abandoned the Pueblo of Isleta and fled to Hopi country. They returned in 1716, brining their Hopi relatives with them. The present Pueblo was built in 1709 by scattered Tigua families. Most of the Hopi later returned to Arizona, but have retained their ties with Isleta. Reservations of Acoma and Laguna migrated to Isleta in the early 1800s because of drought and religious differences at their home pueblos. Thus, Isleta has incorporated a variety of pueblo people (Taken from Connolly, Woodward, and Hawley, 1982, p. 29). **0.1**

39.4 Bear right at cylindrical cement water tank and continue west to plaza. **0.1**

39.5 Cross plaza and church at Isleta. **0.1**

39.6 Turn right (north) at intersection west of plaza. **0.2**

39.8 Turn left onto state Highway NM-147. **0.7**

40.5 Cross railroad tracks and immediately turn left onto NM-314. **0.3**

40.8 Turn right onto Tribal Road TR-74. Drive slow and watch for speed bumps. **0.2**

41.0 Turn left onto NM-45 at stop sign, then make a quick right onto NM-317 towards junction with I-25. **0.8**

41.8 Ascend onto Los Duranes Fm, a late-middle Pleistocene fluvial deposit of the ancestral Rio Grande that is inset against Santa Fe Group basin fill. The top of this deposit was named the Segundo Alto surface by Lambert (1968). The age of the top is constrained by the 98-110 ka Cat Hills flows, which overlies the Los Duranes Fm (Fig. 1-31). About 25 km to north in NW Albuquerque, tongues of the 156±20 ka (U/Th date from Peate et al., 1996) Albuquerque volcanoes are interbedded near the top of the Los Duranes Fm. These constraints indicate that deposition of the Los Duranes Fm ceased between 98-156 ka. A prominent tributary terrace deposit in Socorro Canyon, about 105 km to the south near Socorro, New Mexico, has been dated using cosmogenic ^{36}Cl dating methods, indicates a cessation in deposition at 122±18 ka (Ayarbe, 2000). Correlations to this better-dated deposit have not been made, but suggest that the development of the Segundo alto terrace tread surface may be near this vintage. **0.3**

42.1 Cross I-25 overpass. Continue west. **0.2**

42.3 Cross cattle guard, heading west on Segundo alto surface. Pavement ends. Black hill to right (north) is the 2.78 Ma Isleta volcano (Maldonado et al., 1999). **0.2**

42.5 Low eastern limit of younger flows of Cat Hills volcanic field, which have been ^{40}Ar/^{39}Ar dated between 98-110 ka (Maldonado et al., 1999). **0.8**

Figure 1-31. View, looking west, of late Pleistocene basaltic flows of the Cat Hills volcanic field overlying the Segundo alto surface of the Los Duranes Fm.

43.3 Pass transfer station to your left. The Shell Isleta #2 well was drilled just west of Isleta volcano to the north. **0.7**

44.0 Flows of the late Pleistocene Cat Hills volcanic field to the south. **1.3**

45.3 Cross wash and turn left (southwest) on dirt road. **0.5**

45.8 The prominent hill to south is the Pliocene and early Pleistocene Los Lunas volcano. Volcano intruded deposits of the Arroyo Ojito Fm and Sierra Ladrones Fm. **0.6**

46.4 Pass through locked gate. **0.3**

46.7 Drive on Cat Hills flow 1. **0.4**

47.1 On Arroyo Ojito Fm. **0.2**

47.3 Flow of unit 1 of the Cat Hills basalt field. **0.3**

47.6 Exposures of the Arroyo Ojito Fm. **0.5**

48.1 On flow 1 of Cat Hills field. Excellent view of north side of Los Lunas volcano. **0.2**

48.3 Descend into eroded units of sand and mud exposed in the San Clemente graben. **0.1**

48.4 Cross drainage covered by eolian sandsheets and fine-grained mud and sand dominated deposits that fill the San Clemente graben. **0.4**

48.8 North-trending alignment of vents of the Cat Hills field to the west. **0.5**

49.3 Pass under powerlines. **0.4**

49.7 Bear right at corral and windmill. **0.4**

50.1 Pass Cat Hills basalt flow overlying strongly developed soil on right. **0.1**

50.2 **STOP 1-6.** San Clemente graben and Cat Hills volcanic field. *Dalies 7.5' quadrangle, GPS: NAD 83, UTM Zone 013 S, N: 3,856,670 m; E:332,080 m.*

Deposits within the San Clemente graben are mostly muddy sand and sand of eolian, fluvial, and colluvial origin. These deposits rest on a soil developed on the upper Arroyo Ojito fm (Ceja Mbr) and are overlain by flows of the Cat Hills field (Fig. 1-32). Strongly developed soil with stage III+ carbonate morphology are present at this upper contact. A bed of pumice-bearing pebbly sand is exposed locally in upper part of the San Clemente graben succession (Fig. 1-33). This pebbly sand bed contains pumice that has been chemically correlated to the Bandelier Tuff and yields a $^{40}Ar^{39}Ar$ date of 1.2 Ma, indicating that it is correlated to the upper Bandelier Tuff. These deposits overlie a soil developed on deposits of the Arroyo Ojito Fm. This soil is interpreted to represent a buried correlative of the Llano de Albuquerque soil, which marks the local top of Arroyo Ojito Fm deposition. The presence of Bandelier Tuff suggests that these sandy deposits are part of the ancestral Rio Grande deposits of the Sierra Ladrones Fm and represent the westernmost progradation and temporary spillover of the ancestral Rio Grande into the San Clemente graben during early Pleistocene time (Fig. 1-34).

Turn around and retrace route back to paved road west of I-25. End of day one road log. **8.0**

Figure 1-32. View to west of the 98-110 ka flow of the Cat Hills volcanic field, which overlies a strongly developed soil that exhibits Stage III pedogenic carbonate morphology. This soil is developed on sand and mud of the San Clemente graben, which overlies a soil developed on the Ceja Member of the Arroyo Ojito Fm.

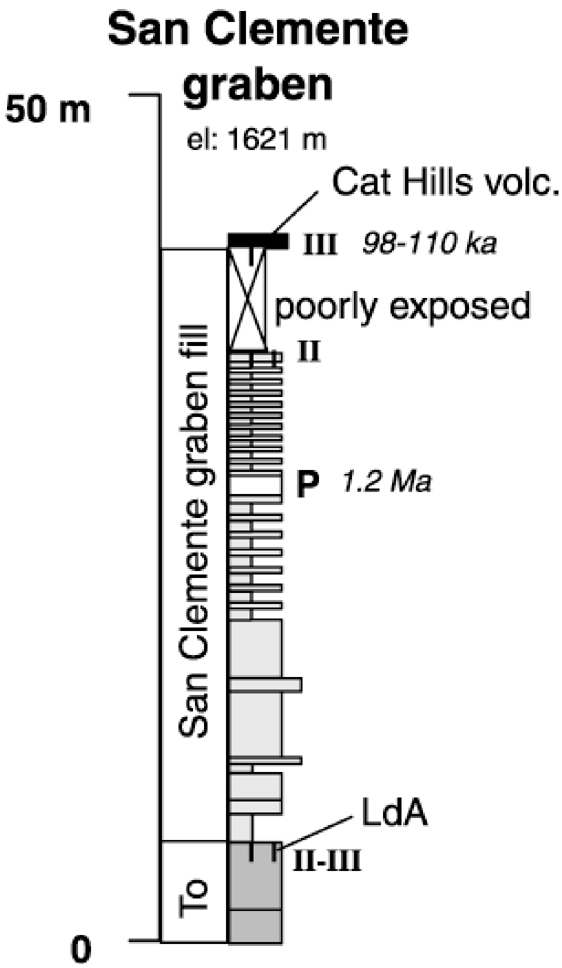

Figure 1-33. Stratigraphic column of San Clemente graben site, illustrating about 40 m of sand and mud overlying a soil developed on deposits assigned to the Ceja Member of the Arroyo Ojito Fm. About 18 m above the basal contact is a bed of sand containing pebbles of fluvially recycled upper Bandelier Tuff (verified by $^{40}Ar/^{39}Ar$ dating and geochemical correlation; W.C., McIntosh, and N. Dunbar, unpubl.). Hachured lines denote soils. Roman numerals indicate pedogenic carbonate morphologic stage.

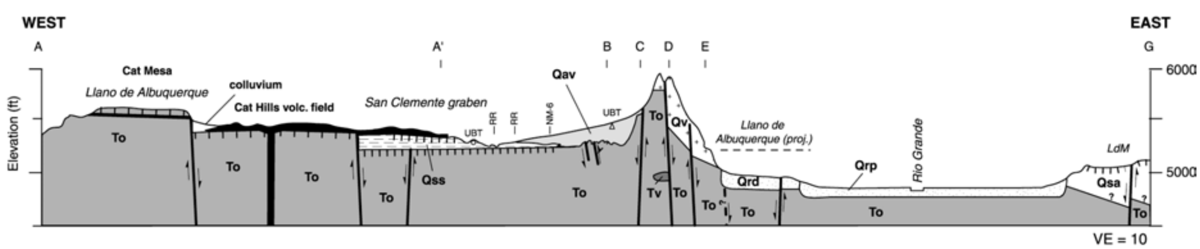

Figure 1-34. Cross section across western edge of basin and Los Lunas volcano. Note that the Llano de Albuquerque is faulted down towards the east and is buried by sediments accumulated in the San Clemente graben, which contains beds of early Pleistocene ancestral Rio Grande deposits in it. The scarp along the eastern edge of Los Lunas volcano is either faulted or is an erosional escarpment formed during entrenchment and subsequent aggradation of the middle Pleistocene Los Duranes Fm. A notch along the eastern flank of Los Lunas volcano marks the edge of an upper flow. Units include the Arroyo Ojito Fm (To), alluvium in San Clemente graben (Qss), ancestral Rio Grande deposits of the Sierra Ladrones Fm (Qsa), alluvium of Los Lunas volcano (Qav), 1.26 Ma trachyandesite of Los Lunas volcano (Qv), older volcanic rocks of Los Lunas volcano (Tv), and inset fluvial deposits of the Los Padillas (Qrp) and Los Duranes (Qrd) fms. Hachured lines denote major geomorphic surfaces, such and the Llano de Albuquerque and Llano de Manzano (LdM). Fallout ash and fluvially recycled pumice of the 1.22 Ma Bandelier Tuff (UBT) is present in units Qss and Qav.

FRIENDS OF THE PLEISTOCENE, ROCKY MOUNTAIN CELL, 45TH FIELD CONFERENCE

PLIO-PLEISTOCENE STRATIGRAPHY AND GEOMORPHOLOGY OF THE CENTRAL PART OF THE ALBUQUERQUE BASIN

SECOND-DAY ROAD LOG, OCTOBER 13, 2001

Geology of Southern Albuquerque and Tijeras Arroyo

SEAN D. CONNELL
New Mexico Bureau of Geology and Mineral Resources-Albuquerque Office, New Mexico Institute of Mining and Technology, 2808 Central Ave. SE, Albuquerque, New Mexico 87106

DAVID W. LOVE
New Mexico Bureau of Geology and Mineral Resources, New Mexico Institute of Mining and Technology, 801 Leroy Place, Socorro, NM 87801

J. BRUCE J. HARRISON
Dept. of Earth and Environmental Sciences, New Mexico Institute of Mining and Technology
801 Leroy Place, Socorro, NM 87801

The following trip examines the geomorphic and stratigraphic setting of the inset (post-Santa Fe Group) fluvial succession of the ancestral Rio Grande, the stratigraphic and geomorphic relationships between the Llano de Albuquerque and Sunport surfaces, and the lithologic makeup and size distribution of the gravel of the western-margin facies and axial Rio Grande facies. During the trip we will also discuss potential problems inherent with extending lithostratigraphic and allostratigraphic concepts through the basin-fill system. Field-trip stops illustrated on Plate I.

Mi **Description**

0.0 **STOP 2-0**. Begin trip at south side of store at the Isleta Lakes Campground, *Isleta 7.5' quadrangle (1991), GPS: NAD 83, UTM Zone 013 S, N: 3,867,855 m; E: 346,955 m. (Note that the UTM ticks on this quad are incorrect)*. This trip begins on the floodplain of the Rio Grande. The stratigraphy of this uppermost Pleistocene and Holocene deposit has been recently studied in detail for a liquefaction susceptibility evaluation (Kelson et al., *this volume*). Drive east and leave Isleta Lakes Campground. The inner valley of the Rio Grande is a floodplain surface bordered by dissected bluffs that are partially buried by coalescent valley border alluvial fan deposits (Fig. 2-1). This lowest and youngest cut-and-fill deposit of the Rio Grande Valley formed very late in the sequence of episodic incision and partial aggradation after the Rio Grande began to incise into Plio-Pleistocene basin fill of the upper Santa Fe Group between 1.2-0.7 Ma. Deposits of the inner valley, informally referred to herein as the Los Padillas formation (Connell and Love, 2000, 2001), represent the latest aggradational phase of the axial Rio Grande. The inner valley is underlain by about 22 m of sand, gravel, and minor silt-clay deposits that form the floodplain of the Rio Grande (MW-1 Isleta and MW-2 Isleta, Hawley, 1996, appendix A). These floodplain deposits do not exhibit soil development and have very little depositional relief and significant portions of the inner valley have historically been flooded (see Kelley, 1982) prior to the construction of Cochiti and Jemez dams upstream. Thus, the inner valley is hydrologically connected to the modern Rio Grande, whereas the late Pleistocene deposits of the Arenal Fm are well above flood stage. The age of the Los Padillas Fm is poorly constrained, but was likely laid down during latest Pleistocene time after the Rio Grande incised about 85 m into ancestral Rio Grande deposits of the late Pleistocene Arenal Fm (a.k.a. Primero Alto terrace surface of Lambert, 1968), which contains soils having Stage I and II+ pedogenic carbonate morphology (Connell et al., 1998a; Machette, 1997). Inner valley aggradation is demonstrated by an archaic site located 4 m below the valley floor in the north valley of Albuquerque (Sargent, 1987). Tributary aggradation may have slowed by middle Holocene time as indicated by a 4550±160 yr BP (Beta 109129; dendrochronologically calibrated to BC 3640-2895 yrs ±2σ) date on charcoal within 2 m of the top of a broad valley border fan near the mouth of Tijeras Arroyo (Connell et al., 1998a). The lack of strong soils between the terrace deposits of the ancestral Rio Grande and piedmont and valley border deposits suggests that piedmont and valley border deposition kept pace with the development of the floodplain.

Upper Pleistocene and Holocene alluvial deposits are aggraded alluvial aprons and channels cut into, or burying, older deposits bordering the valley. The progradation of Holocene valley border alluvial deposits across the floodplain indicates that present discharge of the river along this reach is inadequate to transport accumulated sediment out of the valley. The presence of progressively inset fluvial deposits of the ancestral Rio Grande along the valley margins indicates that episodes of prolonged higher discharge were necessary to flush sediment and erode the valley. Such erosional episodes must have occurred prior to aggradation of fluvial terrace deposits, perhaps during times of increased discharge, such as during full glacial events. Progradation of middle Holocene valley border alluvium across the modern Rio Grande floodplain suggests that deposition of tributary and piedmont facies occurred during drier (interglacial) conditions, possibly coupled with increased monsoonal precipitation. Deposition of fluvial terraces in semi-arid regions has been interpreted to occur during the transition from wetter to drier climates (Schumm, 1965; Bull, 1991). The stratigraphic relationships of the Los Padillas Fm and tributary and valley border alluvial deposits support this concept. Stratigraphic constraints on the deposition of the Los Duranes Fm, a middle Pleistocene deposit of the ancestral Rio Grande, indicate that much of the deposition of this widespread terrace deposit had finished prior to interglacial period of marine oxygen isotope stage 5 (*ca*. 128 ka), although deposition may have continued into the early part of the late Pleistocene. Studies of a lacustrine and eolian succession in the Estanica basin (Allen and Anderson, 2000) indicate a wetter climate in the region existing between about 15-20 ka, which might have driven incision of the inner valley; however, age control is lacking at the base of the Los Padillas Fm.

Drillhole data near Isleta Lakes and just north of Black Mesa, a basalt-capped mesa bordering the western margin of the inner valley, just west of Isleta Lakes, indicates that much of the floodplain succession is mostly pebbly sand and sand. Drillhole data in the inner valley suggests that much of the Los Padillas Fm rests upon Pliocene sediments of the Arroyo Ojito Fm, which were laid down by areally extensive rivers derived from the western margin of the basin. Clay beds, locally recognized within the Los Padillas Fm near Rio Bravo Boulevard (about 8 km to the north; Connell et al., 1998a) are interpreted to represent vertical accretion facies that are probably related to cut-off meander loops of the Holocene Rio Grande (*cf*. Kelson et al., 1999). These clay beds strongly influence the flow of groundwater and the transport of groundwater contamination from the rather heavily industrialized portions of the inner valley. **0.3**

0.3 Railroad Crossing. Ascend valley border alluvium derived from recycled sand and gravel of the upper Santa Fe Group. Valley border alluvium is poorly consolidated, weakly to non-cemented, typically low density, and exhibit weak to no soil-profile development with disseminated calcium carbonate or Stage I pedogenic carbonate morphology at depth. These deposits form a series of coalescent fans along the margins of the valley. These deposits are commonly prone to collapse upon wetting and have resulted in damage to buildings and homes in the Albuquerque area. **0.2**

0.5 Isleta Eagle Golf Course to south, a 27-hole course operated by the tribe and is part of their growing resort complex. **0.4**

0.9 Turn left (north) at stoplight onto highway NM-47. **0.1**

1.4 Cross under I-25 overpass, keep in left lane. **0.2**

1.6 Turn left and head south on NM-47 (South Broadway). **0.1**

1.7 Get into right lane. **0.1**

1.8 Turn right onto southbound I-25 entrance ramp. **0.3**

2.1 Merge with I-25 south (headed west). **0.5**

2.6 East abutment of I-25 bridge over Rio Grande. Rio Grande channel ahead. **0.4**

3.0 Milepost 214. West bridge abutment. **0.5**

3.5 Cross over Isleta Blvd. **0.3**

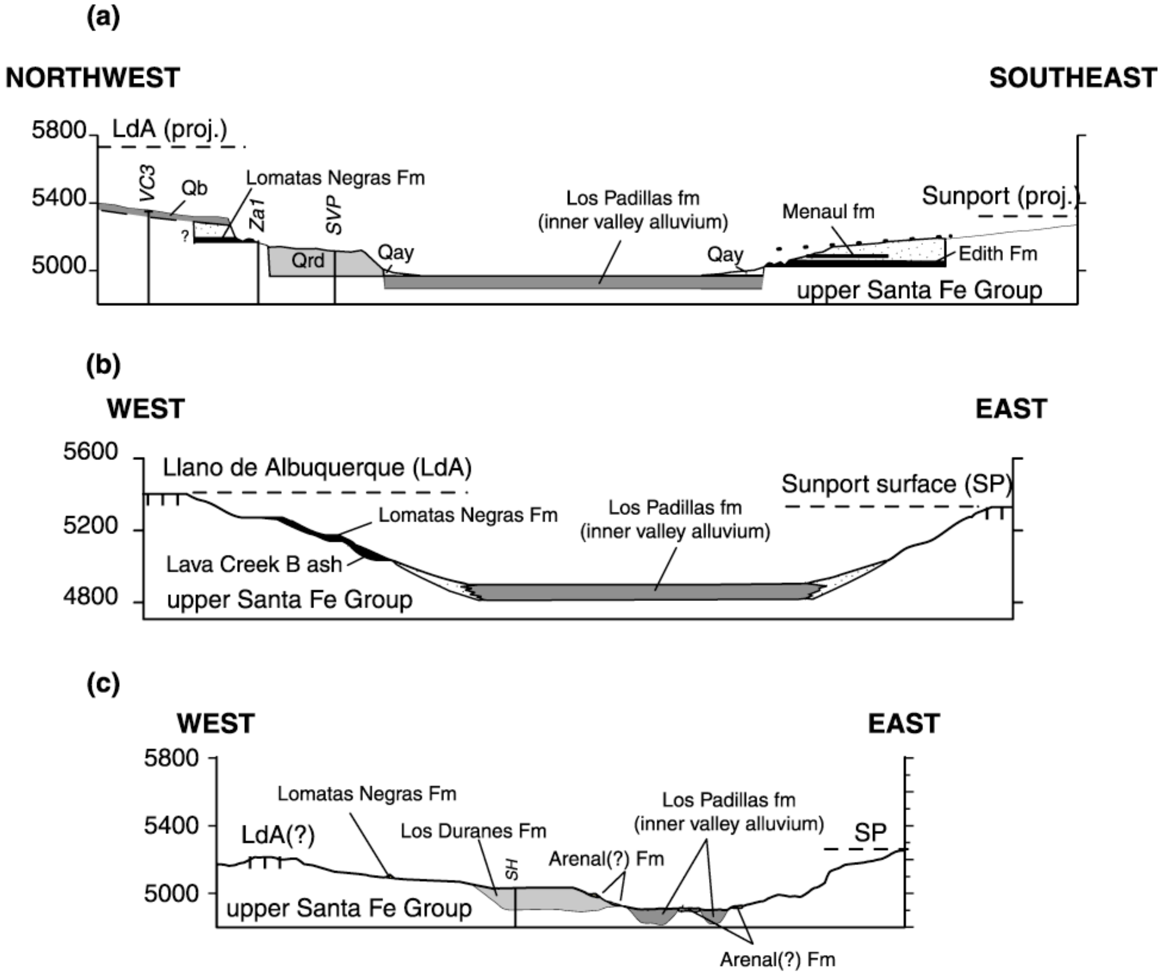

Figure 2-1. Schematic east-trending cross sections (VE=10) across Rio Grande Valley, illustrating inset relationships among middle and late Pleistocene fluvial deposits of the ancestral Rio Grande and upper Santa Fe Group constructional surfaces of the Llano de Albuquerque (LdA) and Sunport (SP). Profile north of I-40 illustrating burial of the Lomatas Negras Fm by the middle Pleistocene basalt of the Albuquerque volcanoes (a). Profile near Isleta Lakes (b). Profile at Isleta Pueblo (c). Approximate elevations of major constructional surfaces of the late Pliocene Llano de Albuquerque, and early Pleistocene Sunport surfaces are illustrated as are inset deposits of the middle Pleistocene Lomatas Negras Fm (containing the ~0.66 Ma Lava Creek B ash), the late-middle Pleistocene Los Duranes Fm (constrained by middle and late Pleistocene lava flows of the 156 ka Albuquerque volcanoes and 98-110 ka Cat Hills volcanic field; Peate et al., 1996; Maldonado et al., 1999), the late Pleistocene Arenal Fm, and the latest Pleistocene-Holocene inner valley deposits of the Los Padillas Fm. The stippled pattern indicates local deposition of valley border fans.

3.8 Entering Isleta Reservation. Overpass of drain and location of Isleta-Black Mesa piezometer, which encountered 22 m of sandy fluvial deposits underlying the Rio Grande floodplain (Los Padillas Fm). Deposits are associated with the last incision/aggradation episode of the Rio Grande. Incision probably occurred during latest-Pleistocene time, and entrenched 40 m below the late Pleistocene Arenal Fm. **0.6**

4.4 Cross bridge over Old Coors Road, which follows a former course of the Rio Grande cut through the lava flow of Black Mesa. Roadcut to right shows the edge of the 2.68±0.04 Ma ($^{40}Ar/^{39}Ar$ date, Maldonado et al., 1999) Black Mesa flow overlying cross-bedded pebbly sands of the Arroyo Ojito Fm and base-surge deposits from Isleta volcano. The tholeiitic Black Mesa flow has no outcrop connection with, and is slightly younger than, Isleta volcano, which forms the dark, rounded hill ahead and to the right of the highway. A buried vent for the Black Mesa flow is suspected in the floodplain area to left (Kelley and Kudo, 1978). **0.3**

4.7 Base-surge deposits of tuff cone associated with emplacement of Isleta volcano in outcrops on both sides of route. **0.5**

5.2 Change in primary dip direction of base-surge deposits at crest of tuff ring on right. Overlying alkali-olivine basalt flows fill tuff ring and extend southeast beyond Isleta volcano. $^{40}Ar/^{39}Ar$ dates indicate that oldest flow is 2.75±0.03 Ma and the second is 2.78±0.06 Ma (Maldonado et al., 1999). Basaltic cinders correlated to the Isleta volcano flows are recognized in the Arroyo Ojito Fm exposed along the eastern margin of the Rio Grande valley. These cinder-bearing deposits are about 70 m (estimated) stratigraphically below exposures of lower Pleistocene, Lower-Bandelier-Tuff bearing sand and gravel of the ancestral Rio Grande facies of the Sierra Ladrones Fm. This stratigraphic relationship indicates that deposition of the Arroyo Ojito Fm continued after 2.72-2.78 Ma, thereby constraining the age of the mesa capping Llano de Albuquerque to between 2.7 to 1.6 Ma. Based on local stratigraphy on both sides of the present valley, it is likely that the Llano de Albuquerque was abandoned as an active fluvial fan prior to deposition of Lower Bandelier ash and pumice gravel at *ca*. 1.6 Ma. Locally, the cinders of Isleta Volcano on the east side of the valley have experienced over 100 m of uplift with consequent erosion of the overlying units before final deposition by the Rio Grande to form the Sunport Surface. Because early Pleistocene terraces of the Rio Grande pass west of Isleta volcano at high levels, the volcanic edifice probably was exhumed during middle and late Pleistocene time (Love et al., 2001). **0.1**

5.3 Entering cut exposing basalt flow of Isleta volcano over base-surge unit (Fig. 2-2). Shell Isleta #2 well is about 1 mi. to the west, where it reached a depth of 6482 m and ended in Eocene rocks. Lozinsky (1994) reports that the Santa Fe Group is 4407 m thick at the Isleta #2 well and is underlain by 1787 m of the Eocene-Oligocene unit of Isleta #2, which overlies more than 288 m of sediments correlated with the Eocene Baca or Galisteo fms. **1.8**

7.1 Leave I-25 at exit 209 overpass to Isleta Pueblo. **0.1**

7.2 Turn left at NM-317 and head east towards Isleta Pueblo. **0.7**

7.9 Descend riser of Segundo Alto surface and middle Pleistocene Los Duranes Fm. A soil described by S. Connell and D. Love, nearby indicates that the Segundo Alto surface exhibits Stage II carbonate morphology. **0.2**

8.1 Water tanks to left. **0.2**

8.3 Turn left at stop sign onto Old Coors Rd (NM-45). **0.2**

8.5 Low rounded quartzite-bearing gravel of an ancestral Rio Grande terrace deposit inset against red cinders of Isleta volcano (2.72-2.79 Ma; Maldonado et al., 1999). **0.3**

8.8 Low inset terrace deposit of the ancestral Rio Grande north of red cinder bluff. **0.1**

8.9 Exposed south end of lava flow beneath terrace gravel. **0.4**

9.3 Descend onto floodplain of the Rio Grande. Basalt flow and underlying base-surge deposits to west. These are part of the tuff ring of Isleta volcano. The 2.68 Ma (Maldonado et al., 1999) Black Mesa flow is straight ahead and overlies deposits of the Arroyo Ojito Fm. **1.4**

11.0 Cross under I-25 overpass and through water gap cut by the Rio Grande. **0.5**

11.5 Leave Isleta Reservation. **0.6**

12.1 Pass intersection with Malpais Rd. Travel along western margin of inner valley floodplain. The low slopes to the west (left) are the toes of coalescent valley border alluvial fans. **1.4**

13.5 Pass intersection with Powers Way (west). **1.2**

14.7 Turn left (west) onto Pajarito Rd. Ascend valley border alluvium. The skyline mesa to the west is the Llano de Albuquerque, the interfluve between the Rio Puerco and Rio Grande drainages. Within next 0.5 miles, note the thin, discontinuously exposed white band at top of Llano de Albuquerque (Cejita Blanca of Lambert, 1968; Kelley, 1977). It is a strongly developed petrocalcic soil of the Llano de Albuquerque surface. Note low east-descending spur ridges, which are inset fluvial deposits of the ancestral Rio Grande. **1.0**

15.7 Pass intersection with Douglas Rd and prepare to stop on left (south) side of road. **0.2**

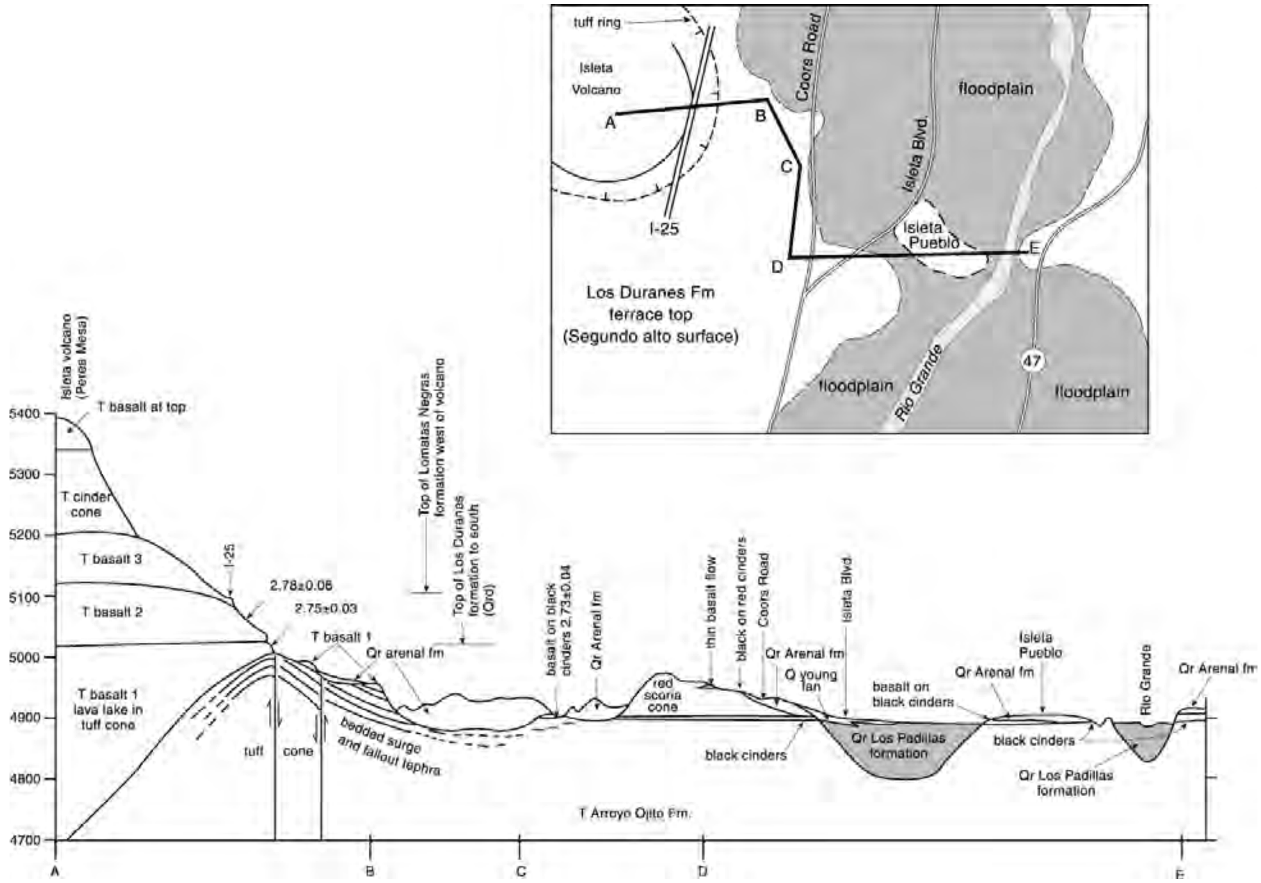

Figure 2-1. Cross Section across eastern flank of Isleta volcano and the Rio Grande Valley, illustrating late Pleistocene and Holocene inset fluvial deposits and the "island" of Isleta.

15.9 **STOP 2-1.** Turn left and park at wide shoulder on south edge of road. Middle Pleistocene inset fluvial terrace deposit of the ancestral Rio Grande (Lomatas Negras Fm). *Isleta 7.5' quadrangle, GPS, NAD 83, Zone 013 S, N: 3,873,725 m; E: 341,260 m.* Walk to the top of the low hill on south side of road.

The purpose of this stop is to examine a remnant of a middle Pleistocene terrace deposit of the Rio Grande and to discuss recent work on the terrace stratigraphy.

Inset stratigraphic relationships require the development of bounding discontinuities along deposit margins. These buttress unconformities are analogous to buried valley margin bluffs that mark the edge of the paleovalley. At this stop, we are less than 300 m east of such a remnant paleobluff line, which is defined by the terminations of low spur ridges that are underlain by the Arroyo Ojito Fm. Rounded, stratified cobbles and pebbles of metaquartzite and various volcanic rocks dominate the gravel underlying this hill. Sparse Pedernal chert and sandstone clasts are also recognized. Sandstone gravel is not typical of the ancestral Rio Grande facies and are probably remnants of an older alluvial deposit that once overlain this deposit, or the sandstone gravel was incorporated from the nearby buttress unconformity. This deposit is about 60 m below the Sunport surface, the broad mesa about 120 m above the Rio Grande on the eastern side of the valley. This deposit is correlated to the Lomatas Negras Fm, one of the oldest definitively inset fluvial terrace deposits.

Terrace deposits were originally given geomorphic names, such as Primero Alto, Segundo Alto, and Tercero Alto (Lambert, 1968; Machette, 1985). Such terms were originally defined by Bryan and McCann (1936) for terraces of the upper Rio Puerco Valley, which has a distinctly different drainage morphology, and transported (sedimentary dominated) lithology compared to the crystalline- and volcanic-dominated deposits of the Rio Grande Valley. Lambert (1968) defined the Edith, Menaul, and Los Duranes formations as lithostratigraphic units. Connell and Love (2001) proposed additional terms to round out Lambert's stratigraphy and to avoid confusion between geomorphic and lithologic terms.

The oldest fluvial deposit is the Lomatas Negras Fm, an early-middle Pleistocene fluvial deposit exposed at this stop. Love (1997) delineated this unit as a terrace complex because the base(s) are poorly exposed and there is a large range in the heights of the gravel beds (from ~30 to ~73 m above the floodplain), and the tops are buried by several meters of alluvium and eolian sand sheets that prograded across these terraces before erosion dissected arroyo valley fills through the terraces.

Inset against the Lomatas Negras (Tercero Alto of Machette, 1985) is the Edith Fm, which is also middle Pleistocene in age. The late-middle Pleistocene Los Duranes Fm is the best-dated terrace in the area. The 156 ka Albuquerque volcanoes (U/Th date of Peate et al., 1996) is interbedded near the top of this deposit. The broad terrace tread, called the Segundo Alto by Lambert (1968) is buried by 98-110 ka flows of the Cat Hills volcanic field. The Menaul Fm is a gravel deposit found east of the Rio Grande. This deposit may be part of the Los Duranes Fm. Inset against the Los Duranes Fm is the Arenal Fm (Primero Alto surface of Lambert, 1968; also Machette, 1985), which contains a fairly weak soil with Stage I and II+ carbonate morphology (Connell et al., 1998b; Machette et al., 1997). The modern valley alluvium of the Los Padillas Fm insets this lowest terrace deposit.

Entrenchment of the upper Santa Fe Group is constrained by the Lomatas Negras Fm. This deposit contains a fallout ash of the ~0.66 Ma Lava Creek B (Yellowstone National Park, Wyoming and Montana) exposed in an active gravel quarry along the western margin of the Valley (Isleta quadrangle), a couple of kilometers south of this stop (Figs. 2-3 and 2-4). This ash, found about 35 m above the Rio Grande, was geochemically correlated to the middle Pleistocene Lava Creek B (~0.66 Ma; Izett et al., 1992) separately by A. Sarna-Wojcicki (U.S. Geological Survey) and N. Dunbar (N.M. Bureau of Geology and Mineral Resources). Unfortunately, continued quarry operations have buried or possibly obliterated this stratigraphically important ash. This terrace deposit is about 44 m below the Sunport surface, which is underlain by a fallout ash of the upper Bandelier Tuff in Tijeras Arroyo. Boulders of upper Bandelier Tuff are found near the top of the ancestral Rio Grande facies of the upper Santa Fe Group. These were probably deposited from a post-eruption breaching of a lake within the caldera. Thus, the development of the Sunport surface is constrained between 0.7-1.2 Ma.

The slightly higher hills to the west are exposures of the Arroyo Ojito Fm. The discontinuous low spur ridges represent the paleobluff, or buttress unconformity, between this fluvial deposit and the upper Santa Fe Group.

Turn left and continue on Pajarito Rd going west. **0.3**

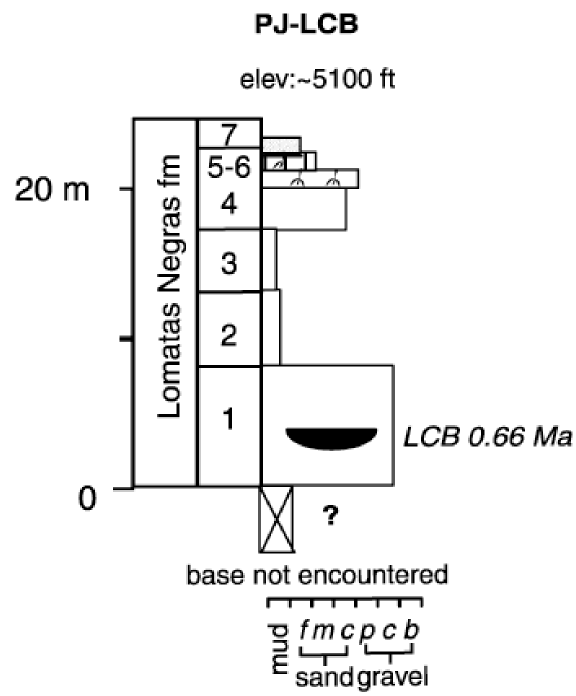

Figure 2-3. Stratigraphic section of the Lomatas Negras Fm at an active gravel quarry in the Pajarito grant. The Lava Creek B ash is within a thick succession of gravel and sand that is overlain by a fining-upward sequence of sand and mud. These fluvial deposits are overlain by a thin tongue of alluvial sediments derived from the western margins of the valley.

16.2 Note slightly higher hill to the northwest (right), which exposes the Arroyo Ojito Fm in a degraded east-facing riser between the Santa Fe Group (ancestral Rio Puerco) and inset fluvial deposits of the ancestral Rio Grande to the east. **0.2**

16.4 Pass under powerlines. The Cejita Blanca is at 1:00. **1.2**

17.6 Top of hill on eastern edge of the Llano de Albuquerque. Turn left (south). Travel south on footwall of west-facing normal fault cutting the Llano de Albuquerque. **0.6**

Figure 2-4. Photograph of fallout ash correlated to the middle Pleistocene Lava Creek B. This ash is within a thick succession of fluvial deposits of the ancestral Rio Grande. Correlative fluvial deposits are 75-85 m above the Rio Grande at the northern end of the basin (Smith et al., 2001).

18.2 Turn right (west) and descend west-facing fault scarp. Light colored hills on horizon between 1:00 and 2:00 are sand dunes that formed along the western edge of the Llano de Albuquerque. Other features on the Llano de Albuquerque include Los Lunas volcano at 10:00, and Wind Mesa, which is cut by a south-trending graben. Between 10:00-11:00 is Gallo Mesa, which is capped by 8 Ma basalt on Colorado Plateau, and lies just west of the rift border Santa Fe fault (Kelley, 1977). **0.4**

18.6 Note brown Quaternary eolian sand with scattered pebbles of Arroyo Ojito Fm. Eolian sand forms a relatively continuous mantle on the Llano de Albuquerque surface, and covers the strongly developed soil, except along its margins or near fault scarps, where gravels are locally exposed. **0.9**

19.5 Ascend one of a number of east-facing fault scarps cut into the Llano de Albuquerque. **0.4**

19.9 Descend west-sloping footwall of fault and descend into another east-facing fault block. **0.4**

20.2 Cross under powerline. We will take this powerline road north to get to Stop 3. **3.2**

23.8 Cinder cones and flows of the middle-to late-Pleistocene Cat Hills volcanic field to the south. Twenty-three cones and seven extensive lava flows, ranging in age from 250 ka to less than 100 ka, mapped by Kelley and Kudo (1978) and Maldonado and Atencio (1998a, b). The Ladron Mts form the skyline to the left. The large facility to the right (north) is the new Bernalillo County Metropolitan Detention center. Water levels from wells drilled in the area indicates about 244 m (800 ft) to water. The water quality on much of the Llano de Albuquerque is poor. At the Detention Center, it is unpotable. Water will likely have to be piped in from the city to accommodate the residents of this institution. **0.6**

24.4 Bear left. **0.1**

24.5 **STOP 2-2.** Ceja del Rio Puerco. Hike south along edge of to Stop. *Dailies NW 7.5' quadrangle. GPS: NAD 83, Z013 S, N: 3,872,220 m; E: 329,510 m.*

The purpose of this stop is to examine the stratigraphy of the uppermost gravels of the Arroyo Ojito Fm (Ceja Mbr) and the overlying soil of the Llano de Albuquerque. We will also discuss the geomorphic development of the Rio Puerco Valley. This stop is at the Ceja del Rio Puerco of Bryan and McCann (1937, 1938), a linear escarpment that defines the eastern margin of the Rio Puerco Valley (Fig. 2-5). Volcanic features of the Llano de Albuquerque are visible to the east (Fig. 2-6).

The broad faulted interfluve between the Rio Puerco and Rio Grande valleys is the Llano de Albuquerque of Bryan and McCann (1938). This surfaces marks a widespread and important local top to the Santa Fe Group and represents the top of the Arroyo Ojito Fm. Kelley (1977) correlated this to the Ortiz surface, which was recognized at the foot of the Ortiz Mts (*cf*. Stearns, 1953). Kelley (1977) extended the Ortiz surface across much of the basin. Other studies (Bachman and Mehnert, 1978; Machette, 1985; Connell et al., 2000, 2001c); however, indicate that a number of surfaces in the basin are of different ages and are not correlative to the Ortiz surface. Lambert (1968) recognized two distinct constructional surfaces in his study of the Albuquerque area. Lambert recognized that the Llano de Albuquerque surface of Bryan and McCann (1938) was probably older than his topographically lower Sunport surface. Machette (1985) also recognized this difference in landscape position and age. On the basis of comparisons of pedogenic carbonate accumulation to other better-dated areas, such as the Mesilla basin of southern New Mexico (Gile et al., 1981), Machette (1985) estimated the age of the Llano de Albuquerque to be around 500 ka, and the Llano de Manzano (Sunport) surface was estimated to be about 300 ka. Geologic mapping, stratigraphic work, and $^{40}Ar/^{39}Ar$ dating indicates that the Llano de Albuquerque surface was formed between 2.58 Ma and 1.6 Ma and the Sunport surface was formed between 1.2 and 0.7 Ma. These revised ages agree somewhat with revised age estimates of similar aged surfaces in the Mesilla basin (i.e., upper and lower La Mesa surfaces, see Gile et al., 1995).

Soils developed on the Llano de Albuquerque are better developed that the Sunport surface and exhibit an ~3-m thick Stage III+ and IV pedogenic carbonate morphology, such as from a trench dug near the center of this surface (Fig. 2-7). This soil forms a discontinuously exposed band along the margins of the Llano de Albuquerque (Fig. 2-6). Soils developed on the Sunport surface commonly exhibit Stage III and III+ pedogenic carbonate morphology. The greater antiquity of the Llano de Albuquerque surface is expressed by the presence of larger fault scarps that cut the surface and the preservation of thick eolian/colluvial wedges adjacent to these intrabasinal faults. In contrast, fault scarps and associated eolian-colluvial wedges are typically shorter and thinner, respectively, on the Sunport surface.

Deposits underlying the Llano de Albuquerque contain cross bedded fluvial sand and gravel and muddy sandstone (Fig. 2-8). Rounded chert, sandstone, and granite, with subordinate amounts of Pedernal chert, porphyritic intermediate to slightly silicic pebbles and cobbles, and scattered basalt, dominate gravel. A bed of pumice-bearing pebble conglomerate with scattered subangular cinders is less than 2 m beneath the base of deposits that contain the Llano de Albuquerque soil (Fig. 2-9). The age of these pumice and cinder gravels are not known, but some of the pumice pebbles correlate may correlate to Pliocene age pumice gravels found beneath the top of the Arroyo Ojito Fm in Rio Rancho, New Mexico and on the Isleta Reservation (N. Dunbar, 2001, personal commun.). $^{40}Ar/^{39}Ar$ dates from these pumice pebbles are pending, but they are similar to other dates pumice pebbles near the top of the Arroyo Ojito Fm section in Rio Rancho and Isleta, New Mexico. Fluvially recycled 2.58 Ma pumice is present the Arroyo Ojito Fm in the Rio Grande Valley to the east. About 4 km south, along the Ceja del Rio Puerco, the 3.00 Ma (Fig. 2-10; date from Maldonado et al., 1999) Cat Mesa basalt is overlain by about 15 m of gravel and sand of the uppermost Arroyo Ojito Fm. These age constraints suggest that the Llano de Albuquerque formed closer to 2.5 Ma, rather than 1.6 Ma. The presence of at least 38-68 m of Arroyo Fm above this 2.58 Ma pumice could also indicate eastward thickening and depositional offlap as deposits of the western margin flowed towards the basin depocenters near the eastern margin of the basin (see Day 1 road log).

Figure 2-5. View to east of the Llano de Albuquerque and late Pliocene and Pleistocene volcanic fields. The Manzano Mountains, in the background, mark the eastern structural margin of the rift.

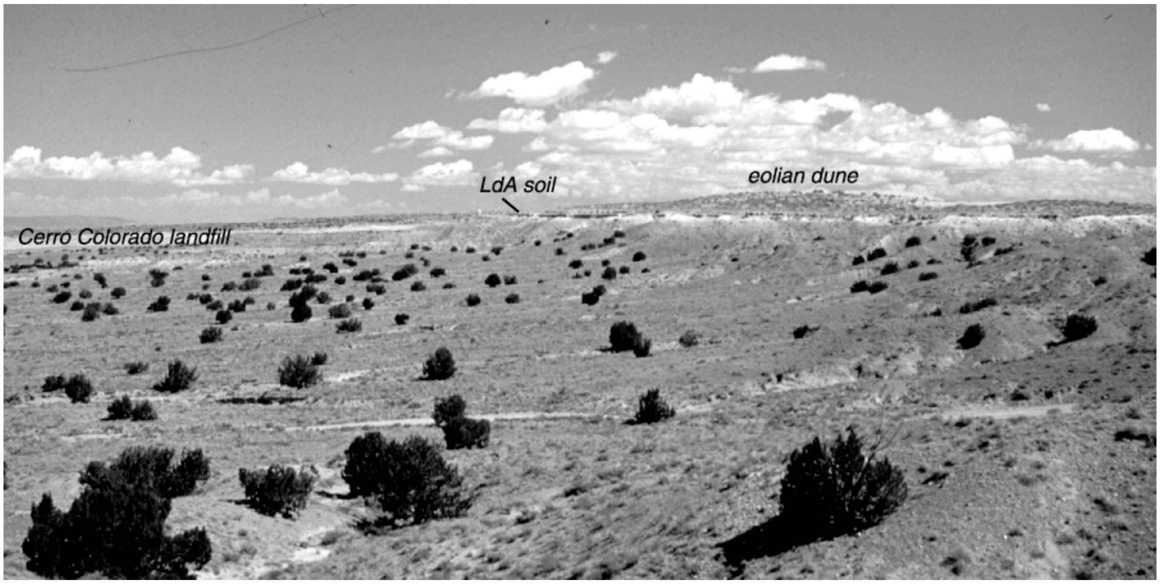

Figure 2-6. View to north along Ceja del Rio Puerco. The white band near the top of the hill is the petrocalcic soil of the Llano de Albuquerque, which is locally overlain by thick dune deposits along the edge.

The Rio Puerco Valley cut about 190 m into the Arroyo Ojito Fm along the western margin of the basin. The presence of ~0.66 Ma Lava Creek B ash (Izett and Wilcox, 1982) about 80 m above the valley floor indicates that this valley was cut prior to 0.7 Ma. A suite of inset, basalt-mantled surfaces are preserved by the Rio Puerco Necks (Hallett, 1990) indicate that these drainages were entrenched on the southeastern Colorado Plateau by late Pliocene time. A longitudinal profile constructed for the lower Rio San Jose (Love, 1986; modified in Love et al., 2001) also indicates Pliocene entrenchment of the Colorado Plateau since about 4 Ma (Fig. 2-11). Aggradation of the upper Santa Fe Group continued after emplacement of the 3.00 Ma (Maldonado et al., 1999) flow and deposition of 2.58 Ma pumice.

Soils of the Llano de Albuquerque contain sparse, scattered pebbles that were probably moved into the soil-profile by bioturbation. Much of the sediment in the soil is fine- to medium-grained sand and is of likely eolian origin. Soils of the Llano de Albuquerque studied to the northeast indicate that horizons contain as much as 53% (weight percent calculation) of micritic carbonate throughout the soil profile (Machette et al., 1997, site 13). This thick petrocalcic soil is overlain at this stop by a 10-m thick succession of eolian sand that contains at least three buried soils.

Differences in height between the Llano de Albuquerque and topographically lower and younger Sunport and Llano de Manzano surfaces are strongly controlled by intrabasinal fault that down-drop the Llano de Albuquerque to the east and to the south (Fig. 2-12; see also Fig. 1-34).

Figure 2-7. Exposure of a petrocalcic soil developed on the Llano de Albuquerque at the Soil Amendment Facility (City of Albuquerque. This exposure is at the east end of a trench cut across an antithetic fault to the San Ysidro (or Calabacillas) fault zone, which was excavated by Jim McCalpin of GEOHAZ, Inc.

The apparent lack of a thick early Pleistocene, Sunport correlative, deposits in the Rio Puerco Valley is puzzling. The lack of preservation of such a thick deposit suggests that erosion within this drainage is quite effective in removing older inset fluvial remnants, or that such older deposits were never deposited along this reach of the Rio Puerco Valley to begin with.

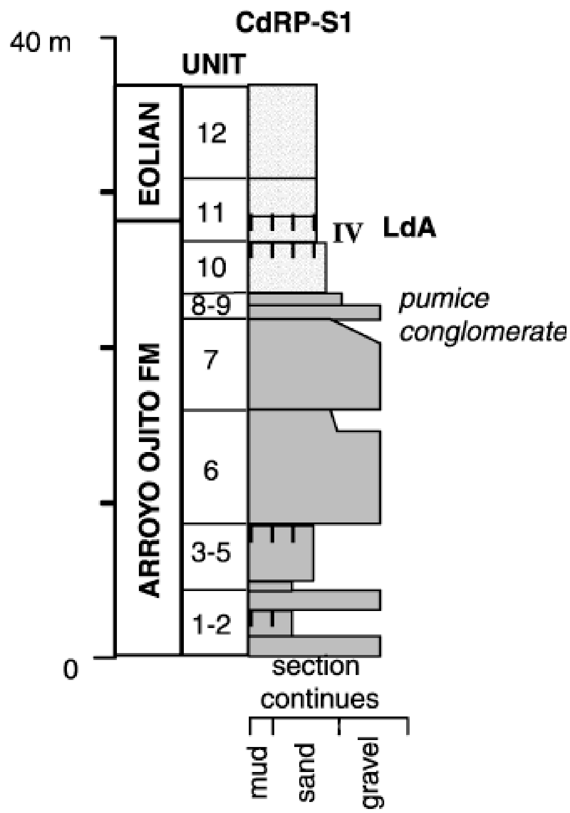

Figure 2-8. Stratigraphic section along Ceja del Rio Puerco at Stop 2-2. A bed of pumice-bearing conglomerate with scattered subangular reddish-brown cinders is less than 2 m below the base of the sandstone that contains the Llano de Albuquerque (LdA) soil.

This lack of preservation of early Pleistocene deposits could be the result of sediment bypass through the valley as a result of a lack of space to accommodate the deposition of such sediment. Activity of the western basin margin faults is not well known, however, projections of Pliocene-aged deposits and volcanic units across the basin boundary (Fig. 2-11) suggest that little significant faulting has occurred since late Pliocene time. Thus, it is possible that faulting did not provide space for significant long-term sediment storage, but rather, sediment was transported out of the Rio Puerco Valley during late Pliocene and early Pleistocene time. This problem warrants further study.

Throughout the literature of the evolution of the Rio Grande one constantly sees references to surfaces, the Llano de Albuquerque, the Llano de Manzano, the Sunport surface etc. What do these surfaces represent and how do you recognize them? Every now and again you also see references to geomorphic surfaces, are they the same as the above surfaces or are they completely different?

Ruhe (1969) defined a geomorphic surface as “ a portion of the land surface comprising both depositional and erosional elements having continuity in space and a common time of origin. It may occupy an appreciable part of the landscape and may include many landforms. A geomorphic surface is established when a stable surface is first exposed to subaerial weathering and soil development”.

Figure 2-9. Uppermost cross bedded gravelly sandstone of the Ceja Mbr. (Arroyo Ojito Fm). A bed of pumice-bearing conglomerate is less than 2 m below the prominent white cliff of the Llano de Albuquerque petrocalcic soil (Stage IV here).

Figure 2-10. The 3.00 Ma Cat Mesa basalt overlies silty sand containing buried paleosols. This basalt is about 15 m below the Llano de Albuquerque. Florian Maldado and Dave Love are kneeling at the foot of this flow.

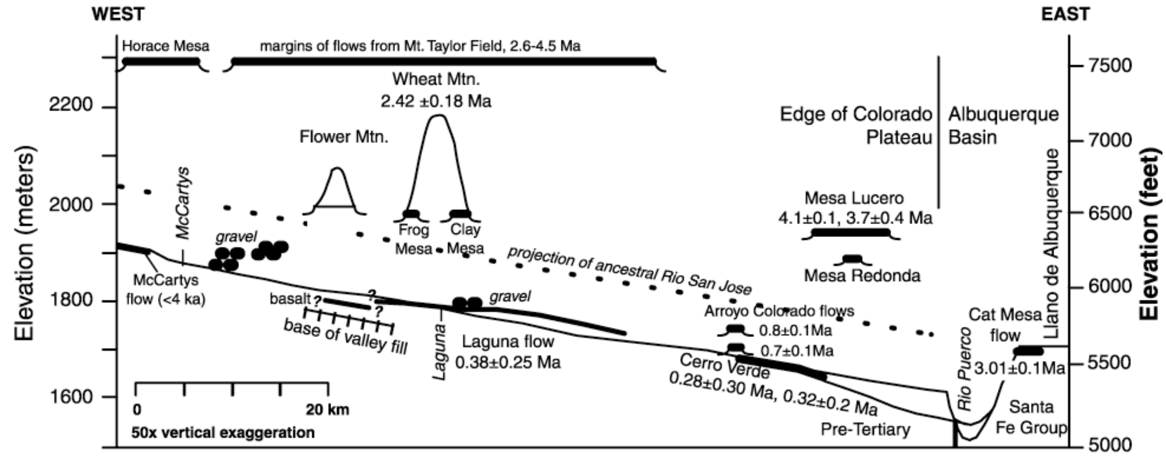

Figure 2-11. Longitudinal profile of the Rio San Jose from the distal end of McCartys flow to the confluence with the Rio Puerco and western edge of the Llano de Albuquerque surface (modified from Love, 1989 with date of Cat Mesa flow from Maldonado et al., 1999). Stratigraphic data indicate that the Llano de Albuquerque is younger than 3.0-2.6 Ma and older than 1.2 Ma. Major incision of the Rio San Jose after about 2.4 Ma suggests that the Llano de Albuquerque surface may have formed somewhat later, perhaps by 2.5-2.0 Ma.

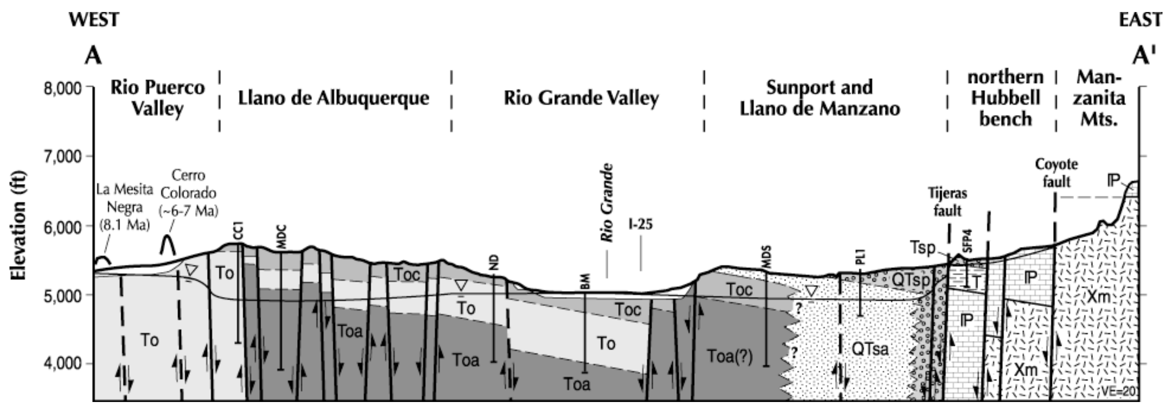

Figure 2-12. Cross section across basin, illustrating structural and geomorphic relationships among the three major lithofacies assemblages. Western fluvial facies of the Arroyo Ojito Fm (undivided, To) are locally subdivided on this diagram into the Ceja Mbr (Toc) and Atrisco unit (Toa, of Connell et al., 1998a). Deposits of the axial Rio Grande (QTsa) and younger (QTsp) and older (Tsp) piedmont facies are east of the Rio Grande deposits. Pre-rift deposits include Paleocene mudstone (T, Thomas et al., 1995), Pennsylvanian limestone and Proterozoic crystalline rocks.

By this definition a geomorphic surface is recognized by the development of a soil profile and it is a time stratigraphic unit. The duration of stability is represented by the degree of soil development. Because of the need to recognize the spatial continuity of erosional and depositional elements the following terms are used: Buried Geomorphic surfaces are parts of former geomorphic surfaces now buried and underlying the present geomorphic surface. Exhumed geomorphic surfaces are former geomorphic surfaces now re-exposed by erosion. Transformation of geomorphic surfaces by erosion or deposition results in the formation of new geomorphic surfaces. The intergrade elements of this continuum are described as degradation and aggradational phases of the present geomorphic surface. These phases are recognized where the soil profile has been modified by degradation exposing B-horizons or aggradation thickening the surface horizons (Tonkin et al., 1981).

The Llano de Albuquerque and Llano de Manzano surfaces as commonly applied in the literature refer to top of the Santa Fe Group gravels, marking the last basin-wide aggradational fill prior to the incision of the Rio Grande Valley in early Pleistocene time. Since this time the surface of these fluvial deposits has been exposed to a wide range of surficial processes, including significant faulting (Machette 1985; McCalpin, 1997) fan progradation from adjacent hillslopes and sand sheet deposition. There are probably very few parts of the original surface existing today and it is unlikely that there are soil profiles that date from that time period and are unaltered by surficial processes. The wide variety of soil profiles described on these surfaces reflects different-aged geomorphic surfaces. This is also true of the incised terrace treads such as the Sunport surface. Thus the bottom line is that soil development cannot be used to identify the Llano de Albuquerque, Llano de Manzano or the Sunport Surfaces.

Turn around and retrace route to intersection of road and powerline at mile marker 20.2. **3.9**

28.4 Turn left (north) at road just east of powerlines. Note prominent west-facing fault scarp to your right (east). **2.8**

31.2 Turn right (east) onto Senator Dennis Chavez Rd. **1.0**

32.2 Descend into valley of the Rio Grande. Deposits of the Arroyo Ojito Fm locally exposed in spur ridges. Valley border fans are incised into the Los Duranes Fm and overlie the Arenal Fm. **2.2**

34.4 Flat surfaces underneath housing development is the Primero Alto surface and underlying Arenal Fm, a late Pleistocene fluvial deposit of the ancestral Rio Grande that is inset against the middle Pleistocene Los Duranes Fm. **0.4**

34.8 Crossing onto floodplain of the Rio Grande. Road is built on fill over this deposit. **0.6**

35.4 Cross Coors Blvd. Continue straight (east) where road becomes Rio Bravo Blvd. (NM-500). **1.9**

37.3 Cross Isleta Blvd (NM-314). Continue east and descend into yazoo along eastern margin of valley. **1.8**

39.1 Ascend valley border alluvium, which prograded over the Rio Grande floodplain. Prepare to turn right. **0.2**

39.3 Turn right (south) onto South Broadway (NM-47). Mesa to left (east) is the Sunport surface and the Albuquerque International Airport (a.k.a. Sunport). **1.4**

40.7 Driving on the sandy alluvium of Tijeras Arroyo. This arroyo contains a mixture of granite, greenstone, gneiss, and sandstone near its mouth at the front of the Sandia Mountains. Deposits derived from the Tijeras Arroyo drainage basin are more heterolithic than alluvium derived from the western front of the Sandia Mts, which contains mostly granite, schist, and minor limestone. **0.4**

41.1 Turn left (east) onto Bobby Foster (Los Picaros) Rd. **0.5**

41.6 Turn right (south) at junction with Los Picaros Rd. Drive uphill towards the Journal Pavilion. Ascend deposits of the Arroyo Ojito Fm. White bed at 2:00 on west side of I-25 is within the Arroyo Ojito Fm. This bed contains a recently discovered microvertebrate site of probable medial Blancan age (Pliocene; G. Morgan, 2001, personal commun.). **0.8**

42.4 Top of hill. Pale beds on top of the mesa contain Stage III+ soils of the Sunport surface, which is developed on a west-thinning wedge of pumice-bearing deposits of the ancestral Rio Grande. The early Pleistocene ancestral Rio Grande fluvial system extended at least 7 km east of here **0.6**

43.0 Disturbed area around road is reclaimed South Broadway landfill, which intermittently operated as an unlined municipal landfill between 1963-1990. **0.4**

43.4 View of range-bounding eastern margin of the Albuquerque Basin. The Sandia Mts at 10:00-12:00, Four Hills salient of the Sandia Mts at 12:00, the flat-topped Manzanita Mts at 12:00-2:00, and the higher Manzano Mts to the south. Tijeras Canyon, one of the largest rift-border drainages in the area and the namesake drainage of Tijeras Arroyo, enters the basin at about 12:00. Scarps of the Hubbell Spring fault zone extend south from the Four Hills. **0.8**

44.2 Large excavations to your right (east), locally known as the "Suez canal," expose the Sunport soil and overlying eolian deposits. **0.3**

44.5 **STOP 2-3.** Pull off road onto shoulder at north end of 3.3 m deep pit. Sunport surface. *Albuquerque East 7.5' quadrangle: GPS, NAD83, Z 013 S, N: 3,874,245 m; E: 352,010 m.*

At this stop we will examine soils of the early Pleistocene Sunport surface, which is commonly overlain by a thick accumulation of eolian sand (Fig. 2-13). The Sunport soil is about 1.6 m thick and commonly exhibits a strongly developed Stage III+ carbonate morphology. Strongly developed platy structure is also present in the strongest developed parts of the soil profile. The top is irregular, eroded, and is overlain by about 1.6 m of eolian sand with weakly to moderately developed soils and is Holocene to latest Pleistocene (?) in age. This soil is developed on loose sand and pebbly sand of the ancestral Rio Grande, which is less than 1 m below the base of this detention pit.

Figure 2-13. Recently constructed flood detention pit on east side of Journal Pavilion parking lot. The Sunport soil is about 1.5 m thick and exhibits Stage III+ carbonate morphology. The top of the soil is irregular and has been modified by relatively deep pipes developed into the profile.

Turn around and leave Journal Pavilion parking area and head towards intersection of Los Picaros and Bobby Foster Rds. **0.5**

45.0 Northern Hubbell bench, and site of stop 2 of the day 1 field trip at 10:00-11:00. The numerous buildings at the foot of the Manzanita Mts and Four Hills salient are part of Sandia National Laboratories. **2.0**

47.0 Cross intersection with Bobby Foster Rd. Continue straight. **0.8**

47.8 Steep-walled arroyo of Tijeras Creek. About 2 m below the surface is a zone containing abundant charcoal. A sample was radiocarbon dated at about 4550 yr. BP. **0.4**

48.2 The exposures to your right (south) contain gray gravel and sand of the ancestral Rio Grande deposits, which overlie brown sand of the Arroyo Ojito Fm. The underlying Arroyo Ojito deposits commonly contain carbonate-cemented sandstone and rhizoconcretionary intervals. **1.3**

49.5 Off-road vehicle recreation area to the south. **0.1**

49.6 Pass intersection with Ira Specter Road. Keep straight. **0.1**

49.7 Pass through gate onto Albuquerque Open-Space Division Headquarters at Montessa Park. Check in with Open-Space division before proceeding east. Drive east towards metal warehouse buildings near end of complex. **0.1**

49.8 **STOP 2-4.** Southeast corner of Kaibab Warehouse #1. Hydrocompactive soils. *Albuquerque East 7.5' quadrangle: GPS, NAD 83, Z 013 S, N: 3,876,195 m; E: 354,435 m.*

Hydrocompactive or collapsible soils lose a significant amount of volume through reduction of porosity when wetted. Hydrocompactive sediments are typically composed of poorly sorted fine-grained sand with minor amounts of silt or clay that were deposited by debris- or hyperconcentrated flows. These deposits typically occur on geologically young, gently sloping alluvial-fan, alluvial-slope, or valley-fill environments that have not been saturated since deposition. Hydrocompactive soils have damaged roads, utility lines, and buildings, such as the Kaibab Warehouse #1 (Fig. 2-14) in several parts of New Mexico (see Haneberg, 1992).

Before collapse, the soil structure of these deposits is porous and has relative low unit weights (typically less than 16 kN/m^3) and high void ratios (typically higher than 1.0). Upon wetting, these deposits typically disaggregate and compact. Because of the geologic age and setting, geologic mapping can be used to predict where such soils may be present. Geologic mapping of the eastern part of the Albuquerque metropolitan area north to Bernalillo, New Mexico (Connell, 1997, 1998; Connell et al., 1995; 1998b) and evaluation of available geotechnical data suggests that the Holocene-latest Pleistocene arroyo and valley border alluvial deposits are particularly susceptible to hydrocompaction. Future studies will attempt to produce predictive hydrocompaction susceptibility maps.

At this stop, we see damage caused by hydrocompactive soils. This building was constructed on about 24 m (80 ft) of poorly sorted sand and mud of Tijeras Arroyo. Note the circular cracks in the asphalt road around a patch of bare ground that was presumably used to drain surface runoff from roads, buildings, and water from a fire hydrant. The concentration of runoff into this patch of bare ground caused collapse of the surrounding soil and foundation, resulting in distress to the warehouse building. Seargent, Hauskins and Beckwith, and Woodward-Clyde studied the Montessa Park facility in 1983 and 1973, respectively (Seargent, Hauskins, Beckwith, 1983). They drilled cores and measured the amount of consolidation, before and after wetting of the sample, under differing static loads (Fig. 2-15). The combined results of this study indicate the presence of hydrocompactive deposits down to the level of groundwater saturation under high loads. Under *in situ* loads, hydrocompaction of up to 5% was reported to a depth of about 18 m. Should the entire column of sediment at this site become saturated, the total consolidation would be about 5.5% and would represent a subsidence of about 1.3 m at *in situ* loads. The addition of greater loads, such as a multi-story building, would increase this subsidence at the more hydrocompactive shallow end of the sediment column. Estimates of ground subsidence, based on elevation differences between the north and south edges of the building, indicate that this structure has undergone approximately 0.6-0.8 m of deformation, mostly on the southern four garage bays. These would be maximum estimates because they assume total saturation of the sediment column, which would create other geotechnical problems, and they also ignore effects of grain bridging of the soil column at depth.

Figure 2-14. Photograph of the south end of the Kaibab Warehouse #1 facility at Montessa Park. Note the arcuate cracks in the asphalt, which have been repaired. These cracks encircle the exposed soil to the left of the building. The doors of this warehouse are out of plumb and rest on the foundation along the right side, but are not supported to the left. Dave Love is at right side of photograph.

Turn around and leave Montessa Park facilities. **0.1**

50.4 Pass through gate. **0.6**

60.0 Turn hard left towards Albuquerque National Speedway. **0.4**

60.4 Exposures of pumice-bearing fluvial deposits of the ancestral Rio Grande to the south are lower in elevation relative to deposits of the Arroyo Ojito Fm at the mouth of Tijeras Arroyo. **0.5**

60.9 Crossing contact between fluvial deposits and overlying piedmont- and eolian-dominated deposits of the Sierra Ladrones Fm. Section contains at least 3 calcic soils. Top of hill is capped by a Stage III+ soil. **0.5**

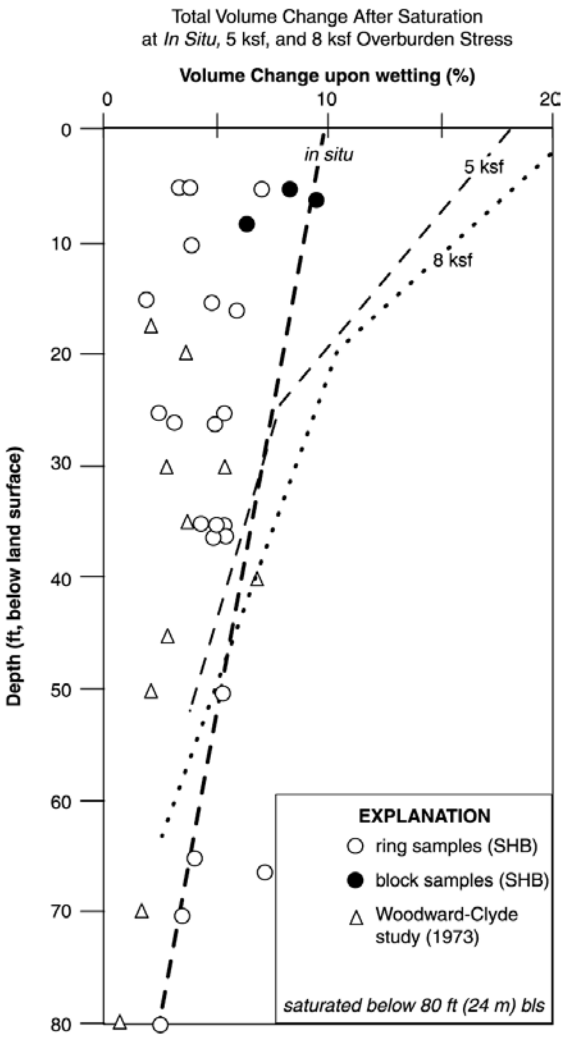

Figure 2-15. Plot of percent consolidation of cored sediment upon saturation with water. From technical report by Seargent, Hauskins & Beckwith (1983)

61.4 **STOP 2-5.** Crest of hill. Turn around and park on right (east) side of road. Walk toward borrow pit to at northeast part of road. Near eastern pinchout of eastern-margin piedmont deposits over ancestral Rio Grande. *Albuquerque East 7.5' quadrangle: GPS, NAD 83, Z 013S, N: 3,875,250 m; E: 354,345 m.*

Recent unpublished geologic mapping of Tijeras Arroyo (Fig. 2-16) delineates the presence of western-fluvial, axial-fluvial, and eastern-piedmont deposits. Gravel from these three major lithofacies assemblages have been studied and indicate that comparing the proportions of metaquartzite can quite easily differentiate among these facies, as can comparisons to chert to sandstone, volcanic, or crystalline rocks (Fig. 2-17).

Gravel was compared among the three lithofacies assemblages. Strong clustering is recognized in comparisons of chert and metaquartzite to sandstone, volcanic, and plutonic/metamorphic constituents (Fig. 2-17). The western fluvial lithofacies assemblage (Arroyo Ojito Fm) contains abundant volcanic tuff, fine-grained red granite, sandstone, and Pedernal chert, whereas the ancestral Rio Grande lithofacies contains abundant volcanic tuffs and well-rounded metaquartzite clasts. These metaquartzite clasts are white, gray, pink, or bluish-purple and are often bedded. Although granites, sedimentary rocks, and Pedernal chert can be found in ancestral Rio Grande deposits, they are not common. Piedmont deposits contain abundant crystalline (plutonic/metamorphic) and sedimentary clasts, and generally lack volcanic detritus in the study area. Chert comprises between 30-60% of the western fluvial lithofacies, and about 2-8% of the axial-fluvial deposits. Metaquartzite is almost entirely composed of the well-rounded metaquartzite variety, comprises between 30-85% of the axial-fluvial lithofacies. In contrast, metaquartzite is a minor constituent of western-fluvial deposits. Volcanic gravel is nearly absent in the eastern-piedmont lithofacies, but is abundant in the western-fluvial and axial-fluvial assemblages. Sedimentary clasts (mostly sandstone) comprise about 35-40% of the western-fluvial lithofacies gravel, but are nearly absent in the axial-fluvial assemblage. Sandstone is locally recognized along the margins of the axial-fluvial assemblage, but only comprises a minor component of those deposits. The absence of the sedimentary component within the piedmont lithofacies in the study area is related to the composition of drainage basins that originate on the footwall uplifts of the Sandia and Manzanita Mts. Plutonic/metamorphic gravel is present in the axial-fluvial and western-margin deposits in similar proportions and comprises the bulk of the piedmont composition in the study area; however, sedimentary gravel is a dominant constituent elsewhere along the piedmont, indicating that the lithologic composition of eastern-margin drainages depends upon on composition of upland drainages.

Discrimination among lithofacies assemblages is best expressed in the ternary relationship among chert-metaquartzite-plutonic/metamorphic and chert-metaquartzite-sedimentary rocks (Figs. 2-17). The field of variation for two standard deviations, around the mean composition, indicates no overlap of the three lithofacies assemblages if chert and metaquartzite are compared to sandstone and volcanic constituents. Strong clustering is also observed in comparisons of chert-metaquartzite-volcanic and to a lesser extent when chert and metaquartzite are combined. The weakest clustering occurs where chert+metaquartzite as compared to other constituents in the absence of the sedimentary component. This is because sedimentary detritus makes up a large component of the western-fluvial lithofacies assemblage.

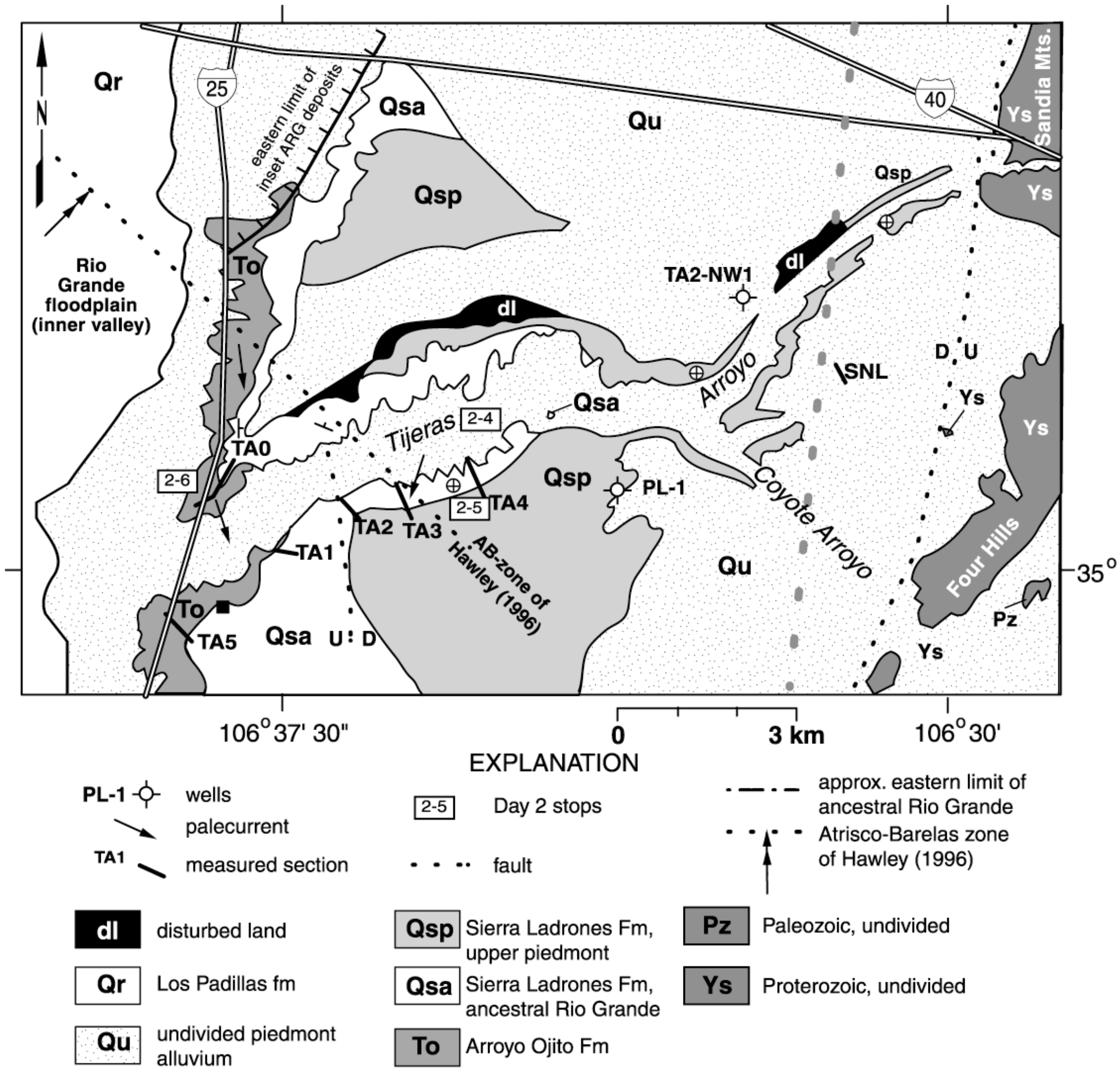

Figure 2-16. Simplified geologic map of Tijeras Arroyo and vicinity (modified from Connell et al., 1998b; Connell, unpubl.; Maldonado et al., *in prep*.).

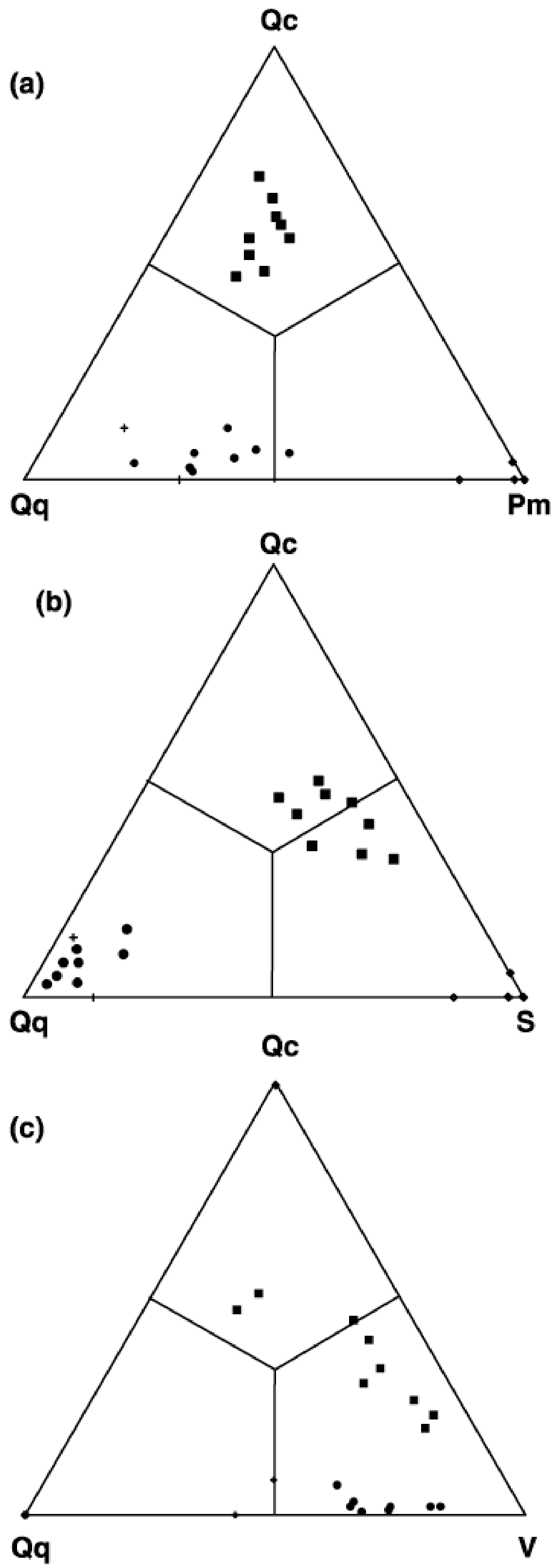

Figure 2-17. Ternary discrimination diagrams of detrital modes of gravel from stratigraphic localities in the southern Albuquerque and Isleta areas. Solid squares, circles, and diamonds indicate western fluvial, axial-fluvial, and eastern piedmont lithofacies assemblages, respectively. The open square, open circle, and "x" denote the mean of the western fluvial, axial-fluvial, and eastern piedmont lithofacies assemblages, respectively. The "+" and open diamond indicate compositions of younger inset (post-Santa Fe Group) fluvial deposits of the ancestral Rio Grande, and Tijeras Arroyo alluvium, respectively. Comparisons of chert (Qc) and quartzite (Qq) to plutonic/metamorphic (Pm) (a) and sandstone (S) (b) constituents indicate the strongest clustering. Comparisons of chert and quartzite to volcanic (V) constituents (c) indicates some overlap of fields of variation.

The spatial variations of lithofacies assemblages in Tijeras Arroyo indicate progradation of the eastern-margin piedmont over the ancestral Rio Grande deposits. Eastern piedmont deposits, which are quite sandy at this stop, pinch out into sandstone about 1.5 km to the west, between TA1 and TA2 (Fig. 2-18). Multiple soils exposed at this site merge into a single soil less than 1.5 km to the west.

Stratigraphic relationships at this stop support the presence of a progradational wedge of early Pleistocene sediment that onlaps onto older sediments of the Arroyo Ojito Fm. Drillhole data also do not support the presence of a buttress unconformity bounding the eastern side of a 6-10 km wide early Pleistocene fluvial terrace as proposed by Cole et al. (2001a, b) and Stone et al. (2001a, b).

Drive towards mouth of Tijeras Arroyo at Bobby Foster-Los Picaros intersection. **3.6**

65.0 Turn right (west) onto Bobby Foster Rd. **0.2**

65.2 Note abundant anthropogenic auto-recyclic deposits at mouth of Tijeras Arroyo. **0.4**

65.6 Turn right (north) onto South Broadway (NM-47). **0.7**

66.3 Turn right (east) onto long dirt driveway at 4500 Broadway SE. The gate may be locked. **0.1**

66.4 Pass through gate. **0.2**

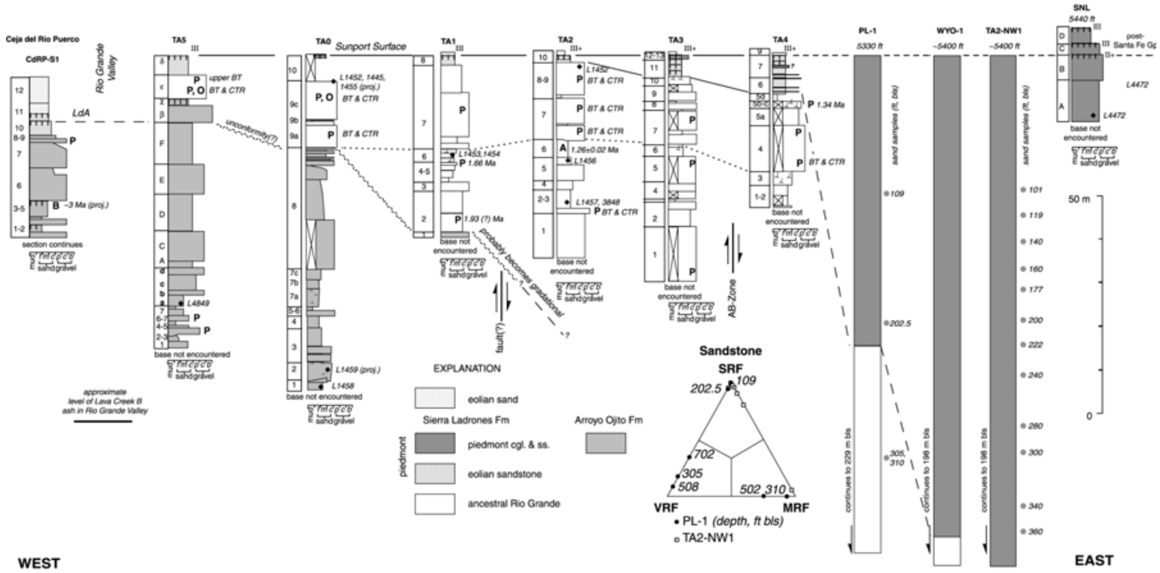

Figure 2-18. Fence diagram of stratigraphic sites for Day 2. Horizontal distances are not to scale. Note westward progradation of eastern-margin piedmont and ancestral Rio Grande deposits. The eastern thickening wedge of piedmont deposits are interpreted from drillhole data from wells on the Sandia National Laboratories. Some of the lithologic interpretations are constrained by sandstone petrography, which shows the proportions of sandstone (SRF), volcanic (VRF), and metamorphic (MRF) rock fragments in these wells (Thomas et al., 1995). The piedmont facies here contain no volcanic detritus, therefore the presence of such material indicates ancestral Rio Grande or Arroyo Ojito sediments. Because of the location of these wells near the eastern side of the basin, the deposits are likely ancestral Rio Grande.

66.6 **STOP 2-6.** Gravel quarry near mouth of Tijeras Arroyo. Walk to northern margin of Tijeras Arroyo along Railroad tracks. Park on north side of gravel quarry. *Albuquerque West 7.5' quadrangle, GPS, NAD 83, UTM Zone 013 S; N: 3,875,400 m; E: 345,000 m.* Walk east to abandoned railroad tracks and under the I-25 overpass to examine the nature and stratigraphic context of the contact between the axial-fluvial Rio Grande and underlying Arroyo Ojito Fm.

Lucas et al. (1993) measured a section at the mouth of Tijeras Arroyo to document the stratigraphic positions of a Pliocene (*medial* Blancan) and numerous early Pleistocene (early Irvingtonian) fossil localities exposed in the arroyo. They suggested the possibility of an unconformity in this section, based mainly on absence of late Blancan fossils and because of an inferred unconformity between Pliocene and lower Pleistocene fluvial sediments near San Antonio, New Mexico (Cather and McIntosh, 1990), in the Socorro Basin, about 140 km to the south. At San Antonio, exposures of pumice-bearing ancestral Rio Grande deposits at the Bosquecito pumice site contain pumice of the lower Bandelier Tuff. This deposit was originally interpreted to be inset against older non-pumiceous deposits of the ancestral Rio Grande (Cather and McIntosh, 1990). Later work, however, demonstrated that this relationship was the result of faulting, and not due to Plio-Pleistocene entrenchment (Dunbar et al., 1996, p. 70). Lucas et al. (1993) note the presence of pumice low in the section that may have represented this unconformity at Tijeras Arroyo. The lowest exposure of pumice in the section would presumably mark the onset of early Pleistocene sedimentation (i.e., contains clasts of Bandelier Tuff). However, the presence of Pliocene-age pumice pebbles in the Arroyo Ojito Fm (see Stop 2-2) indicates that caution must be used in determining age and provenance on the basis of pumice clasts as the sole criterion.

Geologic mapping and preliminary results of gravel and sand petrography indicate that the lower part of the succession at this stop is correlative to the Arroyo Ojito Fm (Fig. 2-16, 2-17; Connell et al., 1998b; Connell and Derrick, unpubl. data). Deposits of the Arroyo Ojito Fm contain sparse scattered pumice pebbles and are overlain by pumice-bearing sand and gravelly sand deposits of the ancestral Rio Grande that are about 20 m below the Sunport surface. Tephra in this upper succession are correlated to the early Pleistocene Bandelier Tuff and Cerro Toledo Rhyolite (Jemez volcanic field) and were laid down by the ancestral Rio Grande during early Pleistocene time. These stratigraphically higher deposits contain early Irvingtonian (early Pleistocene) mammals (Lucas et al., 1993). The ancestral Rio Grande deposits contain more abundant rounded quartzite than the underlying deposits, which contain abundant chert and sandstone clasts. An ash dated at 1.26 Ma is several meters below the top of the ancestral Rio Grande section in an exposure along the southern margin of Tijeras Arroyo.

During repeated reconnaissance of Tijeras Arroyo between 1998-2001, we mapped the geology of the arroyo and re-measured the stratigraphic section of Lucas et al. (1993; Fig. 2-19). Five additional stratigraphic sections supplemented this section in order to document lateral variations in facies (Fig. 2-18). Lucas et al. (1993) recognized, but did not differentiate, two distinct facies in this section. We concur with their observation and have differentiated these facies on our stratigraphic column. At the mouth of Tijeras Arroyo, early Pleistocene-aged, pumice-bearing sand and gravel of the ancestral Rio Grande (Sierra Ladrones Fm) overlie deposits of the Arroyo Ojito Fm.

Comparisons of these two sections indicate significant discrepancies (Fig. 2-19). With the help of Spencer Lucas, we correlated units of the Lucas et al. (1993) section into our recent profile. Comparisons of these marker beds indicate that the overlying Sierra Ladrones Fm is much thinner than portrayed by Lucas et al. (1993). This discrepancy is likely due to mis-correlations of fine-grained marker beds and associated fossil localities into this section and facies variations.

A rich mammalian fossil locality was recently discovered by S. Connell along the southern margin of Tijeras Arroyo at a road cut along I-25. Preliminary studies of this locality indicate a likely *medial* Blancan age (G. Morgan, 2001, personal commun.). This fossil-bearing unit projects to unit 4 of Lucas et al. (1993), which is stratigraphically higher than the unit 2-3 contact of Lucas et al. (1993) (Fig. 2-18).

Aside from the distinctive lithologic changes in the section, there is little evidence for a major unconformity or scour in these exposures. Deposits of the underlying Arroyo Ojito Fm do not contain strongly developed paleosols, however, pauses in sedimentation may be inferred by the presence of locally extensive cemented sandstone intervals and rhizoconcretionary mats. The lack of a buried pedogenic counterpart to the Llano de Albuquerque suggests that some erosion of the top of the Arroyo Ojito Fm has occurred in the Tijeras Arroyo area.

An examination of exposures in Tijeras Arroyo (Fig. 2-18) indicates that the Arroyo Ojito/Sierra Ladrones contact dips to the east and ancestral Rio Grande deposits thicken appreciably to the east. Age constraints in the upper part of the Arroyo Ojito Fm are poor, but the presence of a fluvially recycled pumice at 2.58 Ma indicates that the upper part of the Arroyo Ojito section is younger than 2.58 Ma. Early Pleistocene deposits of the ancestral Rio Grande overlie these deposits. Stratigraphic relationships strongly suggest the presence of an unconformity between these two deposits, which is consistent with angular relationships between these units observed near faults to the south (Fig. 2-20).

Studies of gravel composition (Fig. 2-17) and the discovery of this *medial* Blancan fossil locality support the presence of an unconformity as speculated by Lucas et al. (1993); however, this probable unconformity is stratigraphically higher (at the unit 9/8 contact in TA0, Fig. 2-19) than their reported lowest occurrence of pumice in the section (unit 3 of Lucas et al., 1993). The stratigraphically lower pumice pebbles are likely correlated to the suites of Pliocene-aged pumice pebbles found in the Arroyo Ojito Fm to the south and west, rather than being associated with the early Pleistocene Bandelier Tuff.

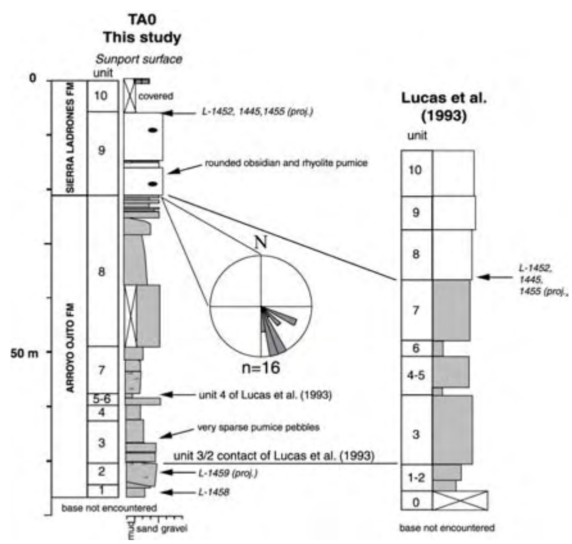

Figure 2-19. Comparison of stratigraphic sections measured at the same location at the northern mouth of Tijeras Arroyo. Left: stratigraphic section TA0. Right: Stratigraphic section of Lucas et al. (1993). Paleocurrent data from the top of the exposed Arroyo Ojito Fm indicates flow to the south-southeast.

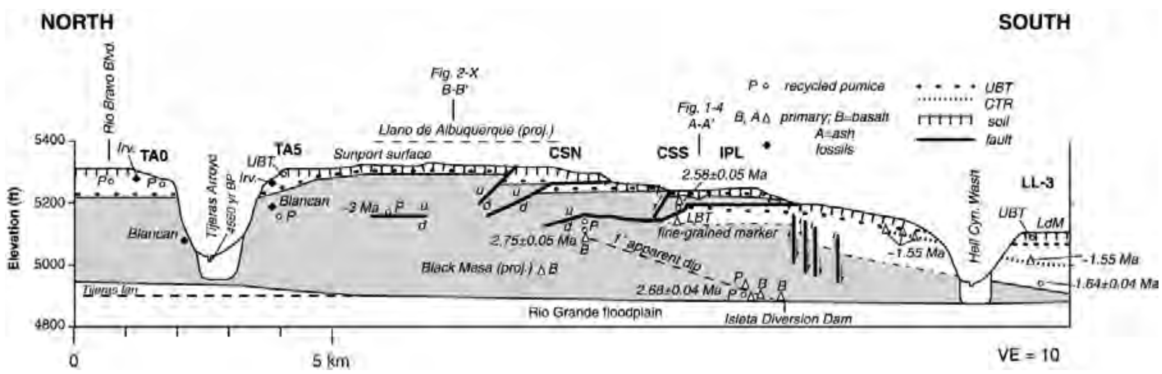

Figure 2-20. Cross section between Rio Bravo Blvd and Hell Canyon Wash showing southward apparent dip of Arroyo Ojito Fm and the preservation and southward thickening of ancestral Rio Grande deposits. Angular unconformity beneath thin ancestral Rio Grande deposits between Tijeras and Hell Canyon arroyos is due to erosion of an intrabasinal horst block. About 100 m of sediment is preserved between 2.7 Ma and 1.6 Ma tephras. About 12-45 m of ancestral Rio Grande deposits that post-date emplacement of a Cerro Toledo Rhyolite ash (~1.55 Ma) are exposed at the mouth of Hell Canyon Wash. This cross section is sub-parallel to faults (shown as bold lines), which have shallow apparent dips.

This unconformity, however, is probably not associated with a Plio-Pleistocene entrenchment event, but rather may represent progressive westward onlap of axial-river facies. Drillhole data to the east of the Tijeras Arroyo measured sections do not support the presence of any significant buttress unconformity between the pumice-bearing ancestral Rio Grande deposits and older basin fill (see Fig. 2-18). This interpretation is supported by studies of the Sandia National Labs by GRAM Inc. and William Lettis and Associates (Thomas et al., 1995) that document interfingering of axial-river and piedmont deposits in the subsurface. The age and stratigraphic significance of such intraformational unconformities is still ambiguous, but ongoing work on the biostratigraphy and pumice pebble correlation should constrain this.

Deposits of the Sierra Ladrones Fm prograde westward and overlie this unconformity with the underlying Arroyo Ojito Fm. Although the stratigraphically significant relationships are buried to the east by Pleistocene fluvial deposits of the ancestral Rio Grande, the geometry of these sediments suggests westward onlap of the Rio Grande over eroded remnants of the Llano de Albuquerque. With few exceptions, deposits of the ancestral Rio Grande are not present west of the Rio Grande Valley, but are quite thick to the east. The location of the Rio Grande Valley could be explained by westward progradation of eastern-margin piedmont deposits and onlap of the Rio Grande during early Pleistocene. During this westward onlap, the Rio Grande entrenched into older basin fill and developed the present valley. This hypothesis is currently being tested by additional field work and dating.

Westward progradation of axial-fluvial and eastern-margin piedmont deposits is recognized along most of the eastern margin of the basin from Isleta Reservation to north of San Felipe Pueblo, about 45 km to the north. Exposures of western, axial, and eastern facies are well exposed in the southern Santo Domingo sub-basin, near San Felipe Pueblo (Fig. 2-21). Pliocene basaltic flows of Santa Ana Mesa and various fluvially recycled and primary tephra constrain the ages of deposits. Stratigraphic sections measured on San Felipe Pueblo document the presence of lithologically indistinguishable pre-2.58 Ma and pre-1.55 Ma vintage ancestral Rio Grande deposits. No unconformities are recognized in the section; however, deposits of the ancestral Rio Grande appear to pinchout to the west and probably buried only part of the eastern edge of the ~1.77-2.58 Ma flows of Santa Ana Mesa (Fig. 2-22).

A significant problem with defining the end of basin aggradation is presented in attempting to correlate unconformities formed along the basin margin, on the up-dip portions of half-graben or asymmetric basins into basin depocenters (see Connell et al., 2001c). Differentiation of stratal discontinuities within deposits of the ancestral Rio Grande would be ambiguous at best, and arbitrary at worst.

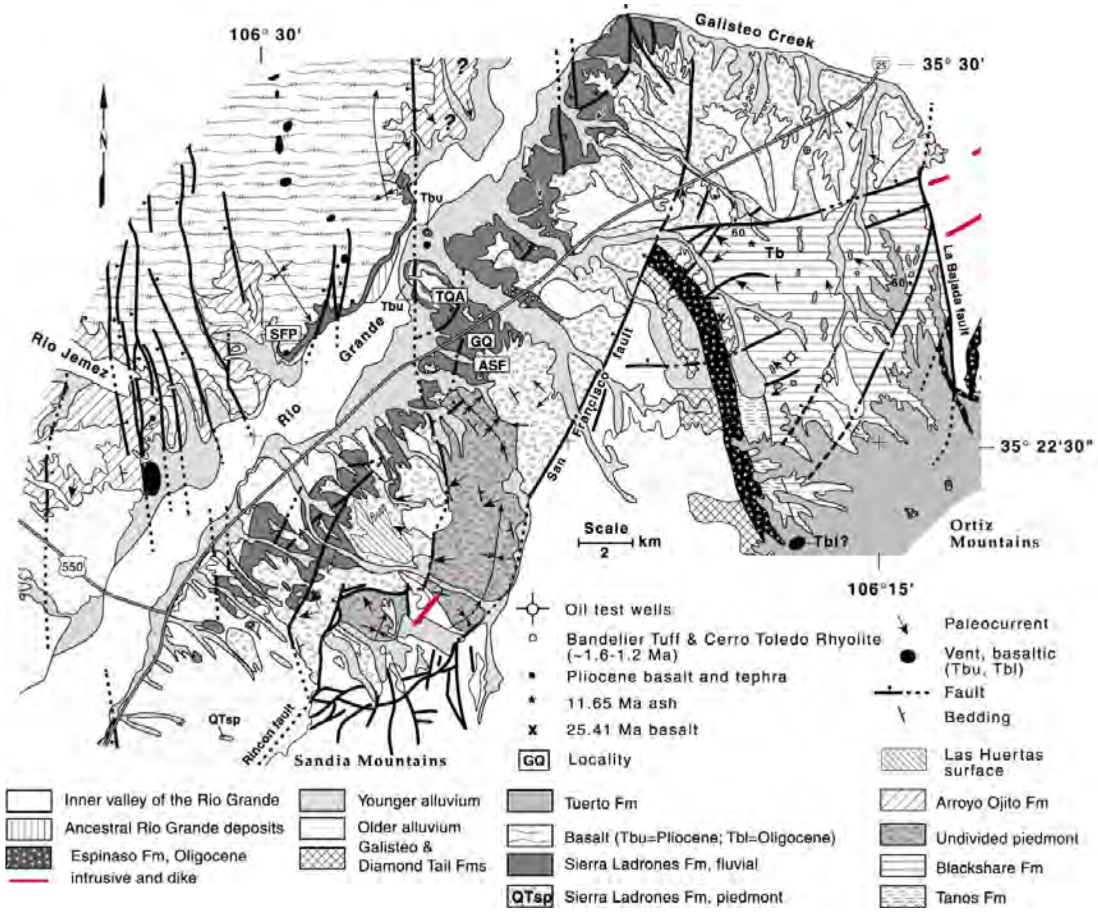

Figure 2-21. Simplified geologic map of the southeastern Santo Domingo sub-basin, illustrating locations stratigraphic sections in San Felipe Pueblo. Compiled from Cather and Connell (1998), Cather et al. (2000), Connell, (1998), Connell et al. (1995), and unpublished mapping.

Pre-Pleistocene deposition of the ancestral Rio Grande is well documented in southern New Mexico, where the earliest appearance is between 4.5 to ~5 Ma (Mack et al., 1996; Mack, 2001). In the San Felipe area, gravel-bearing ancestral Rio Grande deposits are recognized beneath the 1.77-2.58 Ma basalts on the southeastern flank of Santa Ana Mesa. The earliest documented appearance of a probable ancestral Rio Grande deposits in the Albuquerque Basin is near the northern end at Tent Rocks, where metaquartzite-bearing pebbly sandstone is associated with 6.9 Ma tephra of the Peralta Tuff of the Bearhead Rhyolite (Smith et al., 2001).

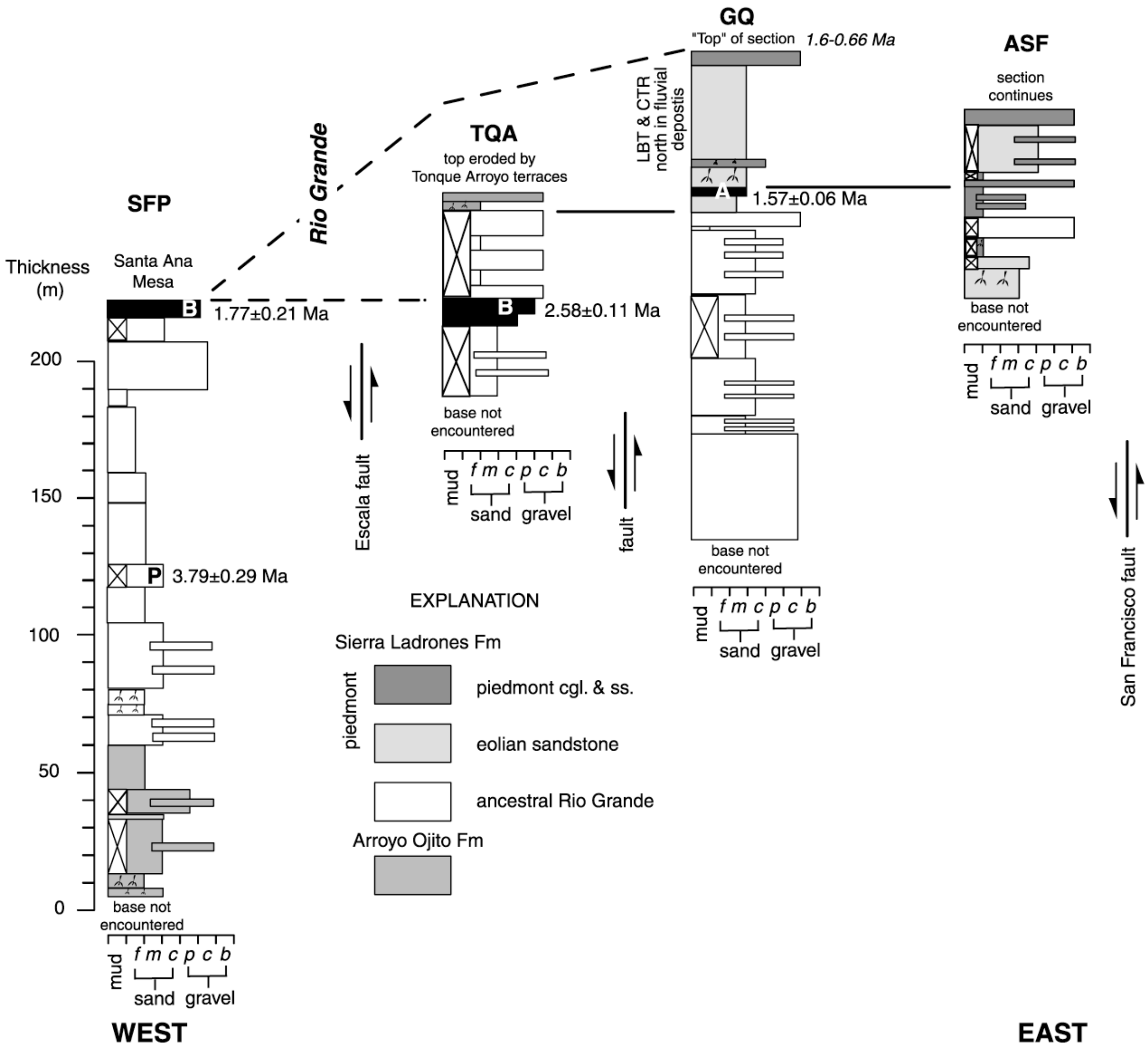

Figure 2-22. Fence diagram on San Felipe Pueblo illustrating stratigraphic relationships among western-fluvial, axial-fluvial, and eastern-margin piedmont deposits (Derrick and Connell, 2001; Derrick, unpubl. data). Santa Fe Group deposits pinchout onto the eastern edge of Santa Ana Mesa. See Figure 2-22 for locations of sections.

If incision of basin fill is climatically driven, then the proposed late Pliocene entrenchment proposed by Stone (2001a, b) and Cole (2001a, b) should be regional in nature. Comparisons of the stratigraphy of the Albuquerque Basin with radioisotopically and paleomagnetically well dated comparable successions of the southern Rio Grande rift (Fig. 2-23; Mack et al., 1993, 1996; Mack, 2001) indicate the presence of nearly continuous aggradation until about 800 ka, when the Rio Grande Valley cut. In the tectonically quiescent part of a southern Basin and Range in southeast Arizona, Smith (1994) documents basin aggradation of the St. David Fm during Pliocene and early Pleistocene times (Fig. 2-23). Thus, it seems reasonable to speculate that this early Pleistocene entrenchment might be climatically driven. However, there is little evidence for the presence of a regional climatically induced unconformity in these basins. These basins tend to coarsen upsection, suggesting that the increased caliber of sediment might be attributed to climate, which presumably became more competent during the late Pliocene. The nature of these stratigraphic changes will no doubt be of continued interest and study.

Return to NM-47. End of Day-two road log.

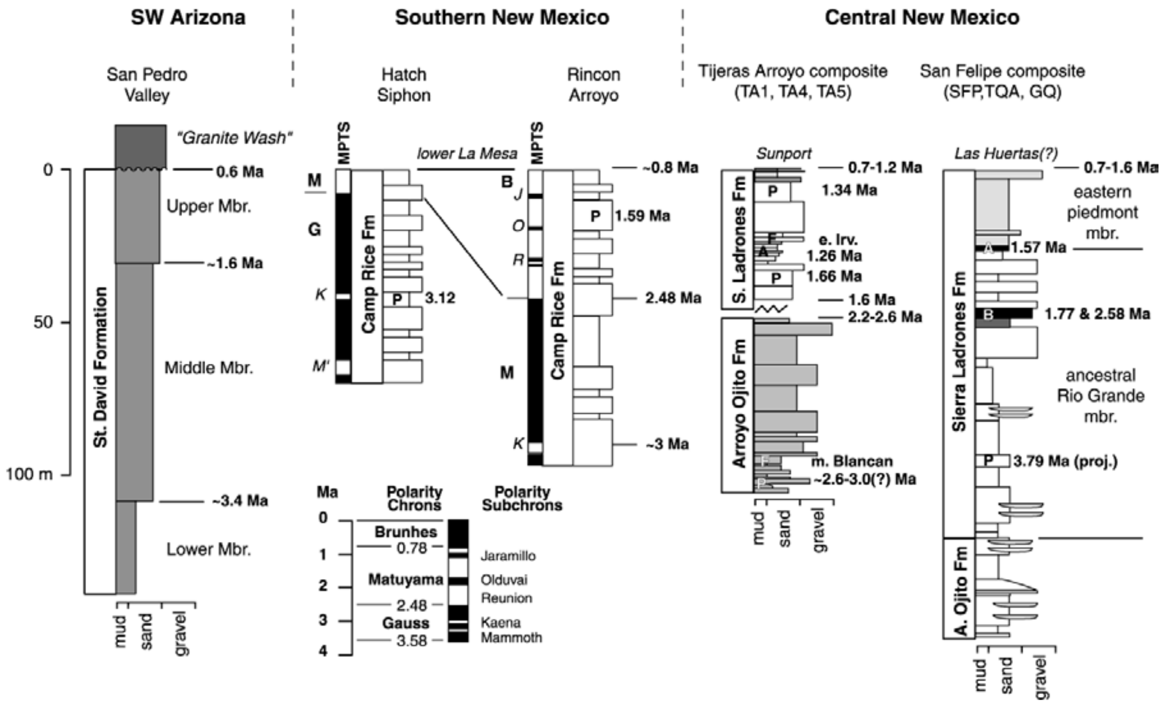

Figure 2-23. Comparison of upper Pliocene and lower Pleistocene alluvial successions in the southern Rio Grande rift, New Mexico, and southeastern Arizona (Smith, 1994; Mack et al., 1993, 1996; Connell, Love, Derrick, unpubl. data). The earliest documented occurrence of the ancestral Rio Grande may be as early as 4.5 or ~5 Ma in southern New Mexico (Mack et al., 1996; Mack, 2001). Entrenchment of the Santa Fe Group is recorded by development of the Rio Grande Valley and the development of constructional surfaces, such as the lower La Mesa surface in southern New Mexico. Aggradation of the St. David Fm is recorded in a tectonically quiescent basin in southeastern Arizona to ~0.6 Ma.

FRIENDS OF THE PLEISTOCENE, ROCKY MOUNTAIN CELL, 45TH FIELD CONFERENCE

PLIO-PLEISTOCENE STRATIGRAPHY AND GEOMORPHOLOGY OF THE CENTRAL PART OF THE ALBUQUERQUE BASIN

THIRD-DAY ROAD LOG, OCTOBER 14, 2001

Geology of Los Lunas volcano

DAVID W. LOVE
New Mexico Bureau of Geology and Mineral Resources, New Mexico Institute of Mining and Technology, 801 Leroy Place, Socorro, NM 87801

SEAN D. CONNELL
New Mexico Bureau of Geology and Mineral Resources-Albuquerque Office, New Mexico Institute of Mining and Technology, 2808 Central Ave. SE, Albuquerque, New Mexico 87106

The following trip presents an overview of the regional setting of Los Lunas volcano(es), some history of geologic work in the area, results of recent geochemistry and geochronology of the eruptives, the relation between the volcanoes and basin fill, deformation associated with the volcanoes, and post-eruption erosion and piedmont deposition. The trip consists of a drive from Isleta Lakes to the flanks of El Cerro de Los Lunas where some vehicles will be parked and orientation/background presented. High clearance vehicles will shuttle the group higher onto the side of the volcano and the group will hike down into a steep canyon and back to the lower vehicles. Along the way the group can examine two spectacular angular unconformities between three packages of basin fill, a disconformity at the base of San Clemente graben-fill, Pliocene fluvial beds with pumice, obsidian, and Blancan fossils, thick and thin-skinned deformation involving tephra of Los Lunas volcano, and post-eruptive piedmont and eolian deposits with multiple soils. Permission from the Huning Land Trust in Los Lunas must be obtained before attempting this trip apart from the Friends of the Pleistocene, October 14, 2001.

Colleague-contributors who helped advance knowledge of the volcano and deserve acknowledgement and thanks (but bear no blame for the field trip leaders mistakes): Charles Reynolds, John Hawley, Rick Lozinsky, Nelia Dunbar, Bill McIntosh, Bruce Hallett, Kurt Panter, Chris McKee, John Young, Bert Kudo, Bill Hall, Jacques Renault, Jim Casten, Becky Thompson, Tad Niemyjski, Bill Haneberg, and Tien Grauch.

Mi.	Description
0.0	Isleta Lakes Store. Follow previous road logs to NM 47 and I-25 south. **0.4**
0.4	Cross railroad; golf course on right. **0.5**
0.9	Stop light with NM-47. **Turn left** and **keep in left lane**. **Prepare to turn left**. **0.5**
1.4	Cross under I-25 overpass, **keep in left lane**. **0.2**
1.6	**Turn left and head south** on NM-47 (South Broadway). **0.1**
1.7	South Broadway. **Get into right lane. 0.1**
1.8	**Turn right** onto southbound I-25 entrance ramp. **0.3**
2.1	**Merge** with I-25 south (headed west). **0.5**
2.6	East abutment of I-25 bridge over Rio Grande. Rio Grande channel ahead. **0.4**
	Milepost 214. West bridge abutment. **0.5**
3.5	Entering Isleta Reservation. Overpass of drain and location of Isleta-Black Mesa piezometer, which encountered 73 ft (22 m) of sandy fluvial deposits underlying the Rio Grande floodplain (Los Padillas Fm of Connell and Love, *this volume*). Deposits are associated with the last incision/aggradation episode of the Rio Grande. Incision probably occurred during latest-Pleistocene time, and entrenched 100 m below the highest inset terrace deposit of the Lomatas Negras fm. **0.6**
4.4	Crossing bridge over Old Coors Road, which follows a former course of the Rio Grande cut through the lava flow of Black Mesa. Roadcut to right shows the edge of the 2.68±0.04 Ma ($^{40}Ar/^{39}Ar$, Maldonado et al., 1999) Black Mesa flow overlying cross-bedded pebbly sands of the Arroyo Ojito Fm and base-surge deposits from Isleta volcano. The tholeiitic Black Mesa flow has no outcrop connection with, and is slightly younger than Isleta volcano, which forms the dark, rounded hill ahead and to the right of the highway. A buried vent for the Black Mesa flow is suspected in the floodplain area to the northeast (Kelley et al., 1976; Kelley and Kudo, 1978). **0.3**

ELEVATIONS OF GEOLOGIC FEATURES, WIND MESA, ISLETA, MESA DEL SOL (SOUTH), BETWEEN I-25 MILE POSTS 212 AND 210

Elevations are in feet above mean sea level as measured from USGS 7.5-minute topographic maps
Arrows point to described features and elevations to your left (east) and right (west) in decreasing order of elevation.

EAST	WEST
	top of east horst of Wind Mesa 5730→
	"bath-tub ring" of gravel, east side of Wind Mesa 5500 →
	top of Isleta volcano 5387 →
← 5340 base of Western Hubbell Spring fault scarp	
← 5240 top of Mesa del Sol	
	east edge of Llano de Albuquerque (down-faulted block) 5240 →
← 5230 top of gravel with Bandelier boulders	
← 5210 base of Rio Grande gravelly sand capping Mesa del Sol	
← 5205 tilted Arroyo Ojito Fm under Mesa del Sol containing Pliocene pumice	
← 5195 Pliocene Isleta (?) basaltic tephra in Arroyo Ojito Fm; 1.58 Ma pumice overlying it.	
← 5130 local top of Pliocene thick reddish-brown sandy clay of Arroyo Ojito Fm	
	top of upper terrrace gravel west of Isleta volcano 5100 →
← 5050 base of thick reddish-brown clay (Pliocene) of the Arroyo Ojito Fm	
	upper edge of lava lake within tuff ring 5050 →
	top of Los Duranes Fm 5020 →
← 4960 Pliocene pumice gravel	
	top of Rio Grande terrace inset against Isleta volcano 5000 →
	basaltic edifice southeast of Isleta volcano with strath terrace at top 4910-4970 →
	base of Rio Grande terrace inset against Isleta volcano 4910 →
← 4910 Pliocene pumice gravel 1.68 Ma	
	Base of lava flow east of Highway 85, 4900 →
← 4885 Isleta (?) tephra 4895 →	
← 4892 Pliocene pumice gravel	
← 4890 Rio Grande flood plain→	
← 4885 Rio Grande floodway channel →	
← 4805 base of Rio Grande paleovalley →	

4.7 Base-surge deposits of tuff cone associated with emplacement of Isleta volcano in outcrops on both sides of route. **0.5**

5.2 Change in primary dip direction of base-surge deposits at crest of tuff ring on right. Overlying alkali-olivine basalt flows fill tuff ring and extend southeast beyond Isleta volcano. Radioisotopic dates ($^{40}Ar/^{39}Ar$ method) indicate that oldest flow is 2.75±0.03 Ma and the second is 2.78±0.06 Ma (Maldonado et al., 1999). Basaltic cinders correlated to the Isleta volcano flows are recognized in the Arroyo Ojito Fm exposed along the eastern margin of the Rio Grande valley. These cinder-bearing deposits are about 70 m (estimated) stratigraphically below exposures of lower Pleistocene, Lower-Bandelier-Tuff bearing sand and gravel of the ancestral Rio Grande facies of the Sierra Ladrones Fm. This stratigraphic relationship indicates that deposition of the Arroyo Ojito Fm continued after 2.72-2.78 Ma, thereby constraining the age of the mesa capping Llano de Albuquerque to between 2.7 and 1.25 Ma. Based on local stratigraphy on both sides of the present valley, it is likely that the Llano de Albuquerque was abandoned as an active fluvial fan prior to deposition of Lower Bandelier ash and pumice gravel at *ca*. 1.6 Ma. Locally, the cinders of Isleta Volcano on the east side of the valley have experienced over 100 m of uplift with consequent erosion of the overlying units before final deposition by the Rio Grande to form the Sunport Surface. Because early Pleistocene terraces of the Rio Grande pass west of Isleta volcano at high levels, the volcanic edifice probably was exhumed during middle and late Pleistocene time (Love et al., 2001). **0.1**

5.3 Entering cut exposing basalt flow of Isleta volcano over base-surge unit (see cross section, Day 2). Shell Isleta #2 well is about 1 mi. to the west, where it reached a depth of 6482 m and ended in Eocene rocks. Lozinsky (1994) reports that the Santa Fe Group is 4407 m thick at the Isleta #2 well and is underlain by 1787 m of the Eocene-Oligocene unit of Isleta #2, which overlies more than 288 m of sediments correlated with the Eocene Baca or Galisteo fms. **1.8**

ELEVATIONS OF GEOLOGIC FEATURES, SAN CLEMENTE TO LOWER HELL CANYON, BETWEEN I-25 MILE POSTS 205 AND 206

Elevations are in feet above mean sea level as measured from USGS 7.5-minute topographic maps

Arrows point to described features and elevations to your left (east) and right (west) in decreasing order of elevation.

EAST **WEST**

base of 100,000-year-old basalt flow 1 of Cat Mesa resting on top of San Clemente graben fill 5315 →
← 5310 top of eastern piedmont aggradation, footwall of western Hubbell Spring fault
Upper Bandelier pumice in cross-bedded sand, San Clemente graben 5300 →
← 5280 Lower Bandelier pumice in ancestral Rio Grande unit, footwall of western Hubbell Spring fault
encroaching piedmont from Los Lunas volcano on graben-fill (1.1 km south) 5280 →
Los Lunas volcano tephra (1.25 Ma) at top of San Clemente section (2.2 km SE) 5260 →
← 5260 top of ancestral Rio Grande deposits bearing Upper Bandelier boulders, north side of Hell Canyon
Blancan fossil camel bones in section tilted 6 degrees SW, east of San Clemente graben 5240 →
thick soil at base of San Clemente graben section 5220 →
pumice in tilted section, east of San Clemente graben 5215 →
← 5140 top of Rio Grande gravel east of Palace-Pipeline fault, south of Hell Canyon
← 5100 top of Rio Grande gravel west of Palace-Pipeline fault
← 5065 top of Hell Canyon gravel and soil, mouth of Hell Canyon
← 5060 top of Rio Grande gravel in section at mouth of Hell Canyon
← 5000 Cerro Toledo (c.a. 1.5 Ma) ash in Janet Slate section , mouth of Hell Canyon
top of Los Duranes Fm 4985 →

←4915 base of exposures of ancestral Rio Grande with Lower Bandelier pumice and ash
← 4865 Rio Grande floodplain →
← 4863 Rio Grande floodway channel →

7.1 Exit 209 overpass to Isleta Pueblo. Road now on upper constructional surface of the Los Duranes Fm, a middle to upper(?) Pleistocene inset fluvial deposit of the ancestral Rio Grande named by Lambert (1968) for exposures in NW Albuquerque. The Los Duranes Fm is inset against middle Pleistocene fluvial deposits correlated to the Lomatas Negras fm, which contains an ash that was geochemically correlated to the 0.60-0.66 Ma Lava Creek B ash, from the Yellowstone area in Wyoming (N. Dunbar, 2000, written commun,; A. Sarna-Wojcicki, 2001, written commun.). At 3:00 is a low dark hill of the 4.01±0.16 Ma Wind Mesa volcano (Maldonado et al., 1999). The late Pleistocene Cat Hill volcanoes between 2:00-3:00. Hell Canyon Wash is at 9:00 on the eastern margin of the Rio Grande Valley. **1.1**

8.2 Railroad overpass. A soil described in exposures of the uppermost Los Duranes Fm indicate that soils are weakly developed with Stage I and II+ pedogenic carbonate morphology (S.D. Connell, and D.W. Love, unpubl. data). **0.8**

9.0 Milepost 208. Between 1:00-2:00 is the rift-bounding uplift of Mesa Lucero, which is about 30 km west of here. **0.6**

9.6 Valencia County Line. **0.4**

10.0 Milepost 207. Late Pleistocene basalt flow of the Cat Hills volcanic field overlies the Los Duranes Fm at 3:00. This flow is the oldest of the Cat Hills seven flows and yielded two $^{40}Ar/^{39}Ar$ dates of 98±20 ka and 110±30 ka (Maldonado et al., 1999). The Albuquerque volcanoes (dated using $^{238}U/^{230}Th$ method at 156±29 ka, Peate et al., 1996) overlie the Lomatas Negras fm and locally interfinger with the top of the Los Duranes Fm in NW Albuquerque. These dates constrain the upper limit of deposition of this extensive terrace deposit to between 98-156 ka, which spans the boundary of marine oxygen isotope stages 5 and 6 (Morrison, 1991). These dates and stratigraphic constraints indicate that much of the deposition of the Los Duranes Fm occurred prior to the interglacial of marine oxygen isotope stage 5. **1.0**

11.0 Milepost 206. Descend possible fault scarp in Los Duranes Fm. Beneath rim of Cat Hills lava flows about 6 km (4 mi.) west of here is the San Clemente graben. It extends northward from near Los Lunas volcano to a graben that splits Wind Mesa (Maldonado et al., 1999). The Arroyo Ojito beds and thick stage III soil beneath the graben-fill near San Clemente are deformed into a flat-floored syncline. At least 37 m of fine sand, silt, and clay with a few coarser pebbly sand units accumulated in this graben where we found a bed of fluvially recycled pumice pebbles about 29 m above the base of the graben-fill section. These pumice pebbles have been geochemically correlated to the Bandelier Tuff and have been dated 1.21±0.03 Ma. Farther south near NM-6, tephra from Los Lunas volcano (*ca*. 1.25 Ma) overlies correlative graben-fill sediments, which lie only a few meters above a stage III soil that is interpreted to mark a break in deposition of the Arroyo Ojito Fm along the easternmost edge of the Llano de Albuquerque. **1.1**

12.1 Southern boundary of Isleta Reservation. El Cerro de Los Lunas between 1:00-2:00. Northwest of the volcano, northwest-tilted beds of the Arroyo Ojito Fm contain multiple layers of pumice pebbles. A pumice pebble collected in the middle of the section of the Arroyo Ojito Fm here has been geochemically correlated to a pumice unit which was $^{40}Ar/^{39}Ar$ dated at 3.12±0.10 Ma in the Arroyo Ojito Fm exposed beneath the Llano de Albuquerque in the valley of the Rio Puerco on the Dalies NW quadrangle (Maldonado et al, 1999). This pumice has been geochemically correlated to a pumice pebble at Day 1, Stop 7 in Rio Rancho. **0.7**

12.8 Borrow pit to right exposes weakly developed soil in Los Duranes Fm. **0.6**

13.4 **Take Exit** 203 to Los Lunas and NM highway 6 to west. **0.3**

13.7 **Turn right** (west) on NM 6. This road was an early alignment of Route 66. El Cerro de Los Lunas at 10:00 consists of several eruptive centers of trachyandesite to dacite. The earliest eruption consisted of andesitic and dacitic vent breccias and lava flows that have an $^{40}Ar/^{39}Ar$ age of 3.81±0.1 Ma (McIntosh, unpubl; Panter et al., 1999). The north edifice with the "LL" on it is a trachyandesite with an $^{40}Ar/^{39}Ar$ age of 1.25±0.1 Ma (McIntosh, unpubl; Panter et al., 1999). A separate, undated vent at the top of the mountain produced red and gray scoraceous tephra that extended over several km^2 to the north, east, and southeast of the volcano. The underlying flow and scoria were then cut by several north-south faults. The scoria vent, underlying flow, and Santa Fe Group strata were tilted and uplifted more than 150 m above the surrounding landscape and rapidly eroded, forming a piedmont apron to the west and northwest. An eroded fault scarp on the east side of the peak has dip-separation of 56 m on the base of the lowest 1.25 Ma flow. The next set of eruptions issued along the fault scarp and buried talus from the scarp. Between eruptions, minor amounts of talus and eolian sand buried the lava flows. The final vent produced at least three lava flows that descended eastward toward the valley. V. Grauch (personal commun., 1999) suggests that the magnetic polarity of these flows is reversed, indicating that they predate the Brunhes chron (older than 780 ka). McIntosh (unpubl.) obtained ages of 1.25±0.1 Ma on some of these upper flows, indicating that the eruptions and concurrent deformation took place in less than twenty thousand years.. **0.5**

14.2 Pass Los Morros Road to business park to your right. **0.2**

14.4 Pass Sand Sage Road and ascend alluvial apron prograded over the Los Duranes Fm. Relict landslide on north side of "LL" edifice at 9:30. **0.6**

15.0 Exposures of northwest-tilted Arroyo Ojito deposits below skyline to the southwest of NM 6. Tilting of the section is due to deformation during emplacement of two batches of magma. An older, more tilted succession is not visible from the highway, but will be visited during a hike from **Stop 3-1**. **0.9**

15.9 V-shaped gray syncline developed in Los Lunas tephra in slopes up drainage to southwest. **1.1**

17.0 Hill to right is eolian falling dune covering reworked piedmont of Los Lunas volcano. **0.1**

17.1 Los Lunas tephra exposed in road cuts at eye level. **0.3**

17.4 Contact between Los Lunas tephra and San Clemente graben fill near elevation of gate to your right (north). **0.1**

17.5 Piedmont alluvium from Los Lunas volcano exposed in road cuts. Stage III calcium carbonate soil horizon near top. **0.3**

17.8 **Turn left** (south) on "AT and T" Road. **0.6**

18.4 **Turn left** just past power pole and before houses. Water table for this housing development at a depth of more than 900 feet. Head east on two-track dirt road. **0.3**

18.7 Pass "No Trespassing" Sign on Huning Ranch and **head southeast**. Permission must be obtained from the Huning Land Trust in Los Lunas prior to entering ranch lands. **0.1**

18.8 **Turn left** on two-track road to east and prepare to leave vehicle. **0.1**

18.9 Separate vehicles to be left here from four-wheel drive, high clearance vehicles that will continue after **Stop 3-1**. Park on left side of road near edge of badlands. *GPS, N: 3,854,000 m; E: 333,819 m, Z013S, NAD83, Dalies 7.5' quadrangle.*

Discussion at Stop 3-1 will address seven items of interest: (1) where are we? (2) who has done work here? (3) what about those volcanoes? (4) what relation does the basin fill have to the volcanoes? (5) what's happened since the last eruption in the way of erosion of the volcano and consequent piedmont deposition? (6) what's the history of post-piedmont erosion on the north, south, and southwest flanks of the piedmont? And most importantly, (7) where do we go from here, what do we see, how long will it take, and what should participants take with them?

1) Where are we?

Regional setting of Los Lunas volcano: Topics and visual aids to cover--position near center of Albuquerque basin, visual landmarks around basin and margins of basin; Mid-basin rift setting—Maldonado et al draft map; Aeromagnetic maps; gravity map; tops of basin fill—Llanos: Albuquerque, Sunport, Manzano, San Clemente, Los Lunas volcano piedmont. Basin fill thickness—Shell Isleta # 2: 6,482 m deep; Santa Fe Group 4,407 m or 4,941m Shell Isleta # 1: 2,679 m of Santa Fe Group/Cretaceous at 3,670 m TransOcean 1,536 m of Santa Fe Group (TD in Precambrian at 3,163 m) Long-Dalies 2,589 m of Santa Fe Group; Harlan 864 m of Santa Fe Group. Sources of basin fill—west, north, northeast (Rio Grande), east (piedmont of Manzano Mountains not found here). Where was the Rio Grande? Post-Santa Fe development of Rio Grande valley in inset steps.

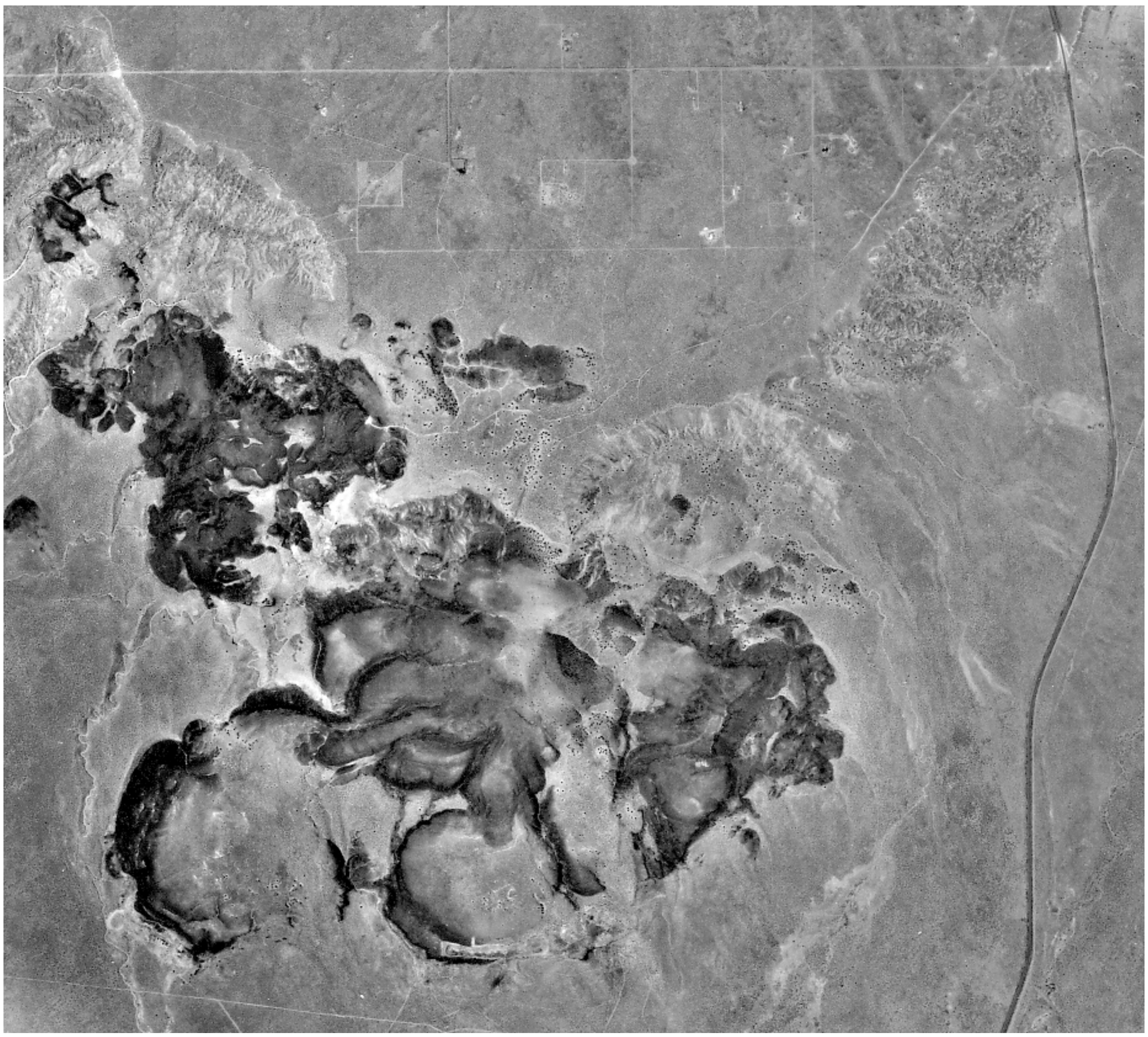

Figure 3-1. Aerial photograph of El Cerro de los Lunas and vicinity. North is to the right (U.S. Geological Survey air photo, 1990, GS-VFN, No. 2-83).

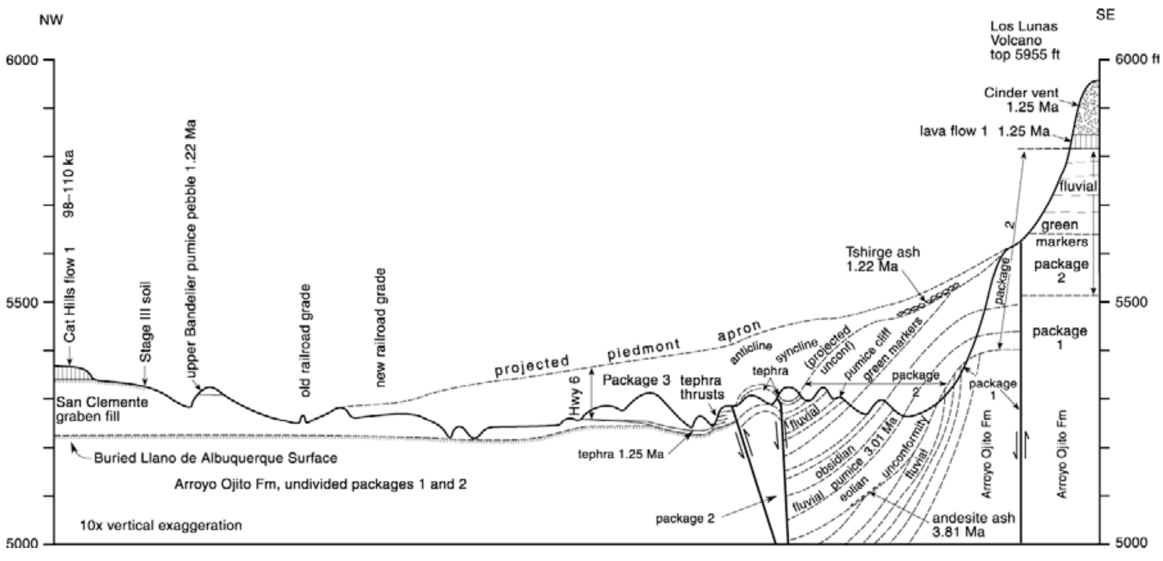

Figure 3-2. Cross section across northwestern flank of Los Lunas volcano.

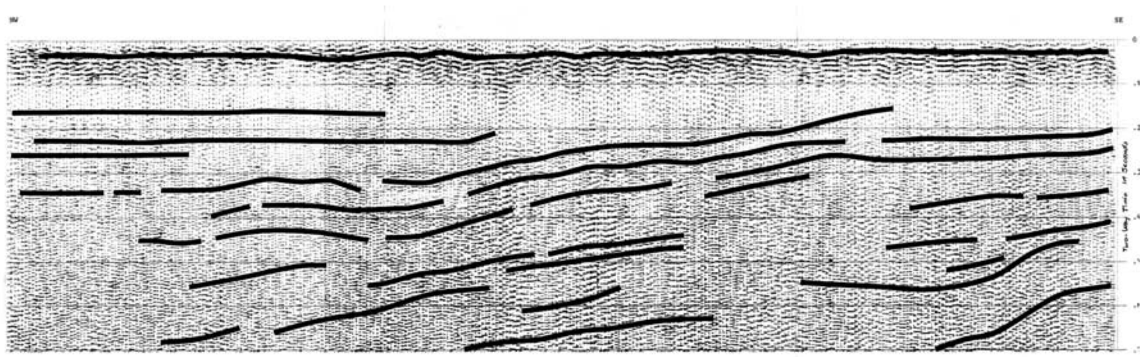

Figure 3-3. Reflection seismic profile along the northwest piedmont slope of Los Lunas volcano (C. Reynolds, unpubl. data). Note dipping reflectors and unconformities at 0.2 to 0.5 seconds two-way travel time (scale on right margin 0 to 0.7 seconds).

Figure 3-4. Photograph of the white Tshirege ash overlying blocks of the 1.25 Ma Los Lunas trachyandesite.

Figure 3-5. View to north of west-tilted Arroyo Ojito Fm (local package 2).

2) Who worked here?

T. Galusha; V. Kelley and A. Kudo; J. Kasten; J. Renault; G. Bachman & J. Mehnert; J. Hawley, R. Lozinsky, J. Young, D. Love; C. Reynolds; K. Panter and B. Hallett; W. Haneberg; N. Dunbar and W. McIntosh; C. McKee; S. L. Minchak; H. D. Southern; H. D. Rowe; J. Geissman.

3) Los Lunas volcano(es) Elevations: Top 5955 ft (1815 m), west side 5300-5700 (1615-1737 m), east side 5050 ft (1539 m), base of badlands to south 5100 ft (1554 m), Dalies to SW 5305 ft (1617 m). High edifices—NE 1.25 Ma, central 1.25, SE scoria on NE flow 1.25 Ma; Low, tilted edifice to SW—3.8 Ma; also outliers to south that we can't see from here (Fig. 3-1)Large north-trending fault offsets first flow (59 m of displacement, down to east; other, smaller faults to east and west. Chemistry of flows—early (3.8) andesite & dacite, late (1.25) trachyandesite.

4) Relation of volcanoes to basin fill: Pre-3.8 Ma sediments (> 40 m exposed)—western-source pebbly sands and eolian; deformation by folds and faults (normal and thrusts). Flow-front deformation of sediments and tephra (normal & thrusts). Post 3.8 Ma tilting, faulting, burial first with eolian (20-40 m), then 150 m of fluvial and eolian section below 1.25 Ma tephra.

Problem with southern "intrusives"—outcrops look intrusive, but they are buried by sediments containing adjacent eroded igneous blocks—so what were these igneous bodies intruding?

1.25 Ma eruptions and deformation: first, "chocolate brown" (CB) flow and edifice; second "red and gray" scoria cone and tephra; deformation of tephra—folds, reverse faults, low-angle thrusts, normal faults, cuspate-lobate structures; normal faults with ~59 m of displacement; uplift beneath volcano of 155 m above rest of Llano de Albuquerque; talus; third edifice and late flows cover faults

5) Post-tephra erosion and piedmont deposition (~50 m of fill) Relation to San Clemente graben; local seismic profiles.

Where is "Llano de Albuquerque" (top of basin fill) in this section?

6) Post-piedmont erosion and deposition of intermediate landscape levels and current deep canyons

7) Where are we going from here? What will we see? How long will it take?

We shuttle the group with as few high-clearance vehicles as possible up slope to edge of steep canyon between us and the volcano. We look at three packages of sediments between angular unconformities. The upper package of local colluvium and alluvium and stage III soils includes fallout of Tshirge ash (upper Bandelier--1.22 Ma) in a paleovalley cut into tilted Pliocene sediments. We descend into the present canyon and see part of the middle package that includes Pliocene pumice mixed with western-margin facies and eolian sand. At the base of exposures in the canyon, we see a profound angular unconformity between an older (Pliocene?) pumice-bearing third package of sediments and the tilted beds we have just examined. Then we walk northward through the tilted section to examine the Pliocene and Pleistocene beds where it is more easily accessible. We look at deformation of sediments by faults and folds. To the north we find the 1.25 Ma tephra from the second eruption of Los Lunas volcano deformed in a syncline and anticline in the section, immediately overlain by sediments reworked from the uplifted volcano.

We will examine unusual reverse faults, cuspate and lobate structures, and low-angle thrust faults involving plates of unconsolidated sediments only a few m thick (who would have thought that unconsolidated sediments would be considered "competent" [see article by Haneberg, *this volume*]). Farther north, we see the Los Lunas tephra flatten out on top of fine-grained sediments in the San Clemente graben. Above the tephra, we walk through 50 m of alluvial sediments derived from the uplifted youngest eruption of Los Lunas volcano and Arroyo Ojito sediments on our way back to the vehicles at the lower parking lot.

We hope to complete this traverse within 4 hours. The climb down is steep, and there is a small chance of finding rattlesnakes among boulders at the bottom. The climb out is not particularly steep, but may require extra effort. Take water, food, sunscreen, and walking tools.

Selected vehicles will drive south (uphill) to upper parking area. Roadlog from lower parking area to upper parking area.

Reset odometer.

0.0 **Return** to larger dirt two-track and turn southeast (left) toward volcano. **0.1**

0.1 Route towards volcano is along the top of undissected piedmont slope covered with Holocene eolian sand dunes. **0.1**

0.2 View of highest part of Los Lunas volcano at 12:00. This consists of a red scoria cone overlying a trachyandesite flow. The volcanic units make up only the upper 40-45 m of the mountain. Underlying the flow is local package 2 of Arroyo Ojito Fm mostly exposed. Package one of Arroyo Ojito Fm is exposed in deep arroyos north and south of this summit. To the east at 11:30 is the fault with ~56 m of offset judging from the base of the trachyandesite flow on either side of the fault. Farther to the east is the "LL" edifice at 10:30 and numerous landslides from 10:30 to 10:00. **0.5**

0.7 Low black outcrops to southwest (1:00) are nearly buried tops of 3.81 Ma tilted lava flows. **0.1**

0.8 **Turn left** (east) on two track road. **0.2**

1.0 **Turn around** where possible and **park** out of roadway. Prepare to hike downslope. *GPS, N: 3,852,855 m; E: 334,640 m, Z013S, NAD83, Dalies 7.5' quadrangle.*

Outline of landscape development around Los Lunas volcano

D. Love, B. Hallett, K. Panter, N. Dunbar, W. McIntosh, J. Hawley, R. Lozinsky, J. Young, C. Reynolds, S. Connell, W. Haneberg

Los Lunas volcano consists of two sets of edifices—an older tilted one (and outliers) to the southwest at 3.81 ± 0.10 Ma, and a younger one to the northeast at 1.25 ± 0.02 Ma. The local landscape consists of the two sets of volcanic edifices, subvolcanic basin fill, piedmont apron around western side, river-cut valley and terrace to east, and erosional drainage basins to NW, S and SW.

Present drainages show influence of differential erosion of basin-fill, structure (faulting and folding), resistance of lava flows; colluvial processes (landslides, slumps, rock falls); and oriented eolian processes.

Events

- Pre-volcanic basin fill from west and north—typical western margin facies (Arroyo Ojito Fm), but deformed and exposed here;
- Deformation precedes first eruptions; faulting and dramatic tilting of Santa Fe Group beds;
- 3.81 Ma andesite and dacite eruptions:
- tephra overridden by andesite flows with concurrent deformation. Flows are tilted.
- Eolian aggradation around and over the top of the flows before fluvial western-margin gravels come back into picture. Then pumice and obsidian arrive with western-margin fluvial clasts. 150 m of section accumulates;
- Stage III soil forms at least in some areas;
- San Clemente graben forms—primarily to north and northwest. Soil develops on margins of graben, sediments accumulate in graben.

1.25 Ma eruptions of El Cerro de los Lunas

1) NE edifice with "chocolate brown" (CB) flow across landscape—on edge of San Clemente graben (some exposures have stage III soil, others just alluvium beneath first flow). Flow in SW area ponds into "lava lake" > 30 m thick.
2) cinder and red scoria edifice erupts to WSW of first edifice
3) cinder edifice is uplifted and offset 56 m along N-S fault, forms top of "El Cerro de Los Lunas"
4) cinders with blocks of first flow are folded into syncline, anticline, and faulted with reverse and thrust faults to northwest of edifice and subsequently buried by erosional debris from southeast
5) N-S faults also cut "chocolate brown" edifice to east; probably NE faults west of cinder edifice
6) talus develops on free face of major N-S fault
7) new edifice erupts along fault and produces flow 3 down east side
8) eolian sand partially covers flow 3 on east side
9) flows 4 descend down east side from edifice on fault, forming symmetrical flow lobes clearly visible in photographs

After eruptions ceased

- East side—very linear—either fault or Rio Grande truncation prior to Los Duranes sedimentation
- NW side—after eruptions and faulting, paleo-valley eroded in uplifted Santa Fe Group sediments, blocks of CB and cinders into the paleovalley, 1.22 Ma Tshirge ash of Bandelier into the valley. Up to 50 m of accumulation in the valley; extension of alluvial apron to northwest, west, and southwest; apron may interfinger with San Clemente graben fill; large eolian component to apron from SW.
- South side—early drainages off SW side of uplifted volcano, development of drainages down south side and across SE flows of volcano; transport of recycled Arroyo Ojito clasts from southwest side onto SE flow lobes, entrenchment of upper flow. Then south-side drainage gets captured to flow west and south. Eolian influence of meander courses; migrates down south-tilted dip slope.
- Creation of renewed erosional relief both north side and south side.
- Recycling of western alluvial apron into intermediate alluvial apron on north side and south side of Los Lunas volcano
- Creation of renewed erosional relief on both north side and south side.
- Recycling of western alluvial apron and intermediate alluvial apron into an even lower alluvial apron on north side and south side of Los Lunas volcano.

- Routing of hairpin turn in drainage on south side—eolian influence here too. Transport from head of SW badlands across old edifice and eastward. Definite eolian influence on west side of SE flow lobes— eolian ramp across top and into ENE area on top of (and between) flows.
- Southwest drainage hangs up on older lava flows, incises meanders with two mouths to drainage across lava, depending on NE trending faults; Far SW drainage through NE trending grabens; curved drainages along strike around uplift of older Tsf—both far southwest side and north side of Los Lunas volcano.
- Southwest drainage establishes new, lower route as badlands are stripped out.
- Landslides, slumps, Toreva blocks continue to develop on steep slopes.
- Eolian dunes, distended parabolic arms, rim dunes on NE side of SW badlands and on parts of the volcanoes on landscape now.

ROAD LOG REFERENCES
(probably incomplete)

Abbott, J.C., and Goodwin, L.B., 1995, A spectacular exposure of the Tijeras fault with evidence for Quaternary motion: New Mexico Geological Society Guidebook 46, p. 117-125.

Allen, B.D., and Anderson, R.Y., 2000, A continuous, high-resolution record of late Pleistocene climate variability from the Estancia Basin, New Mexico: Geological Society of America Bulletin, v. 112, n. 9, p. 1444-1458.

Ayarbe, J. P., 2000, Coupling a fault-scarp diffusion model with cosmogenic ^{36}Cl rupture chronology of the Socorro Canyon fault, New Mexico [M.S. thesis]: Socorro, New Mexico Institute of Mining and Technology, Socorro, 71 p.

Bachman, G. O., and Mehnert, H.H., 1978, New K-Ar dates and the late Pliocene to Holocene geomorphic history of the central Rio Grande region, New Mexico: Geological Society of America, Bulletin, v. 89, p. 283-392.

Black, B.A., and Hiss, W.L., 1974, Structure and stratigraphy in the vicinity of the Shell Oil Co. Santa Fe Pacific No. 1 test well, southern Sandoval County, New Mexico: New Mexico Geological Society, Guidebook 25, p. 365-370.

Blair, T., Bilodeau, W.L., 1988, Development of tectonic cyclothems in rift, pull-apart, and foreland basins; sedimentary response to episodic tectonism, v. 16, n. 6.

Bryan, K and McCann, F. T., 1937, The Ceja del Rio Puerco, a border feature of the Basin and Range province in New Mexico: Journal of Geology, v. 45, p. 801-828.

Bryan, K., and McCann, F.T., 1938, The Ceja del Rio Puerco-a border feature of the Basin and Range province in New Mexico, part II, geomorphology: Journal of Geology, v. 45, p. 1-16.

Bryan, K., McCann, F.T., 1936, Successive pediments and terraces of the upper Rio Puerco in New Mexico: Journal of Geology, 44, n. 2, p. 145-172

Bull, W.B., 1984, Tectonic geomorphology: Journal of Geologic Education, v. 32, p. 310-324.

Bull, W.B., 1991, Geomorphic responses to climate changes: New York, Oxford University Press, 326 p.

Cather, S.M., and Connell, S.D., 1998, Geology of the San Felipe Pueblo 7.5-minute quadrangle, Sandoval County, New Mexico: New Mexico Bureau of Mines and Mineral Resources, Open-File Digital Map 19, scale 1:24,000.

Cather, S.M., and McIntosh, W.C., 1990, Volcanogenic flood deposits near San Antonio, New Mexico- depositional processes and implications: Sediments 1990, 13th International Sedimentological Congress, Nottingham, England, 80 p.

Cather, S.M., Connell, S.D., and Black, B.A., 2000, Preliminary geologic map of the San Felipe Pueblo NE 7.5-minute quadrangle, Sandoval County, New Mexico: New Mexico Bureau of Mines and Mineral Resources, Open-file Digital Map DM-37, scale 1:24,000.

Cather, S.M., Connell, S.D., and Black, B.A., 2000, Preliminary geologic map of the San Felipe Pueblo NE 7.5-Minute quadrangle, Sandoval County, New Mexico: New Mexico Bureau of Mines and Mineral Resources, Open-File Geologic Map OF-GM 37, scale 1:24,000.

Cole, J.C., Stone, B.D., Shroba, R., and Dethier, D., 2001a, Episodic Pliocene and Pleistocene drainage integration along the Rio Grande through New Mexico [abstract]: Geological Society of America, Abstracts with Programs, v. 33, n.7.

Cole, J.C., Stone, B.D., Shroba, R., and Dethier, D., 2001b, Pliocene incision of the Rio Grande in northern New Mexico [abstract]: Geological Society of America, Abstracts with Programs, v. 33, n.5, p. A-48.

Connell, S.D., 1997, Geology of the Alameda 7.5-minute quadrangle, Bernalillo and Sandoval Counties, New Mexico: New Mexico Bureau of Mines and Mineral Resources, Open-File Digital Map 10, scale 1:24,000.

Connell, S.D., 1998, Geology of the Bernalillo 7.5-minute quadrangle, Sandoval County, New Mexico: New Mexico Bureau of Mines and Mineral Resources, Open-File Digital Map 16, scale 1:24,000.

Connell, S.D., and Wells, S.G., 1999, Pliocene and Quaternary stratigraphy, soils, and geomorphology of the northern flank of the Sandia Mountains, Albuquerque Basin, Rio Grande rift, New Mexico: New Mexico Geological Society, Guidebook 50, p. 379-391.

Connell, S.D., and Love, D.W., 2000, Stratigraphy of Rio Grande terrace deposits between San Felipe Pueblo and Los Lunas, Albuquerque Basin, New Mexico [abstract]: New Mexico Geology, v. 22, n. 2, p. 49.

Connell, S.D. Cather, S.M., Karlstrom, K.E., Read, A., Ilg, B., Menne, B., Picha, M.G., Andronicus, C., Bauer, P.W., and Anderson, O.J., 1995, Geology of the Placitas 7.5-minute quadrangle, Sandoval County, New Mexico: New Mexico Bureau of Mines and Mineral Resources, Open-File Digital Map 2, scale 1:12,000.

Connell, S.D., Allen, B.D., and Hawley, J.W., 1998a, Subsurface stratigraphy of the Santa Fe Group from borehole geophysical logs, Albuquerque area, New Mexico: New Mexico Geology, v. 20, n. 1, p. 2-7.

Connell, S.D., Allen, B.D., Hawley, J.W., and Shroba, R., 1998b, Geology of the Albuquerque West 7.5-minute quadrangle, Bernalillo County, New Mexico: New Mexico Bureau of Mines and Mineral Resources, Open-File Digital Geologic Map 17, scale 1:24,000.

Connell, S.D., Koning, D.J., and Cather, S.M., 1999, Revisions to the stratigraphic nomenclature of the Santa Fe Group, northwestern Albuquerque basin, New Mexico: New Mexico Geological Society, Guidebook 50, p. 337-353.

Connell, S.D., Love, D.W., Maldonado, F., Jackson, P.B., McIntosh, W.C., and Eppes, M.C., 2000, Is the top of the Santa Group diachronous in the Albuquerque Basin? [abstract]: U.S. Geological Survey, Open-file report 00-488, p. 18-20.

Connell, S.D., Koning, D.J., and Derrick, N.N., 2001, Preliminary interpretation of Cenozoic strata in the Tamara No. 1-Y well, Sandoval County, north-central New Mexico: New Mexico Bureau of Mines and Mineral Resources, Open-file report 454B, p. K-79-K-88.

Connell, S.D., Love, D.W., Cather, S.M., Smith, G.A., and Lucas, S.G., 2001b, Tectonics, climate, and the transition from aggradation to incision of the upper Santa Fe Group, Albuquerque Basin, central New Mexico [abstract]: Geological Society of America, Abstracts with Programs, v. 33, n.5, p. A-48.

Connell, S.D., Love, D.W., Jackson-Paul, P.B., Lucas, S.G., Morgan, G.S., Chamberlin, R.M., McIntosh, W.C., Dunbar, N., 2001a, Stratigraphy of the Sierra Ladrones Formation type area, southern Albuquerque Basin, Socorro County, New Mexico: Preliminary Results [abstract]: New Mexico Geology, v. 23, n. 2, p. 59.

Connolly, J. R., 1982, Structure and metamorphism in the Precambrian Cibola gneiss and Tijeras greenstone, Bernalillo county, New Mexico: New Mexico Geological society, 33rd Field Conference, p. 197-202.

Connolly J. R., Woodward, L. A., and Hawley, J. W., 1982, Road-Log segment I-A: Albuquerque to Tijeras Canyon: New Mexico Geological Society, 33rd Field Conference, p. 2-8.

Dart, C., Cohen, H.A., Akyuz, H.S, and Barka, A., 1995, Basinward migration of rift-border faults: implications for facies distributions and preservation potential: Geology, v. 23, n. 1, p. 69-72.

Derrick, N.N., and Connell, S.D., 2001, Petrography of upper Santa Fe Group deposits in the northern Albuquerque basin, New Mexico: Preliminary Results [abstract]: New Mexico Geology, v. 23, n. 2, p. 58-59.

Dunbar, N., McIntosh, W.C., Cather, S.M., Chamberlin, R.M., Harrison, B., Kyle, P.R., 1996, Distal tephras from the Jemez volcanic center as time-stratigraphic markers in ancestral Rio Grande sediments from the Socorro area: New Mexico Geological Society, Guidebook 47, p. 69-70.

Ferguson, C. A., Timmons, J. M., Pazzaglia, F. J., Karlstrom, K. E., and Bauer, P. W., 1998, Geologic map of the Sandia Park quadrangle, Bernalillo and Sandoval Counties, New Mexico: New Mexico Bureau of Mines and Mineral Resources, Open-file Report DM-1, 12 p. scale 1:24,000.

Gawthorpe, R.L., Leeder, M.R., 2000, Tectono-sedimentary evolution of active extensional basins: Basin Research, v. 12, n. 3-4, p. 195-218.

Gerson, R., 1982, Talus relicts in deserts: a key to major climatic fluctuations: Israel Journal of Earth Sciences, v. 31, n.2-4, p. 123-132.

Gile, L.H., Hawley, J.W., and Grossman, R.B., 1981, Soils and geomorphology in the Basin and Range area of southern New Mexico-Guidebook to the Desert Project: New Mexico Bureau of Mines and Mineral Resources, Memoir 39, 222 p.

Gile L. H., Hawley, J. W., Grossman, R. G., Monger, H. C., Montoya, C. E., and Mack, G. H., 1995, Supplement to the Desert Project Guidebook, with emphasis on soil micromorphology: New Mexico Bureau of Mines and Mineral Resources Bulletin 142, 96 p.

Grauch, V. J. S., 1999, Principal features of high-resolution aeromagnetic data collected near Albuquerque, New Mexico: New Mexico Geological Society, Guidebook 50, p. 115-118.

Grauch, V.J.S., 2001, High-resolution aeromagnetic data, a new tool for mapping intrabasinal faults: Example from the Albuquerque basin, New Mexico: Geology, v. 29, no. 4 p. 367-370.

Grauch, V.J.S., Gillespie, C.L., and Keller, G.R., 1999, Discussion of new gravity maps for the Albuquerque Basin area: New Mexico Geological Society, Guidebook 50, p. 119-124.

Hallett, R.B., Kyle, P.R., and McIntosh, W.C., 1997, Paleomagnetic and $^{40}Ar/^{39}Ar$ age constraints on the chronologic evolution of the Rio Puerco volcanic necks and Mesa Prieta, west-central New Mexico: Implications for transition zone magmatism: Geological Society of America Bulletin, v. 109, no. 1, p. 95-106.

Haneberg, W.C., 1992, Geologic hazards in New Mexico; Part 2: New Mexico Geology, v. 14, n. 3, p. 45-52.

Haneberg, W.C., 1999, Effects of valley incision on the subsurface state of stress--theory and application to the Rio Grande valley near Albuquerque, New Mexico: Environmental & Engineering Geoscience, v. 5, p. 117-131.

Haneberg, W.C., Gomez, P., Gibson, A., and Allred, B., 1998, Preliminary measurements of stress-dependent hydraulic conductivity of Santa Fe Group aquifer system sediments, Albuquerque Basin, New Mexico: New Mexico Geology, v. 20, p. 14-20.

Hawley, J.W., ed., 1978, Guidebook to Rio Grande rift in New Mexico and Colorado: New Mexico Bureau of Mines and Mineral Resources, Circular 163, 241 p.

Hawley, J. W., 1996, Hydrogeologic framework of potential recharge areas in the Albuquerque Basin, central New Mexico: New Mexico Bureau of Mines and Mineral Resources, Open-file Report 402 D, Chapter 1, 68 p., appendix.

Hawley, J. W., Love, D. W., and Lambert, P. W., 1982, Road-log segment I-C: Abo Canyon –Blue Springs area to Albuquerque via Belen and Los Lunas: New Mexico Geological Society, 33rd Field Conference, p. 24-30.

Hawley, J.W. and Haase, C.S., 1992, Hydrogeologic framework of the northern Albuquerque Basin: New Mexico Bureau of Mines and Mineral Resources, Open-file Report 387, 165 p.

Hawley, J.W., Haase, C.S., Lozinsky, R.P., 1995, An underground view of the Albuquerque Basin: New

Mexico Water Resources Research Institute, Report 290, p. 27-55.

Izett, G. A., and Wilcox, R. E., 1982, Map showing localities and inferred distributions of the Huckleberry Ridge, Mesa Falls, and Lava Creek ash beds (Pearlette family ash beds) of Pliocene and Pleistocene age in the western United States and southern Canada: U. S. Geological Survey, Miscellaneous Investigations Series, Map I-1325, scale 1:4,000,000.

Izett, G. A., and Obradovich, J. D., 1994, ^{40}Ar/^{39}Ar age constraints for the Jaramillo Normal Subchron and the Matuyama-Brunhes geomagnetic boundary: Journal of Geophysical Research, v. 99, p. 2925-2934.

Izett, G.A. Pierce, K.L., Naesser, N.D., and Jawarowski, C., 1992, Isotopic dating of Laver Creek B tephra in terrace deposits along the Wind River, Wyoming: Implications for the post 0.6 Ma uplift of the Yellowstone hotspot: U.S. Geological Survey, Open-file report 92-391, 33 p.

Karlstrom, K.E., Chamberlin, R.C., Connell, S.D., Brown, C., Nyman, M., Cavin, W., Parchman, M., Cook, C., Sterling, J., 1997, Geology of the Mt. Washington 7.5-minute quadrangle, Bernalillo and Valencia Counties, New Mexico, New Mexico Bureau of Mines and Mineral Resources, Open-File Geologic Map OF-GM 8, scale 1:12,000 and 1:24,000.

Karlstrom, K.E., Cather, S.M., Kelley, S.A., Heizler, M.T., Pazzaglia, F.J., and Roy, M., 1999, Sandia Mountains and the Rio Grande rift: ancestry of structures and history of deformation: New Mexico Geological Society, Guidebook 50, p. 155-165.

Kelley, V. C., 1977, Geology of Albuquerque Basin, New Mexico: New Mexico Bureau of Mines and Mineral Resources, Memoir 33, 60 p.

Kelley, V.C., 1982, Albuquerque-its mountains, valley, water, and volcanoes: New Mexico Bureau of Mines and Mineral Resources, Scenic Trips to the Geologic Past No. 9, 106 p.

Kelley, V.C. and Kudo, A.M., 1978, Volcanoes and related basalts of Albuquerque basin, New Mexico: New Mexico Bureau of Mines and Mineral Resources Circular 156, 30 p.

Kelson, K. I., Hitchcock, C. S., and Harrison, J. B. J., 1999, Paleoseismology of the Tijeras fault near Golden, New Mexico: New Mexico Geological Society, 50th field conference, p. 201-209.

Kelson, K.I., Hitchcock, C.S., and Randolph, C.E., 1999, Liquefaction susceptibility in the inner Rio Grande Valley, near Albuquerque, New Mexico: Final Technical Report, U.S. Geological Survey, National Hazards Reduction Program, Award No. 98-HQ-GR-1009, 40 p.

Lambert, P. W., 1968, Quaternary stratigraphy of the Albuquerque area, New Mexico [Ph.D. dissert.]: Albuquerque, University of New Mexico, 329 p.

Leeder, M. R., and Jackson, J. A., 1993, The interaction between normal faulting and drainage in active extensional basins, with examples from the western United States and central Greece: Basin Research, v. 5, no. 2, p. 79-102.

Love, D. W., 1986, A geological perspective of sediment storage and delivery along the Rio Puerco, central New Mexico, *in* Hadley, R. F. (ed.), Drainage basin sediment delivery: International Association of Hydrological Sciences, Publication 159, pp. 305-322.

Love, D. W., 1989, Geomorphic development of the Rio San Jose valley: New Mexico Geological Society 40th Field Conference Guidebook, pp. 11-12.

Love, D. W., 1997, Geology of the Isleta 7.5-minute quadrangle, Bernalillo and Valencia Counties, New Mexico: New Mexico Bureau of Mines and Mineral Resources, Open-file Digital Geologic Map 13, scale 1:24,000.

Love, D.W. and Whitworth, T. M., 2001, Description and models of distinctive calcium-carbonate nodules and discontinuous cementation from shallow ground-water seepage in hanging walls of Pleistocene faults [abstract]: New Mexico Geology, v. 23, no. 2, p. 60.

Love, D.W., Dunbar, N., McIntosh, W.C., McKee, C., Connell, S.D., Jackson-Paul, P.B., and Sorrell, J., 2001, Late-Miocene to early-Pleistocene geologic history of Isleta and Hubbell Spring quadrangles based on ages and geochemical correlation volcanic rocks [abstract]: New Mexico Geology, v. 23, n. 2, p. 58.

Lozinsky, R.P., 1988, Stratigraphy, sedimentology, and sand petrography of the Santa Fe Group and pre-Santa Fe Tertiary deposits in the Albuquerque Basin, central New Mexico [Ph.D. dissert.]: Socorro, New Mexico Institute of Mining and Technology, 298 p.

Lozinsky, R. P., 1994, Cenozoic stratigraphy, sandstone petrology, and depositional history of the Albuquerque basin, central New Mexico: Geological Society of America Special Paper 291, p. 73-81.

Lucas, S.G., Williamson, T.E., and Sobus, J., 1993, Plio-Pleistocene stratigraphy, paleoecology, and mammalian biochronology, Tijeras Arroyo, Albuquerque area, New Mexico: New Mexico Geology, v. 15, n. 1, p. 1-8.

Mack, G.H., 2001, Evolution of Cenozoic extensional block faulting and sedimentation in the southern Rio Grande rift, New Mexico [abstract]: Geological Society of America, Abstracts with Programs, v. 33, n. 5, p. A-47.

Mack, G.H. and Seager, W.R., 1990, Tectonic controls on facies distribution of the Camp Rice and Palomas Formations (Pliocene-Pleistocene) in the southern Rio Grande rift: Geological Society of America Bulletin, v.102, p.45-53.

Mack, G.H., Salyards, S.L., and James, W.C., 1993, Magnetostratigraphy of the Plio-Pleistocene Camp Rice and Palomas Fms in the Rio Grande rift of southern New Mexico: American Journal of Science, v. 293, p. 47-77.

Mack, G.H., McIntosh, W.C., Leeder, M.R., and Monger, H.C., 1996, Plio-Pleistocene pumice floods in the ancestral Rio Grande, southern Rio Grande rift, New Mexico, USA: Sedimentary Geology, v. 103, p. 1-8.

Machette, M. N., 1978, Geologic map of the San Acacia quadrangle, Socorro County, New Mexico: U. S. Geological Survey, Geologic quadrangle Map GQ 1415, scale 1:24,000.

Machette, M.N., 1985, Calcic soils of the southwestern United States: Geological Society of America Special Paper 203, p. 1-21.

Machette, M.N., Personius, S.F., Kelson, K.I., Haller, K.M., and Dart, R.L., 1998, Map and data for Quaternary faults and folds in New Mexico: U.S. Geological Survey Open-File Report 98-821, 443 p., 1 pl.

Machette, M.N., Long, T., Bachman, G.O., and Timbel, N.R., 1997, Laboratory data for calcic soils in central

New Mexico: Background information for mapping Quaternary deposits

Maldonado, F., and Atencio, A., 1998a, Preliminary geologic map of the Wind Mesa quadrangle, Bernalillo County, New Mexico: U.S. Geological Survey, Open-file Report 97-740, scale 1:24,000.

Maldonado and Atencio, 1998b Preliminary geologic map of the Dalies NW quadrangle, Bernalillo County, New Mexico: U.S. Geological Survey, Open-file Report 97-741, scale 1:24,000.

Maldonado, F., Connell, S.D., Love, D.W., Grauch, V.J.S., Slate, J.L., McIntosh, W.C., Jackson, P.B., and Byers, F.M., Jr., 1999, Neogene geology of the Isleta Reservation and vicinity, Albuquerque Basin, New Mexico: New Mexico Geological Society Guidebook 50, p. 175-188.

McCalpin, J. P., 1997, Paleoseismicity of Quaternary faults near Albuquerque, New Mexico: unpublished Final Technical Report submitted to U.S. Geological Survey by GEO-HAZ Consulting, Inc., Contract 1434-HQ-96-GR-02751, October 6, 1997, 18 p.

Morrison, R.B., 1991, Introduction, in Morrison, R.B., ed., Quaternary nonglacial geology: conterminous U.S.: Geological Society of America, The Geology of North America, v. K-2, p. 1-12.

Mozley, P.S. and Davis, J.M., 1996. Relationship between oriented calcite concretions and permeability correlation in an alluvial aquifer, Sierra Ladrones Formation, New Mexico: Journal of Sedimentary Research, v. 66, p. 11-16.

Panter, K., Hallett, B., Love, D., McKee, C., and Thompson, R., 1999, A volcano revisited: A preliminary report of the geology of Los Lunas Volcano, central New Mexico [abstract]: New Mexico Geology, v. 21, p. 44.

Peate, D. W., Chen, J. H., Wasserburg, G. J., and Papanastassiou, D. A., 1996, ^{238}U-^{230}Th dating of a geomagnetic excursion in Quaternary basalts of the Albuquerque volcanoes field, New Mexico (USA): Geophysical Research Letters, v. 23, n. 17, p. 2271-2274.

Personius, S.F., 1999, Paleoearthquake recurrence in the Rio Grande rift new Albuquerque, New Mexico [abstract], in Schwartz, D., and Satake, K. (eds.), Proceedings of the Paleoseismology Workshop, March 15, 1999, Tsukuba, Japan: U.S. Geological Survey, Open-file report 99-400, p. 26- 32.

Personius, S.F., Eppes, M.C., Mahan, S.A., Love, D.W., Mitchell, D.K., and Murphy A., 2001, Log and data from a trench across the Hubbell Spring fault zone, Bernalillo County, New Mexico: U.S. Geological Survey, Miscellaneous Field Studies Map MF-2348, *version 1.1*.

Reneau, S. L., and Dethier, D. P, 1996, Pliocene and Quaternary history of the Rio Grande, White Rock Canyon and vicinity, New Mexico: New Mexico Geological society Guidebook, 47th Field Conference, p. 317-324.

Ruhe, 1967, Geomorphic surfaces and surficial deposits in southern New Mexico: New Mexico Bureau of Mines and Mineral Resources, Memoir 18, 65 p.

Russell, L.R., and Snelson, S., 1994, Structure and tectonic of the Albuquerque basin segment of the Rio Grande rift: Insights from reflection seismic data: Geological Society of America Special Paper 291, p. 83-112.

Schumm, S.A., 1965, Quaternary paleohydrology, in Wright, H.E., and Frey, D.G., eds, The Quaternary of the United States: New Jersey, Princeton University Press, p. 783-794.

Sargeant, K., 1987, Coping with the river: Settlements in Albuquerque's north valley, *in* Poor, A.V., and Montgomery, J., eds., Papers of the Archaeological Society of New Mexico: Santa Fe, New Mexico, Ancient City Press, p. 31-47.

Smith, G.A., 1994, Climatic influences on continental deposition during late-stage filling of an extensional basin, southeastern Arizona: Geological Society of America Bulletin, v. 106, n. 9, p. 1212-1228.

Smith, G.A., Kuhle, A.J., McIntosh, W.C., 2001, Sedimentologic and geomorphic evidence for seesaw subsidence of the Santo Domingo accommodation-zone basin, Rio Grande Rift, New Mexico: Geological Society of America Bulletin, v. 113, n. 5, p. 561-574

Stix, J., Goff, F., Gorton, M., Heiken, G., and Garcia, S.R., 1988, Restoration of compositional zonation in the Bandelier silicic magma chamber between two caldera-forming eruptions: geochemistry and origin of the Cerro Toledo Rhyolite, Jemez Mountains, New Mexico: Journal of Geophysical Research, v. 93, B6, p.6129-6147.

Stearns, C. E., 1953, Tertiary geology of the Galisteo-Tonque area, New Mexico: Geological Society of America Bulletin, v. 64, p. 459-508.

Stone, B.D., Cole, J.C., Shroba, R., 2001a, Control of inset alluvial terrace deposits in the Rio Grande drainage, north central New Mexico [abstract]: Geological Society of America, Abstracts with Programs, v. 33, n.7.

Stone, B.D., Cole, J.C., Shroba, R., 2001b, Quaternary climate-cycle control of inset alluvial terrace deposits in the Rio Grande drainage, northern New Mexico [abstract]: Geological Society of America, Abstracts with Programs, v. 33, n. 5, p. A-49.

Tedford, R.H., and Barghoorn, S., 1999, Santa Fe Group (Neogene), Ceja del Rio Puerco, northwestern Albuquerque Basin, Sandoval County, New Mexico: New Mexico Geological Society, Guidebook 50, p. 327-335.

Thomas, E., Van Hart, D., McKitrick, S., Gillentine, J., Hitchcock, C., Kelson, K., Noler, J., and Sawyer, T., 1995, Conceptual geologic model of the Sandia National Laboratories and Kirtland Airforce Base: Technical Report, Site-Wide Hydrogeologic Characterization Project, Organization 7584, Environmental Restoration Program. Prepared by GRAM, Inc., Albuquerque, New Mexico; and William Lettis and Associates, Oakland, California, various pagination.

Tonkin, P. J., Harrison, J. B. J., Whitehouse, I. E., and Campbell, A. S., 1981, Methods for assessing late Pleistocene and Holocene erosion history in glaciated mountain drainage basins, *in*, Davies, T. R. H.; and Pearce, Andrew J., eds., Erosion and sediment transport in Pacific Rim steeplands, IAHS-AISH Publication No. 132, p. 527-543.

Terraces of Hell Canyon and its tributaries, Memorial Draw and Ojo de la Cabra

DAVID W. LOVE
New Mexico Bureau of Geology and Mineral Resources, New Mexico Institute of Mining and Technology, Socorro, NM 87801-4796

INTRODUCTION

According to Jackson (1997, p. 657) a terrace is only a geomorphic form, a "valley-contained, aggradational form composed of unconsolidated material" at elevations separated from the present drainage system—above channel, floodplain, and graded valley borders. Terraces consist of both steep risers and flat treads. Leopold et al. (1964) argue that deposits beneath the form should not be called terraces, but alluvial fill or alluvium or alluvial deposits. In contrast, Bull (1991) coined terms relating the material beneath the form as well as the form: "fill terrace", "fill-cut terrace", and "strath terrace", depending on whether the terrace is underlain by thick fill, beveled fill, or thin fill on bedrock. Paired terraces are interpreted to imply widespread or long-duration geomorphic episodes related to tectonics and/or climatic regimes whereas unpaired terraces imply local, short-duration, perhaps not climatically, tectonically, or alluvially significant events.

Geomorphologists have conventional expectations of terraces. Generally terraces are preserved along margins of stream valleys. They commonly parallel modern stream gradients or they diverge downstream or converge downstream. Commonly terraces exhibit equal amounts of preservation/degradation along reaches. They relate to one kind of climatic regime (or sequence of regimes) during episodic downcutting and aggradation. Holocene terraces along arroyos may reflect discontinuous downcutting and backfilling (Schumm and Hadley, 1957) but such ephemeral events are not postulated for larger Pleistocene terraces. Schumm and Parker (1973) also interpret terraces as products of complex response wherein multiple terraces result from autogenic changes in water and sediment discharges within a drainage without external changes in climate, slope/base level, or sediment availability. The terraces along Hell Canyon and two of its tributaries do not exhibit these conventional phenomena. In fact, they fly in the face of all common expectations. The terraces of Hell Canyon drainages are described below after introducing the geomorphic fundamentals of the system.

GEOMORPHIC FUNDAMENTALS OF THE HELL CANYON DRAINAGE

Hell Canyon and its subsidiary drainage basins currently encompass about 300 km^2 and are elongate east-west. Hell Canyon drainage arises in the Manzano and Manzanita Mountains at elevations up to 2,880 m and debouches to the Rio Grande floodplain just below 1,500 m. More than half of the drainage is above 1,880 m (6000 ft, roughly lower tree line). The terraces of Hell Canyon are almost exclusively below 1,880 m. The two tributaries preserving multiple terraces, Ojo de la Cabra and Memorial Draw (a northern tributary of Hell Canyon, named here for a small memorial erected to honor Navy personnel killed in a plane crash in the draw in 1946), arise on the piedmont below 1,880 m. Memorial Draw covers about 19 km^2 and Ojo de la Cabra is less than 2.3 km^2, but its drainage has fluctuated in size and connectedness to mountain headwaters through time due to stream capture and piedmont progradation near the mouth of Sanchez Canyon drainage. Annual precipitation ranges from about 200 mm at the lowest elevations to more than 500 mm in the headwaters. Precipitation intensity ranges up to 150 mm per 24 hours (United States Department of Commerce, 1973). At present, much of the small drainage basins appear not to experience even decadal overland flow events. Channel gradients range from 6 to 26 m/km (0.006 to 0.026). Hell Canyon Arroyo ranges up to 40 m wide and 5 m deep and is continuous from the mountains to the Rio Grande valley. Boulder bars along the valley floor outside the arroyo attest to at least one large flood in the first half of the 20th century. Boulders along tributaries suggest prehistoric high-discharge events that reworked adjacent Pleistocene deposits into Holocene channels. All three drainages cross multiple strands of faults. Ojo de la Cabra and Memorial Draw cross strands of the Hubbell Spring fault zone and lower Memorial Draw follows part of the main strand of the McCormick Ranch fault. Hell Canyon crosses the Manzano fault zone, multiple strands of the Hubbell Spring fault zone, McCormick Ranch fault zone, and strands of the Palace-Pipeline fault zone. Downstream from the Western Hubbell Spring and McCormick Ranch faults, Hell Canyon and Memorial Draw are bordered with loose pebbly sand of the ancestral Rio Grande. Upstream, their borders are various ages of piedmont alluvium. Along the periphery of the drainage basins, eolian sand sheets and dunes have disrupted tributary drainages so that very little runoff is contributed to the drainages themselves.

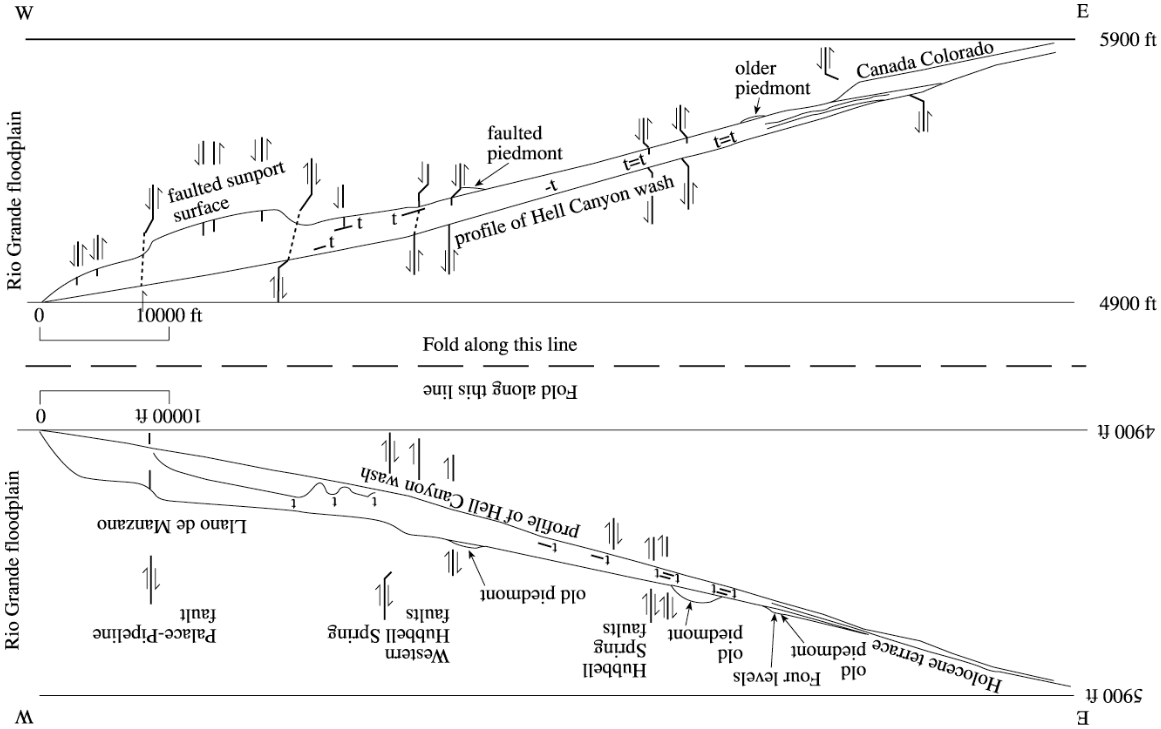

Figure 1. Figure 1. Longitudinal profile of Hell Canyon Wash from the Rio Grande floodplain to the upper piedmont (5900 ft) with terrace reaches and faults shown. Above the fold line is the stream profile, terrace levels, and faults viewed to the north. Below the fold line is the profile, terrace levels, and faults viewed to the south. Kinks in fault symbols portray oblique fault traces. To see differences between the north and south sides of Hell Canyon, fold the paper in half along the fold line and hold it up to strong light or copy the image onto a transparency and fold the two profiles together. Superimposing the two images will show not only the differences between the canyon sides, they will show that one image of both sides would be too complicated for illustrative purposes.

TERRACES

Along these three drainages, geomorphologists may see many subtle stretches of tread surfaces (Fig. 1), but the deposits and soils underneath the surfaces are not well exposed. Similar sub-terrace alluvial deposits occur at different terrace levels; conversely terraces with different sub-terrace deposits and/or soils show up at the same height above the thalweg in different reaches. So-called “fill terraces” crop out near the centers of drainages but these become strath terraces along the valley margins so the terms “fill” and “strath” are a matter of preservation, not fundamental behavior. Terraces may be offset or tilted by faulting, but without better correlation techniques, it is difficult to tell which surface is which across faults. Ephemeral eolian and alluvial cover apparently affects soil development on parts of terraces so that correlations based on soil development are suspect. Finally, on both footwalls and hanging walls of faults shallow, carbonate-precipitating groundwater cemented the deposits and made mounds near the faults and spread laterally and longitudinally to form thin sheets and plates of calcium carbonate (micrite and sparite) both perpendicular and parallel to the ground surface. Degraded spring mounds are not uncommon along some small tributaries and along fault scarps. Yet, springs are rare along the fault traces now (Hubbell Spring and Ojo de la Cabra) and the water table is hundreds of feet below the surface along some stream reaches.

High “terraces” along the lower reach of Hell Canyon are only partially related to the drainage (Fig. 1). The highest surface on the north side of the drainage consists of uplifted and tilted gravelly sands deposited by the Rio Grande, only overtopped locally by piedmont gravels on the downthrown sides of the Palace-Pipeline fault zone. The south rim of the lower reaches of Hell Canyon is capped with piedmont gravel from the Manzanita Mountains and therefore could be considered a “terrace” relative to the inset drainage. Similarly, higher “terraces” along Ojo de la Cabra and Memorial Draw are not related to the streams that currently are cut into them. Rather, some terraces are related to broader aggradational events related to Hell Canyon drainage before it became incised and to local tectonic movements. Such “terraces” are broad surfaces on one side of a tributary (and therefore can not be termed “terraces”), but are inset against uplifted older surfaces on other side. Terraces at similar levels (i.e. the highest levels) on different sides of faults in adjacent reaches may or may not be related.

Along Hell Canyon and Memorial Draw, some inset terraces become wider downstream and overtop the landscape, spreading out to become broad piedmont-like surfaces on both sides of the drainages (Fig. 1). Strands of the Hubbell Spring fault zone cut some of these, particularly along Memorial Draw,; others are unfaulted, but are high on the landscape relative to Hell Canyon drainage and much higher than terraces inset in Hell Canyon.

As one follows terraces upstream along Memorial Draw and Ojo de la Cabra, most of the terraces are very poorly preserved at their downstream ends, are discontinuous and highly eroded, and high on the valley sides in inset positions. As the terraces are followed upstream, they become better preserved and less eroded, more continuous, but still entrenched. Farther upstream they have Holocene alluvium and eolian sands on top of more gravelly alluvium. Even farther upstream, the terraces are unentrenched, occupied by a late Holocene-historic channel and floodplain. New, discontinuous, eroded terraces appear on the landscape above the Holocene drainageway. These new terraces in turn become more continuous and then buried upstream. The higher discontinuous terrace of the lower Ojo de la Cabra canyon may be traced to the upper part of the drainage where it becomes buried by Holocene distal piedmont prograding from the east (in part from lower Sanchez Canyon drainage) and eolian sand prograding across the drainage from the southwest.

The upper part of Memorial Draw is incised into the Canada Colorada surface (Tsp on color map elsewhere in guidebook) as are similar ephemeral drainages to the north. These drainages have intermediate terraces inset below the level of the Canada Colorada and slightly lower piedmont surfaces. They also commonly have only a thin veneer of canyon-bottom Holocene alluvium resting on well cemented Pleistocene conglomerate (not older Tps or Qps; see color map) and groundwater-related platy carbonates. The pervasive platy calcium carbonate cements both within the drainages and along the valley borders suggest (perhaps wrongly) that the drainages are relict from a time when the water table was high and that not much sediment transport or deposition has taken place in the past few thousand years at least. The platy carbonate is commonly broken up and transported short distances downslope, making the shallow exposures difficult to distinguish from degraded Stage IV pedogenic laminar carbonate. These platy carbonate clasts are particularly confusing in young fans along the hanging walls of faults, causing geomorphologists to question the age of the deposits on both sides of fault scarps.

DISCUSSION AND CONCLUSIONS

The terraces of Hell Canyon and its tributaries clearly have a long and complicated history, which remains to be figured out. Details will need to be based on more than 10- and 40-foot contour maps and poor exposures in most reaches. The dynamic shifts in stream entrenchment and episodic terrace formation have taken place during the past million years, ending up with the present incised drainage of Hell Canyon. One can not simply use the “finger method” of counting terraces backward to correlate with the climatic signal recorded by marine oxygen-isotope stages because repeated motions on several faults have affected the terraces, the valley border sediments change downstream, and because the terraces appear to be time-transgressive in part, or at least in their upstream preservation. The upstream preservation and disappearance of terraces imply either incomplete adjustment of the drainages to episodic changes in climate and tectonism (threshold and process-duration phenomena) or dynamic shifts in sediment transport within the upper contributary parts of these small drainages. Is it possible for the small, ephemeral tributary drainages arising on piedmont slopes to generate enough water and sediment discharge within one climatic regime to create a complex response to form more than one terrace in a short period of time, or to generate more than one terrace longitudinally at the same time? Stay tuned.

REFERENCES

Bull, W. B., 1991, Geomorphic responses to climatic change: New York, Oxford University Press, 326 p.

Jackson, J. A., 1997, Glossary of geology [Fourth edition]: American Geological Institute, 769 p.

Leopold, L. B., Wolman, M. G., and Miller, J. P., 1964, Fluvial processes in geomorphology, San Francisco, W. H. Freeman, 522 p.

Schumm, S. A., and Hadley, R. F., 1957, Arroyos and the semiarid cycle of erosion, American Journal of Science, v. 225, p. 161-174.

Schumm, S. A., and Parker, R. S. 1973, Implications of complex response of drainage systems for Quaternary alluvial stratigraphy: Nature, Physical Science (London), v. 243, no. 128, p. 99-100.

United States Department of Commerce, 1973, Precipitation-frequency atlas of the Western United States, v. IV, New Mexico: National Oceanic and Atmospheric Administration, National Weather Service, Atlas 2.

SURFACE GEOLOGY AND LIQUEFACTION SUSCEPTIBILITY IN THE INNER RIO GRANDE VALLEY NEAR ALBUQUERQUE, NEW MEXICO

Keith I. Kelson, Christopher S. Hitchcock, and Carolyn E. Randolph
William Lettis & Associates, Inc.
1777 Botelho Drive, Suite 262
Walnut Creek, California 94596

INTRODUCTION

Historic large earthquakes throughout the world demonstrate that liquefaction-related ground failure commonly causes extensive structural and lifeline damage in urbanized areas. Delineating areas that are susceptible to liquefaction hazards is critical for evaluating and reducing the risk from liquefaction through appropriate mitigation and emergency response. Because liquefaction generally occurs in areas underlain by low-density, saturated granular sediments, liquefaction susceptibility can be mapped using specific, well established geologic and geotechnical criteria. The inner Rio Grande valley near Albuquerque is within the seismically active Rio Grande rift, is underlain by saturated late Holocene floodplain deposits, and thus is particularly vulnerable to liquefaction hazards. The purpose of this study is to delineate areas of the inner Rio Grande valley near Albuquerque that are susceptible to liquefaction (Kelson et al., 1999). The map products developed in the study are useful for insurers, engineers, planners, and emergency-response personnel in order to properly assess and mitigate the risk from future liquefaction hazards in the Albuquerque area.

Methods

Our approach in delineating liquefaction susceptibility in the Albuquerque area is to identify geologic units that are susceptible to liquefaction based on surficial geologic mapping, evaluation of shallow groundwater depths, and analysis of subsurface geotechnical data. These data sets are combined to produce a series of maps showing liquefaction susceptibility in the inner Rio Grande valley. This report presents several 1:24,000-scale maps of the inner valley that depict: (1) surficial geologic units, (2) depth to groundwater, and (3) liquefaction susceptibility. The map area covers the inner Rio Grande valley from the Jemez River on the north to the Isleta Pueblo on the south, and includes parts of the Bernalillo, Alameda, Los Griegos, Albuquerque West, and Isleta 7.5-minute quadrangles. The geologic maps of the inner valley are based primarily on interpretation of aerial photography and geologic mapping, supplemented by geotechnical borehole data compiled from existing databases and logs on file with municipal, state, and federal agencies. The groundwater maps are based on analysis of water-level data from well catalogs, the geotechnical borehole database, shallow drive-point well data, and water-level elevations in drainage ditches.

FLOODPLAIN MATERIALS AND WATER-TABLE DEPTHS

The inner Rio Grande valley is underlain primarily by saturated, unconsolidated sandy alluvium deposited by the Rio Grande and tributary arroyos (Fig. 1). This alluvium consists predominantly of sand and gravel with discontinuous interbeds of silt and clay. Borehole data from these deposits show that most have low Standard Penetration Test (SPT) blow counts. The valley also contains levees, embankments and other man-made features composed of engineered and non-engineered artificial fill. Groundwater in the inner valley is very shallow, with depths beneath most of the valley of less than 12 m (40 ft) (Fig. 2). In this analysis, we use the shallowest historic water level recorded, thus providing conservatively shallow water depths throughout the inner valley. Because of historic declines in groundwater levels near downtown Albuquerque, our analysis provides a conservative assessment of liquefaction susceptibility in areas that continue to experience water-level declines. Lesser amounts of historic groundwater decline in the areas north of Albuquerque (i.e., from Alameda to Bernalillo) and south of Albuquerque (i.e., from Armijo to Isleta Pueblo) suggest that liquefaction susceptibilities in these areas have not been affected by groundwater withdrawals.

LIQUEFACTION SUSCEPTIBILITY

Based on our synthesis of the geologic, geotechnical, and groundwater data, large areas of the inner Rio Grande valley near Albuquerque are susceptible to liquefaction (Fig. 3). Areas underlain by deposits that may liquefy given a peak ground acceleration (PGA) of 0.1g or less, given the occurrence of a magnitude 7.0 earthquake, are classified as having Very High susceptibility. In the inner valley, these areas include the saturated sandy alluvium associated with the present-day channel and active floodplain of the Rio Grande. Where groundwater is less than 9 m (30 ft), areas of artificial fill associated with levees and embankments are conservatively classified as having Very High susceptibility. Areas classified as having High susceptibility have groundwater depths of less than 9 m (30 ft) and are underlain by sandy alluvium that may liquefy with a PGA of 0.2g or less, given the occurrence of a magnitude 7.0 earthquake. Less extensive areas of the inner valley have deeper groundwater and / or are underlain by older, more consolidated deposits that are less susceptible to liquefaction, and are classified as having Moderate or Low susceptibility. Upland areas adjacent to the inner valley generally are classified as having a Low or Very Low susceptibility to liquefaction.

Overall, the areas classified as having a Very High or High liquefaction susceptibility include most of the inner Rio Grande valley. This area involves roughly 240 square kilometers (90 square miles) within the valley north and south of Albuquerque. Downtown Albuquerque is classified as having areas of High susceptibility (roughly southwest of the intersection of Silver Avenue and Sixth Street) and Moderate susceptibility (roughly southwest of the intersection of Marquette Avenue and First Street). The zones identified herein as Very High or High susceptibility encompass the areas most likely to experience liquefaction-related damage from a moderate to large earthquake in central New Mexico. Overall, it is reasonable to assume that large areas of the inner valley will be affected by liquefaction-related damage. Site-specific geotechnical investigations should be performed in areas of Very High or High susceptibility to assess risk to existing facilities and to evaluate and mitigate liquefaction hazards prior to future development.

ACKNOWLEDGMENTS

This research was supported by U.S. Geological Survey (USGS), Department of the Interior, under USGS award number 98-HQ-GR-1009, for the National Earthquake Hazard Reduction Program. The views and conclusions contained in this document are those of the authors and should not be interpreted as necessarily representing the official policies, either expressed or implied, of the U.S. Government.

REFERENCES

Kelson, K.I., Hitchcock, C.S., and Randolph, C.E, 1999, Liquefaction Susceptibility in the Inner Rio Grande Valley Near Albuquerque, New Mexico: unpublished final technical report, U.S. Geological Survey National Earthquake Hazards Reduction Program, Award Number 98-HQ-GR-1009, 40 p., 9 plates, scale 1:24,000.

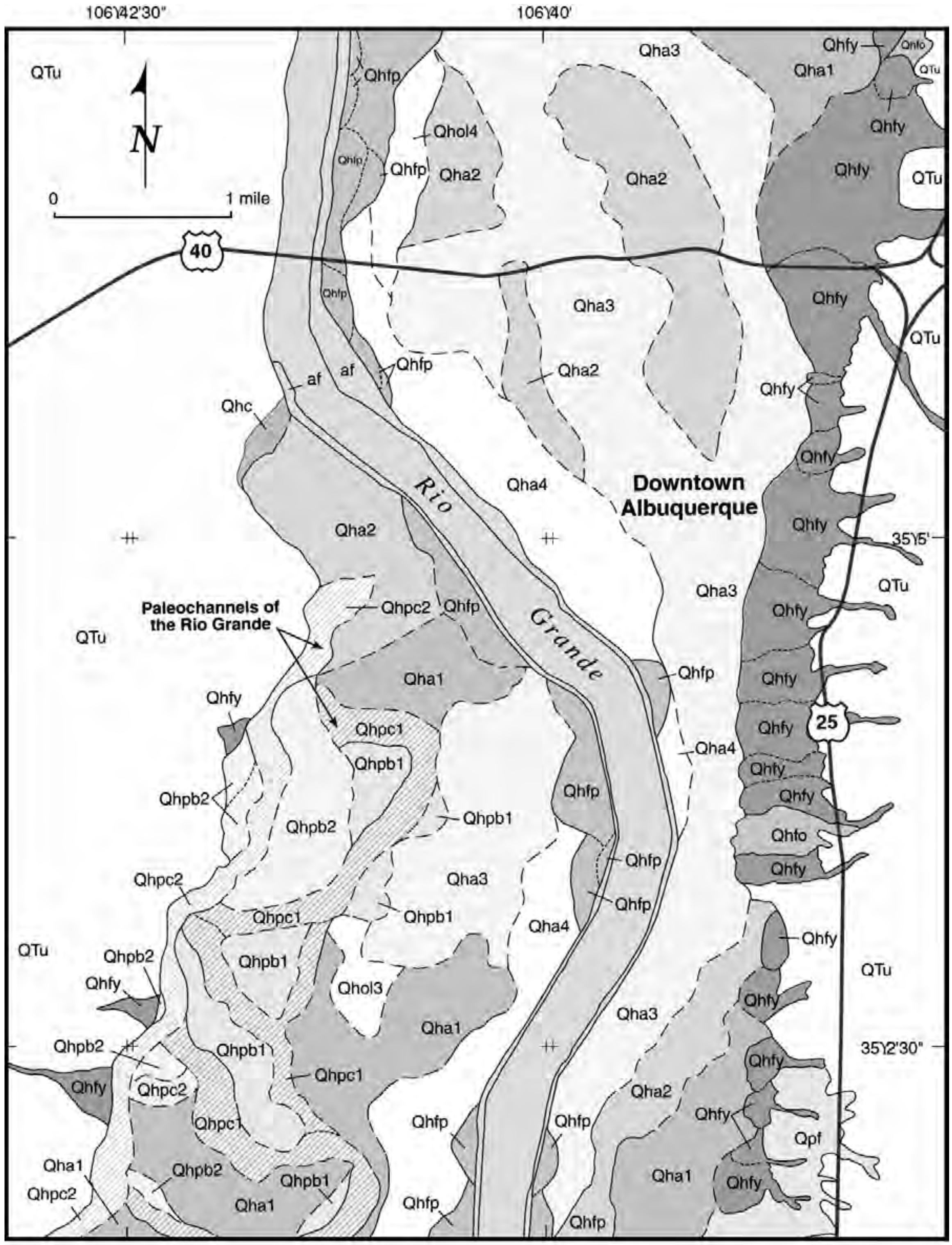

Figure 1. Surficial geologic map of part of the Albuquerque West quadrangle. Units designated by following notation; Q: Quaternary, Pleistocene, fp: floodplain, a: alluvium, ps: paleochannel, ol: overbank levee; pb: point bar; e: eolian, fy: young alluvial fan, fo: old alluvial fan, c: colluvium, af: artificial fill. Numerals indicate relative age of units, with 1=oldest and 4=youngest.

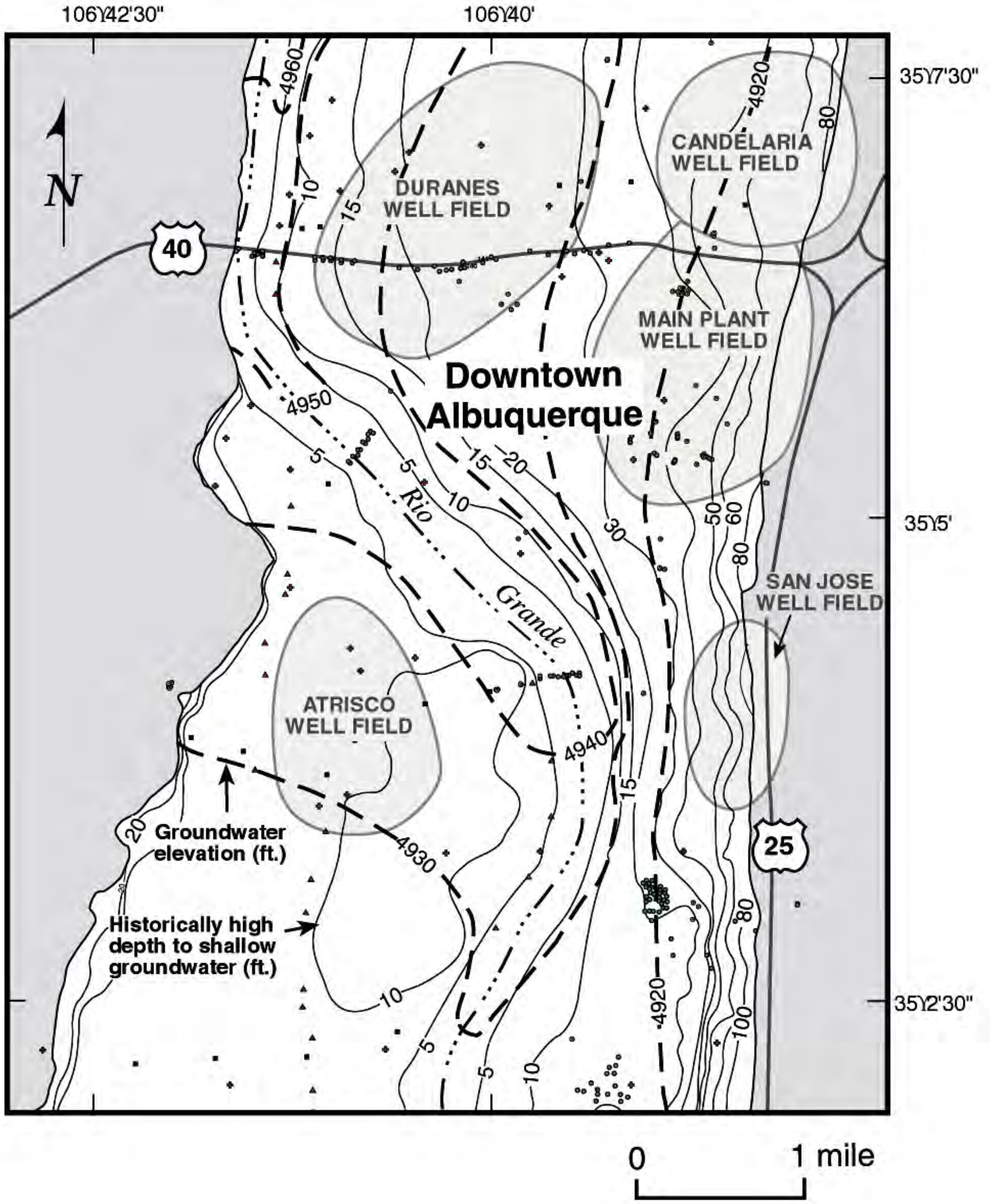

Figure 2. Groundwater elevation map (dashed lines) and depth-to-groundwater contour map (solid lines) of part of Albuquerque West quadrangle. Data point from shallow boreholes, drainage ditches, and drive-point wells (Kelson et al., 1999).

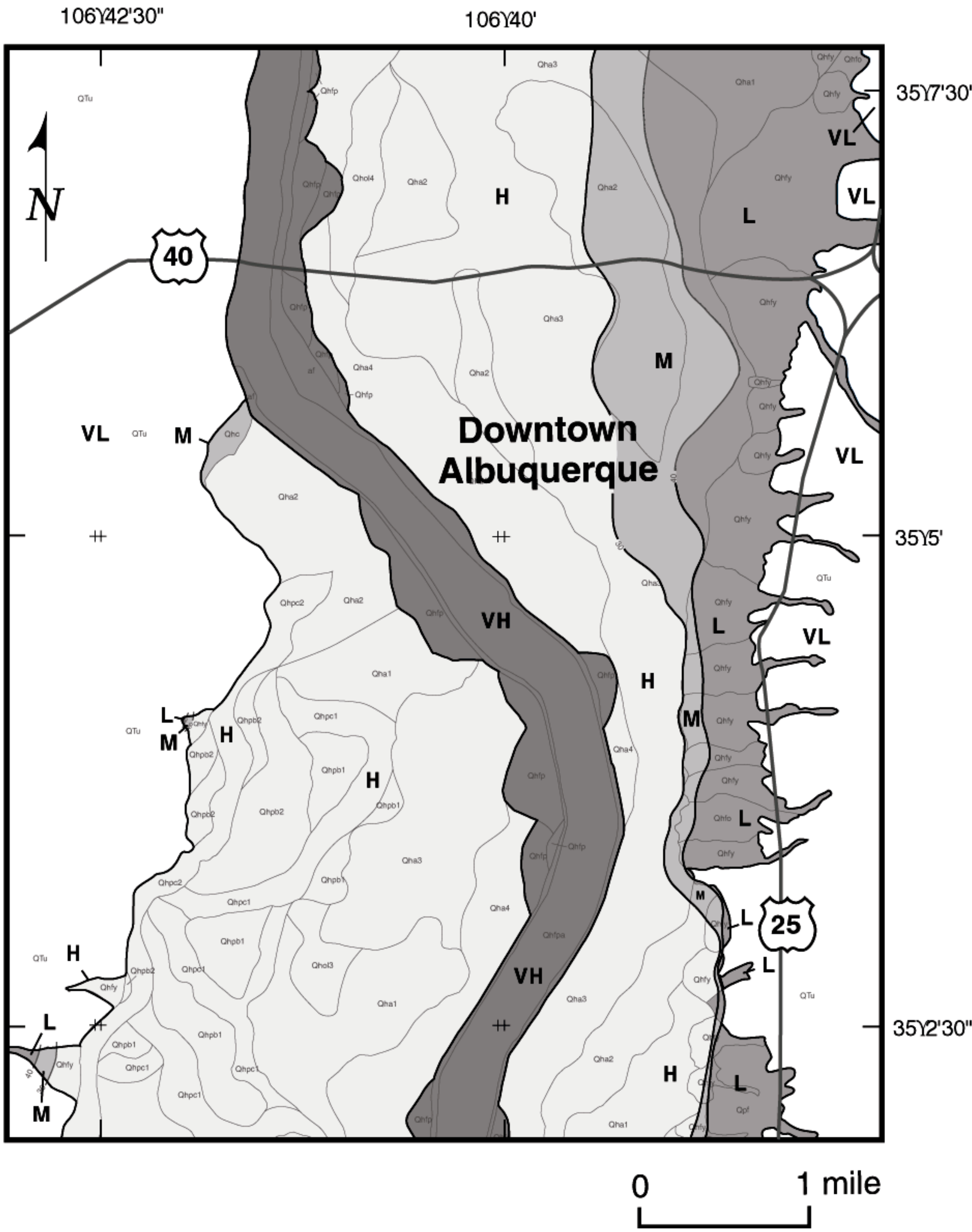

Figure 3. Liquefaction susceptibility of part of the Albuquerque West quadrangle (VH: Very high, H: High, M: Moderate, L: Low, VL: Very Low).

STRATIGRAPHY OF MIDDLE AND UPPER PLEISTOCENE FLUVIAL DEPOSITS OF THE RIO GRANDE (POST-SANTA FE GROUP) AND THE GEOMORPHIC DEVELOPMENT OF THE RIO GRANDE VALLEY, NORTHERN ALBUQUERQUE BASIN, CENTRAL NEW MEXICO

SEAN D. CONNELL
New Mexico Bureau of Mines and Mineral Resources-Albuquerque Office, New Mexico Institute of Mining and Technology, 2808 Central Ave. SE, Albuquerque, NM 87106

DAVID W. LOVE
New Mexico Bureau of Mines and Mineral Resources, New Mexico Institute of Mining and Technology, 801 Leroy Place, Socorro, NM 87801

INTRODUCTION

Alluvial and fluvial deposits inset against Plio-Pleistocene deposits of the upper Santa Fe Group (Sierra Ladrones and Arroyo Ojito formations) record the development of the Rio Grande valley (Fig. 1) in the northern part of the Albuquerque basin since early Pleistocene time. These fluvial terrace deposits contain pebbly to cobbly sand and gravel with abundant rounded quartzite, subordinate volcanic, and sparse plutonic clasts derived from northern New Mexico. Although the composition of the gravel in these deposits is similar, they can be differentiated into distinct and mappable formation- and member-rank units on the basis of landscape-topographic position, inset relationships, soil morphology, and height of the basal contact above the Rio Grande as determined from outcrop and drillhole data (Table 1; Connell and Love, 2000). These fluvial deposits overlie, and locally interfinger with, alluvial deposits derived from paleo-valley margins and basin margin uplands (Fig. 2). Constructional terrace treads are not commonly preserved in older deposits, but are locally well preserved in younger deposits.

Kirk Bryan (1909) recognized two distinct types of ancestral Rio Grande deposits, his older Rio Grande beds (now called upper Santa Fe Group), and his younger, inset Rio Grande gravels (post Santa-Fe Group). Lambert (1968) completed the first detailed geologic mapping of the Albuquerque area and proposed the terms Los Duranes, Edith, and Menaul formations for prominent fluvial terrace deposits associated with the ancestral Rio Grande, however, these terms were not formally defined. Lambert (1968) correctly suggested that a higher and older unit (his Qu(?)g) may be an inset fluvial deposit of the ancestral Rio Grande (Tercero alto terrace of Machette, 1985).

We informally adopt three additional lithostratigraphic terms to clarify and extend Lambert's inset Rio Grande stratigraphy. We propose lithostratigraphic terms to these fluvial deposits principally to avoid confusion in the use of geomorphic terms, such as the primero, segundo, and tercero alto surfaces (Lambert, 1968), for lithologic units. Furthermore, these geomorphic (i.e., "-alto") terms were imported by Lambert (1968) for geomorphic surfaces described by Bryan and McCann (1936, 1938) in the upper Rio Puerco valley without careful comparison of soil-morphologic and geomorphic character of deposits within each drainage basin. Thus, these geomorphic terms may not be applicable in the Rio Grande valley without additional work to establish surface correlations across the Llano de Albuquerque, the interfluve between the Rio Grande and Rio Puerco valleys. Fluvial deposits discussed in this paper are, in increasing order of age, the Los Padillas, Arenal, Los Duranes, Menaul, Edith, and Lomatas Negras formations.

Although these inset ancestral Rio Grande units may be classified and differentiated allostratigraphically, we consider them as lithologic units of formation- and member rank that can be differentiated on the basis of bounding unconformities, stratigraphic position, and lithologic character.

Recent geologic mapping of the Albuquerque area (Cather and Connell, 1998; Connell, 1997, 1998; Connell et al., 1998; Love, 1997; Love et al., 1998; Smith and Kuhle, 1998; Personius et al., 2000) delineate a suite of inset fluvial deposits associated with the axial-fluvial ancestral Rio Grande. Inset terrace deposits record episodic incision and partial aggradation of the ancestral Rio Grande during Pleistocene and Holocene time. Lack of exposure and preservation of terrace deposits between Galisteo Creek and Las Huertas Creek hampers correlation to partially dated terrace successions at the northern margin of the basin and in White Rock Canyon (Dethier, 1999; Smith and Kuhle, 1998), southward into Albuquerque; however, correlation of these units using soil-morphology, landscape position, and stratigraphic relationships provide at least limited local constraints on the Rio Grande terrace stratigraphy.

Soil-morphologic information derived from profiles for fluvial and piedmont deposits are described on well preserved parts of constructional geomorphic surfaces (Connell, 1996). Carbonate morphology follows the morphogenetic classification system of Gile et al. (1966).

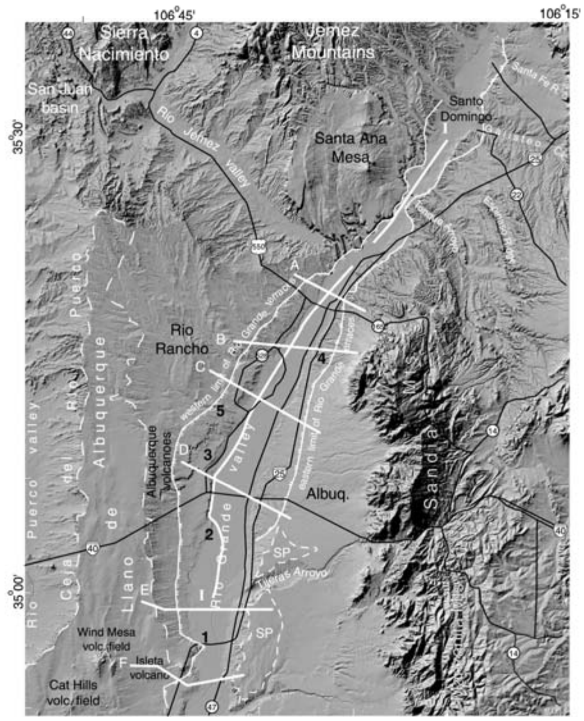

Figure 1. Shaded relief image of the northern part of the Albuquerque Basin (derived from U.S. Geological Survey 10-m DEM data) illustrating the approximate locations of terrace risers (hachured lines), the Sunport surface (SP), stratigraphic sections (1-5), and cross section lines (A-F).

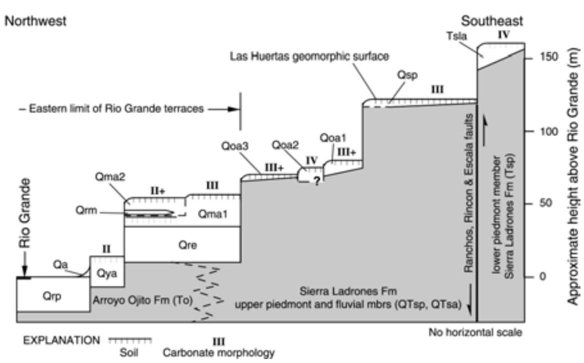

Figure 2. Block diagram of geomorphic relationships among entrenched post-Santa Fe Group deposits along the western piedmont of the Sandia Mountains and east of the Rio Grande valley (from Connell and Wells, 1999).

Lomatas Negras Formation

The highest and presumably oldest preserved Rio Grande terrace deposit in the Albuquerque-Rio Rancho area is informally called the Lomatas Negras Formation for Arroyo Lomatas Negras, where a buttress unconformity between this deposit and the underlying Arroyo Ojito Formation is exposed in the Loma Machete quadrangle (unit Qtag, Personius et al., 2000). The Lomatas Negras Formation is typically less than 16 ft (5 m) thick and consists of moderately consolidated and weakly cemented sandy pebble to cobble gravel primarily composed of subrounded to rounded quartzite, volcanic rocks, granite and sparse basalt (Fig. 3). This unit is discontinuously exposed along the western margin of the Rio Grande valley, where it is recognized as a lag of rounded quartzite-bearing gravel typically between about 215-245 ft (65-75 m) above the Rio Grande floodplain, which is underlain by the Los Padillas Formation (Fig. 4). The basal contact forms a low-relief strath cut onto slightly tilted deposits of the Arroyo Ojito Formation. The top is commonly eroded and is commonly overlain by middle Pleistocene alluvium derived from drainages heading in the Llano de Albuquerque. Projections of the base suggest that it is inset against early Pleistocene aggradational surfaces that define local tops of the Santa Fe Group, such as the Las Huertas and Sunport geomorphic surfaces (Connell et al., 1995, 1998; Connell and Wells, 1999; Lambert, 1968).

Correlative deposits to the south (Qg(?) of Lambert, 1968) underlie the late-middle Pleistocene (156±20 ka, Peate et al., 1996) Albuquerque Volcanoes basalt (Figs. 3-4). Projections of the Lomatas Negras Formation north of Bernalillo are limited by the lack of preserved terraces, so, we provisionally correlate these highest gravel deposits with the Lomatas Negras Formation, recognizing the possibility that additional unrecognized terrace levels and deposits may be present along the valley margins. Similar deposits are recognized near Santo Domingo (Qta1 of Smith and Kuhle, 1998), which contain the *ca*. 0.66 Ma Lava Creek B ash from the Yellowstone area of Wyoming. A gravel quarry in the Pajarito Grant (Isleta quadrangle) along the western margin of the Rio Grande valley exposes an ash within an aggradation succession of fluvial sand and gravel. This ash has been geochemically correlated to the Lava Creek B (N. Dunbar, 2000, personal commun.) It lies within pebbly to cobbly sand and gravels that grade upward into a succession of sand with lenses of pebbly sand. This unit is slightly lower, at ~46 m above the Rio Grande, than Lomatas Negras deposits to the north, suggesting the presence of additional unrecognized middle Pleistocene fluvial units, or intrabasinal faulting has down-dropped the Pajarito Grant exposures. The Lomatas Negras Formation is interpreted to be inset against the Sunport surface, which contains a 1.26 Ma ash near the top of this Santa Fe Group section in Tijeras Arroyo. These stratigraphic and geomorphic relationships indicate that the Lomatas Negras Formation was deposited between about 1.3 and 0.7 Ma.

Table 1. Summary of geomorphic, soil-morphologic, and lithologic data for ancestral Rio Grande fluvial, piedmont and valley border deposits, listed in increasing order of age.

Unit	Height above Rio Grande (m)	Thickness (m)	Carbonate Morphology	Geomorphic/stratigraphic position
Qrp	0	15-24	0	Lowest inset deposit; inner valley floodplain.
Qay	0-3	<21	0, I	Inset against Qpm; grades to Qrp.
Qra	15	3-6	II+	Primero alto surface, inset against Qrd.
Qam, Qpm	~65, eroded top	45	III	Alluvial deposits west of Rio Grande valley; Overlies Qrd.
Qrd	44-48	6-52	II+	Segundo alto surface, inset against Qre
Qpm	8-30	15-51	II+, III+	Piedmont deposits of Sandia Mts; east of Rio Grande valley; interfingers with Qrm.
Qrm	26-36	3	II+	Overlies Qpm and Qre; may be correlative to part of Qrd.
Qre	12-24, eroded top	3-12	not determined	Inset against Qrl, inset by Qrd; underlies Qpm with stage III + carbonate morphology.
Qao, Qpo	~100, eroded top	<30	III to IV	Overlies Qrl; inset by Qpm and Qre.
Qrl	~46-75, eroded top	5-20	III, eroded	Inset against Sunport surface. Contains ash correlated to the Lava Creek B.
Las Huertas	~120	---	III+	Local top of Sierra Ladrones Formation
SP	~95	---	III+	Sunport surface of Lambert (1968): youngest Santa Fe Group constructional basin-floor surface.

Edith Formation

The Edith Formation is a 10-40 ft (3-12 m) thick deposit that typically comprises a single upward fining sequence of basal gravel and overlying sandy to muddy floodplain deposits. The Edith Formation serves as a useful and longitudinally extensive marker along the eastern margin of the Rio Grande valley, between Albuquerque and San Felipe Pueblo, New Mexico. This fluvial deposit can be physically correlated across 33 km, from its type area in Albuquerque (Lambert, 1968, p. 264-266 and p. 277-280), to near Algodones, New Mexico (Lambert, 1968; Connell et al., 1995; Connell, 1998, 1997; and Cather and Connell, 1998). The Edith Formation is a poorly to moderately consolidated, locally cemented deposits of pale-brown to yellowish-brown gravel, sand and sandy clay that forms laterally extensive outcrops along the inner valley escarpment of the Rio Grande. Commonly recognized as an upward-fining succession of a 7-26 ft (2-8 m) thick, basal quartzite-rich, cobble gravel that grades up-section into a 13-32 ft (4-10 m) thick succession of yellowish-brown sand and reddish-brown mud. The upper contact is locally marked by a thin, white diatomite between Sandia Wash and Bernalillo. Gravel contains ~30% rounded quartzite and ~40% volcanic rocks with subordinate granite, metamorphic, and sandstone clasts, and sparse, rounded and densely welded Bandelier Tuff (Connell, 1996). The Edith Formation unconformably overlies tilted sandstone of the Arroyo Ojito and Sierra Ladrones formations and is overlain by piedmont alluvium derived from the Sandia Mountains (Fig. 5). Where the top of the Edith Formation is preserved, it typically contains weakly developed soils with Stage I carbonate morphology. This weak degree of soil development suggests that deposition of piedmont and valley border fan sediments occurred shortly after deposition of the Edith Formation.

The Edith Formation contains Rancholabrean fossils, most notably *Bison*, *Mastodon*, *Camelops*, and *Equus* (Lucas et al., 1988). Lambert (1968) considered the Edith Formation to represent a late Pleistocene terrace deposited during the latest Pleistocene glacial events. Soils developed in these piedmont deposits exhibit moderately developed Bt and Btk horizons with moderately thick clay films and Stage III+ carbonate morphology, suggesting a middle Pleistocene age for these deposits (Connell, 1996; Connell and Wells, 1999).

The base of the Edith Formation forms a prominent strath that lies about 40-80 ft (12-24 m) above the Rio Grande floodplain and is about 30 m higher than the base of the Los Duranes Formation (Connell, 1998). The elevation of this basal strath is lower than the base of the Lomatas Negras Formation suggesting that the Edith Formation is inset against

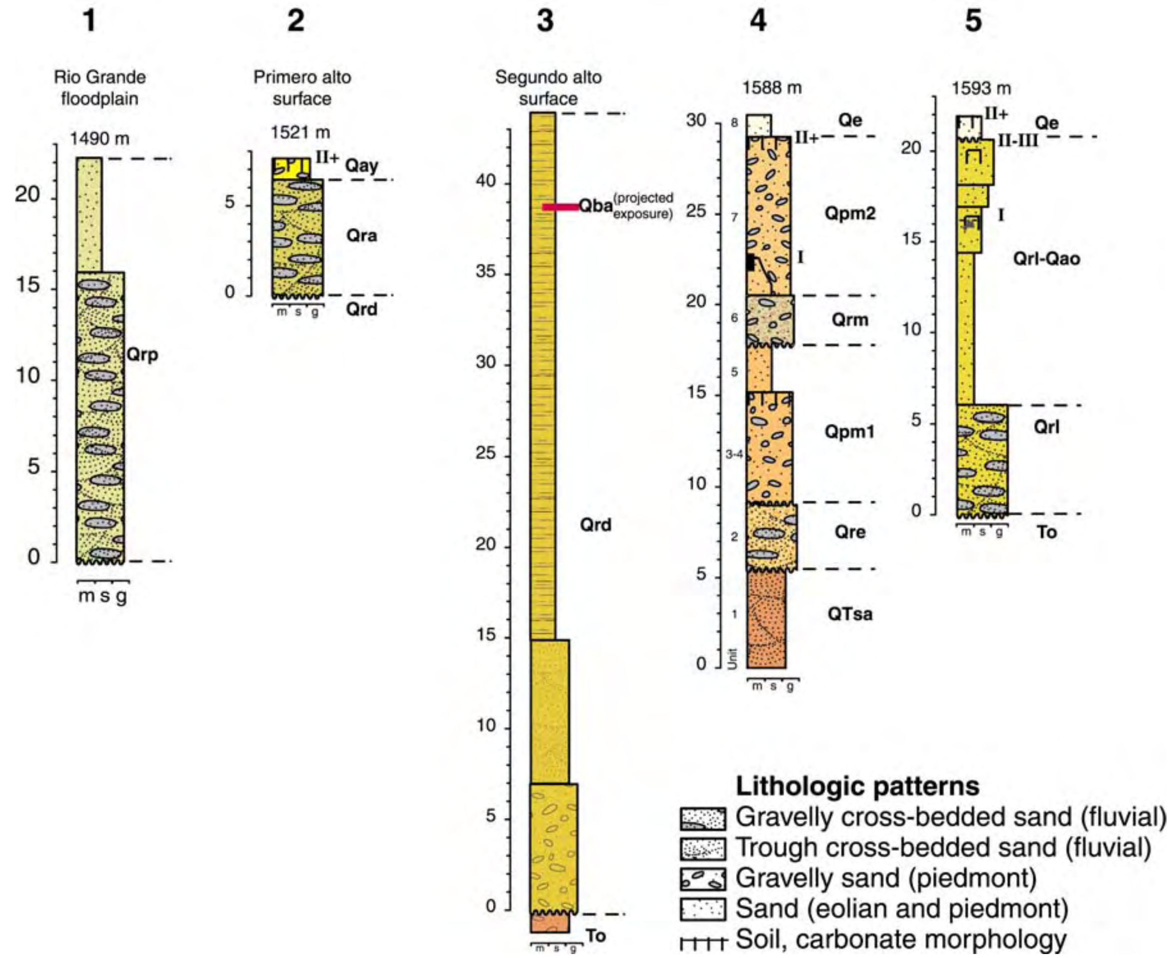

Figure 3. Stratigraphic and drillhole sections of Pleistocene fluvial deposits of the ancestral and modern Rio Grande along the Rio Grande valley: 1) Los Padillas Formation at the Black Mesa-Isleta Drain piezometer nest; 2) Arenal Formation at Efren quarry (modified from Lambert, 1968; Machette et al., 1997); 3) Los Duranes Formation at the Sierra Vista West piezometer nest (data from Chamberlin et al., 1998); 4) Edith and Menaul formations at Sandia Wash (Connell, 1996); and 5) Lomatas Negras Formation at Arroyo de las Calabacillas and Arroyo de las Lomatas Negras.

the Lomatas Negras Formation. A partially exposed buttress unconformity between eastern-margin piedmont alluvium and upper Santa Fe Group deposits marks the eastern extent of this unit. This unconformity is locally exposed in arroyos between Algodones and Bernalillo, New Mexico.

Lambert (1968) recognized the unpaired nature of terraces in Albuquerque, but assigned the Edith Formation to the topographically lower primero alto terrace, which is underlain by the Los Duranes Formation in SW Albuquerque. Lambert (1968) correlated the Edith Formation with the primero alto terrace, and therefore interpreted it to be younger than the Los Duranes Formation. The primero alto terrace is the lowest fluvial-terrace tread in SW Albuquerque and is underlain by rounded pebbly sandstone that is inset against the Los Duranes Formation. Soils on the primero alto terrace are weakly developed (stage I to II+ carbonate morphology, Machette et al., 1997) compared to piedmont deposits overlying the Edith Formation. Therefore, it is likely that the gravels underlying the primero alto terrace are probably much younger than the Edith Formation. Therefore, if the Edith Formation is older than the Los Duranes Formation (see below), it was deposited prior to about 100-160 ka.

The Edith Formation may correlate to fluvial terrace deposits near Santo Domingo Pueblo (Smith and Kuhle, 1998). Deposits at Santo Domingo Pueblo are approximately 30-m thick and about 30-35 m above the Rio Grande (Qta3 of Smith and Kuhle, 1998). The lack of strongly developed soils between the Edith Formation and interfingering middle Pleistocene piedmont alluvium suggests that the Edith Formation was deposited closer in time to the Los Duranes Formation. Thus, the Edith Formation was deposited between 0.66 and 0.16 Ma, and was probably laid down during the later part of the middle Pleistocene.

Los Duranes Formation

The Los Duranes Formation of Lambert (1968) is a 40-52 m fill terrace consisting of poorly to moderately consolidated deposits of light reddish-brown, pale-brown to yellowish-brown gravel, sand, and minor sandy clay derived from the ancestral Rio Grande and tributary streams. The base typically buried by deposits of the Rio Grande floodplain (Los Padillas Formation) in the Albuquerque. The basal contact forms a low-relief strath approximately 20 ft (6 m) above the Rio Grande floodplain near Bernalillo, New Mexico (Figs. 3-4), where the Los Duranes Formation is eroded by numerous arroyos and is about 20-23 ft (6-7 m) thick. The basal contact is approximately 100 ft (30 m) lower than the base of the Edith Formation. The terrace tread on top of the Los Duranes Formation (~42-48 m above the Rio Grande) is about 12-32 m higher than the top of the Edith Formation. Geologic mapping and comparison of subsurface data indicate that the base of the Edith Formation is about 20-25 m higher than the base of Los Duranes Formation, suggesting that the Los Duranes is inset against the Edith. Just north of Bernalillo, New Mexico, deposits correlated to the Los Duranes Formation (Connell, 1998) contain the Rancholabrean mammal *Bison latifrons* (Smartt et al., 1991, SW1/4, NE1/4, Section 19, T13N, R4E), which supports a middle Pleistocene age. The Los Duranes Formation is also overlain by the 98-110 ka Cat Hills basalt (Maldonado et al., 1999), and locally buries flows of the 156±20 ka (Peate et al., 1996) Albuquerque volcanoes basalt. Thus deposition of the Los Duranes Formation ended between 160-100 ka, near the end of the marine oxygen isotope stage 6 at about 128 ka (Morrison, 1991).

Near Bernalillo, the basal contact of the Los Duranes(?) Formation, exposed along the western margin of the of the Rio Grande valley, is approximately 30 m lower than the basal contact of the Edith Formation, which is well exposed along the eastern margin of the valley. This western valley-margin fluvial deposit was originally assigned to the Edith Formation by Smartt et al. (1991), however, these are interpreted to be younger inset deposits that are likely correlative to the Los Duranes Formation (Connell, 1998; Connell and Wells, 1999).

The terrace tread (top) of the Los Duranes Formation is locally called the segundo alto surface in the Albuquerque area (Lambert, 1968; Hawley, 1996), where it forms a broad constructional surface west of the Rio Grande. Kelley and Kudo (1978) called this terrace the Los Lunas terrace, near Isleta Pueblo, however, we support the term Los Duranes Formation as defined earlier by Lambert (1968). The Los Duranes Formation represents a major aggradational episode that may have locally buried the Edith Formation; however, the Edith Formation could also possibly mark the base of the aggrading Los Duranes fluvial succession.

Menaul Formation(?)

The Menaul Formation of Lambert (1968) is generally less than 10 ft (3 m) thick and overlies interfingering piedmont deposits that overlie the Edith Formation. The Menaul Formation consists of poorly consolidated deposits of yellowish-brown pebble gravel and pebbly sand derived from the ancestral Rio Grande. Rounded quartzite pebbles that are generally smaller in size than pebbles and cobbles in the Edith Formation. The Menaul gravel forms discontinuous, lensoidal exposures along the eastern margin o the Rio Grande valley. The basal contact is approximately 85-118 ft (26-36 m) above the Rio Grande floodplain. The Menaul Formation is conformably overlain by younger, eastern-margin piedmont alluvium exhibiting Stage II+ carbonate morphology, and is inset by younger stream alluvium that exhibits weakly developed soils, suggesting a late Pleistocene age of deposition.

Soils on piedmont deposits overlying the Menaul are generally similar to the Los Duranes Formation; however, differences in parent material texture make soil-based correlations somewhat ambiguous. Similarities in height above the Rio Grande and soil development on the Los Duranes Formation and the Menaul Formation suggest that these two units may be correlative. Thus, the Menaul Formation may be temporally correlative to the Los Duranes Formation, and is likely a member of this unit. These units may be associated with an aggradational episode, possibly associated with aggradation of the Los Duranes, middle Pleistocene piedmont alluvium. The Edith Formation may represent the base of a Los Duranes-Menaul aggradational episode during the late-middle Pleistocene. The base Edith Formation is consistently higher than the base of the Los Duranes Formation, suggesting that the Edith is older; however, definitive crosscutting relationships have not been demonstrated.

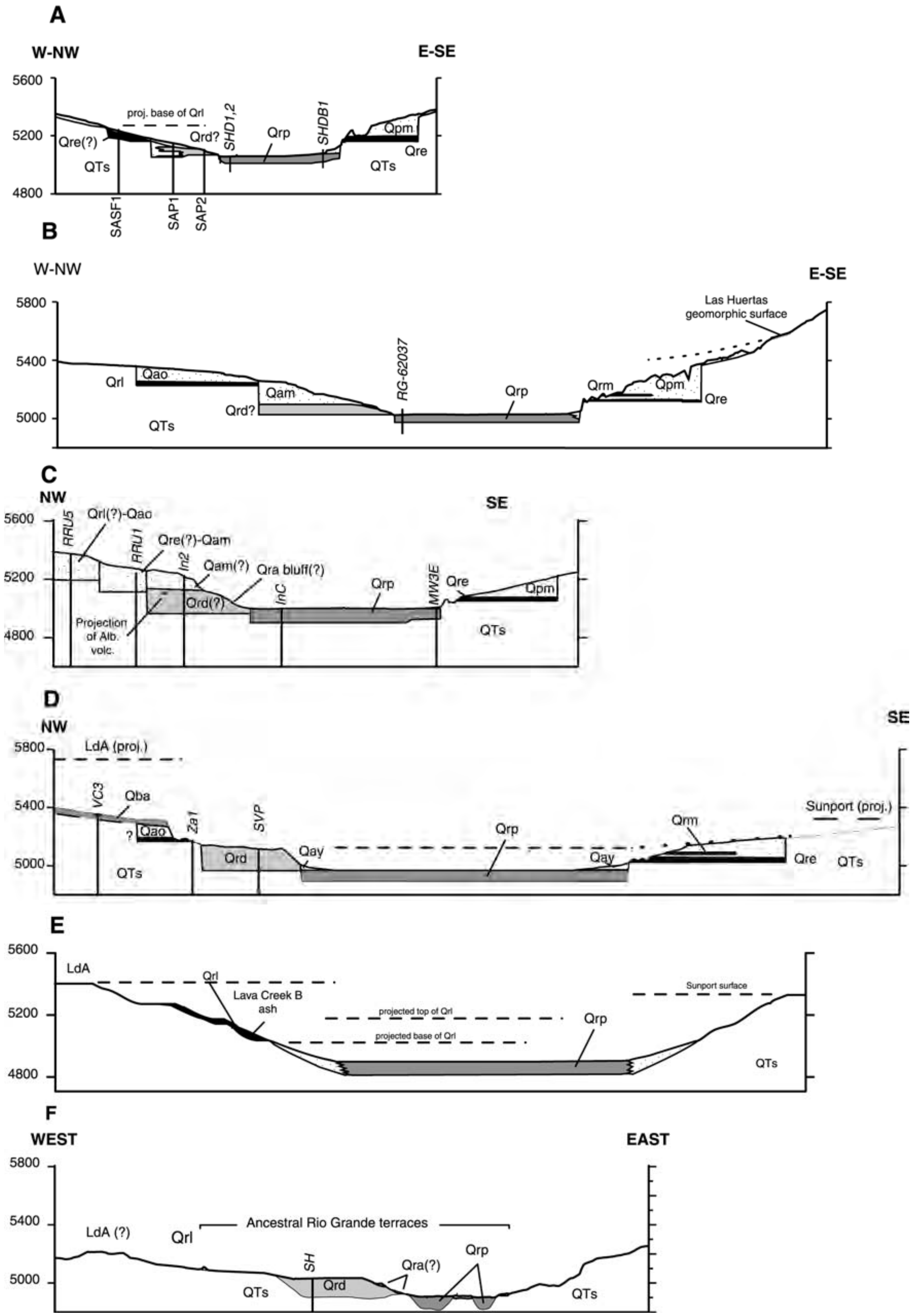

Figure 4. Simplified geologic cross sections across the Rio Grande valley, illustrating inset relationships among progressively lower fluvial deposits. Letters indicate location of profiles on Figure 1 and elevations of cross sections are in feet above mean sea level. See Table 1 for description of symbols. Unit QTs denotes upper Santa Fe Group deposits.

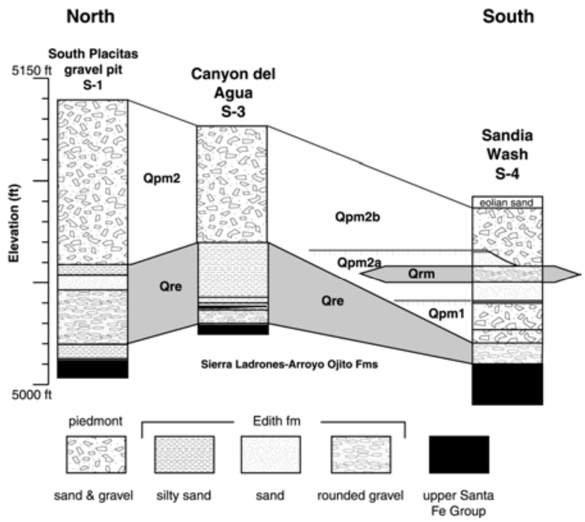

Figure 5. Stratigraphic fence of Edith Formation and piedmont deposits exposed along eastern margin of the Rio Grande valley, between Sandia Wash and highway NM-165, illustrating stratigraphic relationships among fluvial-terrace and piedmont deposits.

Arenal Formation

The lowest preserved terrace deposit is the Arenal Formation, which was named for exposures just west of the Arenal Main Canal in SW Albuquerque (Connell et al., 1998). The Arenal Formation is 3-6 m thick and is inset against the Los Duranes Formation. The Arenal Formation consists of poorly consolidated deposits of very pale-brown to yellow sandy pebble to cobble gravel recognized along the northwestern margin of the Rio Grande inner valley. Gravel clasts are primarily rounded quartzite and subrounded volcanic rocks (welded tuff and rare pumice) with minor granite. Soil development is very weak, with Stage I to II+ carbonate morphology (Machette et al., 1997; Machette, 1985). The top of the Arenal Formation is the primero alto surface of Lambert (1968), which is 15-21 m above the Rio Grande. This deposit is not correlative to the Edith Formation as originally interpreted by Lambert. This unit is interpreted to have been deposited during late Pleistocene time, probably between about 71-28 ka.

Los Padillas Formation

The Las Padillas Formation underlies the modern Rio Grande valley and floodplain and is interpreted to represent the latest incision/aggradation phase of the Rio Grande, which was probably deposited during latest Pleistocene-Holocene time. The Rio Grande floodplain (inner valley) ranges 3-8 km in width in most places and occupies only a portion of the 10-12 km maximum width of the entire ancestral Rio Grande systems tract of the Sierra Ladrones Formation (Connell, 1997, 1998; Connell et al., 1995; Maldonado et al., 1999; Smith and Kuhle, 1998). The top comprises the modern floodplain and channel of the Rio Grande. The Los Padillas Formation is 15-29 m thick and consists of unconsolidated to poorly consolidated, pale-brown, fine- to coarse-grained sand and rounded gravel with subordinate, discontinuous, lensoidal interbeds of fine-grained sand, silt, and clay derived from the Rio Grande. This unit is recognized in drillholes and named for deposits underlying the broad inner valley floodplain near the community of Los Padillas in SW Albuquerque (Connell et al., 1998; Connell and Love, 2000). Drillhole data indicate that the Los Padillas Formation commonly has a gravelly base and unconformably overlies the Arroyo Ojito Formation. This basal contact is locally cemented with calcium carbonate. The Los Padillas Formation is overlain, and interfingers with, late Pleistocene to Holocene valley border alluvial deposits derived from major tributary drainages.

Because this unit has not been entrenched by the Rio Grande, no age direct constraints are available for the base of the alluvium of the inner valley in the study area. This deposit underlies a continuous and relatively broad valley floor that extends south from the Albuquerque basin through southern New Mexico, where radiocarbon dates indicate aggradation of the inner valley by early Holocene time (Hawley and Kottlowski, 1969; Hawley et al., 1976). The base of the Los Padillas Formation was probably cut during the last glacial maximum, which is constrained at ~15-22 ka in the neighboring Estancia basin, just east of the Manzano Mountains. (Allen and Anderson, 2000). Thus, the inner valley alluvium was probably incised during the latest Pleistocene and aggraded during much of Holocene time. Near the mouth of Tijeras Arroyo, charcoal was recovered from about 2-3 m below the top of a valley border fan that prograded across the Los Padillas Formation and forms a broad valley border fan than has pushed the modern Rio Grande to the western edge of its modern (inner) valley. This sample yielded a radiocarbon date of about 4550 yrs. BP (Connell et al., 1998), which constrains the bulk of deposition of the Los Padillas Formation to middle Holocene and earlier.

EVOLUTION OF THE RIO GRANDE VALLEY

Santa Fe Group basin-fill deposits of the ancestral Rio Grande generally differ in the scale and thickness relative to younger inset deposits, which were deposited in well defined valley. During widespread aggradation of the basin (Santa Fe Group time), the ancestral Rio Grande intimately interfingered with piedmont deposits derived from rift-margin uplifts, such as the Sandia Mountains

(Connell and Wells, 1999; Maldonado et al., 1999). Field and age relationships in the near Santa Ana Mesa also indicate that the ancestral Rio Grande also interfingered with fluvial deposits correlated with the Arroyo Ojito Formation (Cather and Connell, 1998). During development of the Rio Grande valley (post-Santa Fe Group time), the Rio Grande cut deeply into older basin-fill, typically leaving large buttress unconformities between inset deposits and older basin fill of the upper Santa Fe Group (Fig. 8).

Younger late Pleistocene-Holocene alluvial deposits are commonly confined in arroyo channels cut into older piedmont deposits east of the Rio Grande valley. These deposits commonly form valley border alluvial fans along bluffs cut by a meandering Rio Grande. These fans commonly prograde across floodplain and channel deposits in the inner valley. The present discharge is inadequate to transport sediment out of the valley. The presence of progressively inset fluvial deposits along the margins of the modern valley indicates that episodes of prolonged higher discharge were necessary to flush sediment and erode the valley. Such episodes must have occurred prior to aggradation of valley fills, such as these fluvial terrace deposits.

Progradation of middle Holocene tributary valley border fans across the modern Rio Grande floodplain suggests that deposition of tributary and piedmont facies occurred during drier (interglacial) conditions. Deposition of fluvial terraces in semi-arid regions probably occurred during the transition from wetter to drier climates (Schumm, 1965; Bull, 1991). The lack of strong soils between the terrace deposits of the ancestral Rio Grande and piedmont and valley border deposits suggests that piedmont and valley border deposition occurred soon after the development of major fluvial terrace deposits.

Age constraints for the Los Duranes Formation indicate that aggradation of fluvial deposits occurred near the end of glacial periods. If we extrapolate ages based on this model of terrace development, then we can provide at least a first order approximation for ages of other poorly dated terrace deposits throughout the study area (Fig. 6). The age of the Edith Formation is still rather poorly constrained. The Edith Formation is Rancholabrean in age and older than the Los Duranes Formation, suggesting that the Edith may have been deposited sometime during MOIS 8, 10, or 12. The lack of strongly developed soils on the top of the Edith Formation suggests that deposition of this unit occurred closer in time to the Los Duranes Formation.

Correlation of these deposits and provisional age constraints indicate that the ancestral positions of the Rio Grande have been modified by tectonic activity (Fig. 7). Most notably, the Edith Formation, which forms a nearly continuous outcrop band from Albuquerque just south of San Felipe, New Mexico, is faulted. The Bernalillo fault displaced this deposit by about 7 m down to the west near Bernalillo (Connell, 1996). Between cross sections B-B' and C-C' of Figure 4, the basal contact of the Edith Formation is down-dropped to the south by about 15 m by the northwest-trending Alameda structural zone. This decrease in height above local base level is also recognized by a change in stratigraphic positions relative to piedmont deposits to the east. Younger piedmont alluvium (Qay, Fig. 2) is typically found overlying the Edith Formation south of the Alameda structural zone (East Heights fault zone), a zone of flexure or normal faults that displace the Edith Formation in a down-to-the-southwest sense. North of the Alameda zone, tributary stream deposits are inset against the Edith Formation and are found in well defined valleys (*see map by* Connell, 1997).

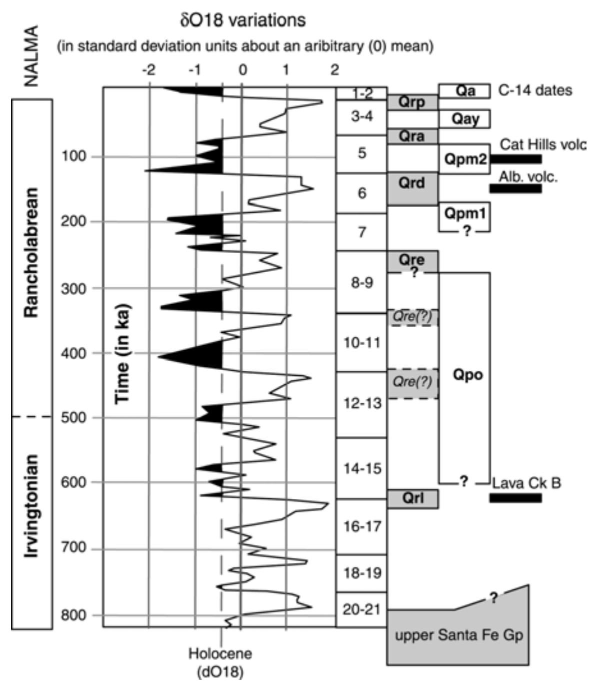

Figure 6. Correlation of fluvial deposits inferred ages. The age of the top of the Los Duranes Formation is constrained by middle and late Pleistocene basalt flows. The Lomatas Negras Formation contains the middle Pleistocene Lava Creek B ash. The Edith Formation contains middle-late Pleistocene Rancholabrean fossils and is older than the Los Duranes Formation, however, its precise age is not well constrained. Younger deposits are constrained by a radiocarbon date of 4550 yr. BP. The Edith Formation is interpreted to be older than the Los Duranes Formation and precise than the Lomatas Negras Formation. More precise age control has not been established and the Edith Formation could have been deposited during different climatic episodes.

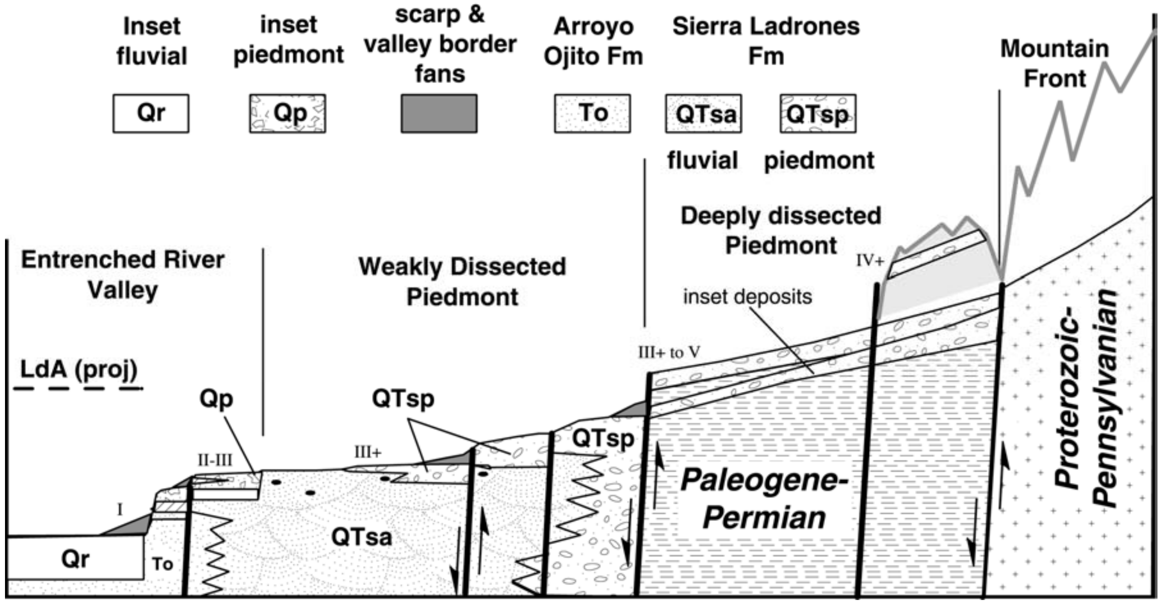

Figure 7. Generalized cross section across part of the piedmont of the Sandia Mountains, illustrating interfingering relationships among aggrading sediments of the upper Santa Fe Group, and inset post-Santa Fe Group deposits. Pedogenic carbonate morphology of constructional deposit surfaces is indicated by roman numerals that indicate the morphogenetic stage of soil development.

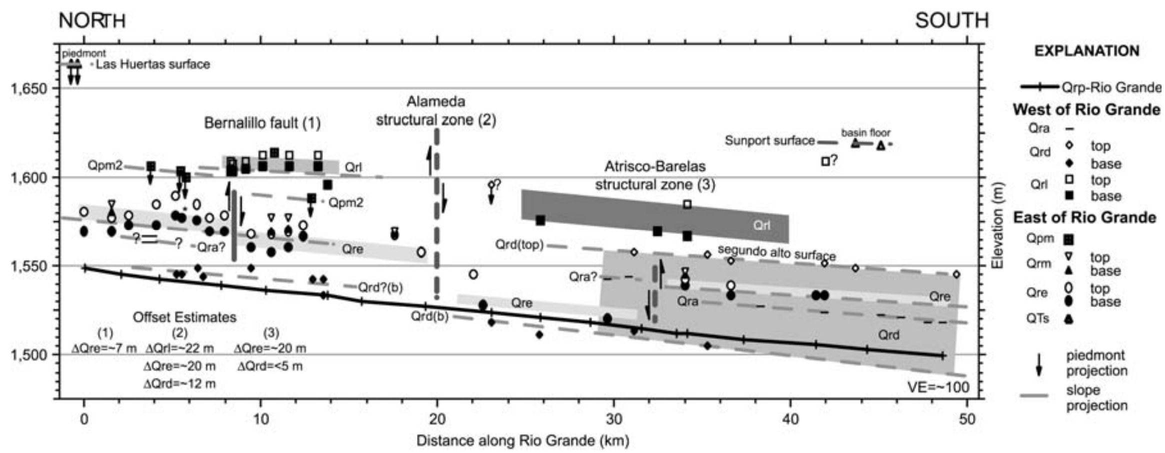

Figure 8. Longitudinal profile along Rio Grande, illustrating inset relationships among ancestral Rio Grande terraces and early Pleistocene aged constructional surfaces that locally mark the end of Santa Fe Group deposition (Las Huertas and Sunport geomorphic surfaces). The Edith and Los Duranes formations are deformed by northwest-trending faults that alter the elevation of the basal contact of these two units.

During late Pliocene time, the ancestral Rio Grande formed an axial-river that flowed within a few kilometers of the western front of the Sandia Mountains (Fig. 9a). During early Pleistocene time, between about 1.3-0.7 Ma, the Rio Grande began to entrench into the basin fill, just west of the modern valley. Piedmont deposits prograded across much of the piedmont-slope of the Sandia Mountains and buried these basin-fill fluvial deposits (Fig. 9b). During middle Pleistocene time, the Rio Grande episodically entrenched into older terrace deposits and basin-fill of the Santa Fe Group. These episodes of entrenchment were followed by periods of partial backfilling of the valley and progradation of piedmont and valley border deposits (Figs. 9c and 9d). The latest episode of entrenchment and partial backfilling occurred during the latest Pleistocene, when middle Pleistocene tributary deposits were abandoned during entrenchment, and valleys partially aggraded later during latest Pleistocene and Holocene time (Fig. 9e).

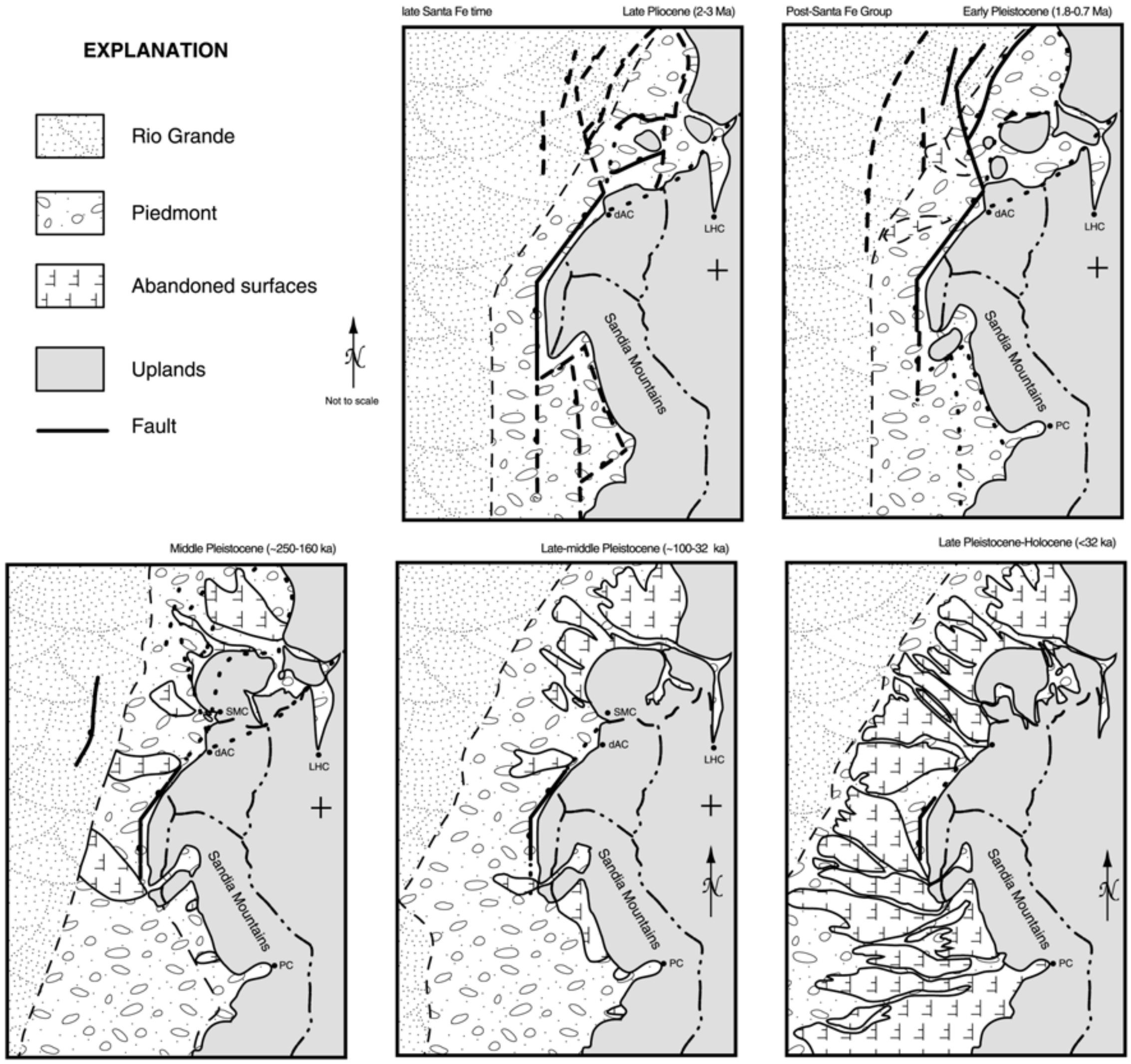

Figure 9. Paleogeographic maps of the latest phase of basin filling of the Santa Fe Group, and Pleistocene development of the Rio Grande valley (modified from Connell, 1996). Las Huertas Creek (LHC), Pino Canyon (PC), and del Agua Canyon (dAC) are shown for reference.

REFERENCES

Allen, B.D., and Anderson, R.Y., 2000, A continuous, high-resolution record of late Pleistocene climate variability from the Estancia Basin, New Mexico: Geological Society of America Bulletin, v. 112, n. 9, p. 1444-1458.

Bryan, K., 1909, Geology of the vicinity of Albuquerque: University of New Mexico, Bulletin No. 3, 24 p.

Bull, W.B., 1991, Geomorphic responses to climate changes: New York, Oxford University Press, 326 p.

Cather, S.M., and Connell, S.D., 1998, Geology of the San Felipe 7.5-minute quadrangle, Sandoval County, New Mexico: New Mexico Bureau of Mines and Mineral Resources, Open-File Digital Geologic Map 19, scale 1:24,000.

Chamberlin, R.M., Jackson, P., Connell, S.D., Heynekamp, M., and Hawley, J.W., 1999, Field logs of borehole drilled for nested piezometers, Sierra Vista West Park Site: New Mexico Bureau of Mines and Mineral Resources Open-File Report 444B, 30 p.

Connell, S.D., 1996, Quaternary geology and geomorphology of the Sandia Mountains piedmont, Bernalillo and Sandoval Counties, central New Mexico: New Mexico Bureau of Mines and Mineral Resources Open-File Report 425, 414 p., 3 pls.

Connell, S.D., 1997, Geology of the Alameda 7.5-minute quadrangle, Bernalillo County, New Mexico: New Mexico Bureau of Mines and Mineral Resources, Open-File Digital Geologic Map 10, scale 1:24,000.

Connell, S.D., 1998, Geology of the Bernalillo 7.5-minute quadrangle, Sandoval County, New Mexico: New Mexico Bureau of Mines and Mineral Resources, Open-File Digital Geologic Map 16, scale 1:24,000.

Connell, S.D., and Love, D.W., 2000, Stratigraphy of Rio Grande terrace deposits between San Felipe Pueblo and Los Lunas, Albuquerque Basin, New Mexico [abstract]: New Mexico Geology, v. 22, n. 2, p. 49.

Connell, S.D., and Wells, S.G., 1999, Pliocene and Quaternary stratigraphy, soils, and geomorphology of the northern flank of the Sandia Mountains, Albuquerque Basin, Rio Grande rift, New Mexico: New Mexico Geological Society, Guidebook 50, p. 379-391.

Connell, S.D., and 10 others, 1995, Geology of the Placitas 7.5-minute quadrangle, Sandoval County, New Mexico: New Mexico Bureau of Mines and Mineral Resources, Open-File Digital Map 2, scale 1:12,000 and 1:24,000, revised Sept. 9, 1999.

Connell, S.D., Allen, B.D., Hawley, J.W., and Shroba, R., 1998, Geology of the Albuquerque West 7.5-minute quadrangle, Bernalillo County, New Mexico: New Mexico Bureau of Mines and Mineral Resources, Open-File Digital Geologic Map 17, scale 1:24,000.

Dethier, D.P., 1999, Quaternary evolution of the Rio Grande near Cochiti Lake, northern Santo Domingo basin, New Mexico: New Mexico Geological Society, Guidebook 50, p. 371-378.

Gile, L. H., Peterson, F. F. and Grossman, R. B., 1966, Morphological and genetic sequences of carbonate accumulation in desert soils: Soil Science, v. 101, n. 5, p. 347-360.

Hawley, J. W., 1996, Hydrogeologic framework of potential recharge areas in the Albuquerque Basin, central New Mexico: New Mexico Bureau of Mines and Mineral Resources, Open-file Report 402 D, Chapter 1, 68 p.

Hawley, J.W. and Kottlowski, F.E., 1969, Quaternary geology of the south-central New Mexico border region: New Mexico Bureau of Mines and Mineral Resources, Circular 104, p. 89-115.

Hawley, J.W., Bachman, G.O. and Manley, K., 1976, Quaternary stratigraphy in the Basin and Range and Great Plains provinces, New Mexico and western Texas; *in* Mahaney, W.C., ed., Quaternary stratigraphy of North America: Stroudsburg, PA, Dowden, Hutchinson, and Ross, Inc., p. 235-274.

Johnson, P.S., Connell, S.D., Allred, B., and Allen, B.D., 1996, Field logs of boreholes for City of Albuquerque piezometer nests, Hunters Ridge Park, May 1996: New Mexico Bureau of Mines and Mineral Resources, Open-File Report 426C, 25 p., 1 log, 1 fig.

Johnson, P.S., Connell, S.D., Allred, B., and Allen, B.D., 1996, Field logs of boreholes for City of Albuquerque piezometer nests, West Bluff Park, July 1996: New Mexico Bureau of Mines and Mineral Resources, Open-File Report 426D, 19 p., 1 log, 1 fig.

Kelley, V. C. and Kudo, A. M., 1978, Volcanoes and related basaltic rocks of the Albuquerque-Belen Basin, New Mexico: New Mexico Bureau Mines Mineral Resources, Circular 156, 30 p.

Lambert, P.W., 1968, Quaternary stratigraphy of the Albuquerque area, New Mexico: [Ph.D. dissertation] Albuquerque, University of New Mexico, 329 p.

Love, D. W., 1997, Geology of the Isleta 7.5-minute quadrangle, Bernalillo and Valencia Counties, New Mexico: New Mexico Bureau of Mines and Mineral Resources, Open-file Digital Geologic Map 13, scale 1:24,000.

Love, D., Maldonado, F., Hallett, B., Panter, K., Reynolds, C., McIntosh, W., Dunbar, N., 1998, Geology of the Dalies 7.5-minute quadrangle, Valencia County, New Mexico: New Mexico Bureau of Mines and Mineral Resources, Open-file Digital Geologic Map 21, scale 1:24,000.

Lucas, S.G., Williamson, T.E., and Sobus, J., 1988, Late Pleistocene (Rancholabrean) mammals from the Edith Formation, Albuquerque, New Mexico: The New Mexico Journal of Science, v. 28, n. 1, p. 51-58.

Machette, M.N., 1985, Calcic soils of the southwestern United States: Geological Society of America, Special Paper 203, p. 1-42.

Machette, M.N., Long, T., Bachman, G.O., and Timbel, N.R., 1997, Laboratory data for calcic soils in central New Mexico: Background information for mapping Quaternary deposits in the Albuquerque Basin: New Mexico Bureau of Mines and Mineral Resources, Circular 205, 63 p.

Maldonado, F., Connell, S.D., Love, D.W., Grauch, V.J.S., Slate, J.L., McIntosh, W.C., Jackson, P.B., and Byers, F.M., Jr., 1999, Neogene geology of the Isleta Reservation and vicinity, Albuquerque Basin, New Mexico: New Mexico Geological Society Guidebook 50, p. 175-188.

Peate, D.W., Chen, J.H., Wasserburg, G.J., and Papanastassiou, D.A., 1996, ^{238}U-^{230}Th dating of a geomagnetic excursion in Quaternary basalts of the Albuquerque volcanoes field, New Mexico (USA): Geophysical Research Letters, v. 23, n. 17, p. 2271-2274.

Personius, S. F., Machette, M. N., and Stone, B. D., 2000, Preliminary geologic map of the Loma Machette quadrangle, Sandoval County, New Mexico: U.S. Geological Survey, Miscellaneous Field Investigations, MF-2334, scale 1:24,000, *ver. 1.0*.

Schumm, S.A., 1965, Quaternary paleohydrology, in Wright, H.E., and Frey, D.G., eds, The Quaternary of the United States: New Jersey, Princeton University Press, p. 783-794.

Smith, G.A. and Kuhle, A.J., 1998, Geology of the Santo Domingo Pueblo 7.5-minute quadrangle, Sandoval County, New Mexico, New Mexico Bureau of Mines and Mineral Resources, Open-file Digital Geologic Map 15, scale 1:24,000.

SUMMARY OF BLANCAN AND IRVINGTONIAN (PLIOCENE AND EARLY PLEISTOCENE) MAMMALIAN BIOCHRONOLOGY OF NEW MEXICO

GARY S. MORGAN and SPENCER G. LUCAS
New Mexico Museum of Natural History, 1801 Mountain Road NW, Albuquerque, NM 87104

Significant mammalian faunas of Pliocene (latest Hemphillian and Blancan) and early Pleistocene (early and medial Irvingtonian) age are known from the Rio Grande and Gila River valleys of New Mexico. Fossiliferous exposures of the Santa Fe Group in the Rio Grande Valley, extending from the Española basin in northern New Mexico to the Mesilla basin in southernmost New Mexico, have produced 21 Blancan and six Irvingtonian vertebrate assemblages (Fig. 1). A medial Irvingtonian fauna is known from a cave deposit in the San Luis basin in northernmost New Mexico (Fig. 2). Three Blancan faunas occur in Gila Group strata in the Gila River Valley in the Mangas and Duncan basins in southwestern New Mexico (Fig. 3). More than half of these faunas contain five or more species of mammals, and many have associated radioisotopic dates and/or magnetostratigraphy, allowing for correlation with the North American land-mammal biochronology (Figs. 2-3).

Two diverse early Blancan (4.5-3.6 Ma) faunas are known from New Mexico, the Truth or Consequences Local Fauna (LF) from the Palomas basin and the Buckhorn LF from the Mangas basin. The Truth or Consequences LF contains five species of mammals indicative of the early Blancan: *Borophagus* cf. *B. hilli*, *Notolagus lepusculus*, *Neotoma quadriplicata*, *Jacobsomys* sp., and *Odocoileus brachyodontus*. Associated magnetostratigraphic data suggest correlation with either the Nunivak or Cochiti subchrons of the Gilbert Chron (between 4.6 and 4.2 Ma), which is consistent with the early Blancan age indicated by the mammalian biochronology. The Truth or Consequences LF is similar in age to the Verde LF from Arizona, and slightly older than the Rexroad 3 and Fox Canyon faunas from Kansas. The Buckhorn LF has 18 species of mammals, including two rodents typical of the early Blancan, *Mimomys poaphagus* and *Repomys panacaensis*. The Buckhorn LF also is similar in age to the Verde LF and has affinities with the Panaca LF from Nevada. Although the Buckhorn and Truth or Consequences LFs have few taxa in common, the similarities of both faunas with the Verde LF suggest they are close in age.

Eight faunas from the central and southern Rio Grande Valley are medial Blancan in age (3.6-2.7 Ma), including the Pajarito and Belen faunas from the Albuquerque basin, the Arroyo de la Parida LF from the Socorro basin, the Cuchillo Negro Creek and Elephant Butte Lake LFs from the Engle basin, the Palomas Creek LF from the Palomas basin, the Hatch LF from the Hatch-Rincon basin, and the Tonuco Mountain LF from the Jornada basin. These faunas are characterized by the presence of taxa absent from early Blancan faunas, including *Geomys* (*Nerterogeomys*) *paenebursarius*, *Equus cumminsii*, *E. scotti*, and *Camelops*, and the absence of South American immigrant mammals found in late Blancan faunas. The Pajarito LF is directly associated with a fluvially recycled pumice dated at 3.12±0.10 Ma (Maldonado et al., 1999). The Cuchillo Negro Creek and Elephant Butte Lake LFs are in close stratigraphic association with a basalt flow dated at 2.9 Ma. Magnetostratigraphy constrains the age of the Tonuco Mountain LF between 3.6 and 3.0 Ma.

The Mesilla A fauna from the Mesilla basin and the Pearson Mesa LF from the Duncan basin are late Blancan in age (2.7-2.2 Ma). Both faunas record the association of *Nannippus* with a South American immigrant, *Glyptotherium* from Mesilla A and *Glossotherium* from Pearson Mesa, restricting their age to the interval after the beginning of the Great American Interchange at about 2.7 Ma and before the extinction of *Nannippus* at about 2.2 Ma. Magnetostratigraphy further constrains the Mesilla A and Pearson Mesa faunas to the upper Gauss Chron, just prior to the Gauss/Matuyama boundary at 2.58 Ma. The Mesilla B and Virden faunas occur higher in the same stratigraphic sequences as the Mesilla A and Pearson Mesa faunas, respectively, and are latest Blancan in age (2.2-1.8 Ma). Both faunas contain taxa restricted to the Blancan, including the camels *Blancocamelus* and *Gigantocamelus* from Mesilla B, and *Canis lepophagus* from Virden. The absence of *Nannippus*, and of *Mammuthus* and other genera that first appear in the Irvingtonian, suggest an age range between 2.2 and 1.8 Ma. Magnetostratigraphic data from Mesilla B support a latest Blancan age.

The Tijeras Arroyo fauna from the Albuquerque basin and the Tortugas Mountain and Mesilla C faunas from the Mesilla basin all include *Mammuthus* and other mammals indicative of an early Irvingtonian age (1.8-1.0 Ma). The association of *Mammuthus* and *Stegomastodon* in the Tortugas Mountain LF indicates an age younger than 1.8 Ma, after the arrival of *Mammuthus* in North America from Eurasia and before the extinction of *Stegomastodon* at about 1.2 Ma. The co-occurrence of *Glyptotherium arizonae*, *Equus scotti*, and the primitive mammoth *M. meridionalis* in Tijeras Arroyo and Mesilla C is typical of southwestern early Irvingtonian faunas. Fossils of *M. meridionalis* from Tijeras Arroyo and Mesilla C are both closely associated with dates of 1.6 Ma on pumice from the lower Bandelier tuff, making them among the oldest dated mammoths in North America. San Antonio Mountain (SAM) Cave in northernmost New Mexico lacks large mammals, but the presence of the microtine rodents *Mictomys kansasensis*, an advanced species of *Allophaiomys*, *Lemmiscus curtatus*, and *Microtus* cf. *M. californicus* indicates a medial Irvingtonian age, between about 1.0 and 0.85 Ma.

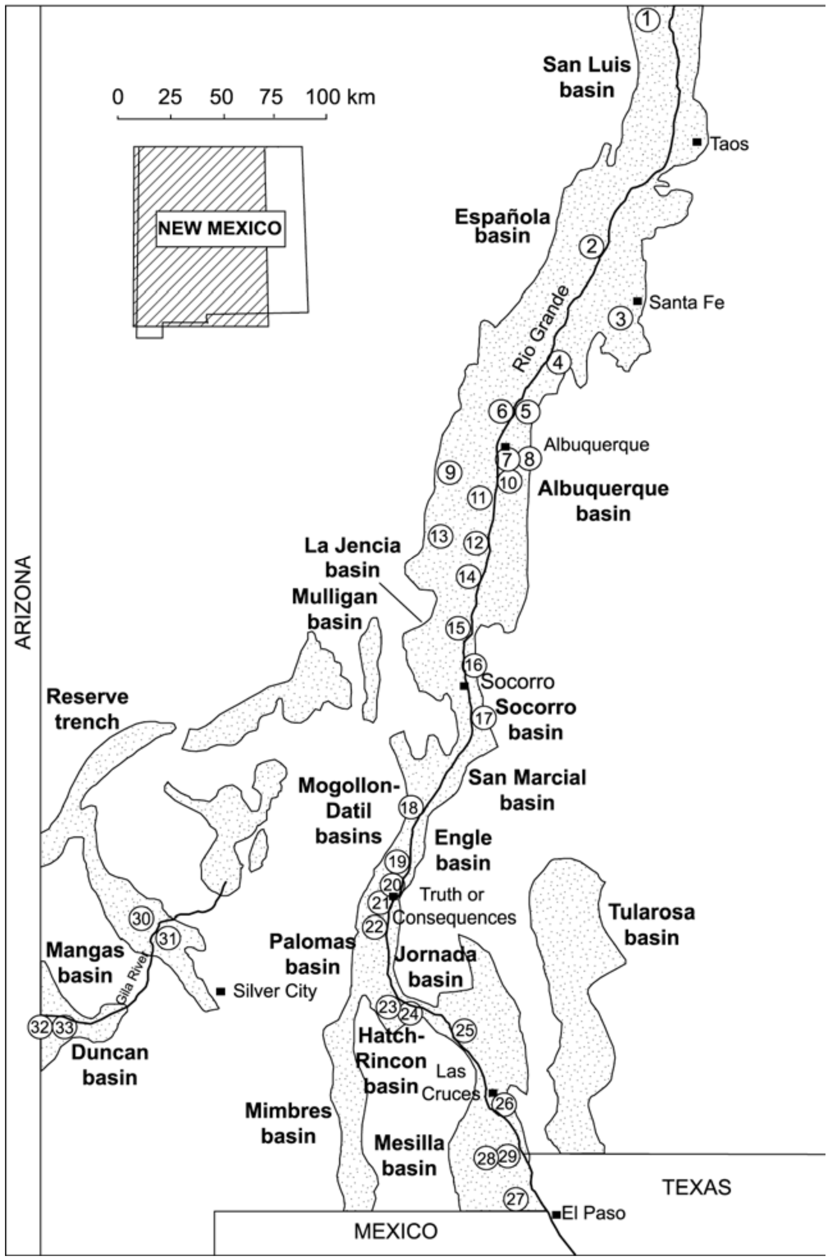

Figure 1. Map of New Mexico showing the location of late Hemphillian, Blancan, and Irvingtonian fossil sites. The structural basins are named and indicated by stippling. Sites are numbered from north to south in the Rio Grande Valley (sites 1-29), followed by sites in the Gila River Valley (sites 30-33). 1. San Antonio Mountain (SAM) Cave, medial Irvingtonian; 2. Puyé Formation site, late Hemphillian; 3. Ancha Formation sites, late Blancan; 4. Santo Domingo, late Blancan; 5. Western Mobile, early Irvingtonian; 6. Loma Colorado de Abajo, early/medial Blancan; 7. Mesa del Sol, Blancan; 8. Tijeras Arroyo, early Irvingtonian; 9. Pajarito, medial Blancan; 10. Isleta, Blancan; 11. Los Lunas, Blancan; 12. Belen, medial Blancan; 13. Mesas Mojinas, Blancan; 14. Veguita, Blancan; 15. Sevilleta, Blancan; 16. Arroyo de la Parida, medial Blancan; 17. Fite Ranch, early Irvingtonian; 18. Silver Canyon, Blancan; 19. Elephant Butte Lake, medial Blancan; 20. Cuchillo Negro Creek, medial Blancan; 21. Truth or Consequences, early Blancan; 22. Palomas Creek, medial Blancan; 23. Hatch, medial Blancan; 24. Rincon Arroyo, late Blancan/early Irvingtonian; 25. Tonuco Mountain, medial Blancan; 26. Tortugas Mountain, early Irvingtonian; 27. Mesilla A, late Blancan; 28. Mesilla B, latest Blancan; 29. Mesilla C, early Irvingtonian; 30. Buckhorn, early Blancan; 31. Walnut Canyon, latest Hemphillian; 32. Pearson Mesa, late Blancan; 33. Virden, latest Blancan.

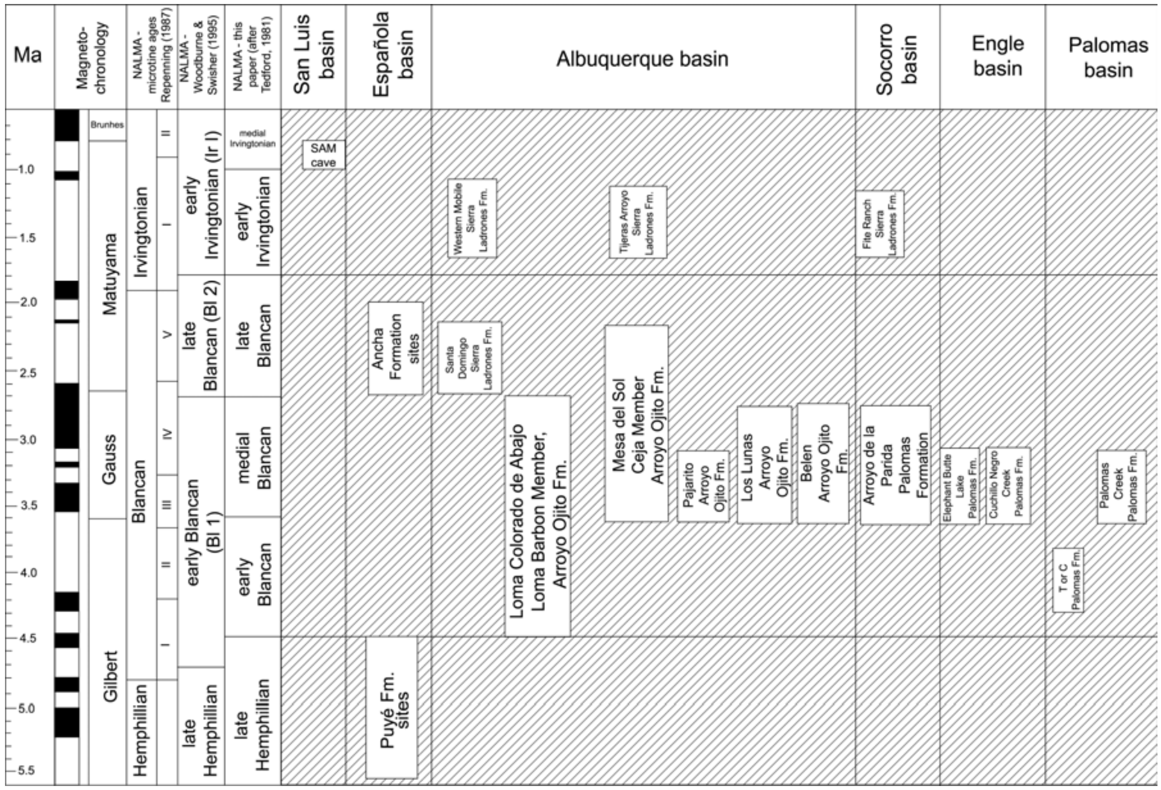

Figure 2. Correlation chart showing the relative ages of late Hemphillian, Blancan, and Irvingtonian vertebrate faunas from the northern and central Rio Grande Valley in New Mexico, including the San Luis, Española, Albuquerque, Socorro, Engle, and Palomas basins. The chronological limits of the mammalian faunas are indicated by the vertical height of the boxes enclosing the fauna or site names. The lithostratigraphic unit from which each fauna or site was derived is also indicated within the box. The magnetochronology is from Berggren et al. (1995). Three different systems for subdividing the Blancan NALMA are indicated on the left side of the chart (Tedford, 1981; Repenning, 1987; Woodburne and Swisher, 1995).

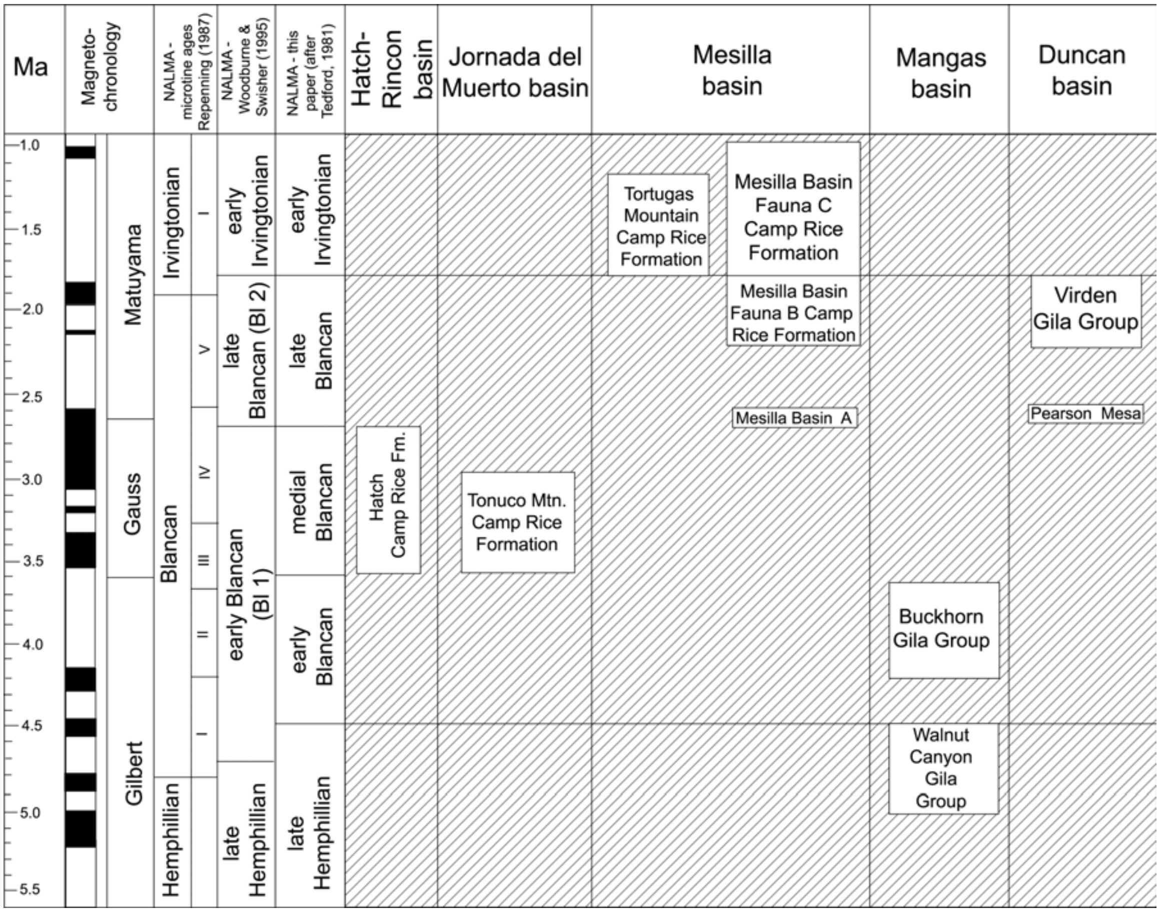

Figure 3. Correlation chart showing the relative ages of late Hemphillian, Blancan, and Irvingtonian vertebrate faunas from the southern Rio Grande Valley and Gila River Valley in New Mexico, including the Hatch-Rincon, Jornada, Mesilla, Mangas, and Duncan basins. Other notes as for Figure 2.

REFERENCES

Berggren, W. A., Hilgen, F. J., Langereis, C. G., Kent, D. V., Obradovich, J. D., Raffi, I., Raymo, M. E., and Shackleton, N. J., 1995, Late Neogene chronology: New perspectives in high-resolution stratigraphy: Geological Society of America Bulletin, v. 107, p. 1272-1287.

Maldonado, F., Connell, S.D., Love, D.W., Grauch, V.J.S., Slate, J.L., McIntosh, W.C., Jackson, P.B., and Byers, F.M., Jr., 1999, Neogene geology of the Isleta Reservation and vicinity, Albuquerque Basin, New Mexico: New Mexico Geological Society Guidebook 50, p. 175-188.

Repenning, C. A., 1987, Biochronology of the microtine rodents of the United States; *in* M. O. Woodburne, ed., Cenozoic mammals of North America: Geochronology and biostratigraphy: University of California Press, Berkeley, p. 236-268.

Tedford, R. H., 1981, Mammalian biochronology of the late Cenozoic basins of New Mexico: Geological Society of American Bulletin, Part I, v. 92, p. 1008-1022.

Woodburne, M. O. and Swisher, C. C., III, 1995, Land mammal high-resolution geochronology, intercontinental overland dispersals, sea level, climate, and vicariance: SEPM Special Publication 54, p. 335-364.

PLIO-PLEISTOCENE MAMMALIAN BIOSTRATIGRAPHY AND BIOCHRONOLOGY AT TIJERAS ARROYO, BERNALILLO COUNTY, NEW MEXICO

SPENCER G. LUCAS and GARY S. MORGAN
New Mexico Museum of Natural History and Science, 1801 Mountain Rd. NW, Albuquerque, NM 87104

Most of the vertebrate fossils from Tijeras Arroyo, located just south of the Albuquerque International Airport in Bernalillo County, are derived from the Sierra Ladrones Formation and are early Irvingtonian in age (Lucas et al., 1993). However, one locality (New Mexico Museum of Natural History and Science [NMMNH] site L-1458) at the base of the exposed stratigraphic section in Tijeras Arroyo (Fig. 1) has produced two species that are indicative of a Blancan age. The fossils from this site were derived from a sandstone comprising unit 1 in the stratigraphic section of Lucas et al. (1993, fig. 2). The lowermost part of the section in Tijeras Arroyo, including unit 1, was recently referred to the Ceja Member of the Arroyo Ojito Formation (Connell and Hawley, 1998; Connell et al., 1999).

Both mammals identified from site L-1458 in the Tijeras Arroyo section, *Hypolagus* cf. *H. gidleyi* and *Equus* cf. *E. cumminsii*, are typical of Blancan faunas, and do not occur in the Irvingtonian. The extinction in the late Pliocene (about 2.2 Ma) of several characteristic Blancan genera, including *Hypolagus*, *Borophagus*, *Rhynchotherium*, and *Nannippus*, is considered one of the most important biochronological events in the late Blancan (Lindsay et al., 1984). The presence of *Hypolagus* thus indicates that site L-1458 is older than 2.2 Ma. *Equus* cf. *E. cumminsii* appears to be absent from early Blancan faunas, so L-1458 is probably middle or early late Blancan in age.

Ten stratigraphically higher localities in Tijeras Arroyo have produced a significant vertebrate fauna of early Irvingtonian age (Lucas et al., 1993; Morgan and Lucas, 2000). More than 75 m of the Sierra Ladrones Formation are exposed in Tijeras Arroyo, consisting of sandstones, pumiceous sandstones, and gravels, with minor amounts of mudstone and diatomite. These sediments represent axial river deposits of an ancestral Rio Grande. The most distinctive lithologic chracteristic of these beds is the presence of reworked Guaje Pumice derived from the Bandelier Tuff, Ar/Ar dated at 1.61 Ma (Izett and Obradovich, 1994), in the units associated with an Irvingtonian fauna (units 3-8 of Lucas et al., 1993). An extensive flora of leaves and pollen from a localized volcanic ash bed was collected in the Tijeras Arroyo section (NMMNH Site L-1445). The Tijeras Arroyo flora indicates that the cottonwood forest or bosque currently found along the banks of the Rio Grande in New Mexico dates back to at least the early Pleistocene (Knight et al., 1996).

The land tortoise *Hesperotestudo* and five species of mammals, including *Glyptotherium* cf. *G. arizonae*, *Equus scotti*, *Equus* sp., *Camelops* sp., and *Mammuthus meridionalis* occur together in the Tijeras Arroyo section above the Blancan site (l-1458) discussed above (Lucas et al., 1993; Morgan and Lucas, 2000). These species constitute a fairly typical fauna of early Irvingtonian age. Three additional species of mammals, a small species of *Equus*, the llama *Hemiauchenia macrocephala* and the mammoth *Mammuthus imperator*, occur somewhat higher in the Tijeras Arroyo section than the remainder of the fauna, but probably are Irvingtonian as well.

A caudal osteoderm of a glyptodont from Tijeras Arroyo (Lucas et al., 1993) probably is not diagnostic at the species level, although this specimen almost certainly represents *Glyptotherium arizonae*. Tentative referral of this osteoderm to *G. arizonae* is reasonable as its association with *Mammuthus* rules out a Blancan age, and the Rancholabrean *G. floridanum* is restricted to the Atlantic and Gulf coastal plains (Gillette and Ray, 1981). The large horse *Equus scotti* is the most common mammal in the Tijeras Arroyo Irvingtonian fauna, represented by mandibles, isolated teeth, and postcrania (Lucas et al., 1993; Morgan and Lucas, 2000). *E. scotti* is the typical large horse in late Blancan and early Irvingtonian faunas in the southwestern United States (Hibbard and Dalquest, 1966), and occurs in medial Blancan through early Irvingtonian faunas in New Mexico (Tedford, 1981; Morgan et al., 1998). A complete equid metacarpal from Tijeras Arroyo is more slender than metacarpals of *E. scotti*, and represents a second, smaller species of *Equus* (Hibbard and Dalquest, 1966; Harris and Porter, 1980). A partial skull of a small *Equus* occurs higher in the Tijeras Arroyo section.

Lucas and Effinger (1991) and Lucas et al. (1993) referred a mandible with left and right m3 from Tijeras Arroyo to the primitive mammoth *Mammuthus meridionalis* on the basis of its low plate count and extremely thick enamel. This is one of only two records of mammoths from New Mexico referred to *M. meridionalis*, indicating that this fauna is almost certainly early Irvingtonian. The other record consists of several partial teeth, tentatively referred to *M. meridionalis*, from an early Irvingtonian fauna in the Mesilla basin (Vanderhill, 1986). Lucas et al (1993) referred a left M3 in a maxillary fragment from Tijeras Arroyo to the mammoth *Mammuthus* *imperator*. The teeth of *M. imperator* are more advanced than *M. meridonalis* in having a higher plate count, higher lamellar frequency, and thinner enamel. The *M. imperator* specimen was found about 12 m higher in the section than the remainder of the Tijeras Arroyo fauna, and thus is somewhat younger, although an Irvingtonian age is still likely (Lucas et al., 1993).

The presence of mammoths in unit 6 of Lucas et al. (1993) and above clearly establishes an Irvingtonian age for the upper part of the Tijeras Arroyo section, as *Mammuthus* is one of the defining genera of the Irvingtonian NALMA. The first appearance of *Mammuthus* in the New World occurred sometime in the early Pleistocene (early Irvingtonian) between about 1.8 and 1.6 Ma. The mammoth jaws from Tijeras Arroyo represent one of the oldest well-documented records of *Mammuthus* from North America, based on an Ar/Ar age of 1.61 Ma on Guaje Pumice from the Sierra Ladrones Formation in Tijeras Arroyo (Lucas et al., 1993; Izett and Obradovich, 1994; Lucas, 1995, 1996). Although the pumice date provides a maximum age for this site, evidence from other pumice deposits of exactly the same age farther south in the Rio Grande Valley (Mack et al., 1996, 1998) indicates that the pumice is very close in age to the fossils. The association of M. *meridionalis* with *Glyptotherium arizonae* and *Equus scotti* is indicative of an early Irvingtonian age for the Tijeras Arroyo fauna. Correlative early Irvingtonian faunas include the Tortugas Mountain LF (Lucas et al., 1999, 2000) and Mesilla Basin Fauna C (Vanderhill, 1986) from the Mesilla basin in southern New Mexico, Gilliland in Texas (Hibbard and Dalquest, 1966), and Holloman in Oklahoma (Dalquest, 1977).

REFERENCES

Connell, S. D. and Hawley, J. W., 1998, Geology of the Albuquerque West 7.5-minute quadrangle, Bernalillo County, New Mexico: New Mexico Bureau of Mines and Mineral Resources, Open File Digital Map 17, Scale 1:24,000.

Connell, S. D., Koning, D. J., and Cather, S. M., 1999, Revisions to the stratigraphic nomenclature of the Santa Fe Group. northwestern Albuquerque basin, New Mexico: New Mexico Geological Society, Guidebook 50, p. 337-353.

Dalquest, W. W., 1977, Mammals of the Holloman local fauna, Pleistocene of Oklahoma: Southwestern Naturalist, v. 22, p. 255-268.

Gillette, D. D. and Ray, C. E., 1981, Glyptodonts of North America: Smithsonian Contributions to Paleobiology, number 40, 255 p.

Harris, A. H. and Porter, L. S. W., 1980, Late Pleistocene horses of Dry Cave, Eddy County, New Mexico: Journal of Mammalogy, v. 61, p. 46-65.

Hibbard, C. W., and Dalquest, W. W., 1966, Fossils from the Seymour Formation of Knox and Baylor Counties, Texas, and their bearing on the late Kansan climate of that region: Contributions from the Museum of Paleontology, University of Michgian, v. 21, n. 1, 66 p.

Izett, G. A. and Obradovich, J. D, 1994, $^{40}Ar/^{39}Ar$ age constraints for the Jaramillo Normal Subchron and the Matuyama-Brunhes geomagnetic boundary: Journal of Geophysical Research, v. 99 (B2), p. 2925-2934.

Knight, P. J., Lucas, S. G., and Cully, A., 1996, Early Pleistocene (Irvingtonian) plants from the Albuquerque area, New Mexico: Southwestern Naturalist, v. 41, p. 207-217.

Lindsay, E. H., Opdyke, N. D., and Johnson, N. M., 1984, Blancan-Hemphillian Land Mammal Ages and late Cenozoic mammal dispersal events: Annual Review of Earth and Planetary Sciences, v. 12, p. 445-488.

Lucas, S. G., 1995, The Thornton Beach mammoth and the antiquity of *Mammuthus* in North America: Quaternary Research, v. 43, p. 263-264.

Lucas, S. G., 1996, The Thornton Beach mammoth: Consistency of numerical age and morphology: Quaternary Research, v. 45, p. 332-333.

Lucas, S. G., and Effinger, J. E., 1991, *Mammuthus* from Lincoln County and a review of the mammoths from the Pleistocene of New Mexico: New Mexico Geological Society Guidebook 42, p. 277-282.

Lucas, S. G., Morgan, G. S. and Estep, J. W., 2000, Biochronological significance of the co-occurrence of the proboscideans Cuvieronius, Stegomastodon, and Mammuthus in the lower Pleistocene of southern New Mexico: New Mexico Museum of Natural History and Science, Bulletin 16, p. 209-216.

Lucas, S. G., Williamson, T. E., and Sobus, J., 1993, Plio-Pleistocene stratigraphy, paleoecology, and mammalian biochronology, Tijeras Arroyo, Albuquerque area, New Mexico: New Mexico Geology, v. 15, p. 1-8, 15.

Lucas, S. G., Morgan, G. S. Estep, J. W. Mack, G. H., and Hawley, J. W., 1999, Co-occurrence of the proboscideans Cuvieronius, Stegomastodon, and Mammuthus in the lower Pleistocene of southern New Mexico: Journal of Vertebrate Paleontology, v. 19, p. 595-597.

Mack, G. H., McIntosh, W. C., Leeder, M. R., and Monger, H. C., 1996, Plio-Pleistocene pumice floods in the ancestral Rio Grande, southern Rio Grande rift, USA: Sedimentary Geology, v. 103, p. 1-8.

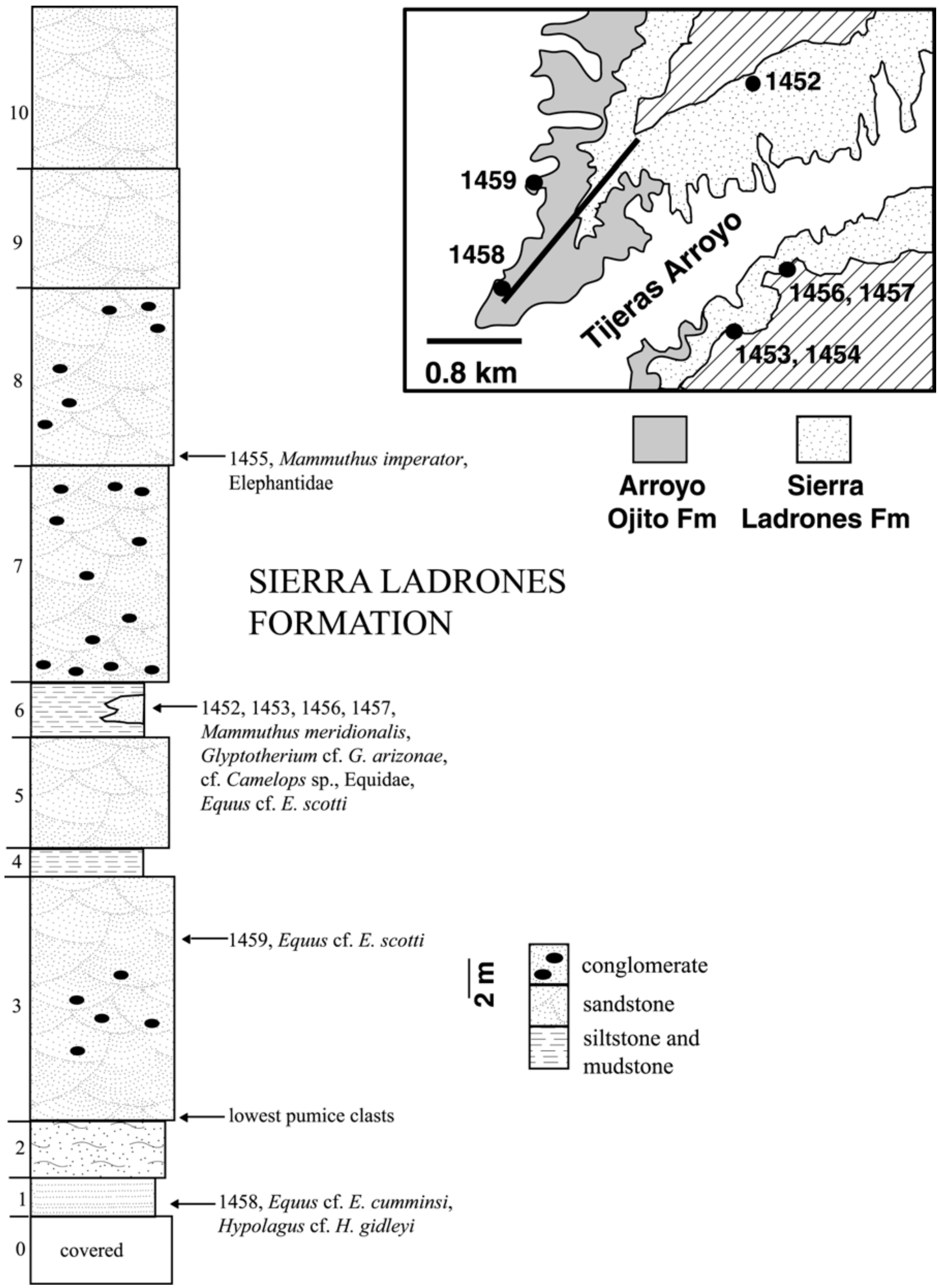

Figure 1. Stratigraphic column of Sierra Ladrones and Arroyo Ojito Formation strata at mouth of Tijeras Arroyo.

Mack, G. H., Salyards, S. L., McIntosh, W. C., and Leeder, M. R., 1998, Reversal magnetostratigraphy and radioisotopic geochronology of the Plio-Pleistocene Camp Rice and Palomas Formations, southern Rio Grande rift: New Mexico Geological Society, Guidebook 49, p. 229-236.

Morgan, G. S. and Lucas, S. G., 2000, Pliocene and Pleistocene vertebrate faunas from the Albuquerque basin, New Mexico: New Mexico Museum of Natural History and Science, Bulletin 16, p. 217-240.

Morgan, G. S., Lucas, S. G., and Estep, J. W., 1998, Pliocene (Blancan) vertebrate fossils from the Camp Rice Formation near Tonuco Mountain, Doña Ana County, southern New Mexico: New Mexico Geological Society Guidebook, 49th Field Conference, p. 237-249.

Tedford, R. H., 1981, Mammalian biochronology of the late Cenozoic basins of New Mexico: Geological Society of American Bulletin, Part I, v. 92, p. 1008-1022.

Vanderhill, J. B., 1986, Lithostratigraphy, vertebrate paleontology, and magnetostratigraphy of Plio-Pleistocene sediments in the Mesilla basin, New Mexico [PhD Dissertation]: Austin, University of Texas, 305 p.

Reprinted with permission from New Mexico Bureau of Mines and Mineral Resources Bulletin 137, p. 162-163 (1991)

CUSPATE-LOBATE FOLDS ALONG A SEDIMENTARY CONTACT, LOS LUNAS VOLCANO, NEW MEXICO

William C. Haneberg[1]
New Mexico Bureau of Mines and Mineral Resources, 801 Leroy Place, Socorro, NM 87801

BACKGROUND

Cuspate-lobate folds are characteristic of strongly compressed interfaces separating media of differing mechanical competence, with the lobate folds cored by the more competent material and the cuspate folds cored by the less competent material (e.g. Ramsay and Huber, 1987, p. 403). Other commonly used terms for this type of feature include *mullion, fold mullion, and arc-and-cusp structure*. Although cuspate-lobate folds are commonly associated with high-grade metamorphic rocks, their morphology is similar to that of alternating load casts and flame structures in sedimentary sequences. In addition to having geologic significance as indicators of both competence contrast and shortening direction, cuspate-lobate folds are also amenable to theoretical and experimental analysis.

Ramsay and Huber (1987, pp. 392-393) maintain that cuspate-lobate folds form only along interfaces separating media of low viscosity contrast, perhaps less than an order of magnitude. Smith (1975, 1977) and Fletcher (1982) analyzed the growth of instabilities along interfaces separating both linear and nonlinear fluids, and concluded that, although so-called mullion instabilities have small growth rates, mullion growth is enhanced in nonlinear fluids. One important conclusion of such analyses is that no first-order dynamic instability, which would maximize the growth of structures with a preferred wavelength, will develop between two semi-infinite fluids. Instead, there is only kinematic amplification of pre-existing perturbations alng the interface. Johnson and Pfaff (1989) provided a detailed geometric analysis of the waveforms necessary to produce different forms of folds, including-cuspate-lobate folds, and showed how cuspate-lobate folds might evolve from sinusoidal folds in linear viscous multilayers subjec[1]ted to shortening of 6-8 %. Recent experimental work with strain-softening silicon putty models (Sokoutis, 1990) has shown that cuspate-lobate structures grow rapidly along a single interface separating two semi-infinite fluids with low viscosity contrast, but again with no preferred wavelength, subjected to shortening greater than 10%.

OBSERVATIONS

A series of exceptionally well developed cuspate-lobate folds is exposed along a sedimentary contact at los Lunas volcano (Fig. 1). Below the contact is a buff to orange alluvium composed of silt and fine sand, with no distinct bedding. Above the contact are a 1-2 cm thick white ash, a 10-15 cm thick gray tephra ranging in size from sand to granule, and a coarser orange [sic] tephra up to 1 m thick. Much of the less-resistant alluvium beneath the contact has been removed by erosion, showing that both cusps and lobes extend at least a meter back into the outcrop; therefore, these folds can be analyzed as two-dimensional structures. Most cusps in the sequence point downward, suggesting that the finer-grained alluvium was generally the more competent material during deformation; however, a few very low-amplitude cusps do point upward. The lobe portions of folds are somwhat flat, similar to a theoretical pattern consisting of a positive first waveform and a negative second waveform (Johnson and Pfaff, 1989, p. 128). Cusp amplitude and peakedness both decrease along the ash and tephra contacts above the alluvium. In addition to the prominent cuspate-lobate folds, the interface is also folded into a gentle syncline with a wavelength on the order of 10^2 m, and cut by two small thrust faults with shortening of 0.19 and 0.48 m. The distribution of 54 fold wavelengths, measured by stretching a tape between adjacent cusps, has a fairly strong central tendency (Fig. 2), with an arithmetic mean of 1.78 m and a standard deviation of 0.76 m.

CONCLUSIONS

The existence of both cuspate-lobate folds and small thrust faults shows that the sedimentary contact described in this paper has been shortened significantly, and cusp orientation shows that the alluvium was from one to ten times more competent than the volcaniclastic sediments during deformation. If mass was conserved during shortening, the thickness of the stratigraphic section must also have grown proportionally. Although measurements of arc-length are appropriate for preferred wavelength studies (Sherwin and Chapple, 1968), straight-line cusp-to-cusp measurements are much easier to collect and provide a useful first approximation of

[1] now at Haneberg Geoscience, 4434 SE Land Summit Court, Port Orchard, WA 98366

wavelength distribution. Because neither theory nor experiment predict the existence of a preferred wavelength for cuspate-lobate folds along a single interface, we are faced with two alternative explanations for our observation of somewhat uniform wavelength. First, the cuspate-lobate folds could represent the amplification of pre-existing perturbations along the interface, for example ripple marks. Second, it is possible that a preferred wavelength evolved because the sediments on one or both sides of the interface behaved as finite layers, for which dynamic instabilities will arise. Smith (1975) for example, suggests that many cuspate-lobate folds along single interfaces in the field are actually the erosional remnants of a finite layer with cuspate-lobate folds along both interfaces. At present, meager knowledge of the depositonal and deformational history of these sediments does not allow either of these explanations to be favored over the other. It is hoped, however, that detailed mapping and mechanical analysis will provide a better understanding of the exceptional structures at Los Lunas volcano.

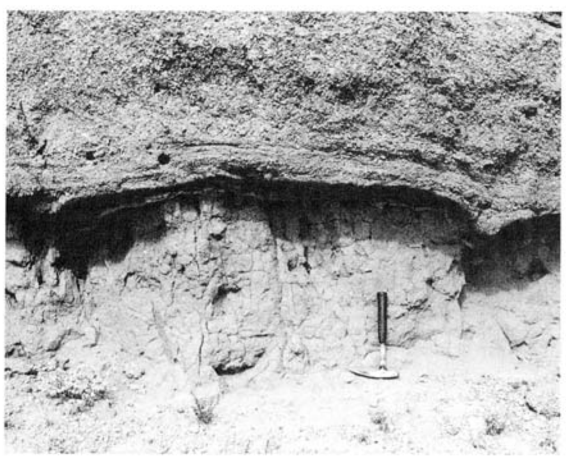

Figure 1. Example of cuspate-lobate folds developed along interface between fine-grained alluvium (lower) and ash-tephra sequence (upper) at Los Lunas volcano. Note changes in cusp amplitude and peakedness along bedding surface in volcaniclastic sediments. Hammer handle is approximately 33 cm long.

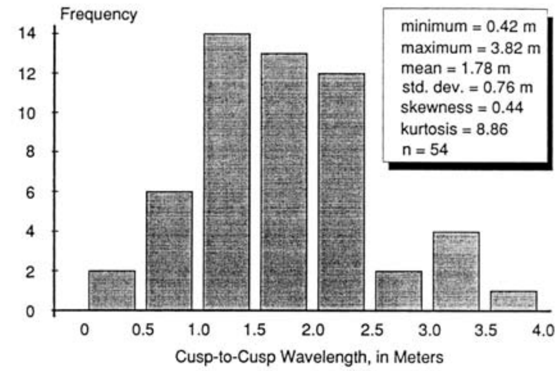

Figure 2. Histogram and sample statistics of cusp-to-cusp wavelengths of 54 cuspate-lobate folds measured at Los Lunas volcano.

ACKNOWLEDGMENTS

This work was supported by the New Mexico Bureau of Mines & Mineral Resources. David Love introduced me to a number of structural problems along the flanks of Los Lunas volcano, assisted with wavelength measurements, and, along with John Hawley, read drafts of this contribution.

REFERENCES

Fletcher, R. C., 1982, Analysis of the flow in layered fluids at small, but finite, amplitudes with application to mullion structures: Tectonophysics, v. 81, pp. 51-66.

Johnson, A. M., and Pfaff, V. J., 1989, Parallel, similar and constrained folds; in Johnson, A. M., Burnham, C. W., Allen, C. R., and Muehlberger, W., (eds.), Richard H. Jahns Memorial Volume: Engineering Geology, v. 27, pp. 115-180.

Ramsay, J. G., and Huber, M. I., 1987, The techniques of modern structural geology, Vol. 2: Folds and fractures: Academic Press, London, 700 pp.

Sherwin, J., and Chapple, W. M., 1968, Wavelengths of single layer folds: a comparison between theory and observation: Americal Journal of Science, v. 266, pp. 167-179.

Smith, R. B., 1975, Unified theory of the onset of folding, boudinage, and mullion structure: Geological Society of America, Bulletin, v. 86, pp. 1601-1609.

Smith, R. B., 1977, Formation of folds, boudinage, and mullions in non-Newtonian materials: Geological Society of America, Bulletin, v. 888, pp. 312-320.

Sokoutis, D., 1990, Experimental mullions at single and double interfaces: Journal of Structural Geology, v. 12, pp. 365-373.

Simplified Preliminary Geologic Map of the Isleta Reservation and surrounding areas

Handout for Friends of the Pleistocene Field Trip (October 12-14, 2001)

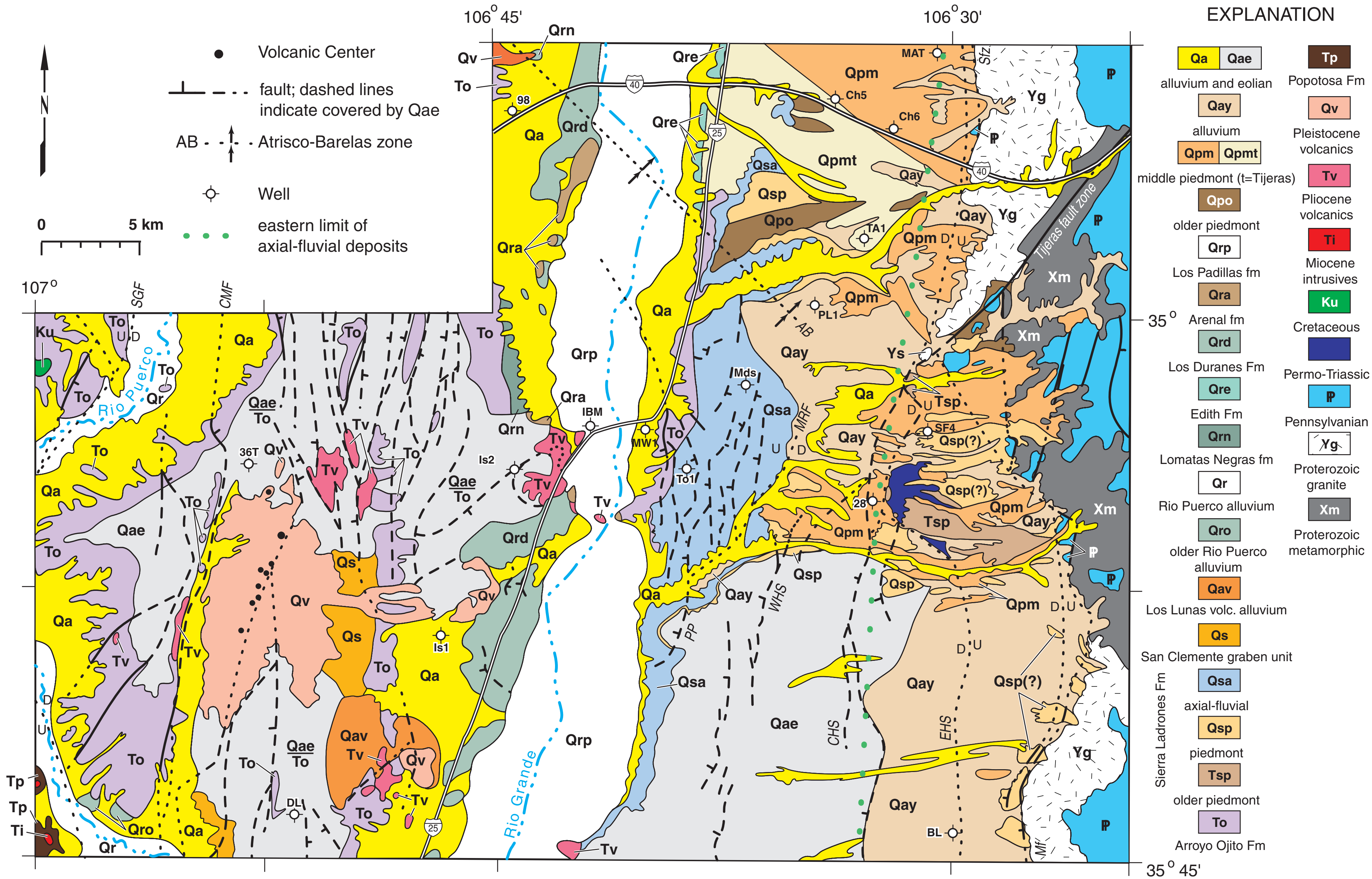

Preliminary draft compiled from Maldonado et al., 1999, and in review; Connell et al., 1998; Connell, unpubl.; Karlstrom et al., 1994)